Advances in Martingale Optimal Transport with Additional Constraints

[Olivier Croissant]

July 25, 2025

Abstract

This paper explores advancements in Martingale Optimal Transport (MOT) enriched with additional constraints, presenting a novel analytical framework that significantly broadens the applicability and computational efficiency of MOT in complex systems. By incorporating constraints that reflect practical scenarios and market conditions, we extend traditional MOT models beyond their conventional boundaries, offering a versatile tool for addressing real-world problems in finance, economics, and beyond.

Our main contribution is an incremental modification of the Sinkhorn algorithm to include these additional constraints as extra projections in the suitable geometry, forming a monotonic sequence of projections utilizing non-commutative analysis. This sophisticated mechanism enhances the transport plan's optimization process under both marginal and martingality constraints.

Additionally, we introduce a novel computational approach that dynamically updates the e-projections (projections with respect to the first dimension of the divergence) and m-projections (projections with respect to the second dimension of the divergence, which plays the role of the loss to be minimized). This enhancement significantly refines the adjustment steps within the Sinkhorn iterations, resulting in an algorithm that is not only more efficient in navigating the complex landscape of MOT problems but also more adept at ensuring convergence to an optimal solution that satisfies all imposed conditions, including those beyond traditional marginal constraints.

Our results demonstrate the efficacy of this integrated approach, showing improvements in computational efficiency and accuracy. Notably, this algorithm represents significant progress towards its implementation for pricing exotic options without the classical limitations introduced by traditional models. This advancement paves the way for more accurate and flexible pricing mechanisms in the financial industry.

Looking ahead, we outline the potential for extending our framework to multi-marginal scenarios (MMOT), anticipating significant contributions to the field. This work not only advances the state-of-the-art in MOT by integrating additional constraints but also represents progress towards implementing these methods for pricing exotic options, heralding

a new era of research and application opportunities at the intersection of mathematics, finance, physics, and operations research.

Contents

1 Introduction to Optimal Transport **7**
- 1.1 Historical Background . . . 7
- 1.2 Mathematical Formulation . . . 7
- 1.3 Optimal Transport in Finance . . . 7

2 General Considerations on the Equinox Payoff **8**
- 2.1 The Use of the Equinox Payoff . . . 8
- 2.2 Use of the Equinox in the Financial Domain . . . 9
- 2.3 Equinox, Optimal Transport, and Volatility Smiles . . . 9
- 2.4 Equinox, as an Exotic Option for Deep Hedging . . . 9

3 Optimal Transport Theory **10**
- 3.1 Application to Financial Derivatives . . . 11

4 Optimal Transport for Equinox Pricing **11**
- 4.1 General Idea of Pricing Using Optimal Transport . . . 11
- 4.2 Kantorovich Duality and Linear Programming . . . 12
- 4.3 Origin of Duality: KKT Conditions . . . 13
- 4.4 The Sinkhorn Algorithm and Optimal Transport . . . 15
- 4.5 A Natural Generalization of the Sinkhorn Algorithm . . . 16
- 4.6 Alternating Projection Algorithms and Information Geometry . . . 17

5 Incorporating Additional Constraints in Optimal Transport **19**
- 5.1 Extended Primal and Dual Problems . . . 19
- 5.2 Lagrange Multipliers and KKT Conditions . . . 19
- 5.3 Mathematical Formulation of the Extended Optimal Transport Problem . . . 20
- 5.4 Formation of the Dual Lagrangian . . . 21
- 5.5 Formulation of the Extended Sinkhorn Algorithm . . . 22
- 5.6 Handling of the Martingality Constraint . . . 24
- 5.7 Linearization of the Martingality Constraint . . . 25

6 Merging BFGS steps in the Bregman projections **27**
- 6.1 Conceptual Subtleties Above Sinkhorn Iterations . . . 29
- 6.2 The BFGS Method . . . 30
- 6.3 Enhancing MOT with BFGS and Sinkhorn through Bregman Projections . . . 30
- 6.4 Bregman Projections via Kullback-Leibler Divergence . . . 31
- 6.5 Mathematical Representation of Projections as KL Divergence Minimization . . . 33
  - 6.5.1 Iterative Proportional Fitting in Sinkhorn Algorithm . . . 34

6.6 Application of E-Projection in the Extended Sinkhorn Algorithm 34

7 Example of Pricing Code **36**
7.1 Market Model Description 37
7.2 Calibrated Model Parameters 38
7.3 Numerical Exemple 42

8 Future Research **42**
8.1 Analysis of "On Schrödinger Bridge Matching and Expectation Maximization" 42
8.2 Multimarginal Optimal Transport : MMOT 43

Appendix A Information Geometry **47**
A.1 Machine Learning and Information Geometry 48
A.2 Divergence Between Two Points 48
A.3 Examples of Divergence 48
A.4 Properties of Divergence 49
A.5 Infinitesimal Distance and Riemannian Structure 49
A.6 Geometry Induced by Divergence Functions 49
A.7 Important examples of Bregman Divergences 51
A.8 Legendre Transform 52
A.9 Relationship Between Duality of Convex Function and Duality of Bregman Divergence 53
A.10 Affine and Dual Affine Coordinate Systems 53
A.11 Tangent Space, Basis Vectors, and Riemannian Metric 54
A.12 Parallel Transport of a Vector 56
A.13 Generalized Pythagorean Theorem 57
A.14 Projection Theorem 59
A.15 Divergence Between Submanifolds 61
A.16 Exponential Family of Probability Distributions 62
A.17 Dually Flat Riemannian Structure Induced by the Log-Partition Function 62
A.18 Bregman Divergence and Thermodynamic Systems 64
A.18.1 Physical Intuition: Free Energy in Thermodynamics . . . 64
A.18.2 Thermodynamic and Information-Theoretic Interpretation 64
A.19 Gaussian Distribution in the Exponential Family 65
A.20 Mixture Family of Probability Distributions 67
A.21 Discrete Distributions as Mixture Families 67
A.22 Flat Structure e-flat and m-flat 67
A.23 Infinite-dimensional Manifold of Probability Distributions 68
A.24 Kernel Exponential Family 71
A.25 Bregman Divergence and Exponential Family 72
A.26 Maximum Entropy Principle 73
A.27 Repeated Observations and Maximum Likelihood Estimators . . 74
A.28 Dual Connections 75
A.29 Dually Flat Manifolds 78

A.30 Canonical Divergences in Dually Flat Manifolds 79
A.31 Estimation 81
A.32 Estimation in the Exponential Family 82
A.33 Estimation in a Curved Exponential Family 83

Appendix B Understanding a few Projection Algorithms **84**
B.1 Iterative Proportional Fitting (IPF) via Alternating e-Projections 84
B.2 Markov Projection algorithm 86
B.3 Iterative Markovian Fitting and Exact Marginal Fitting 86

Appendix C Optimal Transport **88**
C.1 The Monge Problem 88
C.1.1 Other Cost Functions 88
C.1.2 The Transportation Problem in $\mathbb{R}$ 90
C.1.3 The Transportation Problem in $\mathbb{R}^n$ 91
C.1.4 Optimality and cyclical monotonicity 92
C.2 The Kantorovich Problem 94
C.2.1 Existence of a Minimum in the Kantorovich Problem . . . 95
C.3 Dual Problem: Discrete Case 98
C.3.1 Discrete Optimization Problem 98
C.3.2 Linear Program Duality 99
C.3.3 ContinuousMeasures 99
C.4 Convex Sets and Convex Functions 101
C.4.1 Subgradient 102
C.4.2 Ligendre Transforms 103
C.4.3 Legendre Pairs and Dual Problems 107
C.5 Characterising the Optimal Map 109
C.6 Brenier's Polar Factorisation 113
C.7 Viscosity Solution of Monge-Ampere 117
C.8 Viscosity Subsolutions and Solutions 122
C.8.1 General Measures in the Monge-Ampère Equation 123
C.8.2 Monge-Ampère Measure 125
C.8.3 Example of a Generalized Solution 125
C.8.4 Mapping and Gradients 125
C.8.5 Contributions of Luis A. Caffarelli to Regularity of the Solutions of the Monge-Ampère Equation 126
C.9 Boundary Conditions for the Monge-Ampère Equation 127
C.9.1 Uniqueness and Existence for the Monge-Ampère Equation 128
C.9.2 Characterizing the Subdifferential using Danskin's Theorem 131
C.9.3 Example: L cost between parallel planes 134
C.10 Wasserstein Metric 135
C.10.1 Desintegration of Measures 137
C.11 Benamou-Brenier Formulation 138
C.11.1 lagrangian point of view 140
C.12 Gradient Flow in the Wasserstein metric 143
C.12.1 JKO Flows 143

C.12.2 Exemple: Link between entropy and heat equation 146
C.12.3 Exemple: Link between entropy plus potential 147
C.12.4 Exemple: porous medium 147
C.12.5 Exemple: Renyi entropy 147
C.12.6 Exemple: Keller-Segel, chemotaxis 148
C.12.7 Exemple: aggregation model 149
C.13 OT with non-quadratic costs 149
C.13.1 Definitions and Properties of C-transforms 150
C.13.2 Generalization of Subgradient for Quadratic Cost 151
C.13.3 Definition and Properties of the C-superdifferential 151
C.13.4 Analysis of the Optimal Transport Solution 153
C.13.5 Exemple: Recovering the euclidian distance squared for the cost 155
C.13.6 Exemple: L1 cost between two parallel plan 155
C.13.7 Ma-Trudinger-Wang (MTW) Conditions 158
C.14 divergence of divergences 158
C.15 ultra-violet divergence 160
C.16 Renormalizable and Non-Renormalizable Theories in High Energy Physics 163
C.17 Formulations of Quantum Field Theory Using Divergences 168
C.18 Simplified Scenario for Free Field Theory with Discrete Field Values 176

Appendix D Pricing of the Equinox in a Black-Scholes Model 177
D.1 Decomposition into Components 177
D.2 The Ordinary Binary Option 178
D.3 Two Conditional Binaries 178
D.4 Definition of the m-Binary 179
D.5 Algebraic Girsanov Transformation 180
D.6 Normalization of the m-binariy pricing formula 180
D.7 Full m-Binary Formula 181
D.8 Full Equinox Closed Form 182

9 Commented Bibliography 182

10 Quantum gravitation 188
10.0.1 Modified Newtonian Potential Formula 188
10.0.2 Explanation of Terms 189
10.0.3 Significance in Quantum Gravity 189
10.1 The Frontal Approach to Quantum Gravity 189
10.2 What is a Quantum Gravity Theory 190
10.3 Conclusion ("FAQ") 191
10.4 Bayesian Approach to Quantum Gravity Effective Theory through Multi-Marginal Optimal Transport 191

11 Advances in OT techniques **193**
11.1 Frameworks for Stochastic Modeling Tools 193
11.2 Frameworks for Optimal Transport 194
11.3 Lagrangian and Hamiltonian Formulations in Optimal Transport 194
11.4 Entropic Optimal Transport and the Schrödinger Bridge 195
11.5 Schrödinger Bridge Solution for Diffusions and Information Geometry of KL Projections 196
11.6 Iterative Methods in Schrödinger Bridge and Optimal Transport 197
11.7 Exact E-Projection in Optimal Transport 198
11.8 Toward Variational Bridge Matching 199

1 Introduction to Optimal Transport

Optimal transport theory, originally formulated by Gaspard Monge in the 18th century and later extended by Leonid Kantorovich in the 20th century, provides a powerful mathematical framework for measuring the distance between probability distributions. At its core, optimal transport seeks to find the most cost-efficient way of transforming one distribution into another. This concept, while simple in its formulation, unravels deep connections within mathematics, physics, and more recently, finance and machine learning.

1.1 Historical Background

The problem was first posed by Monge in 1781, who considered the task of moving a pile of sand to a construction site in the most efficient manner possible. Although Monge's formulation was quite insightful for its time, it was Leonid Kantorovich who, in the 1940s, reformulated the problem in a way that allowed for the application of linear programming methods, significantly broadening its applicability and computational feasibility.

1.2 Mathematical Formulation

At the heart of optimal transport is the Monge-Kantorovich problem, which can be succinctly described as follows:

Given two probability measures, μ and ν, defined on compact metric spaces X and Y, and a cost function $c : X \times Y \to [0, \infty]$, the problem is to find a transport map, or a coupling, π that minimizes the total transport cost:

$$\min_{\pi \in \Pi(\mu,\nu)} \int_{X \times Y} c(x, y) d\pi(x, y) \tag{1}$$

where $\Pi(\mu, \nu)$ denotes the set of all measures on $X \times Y$ with marginals μ and ν. This formulation is particularly appealing in financial mathematics, where μ and ν can represent the initial and final distributions of asset prices, and the cost function c encapsulates the notion of risk or other financial metrics.

1.3 Optimal Transport in Finance

In finance, the optimal transport problem offers a novel lens through which to view risk management and derivative pricing. By considering the cost of moving from an initial asset distribution to a final one, financial analysts can glean insights into the inherent risks and values of financial instruments, such as the Equinox derivative. This perspective aligns with the fundamental goals of financial mathematics: to quantify and manage risk in an uncertain world.

Furthermore, the intersection of optimal transport with areas such as artificial intelligence and theoretical physics opens up exciting possibilities for advanced modeling techniques. For instance, machine learning algorithms can be employed to find optimal transport plans in high-dimensional spaces, while

concepts from physics might offer new ways to think about the "distance" between financial states or the flow of markets.

As we delve further into the application of optimal transport in the pricing of the Equinox derivative, we will explore these connections in greater depth, highlighting the interplay between mathematics, finance, and beyond.

2 General Considerations on the Equinox Payoff

2.1 The Use of the Equinox Payoff

The Equinox payoff is defined as a structured option whose final payout P is contingent upon the performance of an underlying asset observed at two distinct points in time. In the simplified version we are addressing here it just a callable option. But the callability is automatic and not an exercisability like in American option. the idea is here to be the simplest autocall structure we can imagine . we call it a light exotic. The expected value of the payoff structure is formulated as follows:

$$P = G\left(\mathbb{E}[1_{S_1 \geq B}] + \mathbb{E}[1_{S_1 \leq B \& S_2 \geq K}(S_2 - K)]\right) \tag{2}$$

where:

- G is a constant that denotes the scaling factor or payoff multiplier.
- S_1 is the price of the underlying asset at the first observation date t_1.
- S_2 is the price of the underlying asset at the second observation date, denoted as the maturity t_2 of the option.
- B is the barrier level applicable at the first observation date t_1.
- K is the strike price applicable at the maturity date t_2.
- $\mathbb{E}[\cdot]$ represents the expectation under the risk-neutral probability measure.
- $1_{\{\cdot\}}$ is an indicator function that equals 1 if the condition inside is true, and 0 otherwise.

The first component $\mathbb{E}[1_{S_1 \geq B}]$ denotes the expected payoff from a binary option that yields G if the underlying asset's price S_1 is above the barrier B at time t_1. The second component $\mathbb{E}[1_{S_1 \leq B \& S_2 \geq K}(S_2 - K)]$ accounts for the expected payoff of a conditional call option that grants $G \times (S_2 - K)$ provided that S_1 is below the barrier B at t_1, and S_2 exceeds the strike price K at maturity t_2.

This delineation of the Equinox payoff exemplifies its construction as a hybrid between a binary option and a contingent call option, with the payout conditional upon the underlying asset's prices at two separate time intervals.

2.2 Use of the Equinox in the Financial Domain

The Equinox, by design, epitomizes a versatile structured financial instrument that offers a plethora of coupon types, catering to a wide array of investment strategies and risk appetites. Its allure primarily lies in the potential for high coupon payouts, which is particularly attractive to investors seeking substantial yields in a single investment vehicle. The Equinox option, with its unique payout structure, stands out in the landscape of exotic options as a prototype for deals that entice with varying degrees of profit scenarios. Notably, for the sake of balance and financial engineering precision, the less advertised but equally crucial lower coupon outcomes are integral to the option's overall design. Such structured options, especially those offered to retail investors, typically feature numerous callable dates and a diverse set of coupon types in real-world financial markets. However, for analytical clarity and tractability, our examination will be confined to an option with a solitary intermediate date, simplifying the complexity while preserving the essence of the financial product's valuation and risk assessment.

2.3 Equinox, Optimal Transport, and Volatility Smiles

The Equinox stands as a prominent example within the domain of exotic options where the optimal transport framework shines in its applicability. This is due to the payoff of the Equinox being intricately linked to the volatility smiles of the underlying assets at precisely two distinct time points. The optimal transport method thrives in scenarios where the task at hand is to reconcile two probability density functions, making it a powerful tool for managing the skews and shifts in volatility smiles. It's this congruence between the payoff's dependency on the underlying volatility smiles and the optimal transport's dexterity in handling two probability distributions that underpins the rationale for choosing the Equinox as the subject of scrutiny in the accompanying technical paper. The paper delves into the nuances of pricing exotic options through the lens of optimal transport theory, demonstrating how this mathematical framework can bring a new level of precision to the pricing and hedging of complex financial instruments like the Equinox.

2.4 Equinox, as an Exotic Option for Deep Hedging

The Equinox, in its role as an exotic option, emerges as an ideal candidate for the application of deep hedging strategies. The deep hedging framework is adept at incorporating aspects such as transaction costs, the liquidity constraints of hedging instruments, and mandatory regulatory hedging requirements, as stipulated by both European and American financial authorities. What sets the Equinox apart within this context is the availability of closed-form solutions for its hedging instruments. These analytical solutions facilitate the practical application of Monte Carlo simulations to compute realistic hedging costs. Consequently, the intricate computational demands, which are typically associated

with the risk management of exotic derivatives, become manageable with the computational power of modern-day systems. This suitability of the Equinox for deep hedging approaches underscores its potential for aligning with the stringent requirements of capital adequacy and profitability management, rendering it a pragmatic choice in contemporary regulatory and operational landscapes.

Deep hedging strategies extend beyond the traditional Black-Scholes framework by accounting for practical trading considerations. These strategies incorporate the influence of transaction costs, market liquidity, and regulatory constraints on hedging activities. For the Equinox option, deep hedging is particularly suitable due to the existence of closed-form hedge ratios, which are computationally feasible within current technological capabilities.

Below are the equations that illustrate the foundational concepts of deep hedging:

- **Auto financing Strategy:**

$$\pi_1 = \pi_0 + \delta_0(S_1 - S_0) \tag{3}$$

- **Over N periods:**

$$\pi_n = \pi_0 + \sum_{k=1}^{n} \delta_{k-1}(S_k - S_{k-1}) \quad \text{(Martingale)} \tag{4}$$

- **To remove an exotic option payoff:**

$$\tilde{\pi}_n = \pi_0 + \sum_{k=1}^{n} \delta_{k-1}(S_k - S_{k-1}) - \Gamma(S_1, S_2, \ldots, S_n) \tag{5}$$

where

$$\Gamma(S_1, S_2, \ldots, S_n) = 1_{S_T \geq B} G + 1_{S_T < B}(S_T - K)^+ \tag{6}$$

Here, π_n represents the portfolio value at time n, δ_k represents the hedging strategy in place between times k and $k+1$, S_k represents the price of the underlying at time k, and $\Gamma(S_1, S_2, \ldots, S_n)$ represents the payout function of the exotic option being hedged, in this case, the Equinox.

This section clearly delineates the transition from self-financing to deep hedging strategies and the role of the Equinox in these advanced risk management techniques.

3 Optimal Transport Theory

Optimal transport theory, originating from the work of Gaspard Monge and later extended by Leonid Kantorovich, offers a robust framework for comparing probability distributions. The Monge-Kantorovich problem can be formulated as follows:

Given two probability distributions μ and ν, the optimal transport problem seeks a transport plan π that minimizes the overall cost:

$$\begin{aligned} \underset{\pi}{\text{minimize}} \quad & \int_{X \times Y} c(x, y)\, d\pi(x, y) \\ \text{subject to} \quad & \pi \in \Pi(\mu, \nu), \end{aligned} \tag{7}$$

where $\Pi(\mu, \nu)$ represents the set of all joint distributions with marginals μ and ν, and $c(x, y)$ is the cost function.

3.1 Application to Financial Derivatives

In the context of financial derivatives, optimal transport allows us to model the evolution of the underlying asset's distribution, providing a novel approach to risk-neutral valuation.

4 Optimal Transport for Equinox Pricing

Given the probability distribution μ_t of the underlying asset at time t and a target distribution ν_T at the expiration T, the pricing of the Equinox derivative involves solving the following optimal transport problem:

$$\begin{aligned} \underset{\pi}{\text{minimize}} \quad & \int_{X \times Y} c(x, y)\, d\pi(x, y) \\ \text{subject to} \quad & \pi \in \Pi(\mu, \nu), \end{aligned} \tag{8}$$

where r is the risk-free rate, and $Payoff(X_T)$ is the payoff function of the Equinox derivative at maturity.

4.1 General Idea of Pricing Using Optimal Transport

In the realm of financial derivatives, optimal transport techniques provide a structured approach to pricing by establishing a cost function reflective of the derivative's payoff. The objective is to ascertain a coupling, denoted as π, which minimizes the expected cost that also embodies the expected payoff of the derivative.

For the set U of admissible couplings, certain conditions must be satisfied:

- The couplings must respect the marginal distributions at times T' and T, which correspond to the prices of vanilla options. These margins act as anchors, ensuring that the derived price aligns with the market's observed prices for standard instruments.
- They must maintain martingality of the underlying asset price between T' and T. This is a fundamental financial principle that prevents arbitrage by ensuring the expected value of the asset price, conditional on current information, does not change over time.

- They should incorporate the price of another exotic option which links $S_{T'}$ and S_T. An example of such an exotic option is the Asian option, where the payoff depends on the average price of the underlying asset over a specified period. The coupling should, therefore, be consistent with the observed market price of this Asian option.

Given these constraints, the problem can be formalized as:

$$\text{Lower Bound (Infimum)} : \min_{\pi \in U} \sum_{i,j} \pi_{i,j} c_{i,j} \tag{9}$$

$$\text{Upper Bound (Supremum)} : -\min_{\pi \in U} \sum_{i,j} \pi_{i,j} (-c_{i,j}) \tag{10}$$

where $c_{i,j}$ denotes the cost function that mirrors the payoff between states i and j. The task is to find a transport plan, or coupling π, which minimizes the total cost or payoff, thereby aligning with the derivative's value through the lens of optimal transport.

These constraints ensure that the pricing model encapsulates essential market features and risk preferences, which are integral to deriving a fair price for the derivative. The optimal transport problem, once solved within these parameters, furnishes bounds on the derivative's price, providing critical insights for financial practitioners.

4.2 Kantorovich Duality and Linear Programming

Kantorovich duality establishes a relationship between the primal and dual formulations of an optimization problem, a property elegantly utilized in linear programming. In the context of optimal transport, the primal problem aims to minimize the total cost of transporting a distribution, subject to constraints that ensure the marginals of the distribution are preserved.

The primal form of the optimal transport problem can be written as:

$$\begin{aligned}
\text{Minimize} \quad & \sum_{i=1}^{n} \sum_{j=1}^{m} c_{i,j} \pi_{i,j} \\
\text{Subject to} \quad & \sum_{j=1}^{m} \pi_{i,j} = \mu_i, \quad i = 1, \ldots, n, \\
& \sum_{i=1}^{n} \pi_{i,j} = \nu_j, \quad j = 1, \ldots, m, \\
& \pi_{i,j} \geq 0.
\end{aligned}$$

Conversely, the dual problem seeks to maximize the sum of products of the dual variables with the marginal distributions under the condition that the sum of any pair of dual variables does not exceed the corresponding transport cost.

The dual formulation is expressed as:

$$\begin{aligned} \text{Maximize} \quad & \sum_{i=1}^{n} u_i \mu_i + \sum_{j=1}^{m} v_j \nu_j \\ \text{Subject to} \quad & u_i + v_j \leq c_{i,j}, \quad \forall i \in \{1, \ldots, n\}, j \in \{1, \ldots, m\}. \end{aligned}$$

Kantorovich duality theorem assures us that under certain conditions, the optimal values of the primal and dual problems are equal, providing not just a solution but also a verification of optimality. This duality is of particular importance in financial applications where the cost function corresponds to the payoff of a derivative, and the dual variables can be interpreted as shadow prices or the marginal utility of risk.

In the case of linear programming, the optimal transport problem can be seen as a special case where the cost matrix, constraints, and objectives follow linear relations. This perspective allows for the application of powerful linear programming solvers to find the optimal transport plan, hence the pricing of financial derivatives such as the Equinox can be effectively computed.

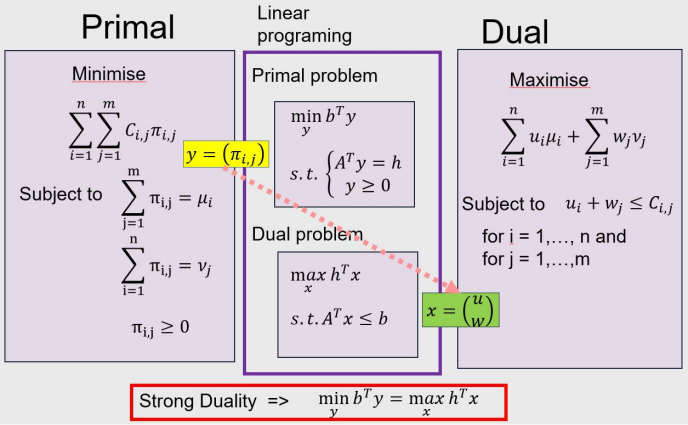

Figure 1: Primal and Dual formulation in linear programming of the optimal transport problem.

This visualization aids in understanding the synergies between the primal and dual aspects of the problem, providing intuitive insights into the nature of the optimization being performed.

4.3 Origin of Duality: KKT Conditions

Duality in optimization has its roots in the conditions for optimality known as the Karush-Kuhn-Tucker (KKT) conditions. These conditions are crucial for solving constrained optimization problems where the objective function and

the constraints are differentiable. The KKT conditions also extend to problems involving subdifferentiable cases, thus broadening their applicability.

For a differentiable case, the KKT conditions can be described by the existence of multipliers λ, u_i, and v_j such that:

$$\lambda \nabla f(x) + \sum_{i=1}^{m} u_i \nabla h_i(x) + \sum_{j=1}^{r} v_j \nabla l_j(x) = 0 \tag{11}$$

where $\nabla f(x)$ denotes the gradient of the objective function f at x, $h_i(x)$ are inequality constraints, and $l_j(x)$ are equality constraints. The multipliers u_i are associated with the inequality constraints and v_j with the equality constraints.

In the case of subdifferentiable functions, the gradients in the KKT conditions are replaced by subgradients, allowing for optimization where the objective function and/or the constraints are not differentiable.

Theorem 12.1: Strong Duality and Slater's Condition A remarkable result connecting these conditions to duality is the strong duality theorem, which states that for problems satisfying Slater's condition (a convex optimization problem with a feasible point strictly satisfying all non-affine inequality constraints), the primal and dual solutions coincide when the KKT conditions are met.

The KKT conditions consist of:

- **Stationarity:**

$$\lambda \nabla f(x) + \sum_{i=1}^{m} u_i \nabla h_i(x) + \sum_{j=1}^{r} v_j \nabla l_j(x) = 0 \tag{12}$$

- **Primal Feasibility:**

$$h_i(x) \leq 0, \quad i = 1, \ldots, m, \tag{13}$$
$$l_j(x) = 0, \quad j = 1, \ldots, r, \tag{14}$$

- **Dual Feasibility:**

$$u_i \geq 0, \quad i = 1, \ldots, m, \tag{15}$$

- **Complementary Slackness:**

$$u_i h_i(x) = 0, \quad i = 1, \ldots, m. \tag{16}$$

These conditions provide a robust framework for establishing the existence of an optimal solution and are integral to the understanding of duality in optimization problems.

The Karush-Kuhn-Tucker (KKT) conditions form the cornerstone for understanding the duality in optimization problems. These conditions, which include

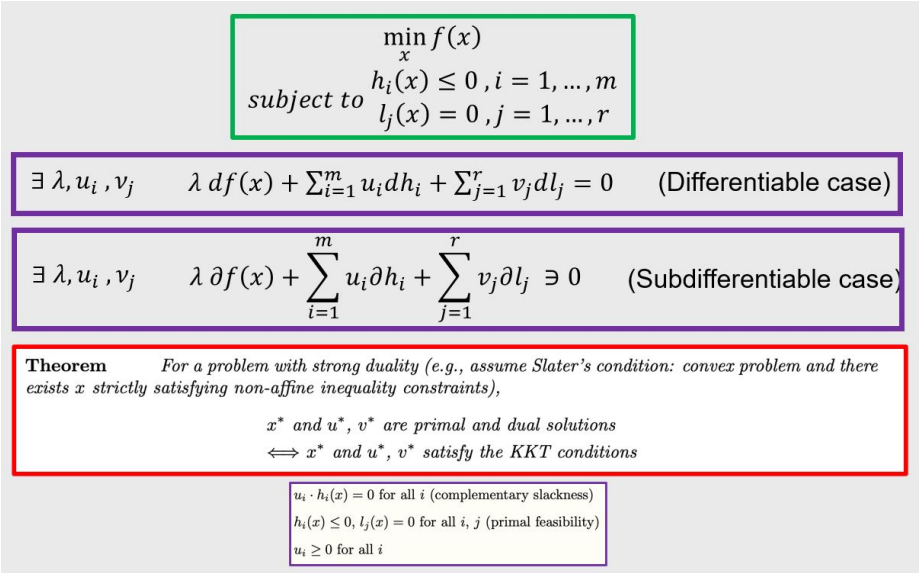

Figure 2: Illustration of the KKT conditions in the context of optimization duality.

stationarity, primal and dual feasibility, and complementary slackness, are visually illustrated below. The diagram helps in comprehending the geometric interpretation of these conditions in both the differentiable and subdifferentiable cases.

This graphical representation underscores the necessary conditions for optimality in a constrained optimization problem, and how they lead to the formulation of dual problems that reflect the same optimal solution under strong duality conditions.

4.4 The Sinkhorn Algorithm and Optimal Transport

The Sinkhorn Algorithm provides a computationally efficient method to solve the entropic regularization of the optimal transport problem. This approach leverages the structure of the problem to yield a solution that satisfies both the KKT conditions and the marginality constraints through an iterative process. The key elements and the iterative steps of the algorithm are illustrated in the figure below.

The Lagrangian for the entropic regularized optimal transport problem incorporates an entropy term, promoting a sparse solution. It is defined as follows:

$$L(\pi, \alpha, \beta) = \sum_{i,j} \pi_{i,j} C_{i,j} + \epsilon \pi_{i,j} (\log(\pi_{i,j}) - 1) + \alpha^T (\pi 1 - \mu) + \beta^T (\pi^T 1 - \nu) \quad (17)$$

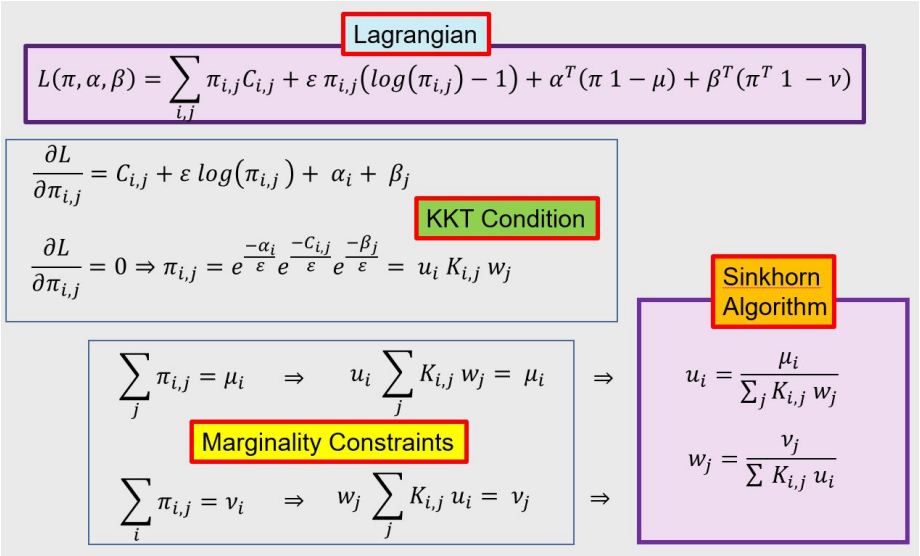

Figure 3: The Sinkhorn Algorithm steps and their relationship with the Lagrangian, KKT conditions, and marginality constraints.

Where ϵ is the regularization parameter, α and β are vectors of Lagrange multipliers associated with the marginal constraints. The KKT conditions guide us to the update rules that define the Sinkhorn Algorithm. These update rules iterate between adjusting row and column scalings to satisfy the marginal constraints, using the variables u_i and w_j. Mathematically, this process can be described by the update formulas:

$$u_i = \frac{\mu_i}{\sum_j K_{i,j} w_j}, \quad w_j = \frac{\nu_j}{\sum_i K_{i,j} u_i} \tag{18}$$

Here, $K_{i,j}$ is an element of the Kernel matrix derived from the cost matrix C and regularization parameter ϵ, and $\pi_{i,j}$ is the transport plan. Through successive iterations, the algorithm refines the transport plan to converge to the optimal solution, ensuring that the entropy-regularized transport problem is solved efficiently.

4.5 A Natural Generalization of the Sinkhorn Algorithm

The Sinkhorn algorithm, an iterative method for solving entropically regularized optimal transport problems, can be seen as an instantiation of a broader class of algorithms within the framework of information geometry. This framework provides tools for understanding the geometric structure of statistical manifolds, where points represent probability distributions and the geometry is defined by the Kullback-Leibler divergence, or the relative entropy.

In information geometry, two types of projections, known as e-projection and m-projection, serve as fundamental operations for minimizing the KL divergence between probability distributions. These operations are generalized by the Sinkhorn algorithm's alternating normalization steps.

Definition (e-Projection): The e-projection onto a set S is the operation that minimizes the KL divergence from a reference distribution $P^{(i)}$ to any member Q of S. Symbolically, it is given by:

$$Q_e = \text{proj}_e^S(P^{(i)}) = \arg\min_{Q \in S} D_{KL}[Q : P^{(i)}]. \tag{19}$$

This projection corresponds to the exponential family of distributions and is related to the mean parameters, or the expected values, of the statistical manifold.

Definition (m-Projection): Conversely, the m-projection onto a set S minimizes the KL divergence from any member of S to a reference distribution $Q^{(i)}$:

$$P_m = \text{proj}_m^S(Q^{(i)}) = \arg\min_{P \in S} D_{KL}[Q^{(i)} : P]. \tag{20}$$

This projection is associated with the mixture family and modifies the natural parameters of the distribution.

The Sinkhorn algorithm can be viewed as a sequence of e-projections and m-projections. Each iteration of the Sinkhorn algorithm performs a scaling of rows and columns of a matrix, effectively projecting onto sets of matrices that satisfy marginal constraints. This scaling process is akin to an e-projection followed by an m-projection, iteratively applied until convergence.

This iterative procedure can be naturally extended by the framework of information geometry, which allows for the design of more complex alternating projection algorithms. These algorithms generalize the Sinkhorn process by incorporating a wider variety of constraints and divergence measures, offering a richer set of tools for solving problems in optimal transport and beyond.

The duality between the e-projection and m-projection captures the essence of the Sinkhorn algorithm's operations and emphasizes their significance in the broader context of information geometric optimization techniques. As a result, the Sinkhorn algorithm can be understood as a practical application of these foundational concepts, harmonizing the computational aspects of optimization with the theoretical underpinnings of information geometry.

4.6 Alternating Projection Algorithms and Information Geometry

The figure below illustrates the alternating projection algorithms within the context of the Schrödinger Bridge (SB) problem, highlighting the geometric interplay between e-projections and m-projections in the solution space.

The Sinkhorn algorithm's generalization, as illustrated in Figure 4, builds upon the framework of alternating KL divergence projections in the space of

probability measures, as discussed by Brekelmans and Neklyodov in their work on Schrödinger Bridge Matching and Expectation Maximization [47].

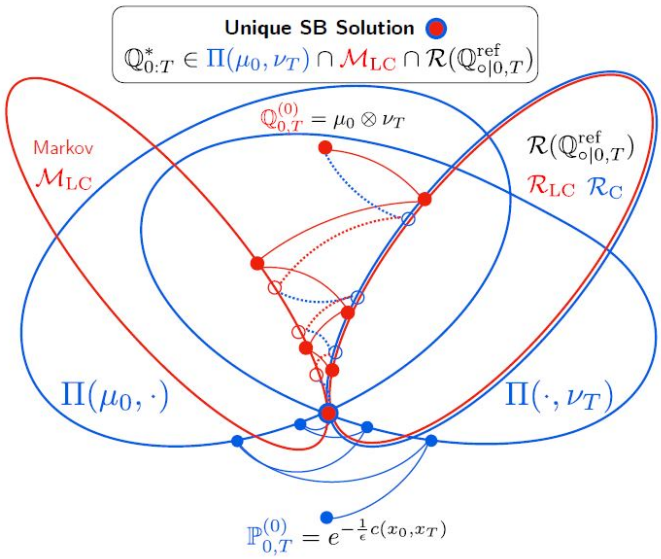

Figure 4: Alternating projection algorithms employing e-projections and m-projections. The unique SB solution is found at the intersection of the feasible sets under consideration (Borrowed from Brekelmans and Neklyodov).

The graphic represents various sets and projections in the space of probability measures. Here, $\Pi(\mu_0, \nu_T)$ denotes the set of all joint distributions with marginals μ_0 and ν_T. The sets $\mathcal{M}_{LC}$ and $\mathcal{R}_{LC}$ are related to the Markov property of transition probabilities. $\mathcal{R}(\mathcal{Q}^{ref}_{0|0,T})$ represents a class of distributions related to a reference process $\mathcal{Q}^{ref}_{0|0,T}$, which is both log-convex and convex.

Alternating projections are used to find a distribution in $\Pi(\mu_0, \nu_T)$ that is also in the intersection of $\mathcal{M}_{LC}$ and $\mathcal{R}(\mathcal{Q}^{ref}_{0|0,T})$. The algorithm iteratively projects between these sets until convergence is achieved. The unique SB solution $\mathcal{Q}^*_{0:T}$ is the distribution that lies in this intersection.

IPF (Iterative Proportional Fitting): This procedure employs both e-projections (denoted by blue solid lines) and m-projections (denoted by red solid lines) to adjust the distribution until it satisfies the constraints imposed by both marginals.

IMF (Iterative Minimization Fitting): Represented by dashed lines, this method iteratively applies m-projections to satisfy constraints, adjusting the distribution to fit the given marginals.

New Alternating Projection Algorithm: Our proposed method combines these projections in a novel way to achieve faster convergence or to address scenarios where traditional methods may not apply.

The initial point $\mathcal{P}_{0,T}^{(0)}$ reflects a starting distribution which adheres to the constraints of the problem and is iteratively updated through the algorithm. The approach effectively balances the entropic regularization with the geometric structure of the problem, resulting in an efficient and robust solution method for the SB problem.

5 Incorporating Additional Constraints in Optimal Transport

In the realm of optimal transport, it is often necessary to consider additional constraints beyond the classical marginal conditions. These constraints can encapsulate complex relationships between the transported measures or account for externalities not captured by standard formulations.

5.1 Extended Primal and Dual Problems

The primal problem traditionally seeks to minimize a cost function subject to marginal constraints. When additional constraints are introduced, the objective function $L(\pi, \phi, \psi, \theta)$ is modified to include terms that enforce these new requirements:

$$L(\pi, \phi, \psi, \theta) = \int\int C(x,y)\pi(x,y)dxdy + \text{additional terms reflecting constraints.} \tag{21}$$

These constraints can be structural, such as ensuring a certain type of dependency or interaction between the variables, or can incorporate additional knowledge about the system being modeled.

5.2 Lagrange Multipliers and KKT Conditions

The dual problem addresses the same optimization task from a different perspective. Lagrange multipliers are introduced for each constraint, converting the constrained optimization problem into an unconstrained one where the multipliers penalize the violation of constraints.

In this extended context, the Lagrange function $L(\pi, \phi, \psi, \theta, \delta)$ incorporates multipliers $\phi(x)$, $\psi(y)$, $\theta(x)$, and δ, corresponding to the various constraints of the primal problem. The KKT conditions then provide the necessary criteria for optimality in the presence of these additional constraints:

$$\frac{\partial L}{\partial \pi(x,y)} = C(x,y) - \phi(x) - \psi(y) - \theta(x)(y-x) - \delta g(x,y) + \epsilon \log(\pi(x,y)) + \epsilon = 0. \tag{22}$$

The interpretation of these conditions remains consistent with the unconstrained setting, where they ensure that the gradient of the Lagrange function with respect to the primal variables vanishes at the optimum.

5.3 Mathematical Formulation of the Extended Optimal Transport Problem

When incorporating additional constraints into the optimal transport problem, the mathematical formulation becomes more complex. These constraints ensure that the transport plan adheres to specific conditions that could represent real-world requirements or conservation laws. The extended primal problem can be expressed as:

$$\begin{aligned} \text{minimize} \quad & L(\pi, \phi, \psi, \theta) \\ \text{subject to} \quad & \int \pi(x,y)\,dx = \nu(y), \\ & \int \pi(x,y)\,dy = \mu(x), \\ & \int y\pi(x,y)\,dy - x\mu(x) = 0, \\ & \int t(x,y)\pi(x,y)\,dx\,dy = p. \end{aligned} \tag{23}$$

The Lagrangian for this problem, which incorporates the additional constraints through Lagrange multipliers, is given by:

$$\begin{aligned} L(\pi, \phi, \psi, \theta, \delta) = \int\int & \left(C(x,y)\pi(x,y) + \epsilon\pi(x,y)\log(\pi(x,y))\right)\,dx\,dy \\ & - \int \phi(x)\Big(\int \pi(x,y)\,dy - \mu(x)\Big)\,dx \\ & - \int \psi(y)\Big(\int \pi(x,y)\,dx - \nu(y)\Big)\,dy \\ & - \theta\left(\int y\pi(x,y)\,dy - x\mu(x)\right) \\ & - \delta\left(\int t(x,y)\pi(x,y)\,dx\,dy - p\right), \end{aligned} \tag{24}$$

where $\phi(x)$, $\psi(y)$, $\theta(x)$, and δ are the Lagrange multipliers for each of the respective constraints.

The dual problem then seeks to maximize the Lagrangian over the Lagrange multipliers:

$$\begin{aligned} \text{maximize} \quad & L(\pi, \phi, \psi, \theta, \delta) \\ \text{subject to} \quad & C(x,y) - \phi(x) - \psi(y) - \theta(x)(y-x) - \delta t(x,y) \geq 0. \end{aligned} \tag{25}$$

The KKT conditions for the optimality at the solution π^* of this problem can be expressed as:

$$C(x,y) - \phi(x) - \psi(y) - \theta(x)(y-x) - \delta t(x,y) + \epsilon\log(\pi^*(x,y)) + \epsilon = 0. \tag{26}$$

These conditions provide a set of equations that must be satisfied simultaneously to ensure that the solution π^* is optimal with respect to both the primal and dual formulations of the extended optimal transport problem.

The introduction of new constraints, and their associated Lagrange multipliers, into the primal and dual formulations fundamentally expands the feasible solution space. This expansion allows for more nuanced modeling of transport problems, such as those with considerations for dynamics, conservation laws, or other physical phenomena.

The analytical and computational implications of these constraints are significant. They necessitate refined algorithms capable of handling the increased complexity, and in the process, provide a richer understanding of the interplay between the cost function, constraints, and the resulting optimal transport plan.

The extended framework showcased in the figure (see Figure 15) provides a powerful lens through which to view and solve more sophisticated optimal transport problems that arise in practical applications, from economics to physics and beyond.

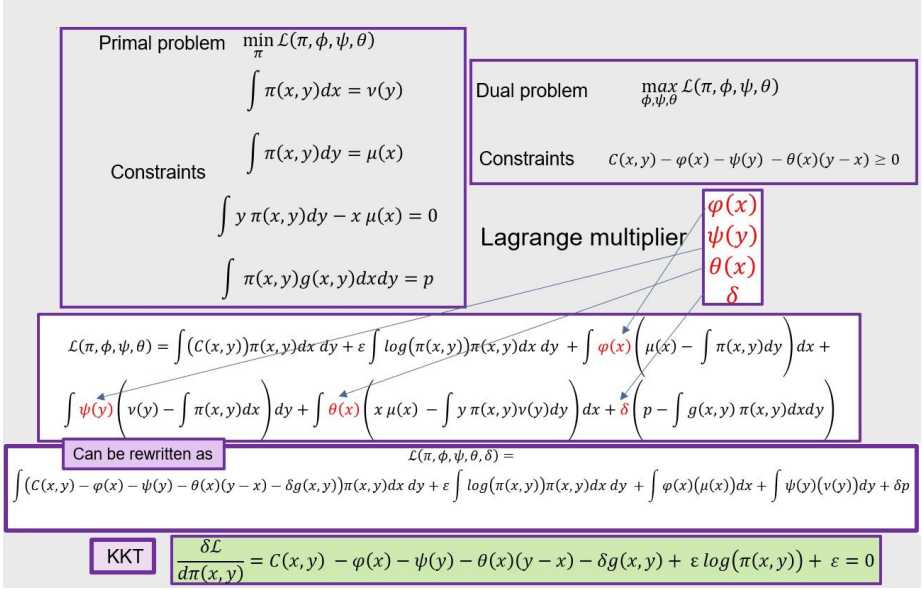

Figure 5: Extended formulations of the primal and dual problems incorporating additional constraints.

5.4 Formation of the Dual Lagrangian

The dual formulation of an optimization problem often provides a different perspective that can be more amenable to analysis or computation. To construct the dual Lagrangian for our extended optimal transport problem, we begin by

defining the total Lagrangian $L(\pi, \phi, \psi, \theta, \delta)$ which incorporates the additional constraints:

$$\begin{aligned} L(\pi, \phi, \psi, \theta, \delta) = \int\int (C(x,y) - \phi(x) - \psi(y) - \theta(x)(y-x) - \delta g(x,y))\, \pi(x,y)\, dx\, dy \\ + \epsilon \int\int \log(\pi(x,y))\pi(x,y)\, dx\, dy \\ + \int \phi(x)\mu(x)\, dx + \int \psi(y)\nu(y)\, dy + \delta p. \end{aligned} \tag{27}$$

The KKT conditions, which serve as a bridge between the primal and dual problems, are derived by setting the gradient of the Lagrangian with respect to π to zero:

$$\pi(x,y) = \exp\left(-\frac{1}{\epsilon}(\phi(x) + \psi(y) + \theta(x)(y-x) + \delta g(x,y) - C(x,y)) - 1\right). \tag{28}$$

By substituting this expression for $\pi(x,y)$ back into the total Lagrangian, we arrive at the dual Lagrangian $L(\phi, \psi, \theta, \delta)$:

$$\begin{aligned} L(\phi, \psi, \theta, \delta) = -\epsilon \int\int \exp\Bigg(-\frac{1}{\epsilon}\,(\phi(x) + \psi(y) \\ +\theta(x)(y-x) + \delta g(x,y) - C(x,y))\Bigg)\, dx\, dy \\ + \int \phi(x)\mu(x)\, dx \\ + \int \psi(y)\nu(y)\, dy \\ + \delta p. \end{aligned} \tag{29}$$

This dual Lagrangian reflects the dual problem's objective to maximize the Lagrangian over the functions ϕ, ψ, θ, and δ. The dual problem formulation provides insights into the properties of the optimal transport plan and offers computational advantages in certain scenarios, such as when dealing with large-scale or high-dimensional problems.

5.5 Formulation of the Extended Sinkhorn Algorithm

In the extended version of the Sinkhorn algorithm tailored for the modified optimal transport (MOT) problem, the traditional cost matrix is augmented by additional terms that account for new constraints. The standard marginal constraints are preserved while new features of the transport plan are encoded within the constraints. The resulting problem formulation involves two coupled integral equations that can be iteratively solved using projections that resemble the Sinkhorn algorithm steps.

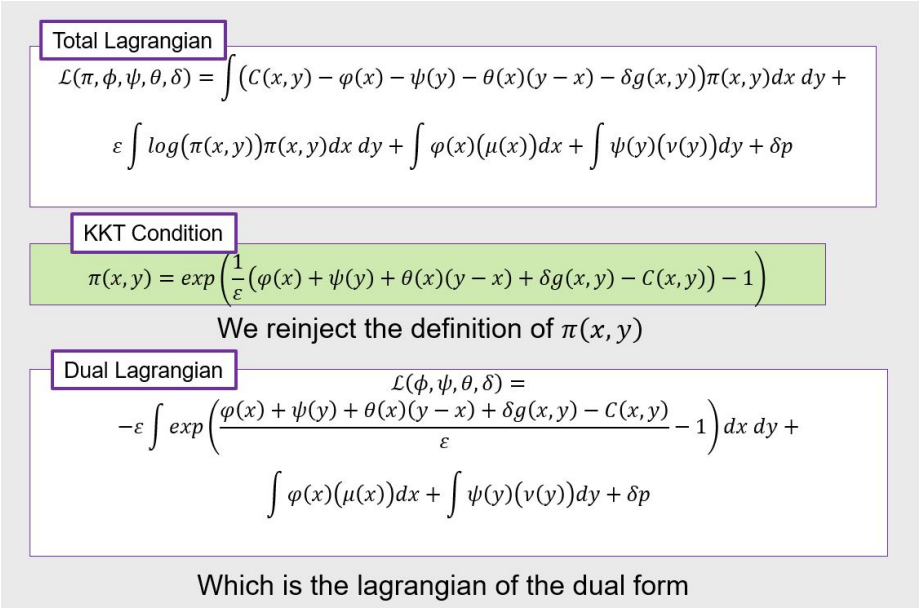

Figure 6: Extended formulations of the primal and dual problems incorporating additional constraints.

Given the KKT condition for the extended problem:

$$\pi(x,y) = \exp\left(\frac{-C(x,y) + \phi(x) + \psi(y) + \theta(x)(y-x) + \delta g(x,y)}{\epsilon} - 1\right), \quad (30)$$

we inject this expression into the marginal constraints, resulting in the following iterative update rules that define the extended Sinkhorn algorithm:

$$\exp\left(-\frac{\phi(x)}{\epsilon}\right) = \frac{\mu(x)}{\int \exp\left(\frac{-C(x,y)+\psi(y)-\theta(x)(y-x)-\delta g(x,y)}{\epsilon}\right) dy}, \quad (31)$$

$$\exp\left(-\frac{\psi(y)}{\epsilon}\right) = \frac{\nu(y)}{\int \exp\left(\frac{-C(x,y)+\phi(x)-\theta(x)(y-x)-\delta g(x,y)}{\epsilon}\right) dx}. \quad (32)$$

These update rules are derived by isolating the Lagrange multipliers $\phi(x)$ and $\psi(y)$ associated with the marginal constraints $\mu(x)$ and $\nu(y)$, respectively. The iterations proceed by alternatively updating $\phi(x)$ and $\psi(y)$ until convergence, at which point the resulting $\pi(x,y)$ satisfies both the marginal constraints and the additional constraints incorporated into the cost function.

The extended Sinkhorn frame thus provides a flexible and computationally efficient mechanism for solving MOT problems with additional structure or requirements not captured by the standard optimal transport formulation.

This adaptation of the Sinkhorn algorithm facilitates the incorporation of complex system dynamics and additional information, extending the applicability of MOT methods to a wider range of practical problems.

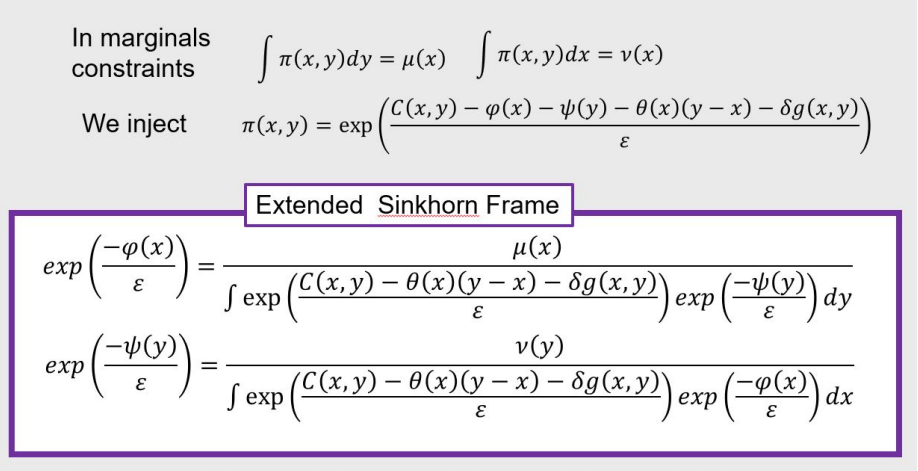

Figure 7: Extended formulations of the primal and dual problems incorporating additional constraints.

5.6 Handling of the Martingality Constraint

The martingality constraint is crucial in financial mathematics as it ensures that the expected value of the asset or portfolio remains constant in a risk-neutral world. In the context of the modified optimal transport problem, this constraint can be incorporated to guarantee that the transport plan respects the martingality property of the underlying stochastic processes.

We consider the additional constraint on the transport plan $\pi(x, y)$, which takes the form of an integral equation representing the expected value of the transported quantity:

$$\int y \exp\left(\frac{\phi(x) + \psi(y) + \theta(x)(y-x) + \delta g(x,y) - C(x,y)}{\epsilon} - 1\right) dy = x\mu(x). \tag{33}$$

The presence of the martingality constraint implies that the above equation must hold for all x, ensuring that the expected outcome under the transport plan corresponds to the current state x.

To handle this constraint within the extended Sinkhorn algorithm, we reformulate it through the following manipulations:

$$\int y \exp\left(\frac{\theta(x)(y-x)+\delta g(x,y)}{\epsilon}\right) \exp\left(\frac{\psi(y)-C(x,y)}{\epsilon}\right) dy = \frac{x\mu(x)}{\exp\left(\frac{\phi(x)}{\epsilon}-1\right)}. \tag{34}$$

This exact equation links the dual variables $\phi(x)$, $\psi(y)$, and $\theta(x)$ with the transport plan $\pi(x,y)$. The term $\delta g(x,y)$ encapsulates the additional constraint, while $\exp\left(\frac{\phi(x)}{\epsilon}-1\right)$ normalizes the constraint to adhere to the distribution $\mu(x)$.

The introduction of these terms in the Sinkhorn iteration leads to an updated algorithm that can efficiently compute a transport plan satisfying both the standard marginal constraints and the martingality condition. This forms an integral part of solving the extended optimal transport problem, particularly in financial applications where martingality is a fundamental concept.

$$\int y\, exp\left(\frac{\varphi(x)+\psi(y)+\theta(x)(y-x)+\delta g(x,y)-C(x,y)}{\varepsilon}-1\right)dy = x\,\mu(x)$$

But marginality in x implies : $\int exp\left(\frac{\varphi(x)+\psi(y)+\theta(x)(y-x)+\delta g(x,y)-C(x,y)}{\varepsilon}-1\right)dy = x\,\mu(x)$

So with a few manipulations we can rewrite:

Exact Equation

$$\int y\, exp\left(\frac{\theta(x)(y-x)+\delta g(x,y)}{\varepsilon}\right) exp\left(\frac{\psi(y)-C(x,y)}{\varepsilon}\right) dy = \frac{x\,\mu(x)}{exp\left(\frac{\varphi(x)}{\varepsilon}-1\right)}$$

Figure 8: Extended formulations of the primal and dual problems incorporating additional constraints.

5.7 Linearization of the Martingality Constraint

The martingality constraint is inherently nonlinear due to the product of variables involved. However, for computational efficiency, especially within iterative schemes such as the Sinkhorn algorithm, linear constraints are preferable. The linearization of the martingality constraint involves approximating the nonlinear constraint with a linear one that closely mimics its behavior within a certain regime or under certain assumptions.

Consider the martingality constraint in its original form:

$$\int y\pi(x,y)\, dy = x\mu(x) \quad \forall x \in \mathcal{X}. \tag{35}$$

This equation ensures that the expected value of the process at the next time step, weighted by the transport plan $\pi(x, y)$, is equal to the current value x, maintaining the martingale property. To linearize this constraint, we consider a first-order Taylor expansion of the function around a point x_0, resulting in an approximate linear relationship.

By defining a suitable perturbation term and using a first-order approximation, the martingality constraint can be recast into a linear form that is easier to handle within optimization algorithms. The linearized version of the martingality constraint then serves as a surrogate for the original nonlinear constraint in the optimization problem, simplifying the computational process while still preserving the essential characteristics of a martingale.

The linearized constraint is particularly useful when employing algorithms that can efficiently handle large-scale linear programming problems, making it a practical approach for extended optimal transport problems in high-dimensional spaces or with complex constraints.

Through such linearization, the extended Sinkhorn algorithm can incorporate the martingality constraint without significantly increasing the computational complexity, thereby maintaining its applicability and scalability to a wide range of problems in finance and economics where martingale measures are of central importance.

To facilitate the computational handling of the martingality constraint within the extended Sinkhorn algorithm, we employ an approximation technique. This approximation is grounded in the observation that the exponential function, which appears in the constraint, can be linearized around zero. Specifically, we use the first-order Taylor approximation:

$$\exp\left(\frac{\theta(x)(y-x)+\delta g(x,y)}{\epsilon}\right) \approx 1+\frac{\theta(x)(y-x)+\delta g(x,y)}{\epsilon}. \tag{36}$$

With this approximation, the integral equation involving the martingality constraint can be rewritten in a simplified form:

$$\int y\left(1+\frac{\theta(x)(y-x)+\delta g(x,y)}{\epsilon}\right)\exp\left(-\frac{\psi(y)-C(x,y)}{\epsilon}\right)dy = \frac{x\mu(x)}{\exp\left(-\frac{\phi(x)}{\epsilon}-1\right)}. \tag{37}$$

This simplification allows us to isolate $\theta(x)$ and express it in terms of known quantities and the transport plan $\pi(x, y)$, yielding an approximated solution for $\theta(x)$:

$$\begin{aligned}\theta(x) = \epsilon\Bigg(&\frac{x\mu(x)}{\exp\left(\frac{\phi(x)}{\epsilon}-1\right)} \\ &-\int y\pi(x,y)\exp\left(-\frac{\theta(x)(y-x)}{\epsilon}\right)dy\Bigg) \\ &\times\left(\int(y-x)\pi(x,y)\exp\left(-\frac{\theta(x)(y-x)}{\epsilon}\right)dy\right)^{-1}.\end{aligned} \tag{38}$$

This expression for $\theta(x)$ can be utilized within the iterative scheme of the extended Sinkhorn algorithm, enabling the integration of the martingality constraint in a manner that is computationally tractable. This approach highlights the power of approximation methods in tackling complex constraints within optimization problems.

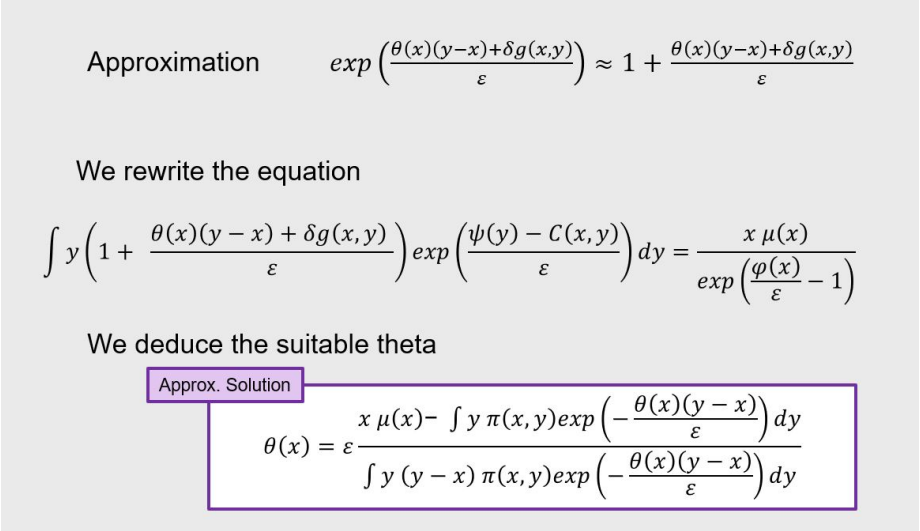

Figure 9: Extended formulations of the primal and dual problems incorporating additional constraints.

6 Merging BFGS steps in the Bregman projections

In certain financial models, it is essential to impose additional constraints that anchor the model to market observables. For instance, when modeling the joint distribution of asset prices at different times, the price of an Asian option can provide a constraint that fixes the copula between t_1 and t_2. This ensures that the model is consistent with observed market prices of derivatives.

The constraint can be formulated as follows:

$$p = \int \int g(y, x)\pi(x, y)\, dx\, dy, \tag{39}$$

where p is the market price of the Asian option, and $g(y, x)$ is the payoff function. Incorporating this constraint into the optimal transport problem involves adjusting the transport plan $\pi(x, y)$ so that the expected payoff under π aligns with p.

Given the complexity of the constraint, especially when $g(y, x)$ is a nonlinear function of x and y, numerical optimization methods are employed. The BFGS algorithm is particularly suitable for this task:

$$\begin{aligned} &\text{Minimize :} \quad f(\delta, \pi), \\ &\text{Subject to :} \\ &\int\int g(y,x) \exp\left(\frac{\phi(x) + \psi(y) + \theta(x)(y-x)}{\epsilon}\right. \\ &\quad \left. + \frac{\delta g(x,y) - C(x,y)}{\epsilon} - 1\right) dx\, dy = p, \end{aligned} \tag{40}$$

where $f(\delta, \pi)$ is the objective function to be minimized, possibly the negative log-likelihood or a regularized version thereof, and the BFGS method is used to update the parameters δ and the plan π to satisfy the price constraint.

The BFGS algorithm, one of the most efficient quasi-Newton methods, iteratively improves the estimate of the inverse Hessian matrix and searches for the optimal parameters by using gradient information. It is particularly well-suited for problems where the exact Hessian is costly to compute or not available.

Employing the BFGS method allows for the efficient calibration of the model to market prices, ensuring that the resulting model is both theoretically sound and practically relevant.

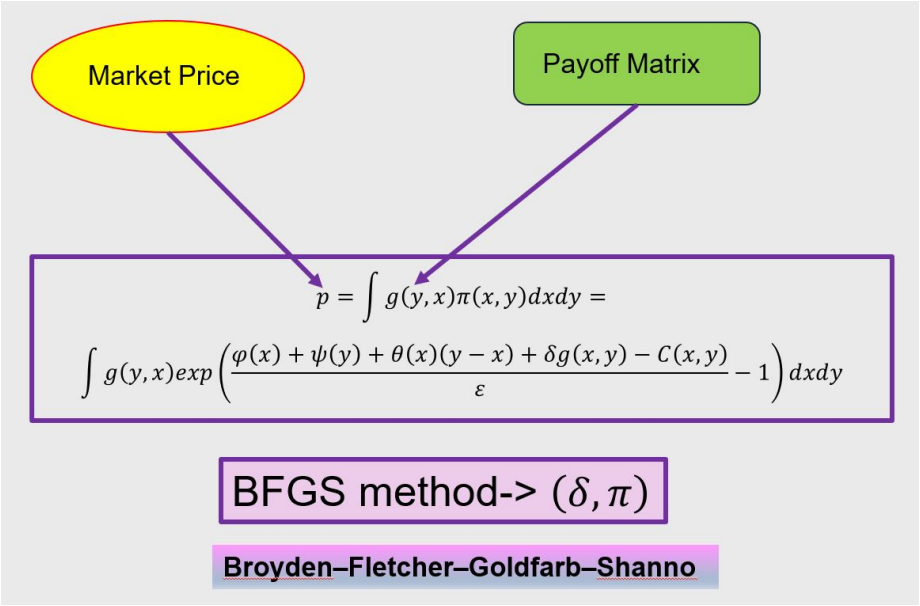

Figure 10: Extended formulations of the primal and dual problems incorporating additional constraints.

6.1 Conceptual Subtleties Above Sinkhorn Iterations

The Sinkhorn algorithm's efficiency and robustness in solving entropic-regularized optimal transport problems are significantly enhanced by underlying mathematical concepts, notably the e-projections and m-projections. These are specialized instances of Bregman projections, rooted in the broader framework of information geometry and the theory of Bregman divergences.

Bregman Divergence: Bregman divergence is a versatile measure of difference defined for a strictly convex, differentiable function Φ as:

$$D_\Phi(p, q) = \Phi(p) - \Phi(q) - \langle \nabla\Phi(q), p - q \rangle,$$

where p and q are points in the domain of Φ, and $\nabla\Phi(q)$ represents the gradient of Φ at q. Distinctive for its asymmetry and the lack of the triangle inequality, Bregman divergence generalizes the concept of Euclidean distance to more complex spaces.

e-projections and m-projections: Within the context of Sinkhorn iterations:

- **e-projections (exponential projections)** minimize the Bregman divergence subject to expectation constraints, aligning closely with the exponential family of distributions. They are pivotal in information-theoretic applications and play a crucial role in the entropic regularization of optimal transport, facilitating efficient distribution adjustments.
- **m-projections (mixture projections)** focus on minimizing the divergence within mixture spaces, crucial for maintaining the weights of distribution components intact. These projections are integral to understanding the geometry of probability spaces and optimizing within them.

Connection to Bregman Projections and Sinkhorn Iterations: Labeling e-projections and m-projections as Bregman projections underscores their mathematical genesis in minimizing Bregman divergences. This characterization is particularly relevant in the entropic regularization context of optimal transport problems solved by the Sinkhorn algorithm. The iterative nature of Sinkhorn adjustments, employing these projections, ensures that distributions converge to a solution that respects both the cost function minimization and the constraints imposed by the problem—marginal conditions in the case of MOT problems.

In essence, the conceptual foundation provided by e-projections and m-projections as Bregman projections not only enriches the mathematical understanding of Sinkhorn iterations but also highlights the algorithm's adaptability and power in tackling complex transport problems.

6.2 The BFGS Method

The Broyden–Fletcher–Goldfarb–Shanno (BFGS) method is an iterative technique for solving nonlinear optimization problems. It is particularly effective for unconstrained optimization problems formulated as:

$$\min_{x \in \mathbb{R}^n} f(x), \tag{41}$$

where $f : \mathbb{R}^n \to \mathbb{R}$ is a differentiable scalar function. The BFGS method belongs to the family of quasi-Newton methods, which seek to find the stationary points of f where its gradient $\nabla f(x)$ is zero, without requiring the computation of the Hessian matrix $H(x)$.

At each iteration k, the BFGS method updates an approximation B_k to the inverse Hessian matrix of f at x_k. The update formula for B_{k+1} is given by:

$$B_{k+1} = B_k + \frac{y_k y_k^T}{y_k^T s_k} - \frac{B_k s_k s_k^T B_k}{s_k^T B_k s_k}, \tag{42}$$

where $s_k = x_{k+1} - x_k$ is the step taken in parameter space, and $y_k = \nabla f(x_{k+1}) - \nabla f(x_k)$ is the change in the gradient.

The search direction at each iteration is then given by:

$$p_k = -B_k \nabla f(x_k), \tag{43}$$

and the next point x_{k+1} is computed by:

$$x_{k+1} = x_k + \alpha_k p_k, \tag{44}$$

where α_k is the step size determined by a line search that satisfies the Wolfe conditions.

The BFGS method iteratively repeats this process, updating the approximation to the inverse Hessian and taking steps in the direction that locally minimizes the function until convergence criteria are met.

The method is known for its superlinear convergence properties under appropriate conditions and is one of the most widely used quasi-Newton methods due to its efficiency and robustness for a broad class of optimization problems.

6.3 Enhancing MOT with BFGS and Sinkhorn through Bregman Projections

To address the computational challenges of Martingale Optimal Transport (MOT) problems efficiently, we introduce a refined approach that combines the Broyden–Fletcher–Goldfarb–Shanno (BFGS) methodology with the Sinkhorn algorithm, utilizing Bregman projections in the form of e-projections and m-projections for the iterative process. This innovative amalgamation capitalizes on the unique strengths of both algorithms to foster rapid convergence and adherence to the martingality constraint, with a special emphasis on the initialization phase to set a robust foundation for optimization.

Algorithmic Framework: Our strategy unfolds across several key steps:

1. **Warm-Up Pre-Iterations with pure Bregman projections:** Prior to addressing the full complexity of the MOT problem, the algorithm undergoes several hundred pre-iterations. This initial phase, devoid of the additional constraints, serves to "warm up" the algorithm, creating a stable starting point for subsequent optimization. These pre-iterations utilize the Sinkhorn algorithm to align the transport plan closer to satisfying the marginal conditions.

2. **Mixed Bregman Projections:** Following the warm-up phase, Sinkhorn iterations are employed to refine the transport plan. Here, we introduce Bregman projections, specifically e-projections and m-projections, to iteratively adjust the transport plan. This adjustment aims at satisfying both the marginal conditions and the martingality constraint, the latter being continually updated and linearized to reflect the evolving solution landscape.

3. **BFGS Iterations for The additional prices Constraint:** Concurrently, the BFGS method is applied to optimize the linear approximation of the martingality constraint. This optimization is critical for navigating the solution space defined by the martingality condition efficiently.

4. **Linearization of the Martingality Constraints:** The martingality constraint is linearized to ensure that the BFGS iterations are based on an accurate and current approximation. Despite being slow to converge This iterative linearization does converge if the meteparameters are correctly tuned , coupled with the e-projection and m-projection mechanisms, guides the algorithm towards convergence, ensuring the solution adheres to the MOT framework.

Efficiency and Convergence: By integrating the BFGS method with Sinkhorn iterations enhanced by e-projections and m-projections, our algorithm not only achieves computational efficiency but also ensures robust convergence. The initial warm-up phase establishes a solid groundwork for optimization, while the strategic use of Bregman projections allows for a nuanced adjustment of the transport plan, accommodating complex constraints inherent in MOT problems.

This advanced approach, leveraging the synergy between BFGS optimization and Sinkhorn algorithm's flexibility, marks a significant advancement in solving MOT problems. It underscores the potential of combining robust optimization techniques with principled iterative methods to tackle the intricacies of martingale constraints and multiple marginals in transport problems.

6.4 Bregman Projections via Kullback-Leibler Divergence

Bregman projections, including those used in the Sinkhorn algorithm for Optimal Transport (OT), are based on Bregman divergences—a class of functions

measuring the distance between points in a convex space. The Kullback-Leibler (KL) divergence is a specific instance of Bregman divergence that is commonly used in information theory and statistics.

Bregman Divergence A Bregman divergence is defined for a strictly convex, differentiable function ϕ and points p and q in its domain. The Bregman divergence D_ϕ is given by:

$$D_\phi(p, q) = \phi(p) - \phi(q) - \langle \nabla\phi(q), p - q \rangle, \tag{45}$$

where $\nabla\phi(q)$ is the gradient of ϕ at q, and $\langle \cdot, \cdot \rangle$ denotes the inner product. This divergence measures the 'error' introduced by approximating the value of ϕ at p with its first-order Taylor expansion around q.

Kullback-Leibler Divergence as a Bregman Divergence When the convex function ϕ is chosen to be the negative entropy function, the Bregman divergence becomes the KL divergence. For two probability distributions P and Q, the KL divergence is:

$$D_{KL}(P \parallel Q) = \int P(x) \log \left(\frac{P(x)}{Q(x)} \right) dx, \tag{46}$$

which can be derived from the more general Bregman divergence by setting ϕ to be the Shannon entropy $H(P) = -\sum P(x) \log P(x)$.

Projection and Optimization In the context of the Sinkhorn algorithm, a Bregman projection with respect to the KL divergence is used to iteratively update a transport plan to satisfy marginal constraints. The projection onto a constraint set is formulated as an optimization problem minimizing the KL divergence:

$$Q^* = \arg\min_{Q \in \mathcal{C}} D_{KL}(P \parallel Q), \tag{47}$$

where $\mathcal{C}$ is the set of distributions meeting the constraints, and P is the current estimate of the transport plan.

Advantages in Optimal Transport The use of KL divergence for Bregman projections in OT algorithms such as Sinkhorn's has several advantages:

- **Computational Efficiency:** It leads to algorithms that can be efficiently computed using matrix-scaling techniques.
- **Stability:** The entropic regularization inherent in the KL divergence promotes solutions that are stable and less sensitive to small changes in the input distributions.
- **Flexibility:** It allows for the seamless incorporation of additional linear constraints into the iterative procedure.

The connection between Bregman projections and the KL divergence offers a rich theoretical framework for developing efficient and robust algorithms for solving complex OT problems. This intersection of convex analysis, information theory, and computational optimization is pivotal to the ongoing development of the field.

6.5 Mathematical Representation of Projections as KL Divergence Minimization

Projections in the extended Sinkhorn algorithm framework can be intrinsically characterized as the minimization of Kullback-Leibler (KL) divergence, facilitating the alignment of a transport plan with the prescribed constraints of an Optimal Transport (OT) problem. Here we elucidate the mathematical underpinnings of this representation.

Kullback-Leibler Divergence The KL divergence from a distribution Q to a distribution P, denoted $D_{KL}(P \parallel Q)$, measures the information loss when Q is used to approximate P. Formally, it is defined as:

$$D_{KL}(P \parallel Q) = \int P(x) \log\left(\frac{P(x)}{Q(x)}\right) dx, \tag{48}$$

where $P(x)$ and $Q(x)$ denote the probability densities of P and Q, respectively.

E-Projection and M-Projection The e-projection and m-projection can be expressed as the solutions to optimization problems involving the minimization of KL divergence. Specifically, for a set S and a reference distribution $\mathbb{P}$, the e-projection is defined as the measure $Q^e \in S$ that minimizes the divergence to $\mathbb{P}$:

$$Q^e = \arg\min_{Q \in S} D_{KL}(\mathbb{P} \parallel Q). \tag{49}$$

Similarly, the m-projection is the measure $P^m \in S$ that minimizes the divergence from $\mathbb{P}$:

$$P^m = \arg\min_{P \in S} D_{KL}(P \parallel \mathbb{P}). \tag{50}$$

Projection as Information Minimization The e-projection minimizes the expected information loss of representing $\mathbb{P}$ with a distribution in S, whereas the m-projection minimizes the information loss of approximating distributions in S with $\mathbb{P}$. This aligns with the principle of entropy regularization in OT, where the goal is to find a transport plan with minimal "surprise" relative to the reference measure.

6.5.1 Iterative Proportional Fitting in Sinkhorn Algorithm

The Sinkhorn algorithm makes use of Iterative Proportional Fitting (IPF), which is a sequence of projection steps designed to satisfy the marginal constraints in an optimal transport problem. This method iterates between two projection steps to converge towards the solution:

First Projection Step The first half-bridge update brings the current transport plan closer to satisfying the marginal constraints associated with ν_T. Mathematically, this is expressed as:

$$P_{0,T}^{(n+1)} \leftarrow \arg\min_{Q_{0,T} \in \Pi(\cdot, \nu_T)} D_{KL}(Q_{0,T} \parallel P_{0,T}^{(n)}), \tag{51}$$

where $P_{0,T}^{(n+1)}$ represents the updated transport plan, $Q_{0,T}$ denotes a candidate transport plan within the set of all plans Π that agree with the target marginal ν_T, and D_{KL} is the Kullback-Leibler divergence, which measures the informational discrepancy between the two distributions.

Second Projection Step The second half-bridge update then adjusts the transport plan to satisfy the marginal constraints associated with μ_0:

$$P_{0,T}^{(n+2)} \leftarrow \arg\min_{Q_{0,T} \in \Pi(\mu_0, \cdot)} D_{KL}(Q_{0,T} \parallel P_{0,T}^{(n+1)}), \tag{52}$$

where $P_{0,T}^{(n+2)}$ is the subsequent update to the transport plan. This step involves minimizing the KL divergence from the newly updated plan $P_{0,T}^{(n+1)}$ to a new candidate $Q_{0,T}$ that satisfies the marginal μ_0.

Intuition and Commentary Each iteration of the IPF effectively tightens the transport plan's adherence to the marginal distributions through an entropic lens, gradually reducing the 'informational cost' of transporting mass from the source to the target distribution. These half-bridge updates alternate, continually refining the transport plan's alignment with the marginals. After every two updates (completing one full cycle), the index n is incremented by 2, signifying a new iteration within the sequence of Sinkhorn updates.

These two steps are repeated until the transport plan's successive projections converge, indicating that the transport plan has reached an equilibrium where it satisfies both marginal constraints as closely as possible, given the entropic regularization.

6.6 Application of E-Projection in the Extended Sinkhorn Algorithm

Integrating e-projection into the extended Sinkhorn algorithm involves minimizing the Kullback-Leibler (KL) divergence, which measures the difference

between two probability distributions. The KL divergence from a distribution Q to a distribution P, denoted as $D_{KL}(P \parallel Q)$, is defined as:

$$D_{KL}(P \parallel Q) = \int P(x) \log \left(\frac{P(x)}{Q(x)} \right) dx, \tag{53}$$

where $P(x)$ and $Q(x)$ represent the probability densities of distributions P and Q, respectively. In the context of e-projection, P corresponds to the adjusted transport plan aiming to satisfy the martingality constraint, and Q represents the current iteration of the transport plan.

Integration into Sinkhorn Iterations To incorporate the martingality constraint into the Sinkhorn algorithm through e-projection, we iteratively minimize the KL divergence between the transport plan and a target distribution that meets the desired constraints. The process can be detailed as follows:

1. **Marginal Adjustment and Martingality Constraint**: Given the initial transport plan Q, we seek a new plan P that better satisfies the marginals and martingality constraint by minimizing the KL divergence. This leads to an updated plan where:

$$P^*(y|x) = \arg\min_P D_{KL}(P \parallel Q), \tag{54}$$

   subject to $E_P[Y|X = x] = T(x)$, where $T(x)$ represents the target martingale condition for the transport plan.

2. **E-Projection Update**: The e-projection modifies the transport plan by solving for:

$$P^*(y|x) = Q(y|x) \exp\left(\theta(x)(y - x) - \lambda(x)\right), \tag{55}$$

   where $\theta(x)$ adjusts for the martingality and $\lambda(x)$ ensures normalization. This step is iterated until convergence, effectively embedding the martingality constraint into the transport plan through the KL divergence minimization framework.

Enhanced Convergence through KL Divergence Minimization By utilizing the KL divergence as a mechanism for enforcing the martingality constraint, the extended Sinkhorn algorithm benefits from a more principled approach to integrating additional constraints. This not only refines the accuracy of the transport plan but also enhances the convergence properties of the algorithm, demonstrating the utility of e-projection in complex MOT problems.

Through this rigorous application of the KL divergence within the e-projection framework, our extended Sinkhorn algorithm achieves a robust balance between adherence to the probabilistic constraints of MOT problems and computational efficiency.

7 Example of Pricing Code

The following Python function illustrates the implementation of the MOT pricing with market price constraints using the BFGS algorithm for numerical optimization.

```
  def MOT_price_log_primal_with_PriceConstraint(cost_mat0, mu, nu,x,y,sink_eps,
     ↪ cost_matrix2, marketPrice_Option, theta=0.9,
  max_pre_iter=100, nb_iter_constraints= 20,max_iter=10**4,
     ↪ period_test_constraints = 10,err_th=10**-9,theta_prix=0.5):
  minval = np.min(cost_mat0)
  cost_mat =cost_mat0 - minval
  cost_mat = cost_mat / sink_eps
  log_mu, log_nu = np.log(mu), np.log(nu)
  log_x ,log_y = np.log(x),np.log(y)
  log_sink_eps = log(sink_eps)
  log_theta = log(theta)
  log_err_th=log(err_th)
  log_opti_pi2 = -cost_mat + [log_nu] +np.transpose([log_mu])
  log_Ap = logsumexp(log_opti_pi2)
  log_opti_pi = log_opti_pi2 - log_Ap
  delta_deltan = np.zeros(mu.size)
  cost_matrix2_v =cost_matrix2.ravel()
  mem_optim=[]
  # pre convergence of marginals
  for i in range(max_pre_iter):
    log_opti_pi += log_mu - logsumexp(log_opti_pi, axis=1, keepdims=1)
    log_opti_pi += log_nu - logsumexp(log_opti_pi, axis=0, keepdims=1)
  #joint convergence of marginaes and martingality
  for i in range(max_iter):
    log_opti_pi += log_mu - logsumexp(log_opti_pi, axis=1, keepdims=1)
    log_opti_pi += log_nu - logsumexp(log_opti_pi, axis=0, keepdims=1)
    if (i % period_test_constraints == 0):
      log_opti_pi , optim = Adjust_MOT_Price_Constraint_new2(log_opti_pi,log_y,y,
     ↪ log_x,x,log_mu,mu,theta,cost_matrix2_v,marketPrice_Option)
      mem_optim.append(optim)
    if np.sum(np.abs(logsumexp(log_opti_pi, axis=0, keepdims=1)-log_nu)) + np.sum
     ↪ (np.abs(logsumexp(log_opti_pi, axis=1, keepdims=1)-log_mu)) <
     ↪ log_err_th:
      break
  log_opti_pi,optim= Adjust_MOT_Price_Constraint(log_opti_pi,log_y,y,log_x,x,
     ↪ log_mu,mu,theta,
  cost_matrix2_v,marketPrice_Option,nb_iter_constraints=nb_iter_constraints)
  mem_optim.append(optim)
  opti_pi = np.exp(log_opti_pi)
  u = mu / np.sum(opti_pi, axis=1, keepdims=1)
  v = nu / np.sum(opti_pi, axis=0, keepdims=1)
  return opti_pi,u,v,mem_optim
```

Listing 1: Python code for MOT pricing with market price constraints.

```
def Adjust_MOT_Price_Constraint(log_opti_pi,log_y,y,log_x,x,log_mu,mu,theta,
    ↪ cost_matrix2_v,price2, nb_iter_constraints = 20):
  def f(log_opti_v):
  return  Control_Log_Martingality(log_opti_v,y,x,mu,matrix_shape)+Control_Prix(
    ↪ np.exp(log_opti_v), cost_matrix2_v,price2)
  # Initial guess : input of optimal matrix
```

```
  matrix_shape = log_opti_pi.shape
  x0 =log_opti_pi.ravel()
  result = minimize(f, x0,options={'maxiter':nb_iter_constraints,'disp':False,'
     ↪ method':'BFGS'})
  log_opti_pi_aux = result.x
  optim = f(log_opti_pi_aux)
  log_opti_pi_aux2 = log_opti_pi_aux.reshape(matrix_shape)
  log_opti_pi2 = (1-theta)* log_opti_pi + theta* log_opti_pi_aux2
  return log_opti_pi2,optim # output : optimal matrix

def Control_Log_Martingality(log_opti_pi,y,x,mu,matrix_shape):
  # nullification of : np.sum(opti_pi * y, axis=1)   - x* mu
  martingality = np.sum(np.exp(log_opti_pi.reshape(matrix_shape)) * y, axis=1)
     ↪ - x* mu
  return np.linalg.norm(martingality)

def Control_Prix(opti, cost_matrix, price):
  p=np.sum(opti * cost_matrix) -price
  return p*p

def Control_Prix_sqr(opti, cost_matrix, price):
  p=np.sum(opti * cost_matrix) -price
  return sqrt(p*p)
```

Listing 2: Python code for auxillary function.

The code optimizes a transport matrix with respect to a given cost matrix, source and target distributions μ and ν, and additional market constraints. The BFGS method is encapsulated in the `Adjust_Price_Constraint` function, which is called within the iterative scheme to ensure that the market price constraints are met.

7.1 Market Model Description

The market on which the algorithm has been tested is characterized by a stochastic model with parameters calibrated to the current cash and option market for the SX5E index. The dynamics of the model are governed by the following set of stochastic differential equations (SDEs):

$$dS_t = (\alpha_t dW_t^1 + \mu dt)S_t, \tag{56}$$

$$d\alpha_t = \phi(\alpha_0 - \alpha_t)dt + \nu_\alpha \gamma dW_t^2, \tag{57}$$

$$d\langle W^1, W^2\rangle_t = \tanh(\lambda_t), \tag{58}$$

$$d\lambda_t = \eta(\lambda_0 - \lambda_t)dt + \chi_\lambda dW_t^3, \tag{59}$$

$$d\langle W^2, W^3\rangle_t = 0, \tag{60}$$

$$d\langle W^1, W^3\rangle_t = \rho_p, \tag{61}$$

where S_t represents the asset price, α_t the stochastic volatility process, and λ_t an additional state variable driving the correlation dynamics. The processes W_t^1, W_t^2, and W_t^3 are standard Brownian motions with correlations specified

by the terms $d\langle W^i, W^j\rangle_t$. The parameters $\mu, \alpha_0, \phi, \nu_\alpha, \gamma, \lambda_0, \eta, \chi_\lambda$, and ρ_p are constants resulting from the calibration process.

This model captures the essential features of market dynamics, including the stochastic volatility and correlation between different factors, making it well-suited for the pricing of options and other derivative securities indexed on the SX5E.

7.2 Calibrated Model Parameters

The calibrated parameters for the stochastic model based on the SX5E index market data are as follows:

$$\begin{aligned}
\alpha_0 &= 0.15, \\
\mu &= 0.2, \\
\phi &= 5, \\
\nu &= 2, \\
\gamma &= 1, \\
\lambda_0 &= -0.7, \\
\eta &= 5, \\
\chi &= 0.3, \\
\rho_p &= 0.
\end{aligned}$$

These parameter values are the result of a fitting procedure that aligns the model with observed market prices for options and other derivatives tied to the SX5E index. It has been used for their determination adavanced risk neutral calibration procedures and historical estimation which beyond the scope of this article. They serve as inputs to the stochastic differential equations that describe the market dynamics in the model.

In order to make seense of them, the following praphics are provided:

because we are going to examine two particular smiles, it makes sense to look at the implied density associated with the vanilla option smiles for the 15 weeks and 25 weeks

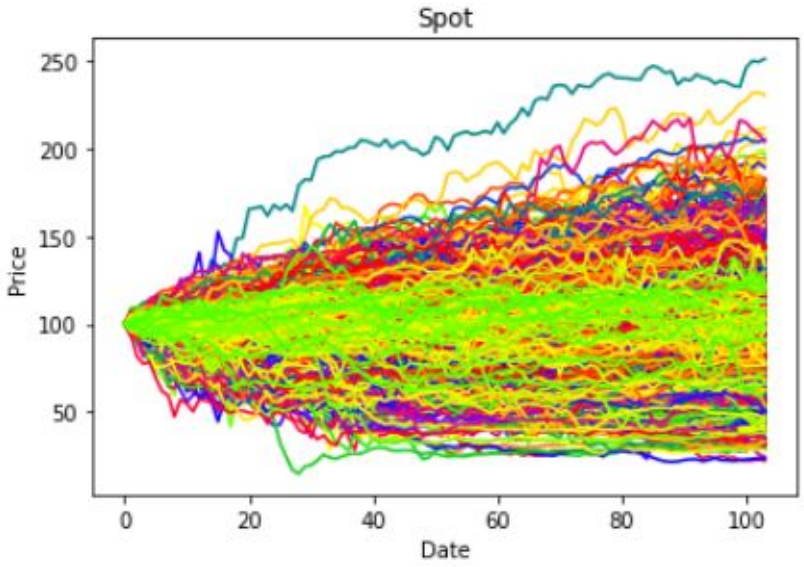

Figure 11: spot scenarii for the next 104 weeks.

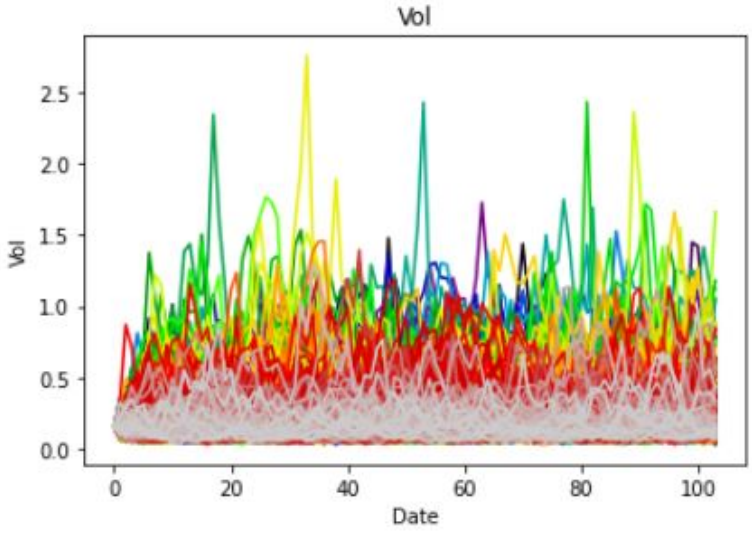

Figure 12: instantaneous volatility scenarii for the next 104 weeks.

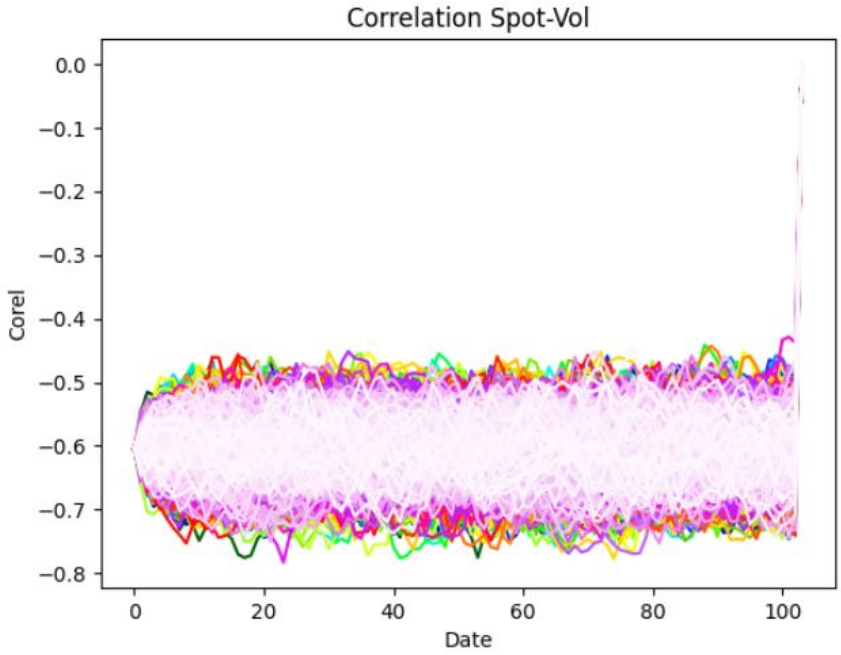

Figure 13: instantaneous correlation vol-spot scenarii for the next 104 weeks.

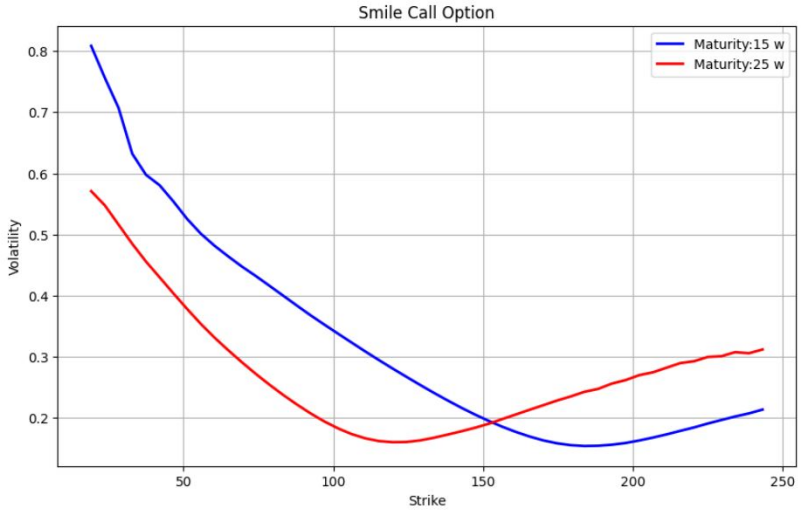

Figure 14: volatility smiles for the 15 weeks and the 25 weeks.

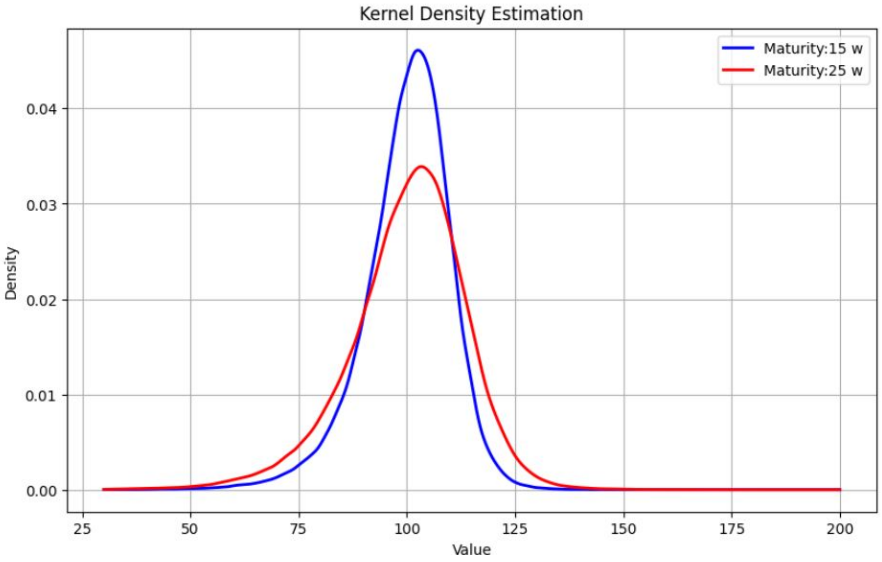

Figure 15: implied forward stock density for the 15 weeks and the 25 weeks.

7.3 Numerical Exemple

In this section, we illustrate the application of the Martingale Optimal Transport (MOT) framework with price constraints using a real-world example. We consider an Equinox product based on the SX5E index with specific maturities $T_1 = 15$ weeks and $T_2 = 25$ weeks.

We present the implied volatility smiles derived from the MOT model, comparing the upper and lower price bounds, the average of these bounds, and the true price obtained from a Monte Carlo simulation tailored to the market conditions. The price constraints are incorporated using the price of an option on the average of S_1 and S_2 with a strike of 105.

The following figure displays the implied volatility smiles for each of these pricing measures:

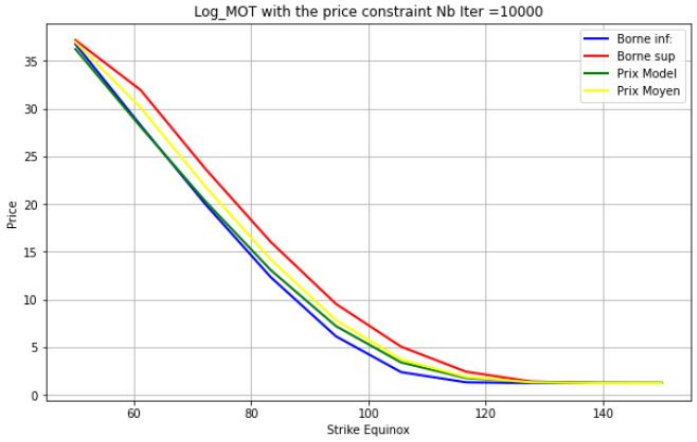

Figure 16: Implied volatility smiles for the Equinox product. The plot shows the upper bound (borne sup), lower bound (borne inf), model price (prix model), and average price (prix moyen) alongside the market price (prix moyen) computed via Monte Carlo simulation.

The results demonstrate the effectiveness of the MOT approach in capturing the essential features of the market price dynamics and providing robust price bounds for complex structured products.

8 Future Research

8.1 Analysis of "On Schrödinger Bridge Matching and Expectation Maximization"

The work "On Schrödinger Bridge Matching and Expectation Maximization" by Rob Brekelmans and Kirill Neklyodov [47] marks a significant advancement in the field of computational optimal transport and generative modeling. The

paper delves into the Schrödinger Bridge (SB) problem, which is integral to entropy-regularized optimal transport, with applications that cut across generative modeling, Bayesian inference, and dynamical systems.

The Schrödinger Bridge Problem

The SB problem is at the core of finding the most plausible evolutionary path of distribution of data points from an initial to a target distribution, subject to certain constraints. Its formulation bears a close relation to entropy-regularized optimal transport, positioning it as a pivotal concept within stochastic processes.

Key Contributions

Brekelmans and Neklyodov's paper offers several key contributions to the field:

- **Unified View:** The paper provides a unified framework for analyzing existing methods for solving the SB problem. By viewing Iterative Proportional Fitting and Iterative Markovian Fitting through the lens of alternating KL-divergence minimization, they uncover a theoretical kinship between seemingly disparate methods.
- **Joint Optimization:** Drawing on principles from information geometry, the authors suggest an approach that optimizes a singular KL-divergence objective. This innovation paves the way for partial, stochastic gradient updates, drawing a parallel to the mechanism of the variational Expectation-Maximization (EM) algorithm.
- **Connections and Contextualization:** The paper adeptly contextualizes the SB matching problem within a broader scope, drawing parallels to flow-matching and few-step generative modeling. It provides fresh insights into the parameterization of coupling distributions, enhancing our understanding of the underlying mechanisms of these models.

In summary, Brekelmans and Neklyodov's research provides a comprehensive and insightful analysis of the SB problem, proposing novel solutions that contribute to the ongoing development of the field. Their approach to joint optimization and the establishment of new connections within different domains of generative modeling highlights the interdisciplinary nature of the problem and sets the stage for future research and applications.

8.2 Multimarginal Optimal Transport : MMOT

Current research in Martingale Optimal Transport (MOT) has predominantly focused on scenarios with a single maturity or a limited number of maturities, often due to computational constraints and the complexity of the problem. However, there is a clear path for future research to explore MOT with multiple maturities. Here are the theoretical formulations for different maturity structures:

For one maturity, the problem does not present interesting use cases:

$$\min_{\pi \mid \pi(x)=\mu(x)} C(x)p(x) = \mathbb{E}_x[C]$$

With three maturities, it becomes feasible, especially under the assumption of Markovianity:

$$\min_{\pi \mid \pi \in U} C(x,y,z)\pi(x,y,z) = U = \begin{cases} \int\int \pi(x,y,z)dxdy = \mu(z), \\ \int \pi(x,y,z)dxdz = \nu(y), \\ \int \pi(x,y,z)dydz = \xi(x) \end{cases}$$

For N maturities, we require additional structure, such as Markovianity and sparsity:

$$\min_{\pi \mid \pi \in U} C(x_1,\dots,x_N)\pi(x_1,\dots,x_N) = U = \begin{cases} \int \dots \int \pi(x_1,\dots,x_N)\, dx_1 \dots dx_{N-1} = \mu_N(x_N), \\ \vdots \\ \int \pi(x_1,\dots,x_N)\, dx_2 \dots dx_N = \mu_1(x_1) \end{cases}$$

The expansion to models with multiple maturities opens new challenges and opportunities, such as considering the sparsity of the transport plan, which can significantly reduce the complexity of the problem. Future work may also delve into the development of efficient computational methods that leverage the inherent structure of MOT problems with many maturities, as well as rigorous theoretical analysis of their properties.

Multi Marginals Martingale Optimal Transport: Theoretical Considerations

The problem of multi-marginal martingale optimal transport (MMOT) presents a formidable challenge, particularly due to the large number of maturity smiles required for pricing standard autocallable products in the financial industry. Autocalls with schedules ranging from 100 to 1000 dates are commonplace, and each requires a precise and computationally efficient approach for accurate pricing.

Several authors have already initiated studies into MMOT, offering various methodologies to address its inherent complexities:

- Nenna and Pass [23] offer an innovative approach to MMOT problems using a system of ordinary differential equations (ODEs). This method simplifies computations and scales linearly with the number of marginals,

a significant improvement over the exponential complexity of traditional methods.

- Albergo et al. [24] focus on generative modeling within the MMOT framework. Their approach captures complex data relationships and utilizes stochastic interpolants, which shows promise for applications in generating realistic and relationally consistent data samples.

- Zhou and Parno [25] tackle the computational demands of MMOT, particularly the issue of dimensionality. They propose an algorithm that not only computes quickly but also guarantees the exactness of the optimal transport plan, thus addressing both efficiency and scalability.

Moreover, Sester [26] adds to this growing body of literature with a theoretical exploration of MMOT, offering a duality theorem within this context. This theorem elucidates the relationship between the primal and dual problems and could be highly influential for financial models involving multiple time periods.

Collectively, these papers pave the way toward resolving some of the most pressing issues in MMOT. They provide theoretical foundations, propose novel computational techniques, and open new possibilities for practical applications in finance and economics.

Multi Marginals Martingale Optimal Transport : more is coming

The problem of multi-marginal martingale optimal transport (MMOT) poses significant computational challenges due to the large number of maturity smiles needed to price standard industry autocalls, which can range from 100 to 1000 dates. Addressing this issue requires innovative approaches that can efficiently handle high-dimensional probability distributions and the associated cost functions.

Optimal Control (Overview)

Optimal control is focused on determining the best sequence of actions for a dynamical system to achieve a specific goal, involving the minimization of a cost function dependent on the system's state and the controls applied.

Multi-Marginal Optimal Transport (Overview)

MMOT extends the classical optimal transport problem to multiple probability distributions. It seeks the most efficient mass transport across these distributions, with efficiency gauged by a cost function.

The Connections

- Both areas can be cast as minimization problems, whether it is over control space or transport plans.

- Entropy regularization is employed in both to ease computational efforts and relate to stochastic control.
- The Schrödinger Bridge problem links the two by solving for optimal paths with entropy regularization, similar to an optimal control problem.

Contributions to Optimal Control

- MMOT offers model-free control design, which is valuable for systems with complex or unknown dynamics.
- Robust control strategies can be developed by considering multiple potential system states, leading to less disturbance-sensitive controls.
- The framework is beneficial for analyzing and designing control strategies for large-scale systems, also known as mean-field control.

Resources for Further Exploration

Important works in this field include:

- The exploration of no-arbitrage conditions in finance by Galichon et al. (2014) [27].
- Foundational research on mean-field control by Lasry and Lions (2006) [28].
- A thorough introduction to mean-field games by Achdouri and Lasry (2010) [29].

Furthermore, the paper "An Optimal Control Perspective on Diffusion-Based Generative Modeling" by Berner, Richter, and Ullrich [48] presents a unifying perspective linking diffusion models in generative learning with optimal control, offering novel insights and sampling methods derived from control theory.

Significance

This paper is significant for its theoretical framework that bridges generative modeling and optimal control, suggesting potential for methodological advancements in both fields.

Key Contributions:

Unifying Perspective: The paper establishes a strong link between diffusion-based generative models and optimal control theory. It provides a framework to interpret diffusion models through a control theory lens, offering new insights and potential avenues for improvement. Hamilton-Jacobi-Bellman (HJB) Equation: The authors derive a Hamilton-Jacobi-Bellman equation for the log-densities of marginals in a diffusion process. They show how this relates to the variational objectives used to train diffusion models. Evidence Lower Bound

(ELBO): The paper demonstrates that the commonly used ELBO objective in diffusion models emerges as a direct consequence of the well-known verification theorem in optimal control theory. Path Space Formulation: The optimal control perspective allows for formulating diffusion-based modeling as minimizing the Kullback-Leibler divergence between suitable probability measures in path space. This can lead to new divergence metrics and loss functions. Novel Sampling Method: The authors develop a Time-Reversed Diffusion Sampler (DIS), a new technique for sampling from unnormalized densities using insights from optimal control.

This paper provides a valuable theoretical bridge between two important areas of research:

- Generative Modeling: It offers a novel way to understand and analyze diffusion-based generative models, which have garnered lots of attention in recent years.
- Optimal Control: It showcases the application of optimal control techniques to machine learning problems, potentially inspiring the development of new methods.

Additional Resources

For a deeper understanding, consider the following resources:

- An insightful talk by Julius Berner on the subject. https://m.youtube.com/watch?v=wQpQg1xIlBA
- Accessible blog posts that distill the paper's main ideas for a general audience.

Link with MMOT

current on going research

A Information Geometry

Acknowledgments

The appendix that follows is based on a series of courses available on YouTube. The courses were delivered by Professor Melvin Leok, who is a professor of mathematics at the University of California, San Diego. The YouTube series can be accessed through the following link: https://www.youtube.com/@melvinleok

Furthermore, the translation and interpretation of the course materials were greatly facilitated by the exceptional capabilities of ChatGPT 4.0, an advanced language model developed by OpenAI.

A.1 Machine Learning and Information Geometry

- Some machine learning algorithms can be viewed abstractly as the optimization problem of finding a parametric probability distribution that minimizes the mismatch with the data.
- Divergence (or contrast) functions are asymmetric analogues of distance functions that provide a unified way of measuring information, energy, and entropy.
- Divergence functions induce metrics and connections on the information manifold, and these differential geometric structures yield more natural optimization algorithms in the sense of optimization on manifolds than working in the parametric representation.

A.2 Divergence Between Two Points

Let us consider two points P and Q in a manifold M, whose coordinates are $\boldsymbol{\xi}_P$ and $\boldsymbol{\xi}_Q$, respectively. A divergence $D[P:Q]$ is a function of $\boldsymbol{\xi}_P, \boldsymbol{\xi}_Q$ which satisfies certain criteria, and often we will write, $D[P:Q]$ as $D[\boldsymbol{\xi}_P : \boldsymbol{\xi}_Q]$.

Definition: $D[P:Q]$ is a divergence when it satisfies the following:

1. $D[P:Q] \geq 0$.
2. $D[P:Q] = 0$ if and only if $P = Q$.
3. When P, Q are sufficiently close, by denoting their coordinates by $\boldsymbol{\xi}_P, \boldsymbol{\xi}_Q = \boldsymbol{\xi}_P + d\boldsymbol{\xi}$, the Taylor expansion of D is given by:

$$D[\boldsymbol{\xi}_P : \boldsymbol{\xi}_P + d\boldsymbol{\xi}] = \frac{1}{2} \sum_{ij} g_{ij}(\boldsymbol{\xi}_P) d\xi^i d\xi^j + \mathcal{O}(|d\boldsymbol{\xi}|^2), \tag{62}$$

where $G = (g_{ij})$ is a positive-definite matrix depending on $\boldsymbol{\xi}_P$.

A.3 Examples of Divergence

K-L divergence for positive measures: The Kullback-Leibler (K-L) divergence for two positive measures m_1 and m_2 is given by

$$D_{KL}[m_1 : m_2] = \sum_i m_{1i} \log \frac{m_{1i}}{m_{2i}} - \sum_i m_{1i} + \sum_i m_{2i}, \tag{63}$$

where when the total mass of the two measures m_1, m_2 equals 1, they are probability distributions, and this definition reduces to the definition of K-L for probability distributions.

Divergence for positive-definite matrices: The divergence for positive-definite matrices P and Q is

$$D[P:Q] = \mathrm{tr}(P \log P - P \log Q - P + Q), \tag{64}$$

which is related to the von Neumann entropy of quantum mechanics. Furthermore, the divergence of two Gaussian distributions P and Q is

$$D[P:Q] = \mathrm{tr}(PQ^{-1} - \log PQ^{-1} - n), \tag{65}$$

where n is the dimensionality, and this is due to the K-L divergence of multivariate Gaussian distributions.

A.4 Properties of Divergence

A divergence represents a degree of separation between two points, but neither it nor its square root is a distance. It does not necessarily satisfy the symmetry condition, so in general

$$D[P:Q] \neq D[Q:P]. \tag{66}$$

It also does not (in general) satisfy the triangle inequality. When we write $D[P:Q]$, we refer to the divergence from P to Q, and it has the dimension of the square of a distance.

One can symmetrize a divergence using the formula:

$$D_S[P:Q] = \frac{1}{2}\left(D[P:Q] + D[Q:P]\right), \tag{67}$$

but asymmetry is an important property and plays an role as we will see later.

A.5 Infinitesimal Distance and Riemannian Structure

When points P and Q on a manifold M are sufficiently close, we can define the square of an infinitesimal distance ds,

$$ds^2 = 2D[\boldsymbol{\xi} : \boldsymbol{\xi} + d\boldsymbol{\xi}] = \sum_{i,j} g_{ij} d\xi^i d\xi^j, \tag{68}$$

where $D[\boldsymbol{\xi} : \boldsymbol{\xi} + d\boldsymbol{\xi}]$ is the divergence between the points P and Q expressed in coordinates $\boldsymbol{\xi}$ and $\boldsymbol{\xi} + d\boldsymbol{\xi}$, and g_{ij} are the components of the positive-definite metric tensor $G(\boldsymbol{\xi})$.

A manifold M is said to be Riemannian when a positive-definite matrix $G(\boldsymbol{\xi})$ is defined on M, and the square of the local distance between two nearby points is given by ds^2. Given a divergence, there is an induced Riemannian structure

A.6 Geometry Induced by Divergence Functions

A divergence function induces a Riemannian metric g and a pair of torsion-free dual connections Γ and Γ^*.

The induced metric is given by:

$$g_{ij}(x) = -D_{i,j}(x,y)\big|_{x=y}, \tag{69}$$

where $D_{i,j}$ represents the partial derivatives of the divergence function with respect to the coordinates i and j.

The torsion-free dual connections are defined as:

$$\Gamma_{ijk}(x) = -D_{ij,k}(x,y)\big|_{x=y}, \tag{70}$$

$$\Gamma^*_{ijk}(x) = -D_{k,ij}(x,y)\big|_{x=y}. \tag{71}$$

Here, Γ_{ijk} and Γ^*_{ijk} are the connection coefficients, and the semicolon in the subscript denotes the covariant derivative.

The connections Γ and Γ^* are torsion-free and are dual with respect to the induced metric g. This duality is particularly important as it relates the geometric structure with the underlying statistical model.

In the geometry induced by divergence functions, the connections Γ and Γ^* can be related to the Levi-Civita connection Γ^0 as follows:

$$\Gamma_{ijk} = \Gamma^0_{ijk} - \frac{1}{2}T_{ijk}, \tag{72}$$

where Γ^0_{ijk} is the Levi-Civita connection, and T_{ijk} is the skewness tensor.

Similarly, the dual connection Γ^* is given by:

$$\Gamma^*_{ijk} = \Gamma^0_{ijk} + \frac{1}{2}T_{ijk}. \tag{73}$$

The tensor T_{ijk} is the difference between the dual connections:

$$T_{ijk} = \Gamma^*_{ijk} - \Gamma_{ijk}. \tag{74}$$

Given a divergence function D, we induce a metric g and a pair of dual connections Γ, Γ^*. An interesting question arises:

Question: If we have a metric g and a pair of dual connections Γ, Γ^*, can we find a divergence function D that induces them?

Geometry can be induced by divergence functions. Specifically, one can construct a canonical divergence by applying Hamilton-Jacobi theory for the following Lagrangian:

$$L(q,v) = \frac{1}{2}g_{ij}v^iv^j + \frac{1}{12}T_{ijk}(q)v^iv^jv^k, \tag{75}$$

where g_{ij} is the Riemannian metric and T_{ijk} is the skewness tensor. This Lagrangian will then yield a generating function which is a canonical divergence.

Divergence functions can be seen as generating functions of symplectic maps. This has connections with discrete mechanics. If D is a generating function, we can define a map $\mathbf{D}$: $T^*M \to T^*M$, where $(q,p) \mapsto (q',p')$, and M is the manifold under consideration.

The transformation of coordinates in a symplectic map given a divergence function D can be described by:

$$p_i = -\frac{\partial D}{\partial q^i}(q,p'), \tag{76}$$

$$p'_i = \frac{\partial D}{\partial q'^i}(q,p'). \tag{77}$$

Given a divergence function D, not only is there an induced Riemannian metric g, but also considering $\frac{1}{2}D$ as a generating function of a symplectic map allows us to question the approximation quality of such a function. Specifically, we assess whether $\frac{1}{2}D$ is a good approximation of the time-h geodesic flow (cost $\frac{1}{2}D$). This approach is always consistent (first-order accurate), and if D is a Bregman divergence, then the approximation is second-order accurate. Such considerations are crucial for the analysis of the geometric and dynamical properties of the system.

A.7 Important examples of Bregman Divergences

Example: Generalized KL-Divergence

For the negative entropy, the function $\Phi(\xi)$ is defined as follows:

$$\Phi(\xi) = -\sum_i \xi_i \log \xi_i, \tag{78}$$

and the associated Bregman divergence is the KL divergence, given by:

$$D_\Phi[\xi : \xi'] = \sum_i \left(\xi_i \log \frac{\xi_i}{\xi'_i} - \xi_i + \xi'_i \right) \tag{79}$$

When $\sum_i \xi'_i = \sum_i \xi_i = 1$, this is the KL divergence for probability vectors. When these normalization do not hold, this a generalization that may be used to describe circonstances when the quantity of matter or number of particules is not conserved.

Example: Free Energy of the Exponential Family

In the exponential family of distributions, there is a normalizing factor $\Psi(\theta)$, defined by:

$$\Psi(\theta) = \log \int \exp\left(\sum_i \theta_i x_i + k(x) \right) dx. \tag{80}$$

We want to compute the associated Bregman divergence. The integral I is given by:

$$I = \int p(x, \theta)\, dx = \int \exp\left(\sum_i \theta_i x_i + k(x) - \Psi(\theta) \right) dx. \tag{81}$$

Differentiating with respect to θ_i, we have:

$$\int \left(x_i - \frac{\partial}{\partial \theta_i} \Psi(\theta) \right) \phi(x, \theta)\, dx = 0. \tag{82}$$

A.8 Legendre Transform

Given a convex function $\Psi(\xi)$, consider,

$$\xi^* = \nabla\Psi(\xi),$$

which is the normal vector to the supporting tangent hyperplane to Ψ at ξ. Observe that the map from ξ to ξ^* is one-to-one, and differentiable.

We can view this as a change of coordinates, and this transformation is referred to as the Legendre transform. The transformation $\xi \to \xi^*$ is given by

$$\xi^* = \nabla\Psi(\xi).$$

Question: Is there a Ψ^* such that

$$\xi = \nabla\Psi^*(\xi^*)?$$

Consider

$$\Psi^*(\xi^*) = \xi \cdot \xi^* - \Psi(\xi), \quad \text{with} \quad \xi^* = \nabla\Psi(\xi).$$

We differentiate Φ with respect to ξ^* and we have

$$\nabla\Phi(\xi^*) = \xi + \frac{\partial^2}{\partial {\xi^*}^2}\Phi(\xi^*) \cdot \xi^* - \nabla\Phi(\xi)\frac{\partial}{\partial \xi^*}\xi^*. \tag{83}$$

Since $\xi^* = \nabla\Phi(\xi)$, the last two terms cancel, and we are left with

$$\nabla\Phi^*(\xi^*) = \xi. \tag{84}$$

So, $\xi^* = \nabla\Phi(\xi)$, $\xi = \nabla\Phi^*(\xi^*)$, and thus, Φ^* is the Legendre dual of Φ.

Observe that

$$\Phi^*(\xi^*) = \text{ext}_\xi \left\{\xi \cdot \xi^* - \Phi(\xi)\right\} = \xi \cdot \xi^* - \Phi(\xi)\Big|_{\xi=\nabla\Phi^*(\xi^*)}. \tag{85}$$

The use of the extremum operator is interesting when we apply the legendre transform to functions Φ which are not necessarely convex and therefore , it may exist several inverse to the equation $\xi^* = \nabla\Phi(\xi)$

We want to check that Φ^* is convex.

We can check that the Hessian of Φ^*

$$G^*(\xi^*) = \nabla^2\Phi^*(\xi^*) = \frac{\partial^2}{\partial {\xi^*}^2}\Phi^*(\xi^*) \tag{86}$$

which is the Jacobian of the inverse transform from ξ^* to ξ, which is inverse of the Hessian of the convex function Φ. So, the Jacobian is also positive definite, since it is the inverse of a positive definite matrix. Hence, Φ^* is convex.

A.9 Relationship Between Duality of Convex Function and Duality of Bregman Divergence

Given ξ, ξ' and their dual coordinates ξ^*, $\xi^{*'}$, we define the Bregman divergence D_Φ and its dual divergence D_{Φ^*} as follows:

$$D_\Phi[\xi : \xi'] =? \tag{87}$$

$$D_{\Phi^*}[\xi^* : \xi^{*'}] =? \tag{88}$$

A new Bregman divergence can be derived from the dual convex function Φ^*:

$$D_{\Phi^*}[\xi^* : \xi^{*'}] = \Phi^*(\xi^*) - \Phi^*(\xi^{*'}) - \nabla\Phi^*(\xi^{*'})^T(\xi^* - \xi^{*'}), \tag{89}$$

which is the dual divergence:

$$D_{\Phi^*}[\xi^* : \xi^{*'}] = D_\Phi[\xi' : \xi] \tag{90}$$

We can check that this is true.

Theorem 1. *The Bregman divergence $D_\Phi[P : Q]$ is given by*

$$D_\Phi[P : Q] = \Phi(\xi_P) + \Phi^*(\xi^*_Q) - \langle \xi_P, \xi^*_Q \rangle, \tag{91}$$

where ξ_P is the coordinates of P in ξ coordinate system, and ξ^*_Q is the coordinates of Q in ξ^* coordinate system.

Proof. The convex conjugate Φ^* at ξ^*_Q is given by

$$\Phi^*(\xi^*_Q) = \langle \xi_Q, \xi^*_Q \rangle - \Phi(\xi_Q). \tag{92}$$

Substituting this into (1) and using the property $\nabla\Phi(\xi_Q) = \xi^*_Q$ gives the theorem. □

This theorem justifies the concept of Bregman divergence because it shows that thanks to the relationships between Bregman divergence and convex duality, we have an expression of the Bregman divergence which uses only the convex duality concept and avoid any reference to gradient and differentials. The symmetry of this expression with respect of the use of functions and its dual makes it also powerful, as we will see.

A.10 Affine and Dual Affine Coordinate Systems

Observe that when a function $\Phi(\Theta)$ is convex in a coordinate system Θ, the same function expressed in another coordinate system ζ,

$$\hat{\Phi}(\zeta) := \Phi(O(\zeta)) \tag{93}$$

is not necessarily convex as a function of ζ. The notion of convexity is invariant under affine transformations

$$O' := A \cdot O + b, \tag{94}$$

where A is a nonsingular constant matrix, b is a constant vector.

Now, we fix a coordinate system Θ in which $\Phi(\Theta)$ is convex, and we introduce geometric structures on M based on it. Consider Θ as an affine coordinate system, which endows M with an affine flat structure .

M is a flat manifold, and the coordinate axes are straight lines. Any curve $\Theta(t) \in M$ of the form,

$$\Theta(t) = at + b \tag{95}$$

is a straight line, where a, b are constant vectors.

We refer to such curves as geodesics of an affine manifold. In this context, geodesics do not mean the shortest path connecting two points, but one where the curve keeps pointing in the same direction.

The geodesics (of an affine manifold) is invariant under affine transformations.

As before, we can consider the dual coordinates Θ^*,

$$\Theta^* = \nabla\Phi(\Theta) \tag{96}$$

and consider this as another affine coordinate system,

So, this gives two notions of geodesics and flatness. We say that a manifold M with these dual structures are dually flat, and the two flat coordinates are related by the Legendre transform,

A.11 Tangent Space, Basis Vectors, and Riemannian Metric

When $d\Theta$ is an (infinitesimally) small line segment, the square of its length ds is given by,

$$ds^2 = 2D_\Phi[\Theta : \Theta + d\Theta] = \sum_{i,j} g_{ij} d\Theta^i d\Theta^j, \tag{97}$$

where the upper indices i, j represent components.

Then, we can deduce that the Riemannian metric g_{ij} is given by the Hessian of Φ,

$$g_{ij}(\Theta) = \frac{\partial^2 \Phi}{\partial\Theta^i \partial\Theta^j}(\Theta). \tag{98}$$

Remark: The tangent space is spanned by the tangent vectors to the coordinate axes of the chart.

$$\frac{\partial}{\partial q^i} = \mathbf{e}_i$$

The vector space spanned by $\{\partial/\partial\Theta^i\}$ is the tangent space of M at each point. Since Θ is an affine coordinate system, $\{\partial/\partial\Theta^i\}$ looks the same at every point.

We can write any tangent vector A as,

$$A = \sum_i A^i e_i \tag{99}$$

A small line segment $d\Theta$ can be expressed as,

$$d\Theta = \sum_i d\Theta^i e_i \tag{100}$$

We can construct $\{e^i\}$ which are the tangent vectors of the dual affine coordinate curves of Θ^*.

$$d\Theta^* = \sum_i d\Theta^i e^{*i} \tag{101}$$

We can express a vector A in terms of its components and basis vectors as:

$$A = \sum_i A^i e_i = \sum_i A_i e^{*i} \tag{102}$$

In general, $A^i \neq A_i$.

Einstein Summation Convention

When the same index appears twice, once as an upper index, and another as a lower index, then summation over that repeated index is assumed, even without the summation symbol. For example:

$$A = A^i e_i = A_i e^{*i} \tag{103}$$

Also, for a line element ds, we have:

$$ds^2 = \langle d\Theta, d\Theta\rangle = g_{ij} d\Theta^i d\Theta^j \tag{104}$$

$$= \langle d\Theta^i e_i, d\Theta^j e_j\rangle = \langle e_i, e_j\rangle d\Theta^i d\Theta^j \tag{105}$$

$$\Rightarrow g_{ij} = \langle e_i, e_j\rangle \tag{106}$$

n Euclidean space, with an orthonormal coordinate system, the metric tensor g_{ij} is defined as:

$$g_{ij} = \delta_{ij} = \begin{cases} 1 & \text{if } i = j, \\ 0 & \text{if } i \neq j, \end{cases} \tag{107}$$

where δ_{ij} is the Kronecker delta.

In general, a manifold induced by a convex function is non-Euclidean.

The Riemannian metric can be represented in the dual affine coordinate system Θ^*.

$$d\Theta^* = d\Theta^*_i e^{*i}$$

$$ds^2 = \langle d\Theta^*, d\Theta^* \rangle = g^{ij} d\Theta_i d\Theta_j$$

where

$$g^{ij} = \langle e^{*i}, e^{*j} \rangle$$

$$d\Theta^{*i} = g^{ij} d\Theta_j \quad \text{and} \quad d\Theta^j = g_{ij} d\Theta^{*i}$$

where $G = G^{-1}$, so the Riemannian metric tensors are mutual inverses.

$$e^{*i} = g^{ij} e_j \quad \text{and} \quad e_i = g_{ij} e^{*j}$$

$\{e_i\}$ and $\{e^{*i}\}$ are dual in the sense that

$$\langle e_i, e^{*j} \rangle = \delta_i^j$$

because $G = G^{-1}$. So, the bases are dual with respect to the Riemannian inner product.

$$A = A^i e_i = A_i e^{*i}$$
$$\langle A, e^{*j} \rangle = \left\langle A^i e_i, e^{*j} \right\rangle = A^i \langle e_i, e^{*j} \rangle = A^j$$
$$\langle A, e_j \rangle = \left\langle A_i e^{*i}, e_j \right\rangle = A_i \langle e^{*i}, e_j \rangle = A_j$$

A.12 Parallel Transport of a Vector

In the context of a dually flat manifold, this simple notion of parallel transport by keeping the coefficients fixed applies.

But, in a dually flat manifold, we have two sets of bases for the tangent space, $\{e_i\}$ and $\{e^{*i}\}$, so each of them induces a specific notion of parallel transport, which are not the same.

To define parallel transport on a manifold, we need additional structure, in particular, an affine connection.

Since M is Riemannian and not Euclidean in general, even though we can define the parallel transport easily, the length of the parallel transported vector is not constant:

$$A = A^i e_i = A_i e^{*i} \tag{108}$$

$$|A|^2 = \langle A, A \rangle = g_{ij}(\Theta) A^i A^j = A^i A_j g^{ij}(\Theta) \tag{109}$$

This depends on Θ.

We define two parralel transports via the two basis we have at our disposal

$$\langle \pi A, \pi^* B \rangle = \left\langle A^i e_i(\Theta), B_j g^{jk}(\Theta) e_k(\Theta) \right\rangle$$
$$= A^i B_j g^{jk}(\Theta) \langle e_i(\Theta), e_k(\Theta) \rangle$$
$$= A^i g_{ik}(\Theta) B^k$$
$$= A_k B^k$$

The last line simplifies the expression by recognizing that $\langle e_i(\Theta), e_k(\Theta)\rangle$ yields the Kronecker delta which further simplifies the summation. it shows that by transportting one vector with a connection and the other with its dual connection, we keep the scalar product, which is the essence of the geometry.

Dually flat manifolds play a crucial role in information geometry by providing a framework where the geometric structure significantly simplifies the complexity of statistical models. These manifolds are endowed with two affine connections, which are flat and dual to each other, facilitating a unique geometric interpretation of statistical parameters.

Definition and Properties

A dually flat manifold is defined by the presence of two connections: the Levi-Civita connection ∇ and a flat, torsion-free connection ∇^* that is dual to ∇. These connections satisfy:

- ∇ is metric-compatible and torsion-free.
- ∇^* is flat and metric-compatible, but not necessarily torsion-free.
- Both ∇ and ∇^* have vanishing curvature, making them flat.

The flatness implies that locally, the manifold behaves like Euclidean space, which simplifies the computation and understanding of geodesic paths.

A.13 Generalized Pythagorean Theorem

We are goin to generalize the classical pythagoean theorem known for euclidian spaces:

Theorem 2 (Generalized Pythagorean Theorem)**.** *When triangle PQR is orthogonal such that the dual geodesic connecting P and Q is orthogonal to the geodesic connecting Q and R, then the generalized Pythagorean relationship holds:*

$$D_\Phi[P : R] = D_\Phi[P : Q] + D_\Phi[Q : R].$$

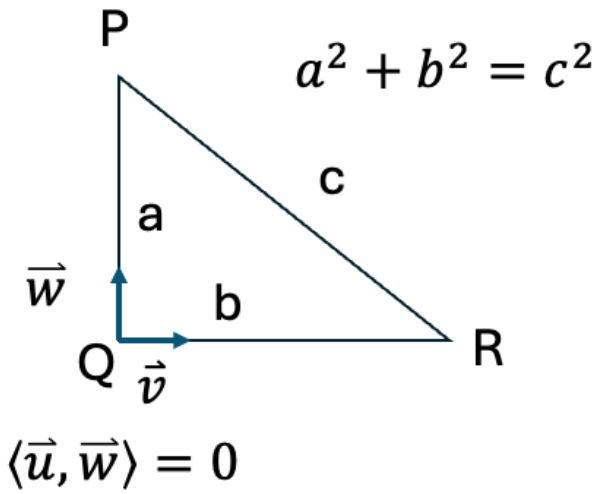

Figure 17: The pythagorean relationship when $\langle \vec{QP}, \vec{QR} \rangle = 0$.

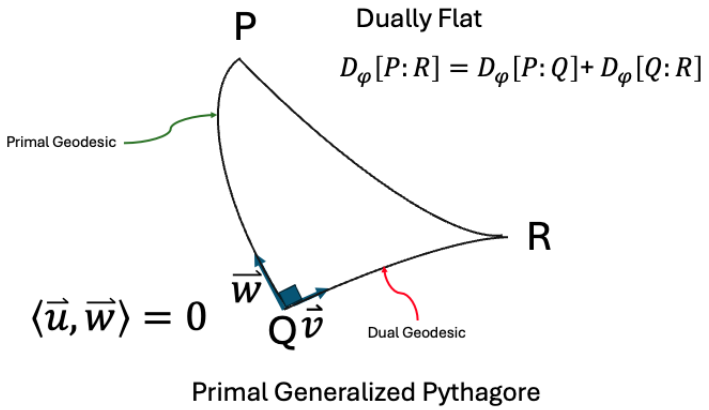

Figure 18: The pythagorean relationship when $\vec{QP}$ and $\vec{QR}$ are carried by dual vectors.

Proof of the Generalized Pythagorean Theorem

Using

$$D_\Phi[P:Q] = \Phi(\Theta_P) + \Phi^*(\Theta_Q^*) - \langle \Theta_P, \Theta_Q^* \rangle,$$

we show that

$$\begin{aligned} D_\Phi[P:Q] + D_\Phi[Q:R] - D_\Phi[P:R] &= (\Theta_P^* - \Theta_Q^*) \cdot (\Theta_Q - \Theta_R) \\ &= \text{the dual geodesic connecting } P, Q \text{ is} \\ \Theta_{PQ}^*(t) &= (1-t)\Theta_P^* + t\Theta_Q^*, \\ \text{Tangent vector is } \Theta_Q^* - \Theta_P^*. & \end{aligned}$$

Similarly, $\Theta_Q - \Theta_R$ is the tangent vector to the primal geodesic. But these two vectors are orthogonal, so $\star$ vanishes.

Theorem 3 (Dual Pythagorean Theorem)**.** *When triangle PQR is orthogonal such that the geodesic connecting P and Q is orthogonal to the dual geodesic connecting Q and R, the dual of the Generalized Pythagorean relation holds:*

$$D_{\Phi^*}[P:R] = D_\Phi[P:Q] + D_{\Phi^*}[Q:R].$$

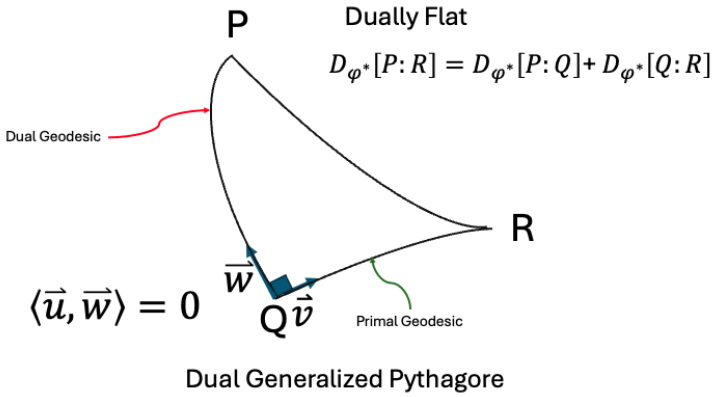

Figure 19: The dual pythagorean relationship when $\vec{QP}$ and $\vec{QR}$ are carried by dual vectors.

A.14 Projection Theorem

Geodesics for a connection ∇ are curves $\gamma(t)$ such that:

$$\nabla_{\dot\gamma(t)} \dot\gamma(t) = 0$$

where $\dot\gamma(t)$ is the tangent vector to γ at t.

Dual Geodesics for the connection ∇^* are curves $\gamma^*(t)$ that satisfy:

$$\nabla^*_{\dot{\gamma}^*(t)} \dot{\gamma}^*(t) = 0$$

Consider a point P and a smooth submanifold S in a dually flat manifold M. The divergence from a point P to the submanifold S is,

$$D_\Phi[P : S] = \inf_{R \in S} D_\Phi[P : R]. \tag{110}$$

It is natural to consider the question of finding a point in S that is closest to P in the sense of divergence. We can define the geodesic projection and dual geodesic projection of P to S in M. A curve $\Theta(t)$ is said to be orthogonal to S when its tangent vector $\dot{\Theta}(t)$ is orthogonal to any tangent vector to S at the intersection of $\Theta(t)$ with S.

Definitions : The point $\hat{P}_S$ is the geodesic projection of P to S when the geodesic connecting P to $\hat{P}_S$ is orthogonal to S.

Dual of this is that $\hat{P}^*_S$ is the dual geodesic projection of P to S, where the dual geodesic P to $\hat{P}^*_S$ is orthogonal to S.

Orthogonality at Intersection

When a geodesic γ intersects a submanifold S at a point $p = \gamma(t_0)$, it has the property that $\dot{\gamma}(t_0)$ is orthogonal to the tangent space T_pS at p. Mathematically,

$$g(\dot{\gamma}(t_0), v) = 0 \quad \forall v \in T_pS$$

where g is the metric tensor on the manifold. A similar property holds for dual geodesics γ^* intersecting S.

Geodesic vs. Dual Geodesic Projections

The projection of points via geodesics γ and dual geodesics γ^* onto S yields different intersection points (p and p^* respectively), generally with $p \neq p^*$. The tangent vectors at these points ($\dot{\gamma}(t_0)$ and $\dot{\gamma}^*(t_0^*)$) are orthogonal to T_pS and $T_{p^*}S$ respectively, but are not necessarily the same since they are determined by different connections and thus follow different paths.

Theorem 4 (Projection Theorem)**.** *Given $P \in M$ and a smooth submanifold $S \subseteq M$, then*

The point $\hat{P}^*_S$ that is the dual geodesic projection of P to S is the point in S that minimizes the divergence $D_\Phi[P : R]$, $R \in S$.

The point $\hat{P}_S$ that is the geodesic projection of P to S minimizes the dual divergence $D^*_\Phi[P : R]$, $R \in S$.

Proof: Let $\hat{P}^*_S$ be the dual geodesic projection of P to S. By the generalized Pythagorean theorem, we have

$$D_\Phi[P : Q] = D_\Phi[P : \hat{P}^*_S] + D_\Phi[\hat{P}^*_S : Q], \tag{111}$$

for any point Q on the geodesic S, and this quantity is greater than or equal to 0. It equals 0 when $Q = \hat{P}_S^*$. By properties of D_Φ, the right-hand side is minimized when $Q = \hat{P}_S^*$, so $\hat{P}_S^*$ is the point in S that minimizes $D_\Phi[P : Q]$, $Q \in S$.

Theorem 5 (Uniqueness of the projection)**.** *When S is a flat submanifold of a dually flat manifold M, the dual projection of P to S is unique and minimizes the divergence. Dually, when S is a dual flat submanifold in a dually flat manifold, the projection of P to S is unique and minimizes the dual divergence.*

A.15 Divergence Between Submanifolds

When you have two submanifolds K and S in a dually flat manifold M, we can define the divergence between K and S as

$$D[K : S] = \inf_{P \in K, Q \in S} D[P : Q] = D[\hat{P} : \hat{Q}], \tag{112}$$

where $\hat{P} \in K, \hat{Q} \in S$ are the closest pair between K and S. To obtain this pair of points $\hat{P}, \hat{Q}$, consider an alternating minimization algorithm.

Observe that such a method has the property,

$$D[P_{k-1} : Q_k] \geq D[P_k : Q_k] \geq D[P_k : Q_{k+1}], \tag{113}$$

and the procedure converges. It is unique when S is flat and K is dually flat. Otherwise, the limit point may depend on the initial guess.

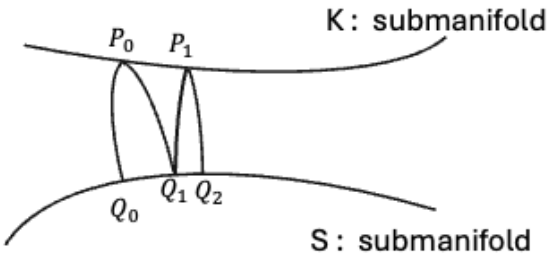

Figure 20: Convergence of successive projections.

Remark

In the latter part of the paper, geodesic projection is called e-projection (exponential projection) and dual geodesic projection is called m-projection (mixture

projection). Also, the alternating primal-dual projection algorithm is called the EM algorithm.

A.16 Exponential Family of Probability Distributions

The probability distribution $p(x, \Theta)$ belonging to the exponential family is expressed as:

$$p(x, \Theta) = \exp\{\Theta^\top h(x) + k(x) - \Psi(\Theta)\}. \tag{114}$$

Here, x is the random variable, and $\Theta = (\Theta^1, \ldots, \Theta^n)$ is an n-dimensional vector parameter. The functions $h_i(x)$ are n functions of x which are linearly independent, and $k(x)$ is a function of x. The term $\Psi(\Theta)$ is the normalization factor.

We can introduce a new vector random variable, $\chi = (x_1, \ldots, x_n)$, where $x_i = h_i(x)$. We also introduce a measure on the sample space X given by $d\mu(x) = \exp(k(x))\, dx$. So we can rewrite the density of this family as :

The differential form of the exponential family of distributions is given by:

$$p(x; \theta)dx = \exp(\theta \cdot x - \Psi(\theta))d\mu(x), \tag{115}$$

where $p(x; \theta)$ is a probability density function with respect to the measure $d\mu$. The set $M : \{p(x; \theta)\}$ forms an n-dimensional manifold, where θ is a coordinate system.

The normalization condition

$$\int p(x; \theta)d\mu(x) = 1, \tag{116}$$

implies that

$$\Psi(\theta) = \log \int \exp(\theta \cdot x)d\mu(x). \tag{117}$$

The function $\Psi(\theta)$ is a convex function. This is the cumulant generating function in statistics, or the free energy in physics.

A.17 Dually Flat Riemannian Structure Induced by the Log-Partition Function

Given the log-partition function $\Psi(\theta)$, we induce a dually flat Riemannian structure on M. The affine coordinates are θ, which is called the natural or canonical parameter of an exponential family. The dual affine parameter is given by the Legendre transform,

$$\theta^* = \nabla\Psi(\theta). \tag{118}$$

This θ^* is the expectation of x, $\eta = (\eta_1, \ldots, \eta_n)$, where η is given by

$$\eta = \mathbb{E}[x] = \int xp(x; \theta)d\mu(x). \tag{119}$$

This η is the expectation parameter in statistics. So, in place of θ^*, we use η, which is also the gradient of Ψ with respect to θ,

$$\eta = \nabla\Psi(\theta). \tag{120}$$

We can denote the dual convex function $\Psi^*(\eta)$ by the Legendre transform of $\Psi(\theta)$ as follows:

$$\Psi^*(\eta) = \text{ext}_\theta\{\theta \cdot \eta - \Psi(\theta)\}. \tag{121}$$

To obtain $\Psi^*(\eta)$, we first compute the negative entropy of $p(x;\theta)$:

$$E[\log p(x;\theta)] = \int p(x;\theta) \log p(x;\theta) d\mu(x) = \theta \cdot \eta - \Psi(\theta). \tag{122}$$

The dual convex function Ψ^* of Ψ is denoted by Φ and is given by the negative entropy,

$$\Phi(\eta) = \int p(x;\theta) \log p(x;\theta) d\mu(x), \tag{123}$$

where θ is regarded as a function of η via $\eta = \nabla\Psi(\theta)$ and consequently, $\theta = \nabla\Phi(\eta)$.

The divergence from $p(x,\theta')$ to $p(x,\theta)$ is given by,

$$D_\Phi[\theta' : \theta] = \Psi(\theta') - \Psi(\theta) - \nabla\Psi(\theta) \cdot (\theta' - \theta), \tag{124}$$

which can be interpreted as

$$D_\Phi[\theta' : \theta] = \int p(x;\theta) \log \frac{p(x;\theta)}{p(x;\theta')} d\mu(x) = D_{KL}[\theta : \theta']. \tag{125}$$

The Riemannian metric is given by the second derivatives of Ψ,

$$g_{i,j}(\theta) = \frac{\partial^2 \Psi(\theta)}{\partial\theta^i \partial\theta^j}, \tag{126}$$

$$g^{i,j}(\eta) = \frac{\partial^2 \Phi(\eta)}{\partial\eta_i \partial\eta_j}. \tag{127}$$

Here, ∂_i denotes $\frac{\partial}{\partial\theta^i}$ and ∂^j denotes $\frac{\partial}{\partial\eta_j}$.

Theorem 6 (Link with the Fisher information)**.** *The Riemannian metric, in the exponential family is the Fisher information matrix given by,*

$$g_{ij} = \mathbb{E}\left[\frac{\partial \log p(x;\theta)}{\partial\theta^i} \frac{\partial \log p(x;\theta)}{\partial\theta^j}\right]. \tag{128}$$

Proof:

Starting with the partial derivatives of the log-probability,

$$\partial_i \log p(x;\theta) = x_i - \partial_i \Psi(\theta) = x_i - \eta_i, \tag{129}$$

we consider the expectation of the product of these derivatives:

$$\mathbb{E}\left[\partial_i \log p(x;\theta)\partial_j \log p(x;\theta)\right] = \mathbb{E}\left[(x_i - \eta_i)(x_j - \eta_j)\right], \tag{130}$$

which simplifies to the covariant derivative of the log-partition function:

$$= \nabla_i \nabla_j \Psi(\theta). \tag{131}$$

This result shows that the Fisher information matrix can be expressed as the Hessian of the log-partition function $\Psi(\theta)$.

A.18 Bregman Divergence and Thermodynamic Systems

A.18.1 Physical Intuition: Free Energy in Thermodynamics

In thermodynamics, the concept of free energy describes the total amount of usable work obtainable from a system, represented as:

$$\text{Free Energy} = \text{Internal Energy} - T \times \text{Entropy}.$$

Applying this to the exponential family:

- **Energy Contributions:** $\theta^i T_i(x)$ analogous to various forms of energy (e.g., kinetic, potential).
- **Log-Partition Function $\psi(\theta)$:** Serves as the cumulant generating function for these energies, akin to the partition function in statistical mechanics.

A.18.2 Thermodynamic and Information-Theoretic Interpretation

if we remember that a Bregman divergence associated with a convex function ϕ is defined by:

$$D_\phi(p, q) = \phi(p) - \phi(q) - \langle \nabla\phi(q), p - q\rangle,$$

- **Entropy and Work:** The term $\langle \nabla\psi(q), p - q\rangle$ can be seen as the 'work' required to change the system's parameters from q to p, reflecting changes in entropy and internal energy.
- **Bregman Divergence as Information:** $D_\psi(p, q)$ quantifies the inefficiency or 'informational cost' of moving from state q to state p, measuring the non-recoverable work due to entropy production or equivalent informational loss.

This approach not only provides a bridge between statistical mechanics and information geometry but also enriches our understanding of statistical distributions and parameter updates in learning algorithms and complex systems analysis.

A.19 Gaussian Distribution in the Exponential Family

The Gaussian distribution with mean μ and variance σ^2 has the probability density function given by:

$$p(x;\mu,\sigma) = \frac{1}{\sqrt{2\pi\sigma^2}} \exp\left(-\frac{(x-\mu)^2}{2\sigma^2}\right). \tag{132}$$

Consider the random vector $X = (X_1, X_2)$ where $X_1 = h_1(X) = X$ and $X_2 = h_2(X) = X^2$.

Note that X and X^2 are dependent, but linearly independent as functions. The new parameters are

$$\theta'^1 = \frac{\mu}{\sigma^2}, \tag{133}$$

$$\theta'^2 = -\frac{1}{2\sigma^2}. \tag{134}$$

Thus, the pdf $p(x)$ can be written in the exponential family form as:

$$p(x;\theta) = \exp(\theta \cdot x - \Psi(\theta)), \tag{135}$$

where θ represents the natural parameters θ'^1 and θ'^2.

Continuous Distribution

The log-partition function $\Psi(\theta)$ for the Gaussian distribution is given by:

$$\Psi(\theta) = \frac{(\theta^1)^2}{4\theta^2} + \log\left(\sqrt{2\pi\sigma}\right), \tag{136}$$

which can be reparametrized using $\theta^1 = \frac{\mu}{\sigma^2}$ and $\theta^2 = -\frac{1}{2\sigma^2}$, leading to:

$$\Psi(\theta) = -\frac{1}{2}(\theta^1)^2 \log(-\theta^2) + \frac{1}{2}\log\pi. \tag{137}$$

Here, X_1 and X_2 are not independent, with $X_2 = X_1^2$. To enforce this condition, we introduce a measure:

$$d\mu(X) = \delta(X_2 - X_1^2)dX, \tag{138}$$

where δ is the Dirac delta function.

The dual affine coordinates η are given by the expectations:

$$\eta_1 = \mathbb{E}[X_1] = \mu, \tag{139}$$

$$\eta_2 = \mathbb{E}[X_1^2] = \mu^2 + \sigma^2. \tag{140}$$

Discrete Distribution

Distributions of discrete random variable x over $X = \{0, 1, \ldots, n\}$ form a probability simplex S_n. A distribution $p = (p_0, \ldots, p_n)$ is represented by:

$$p(x) = \sum_{i=0}^{n} p_i \delta_i(x), \tag{141}$$

where $\delta_i(j)$ equals 1 if $i = j$ and 0 otherwise.

We show that S_n is an exponential family. The logarithm of $p(x)$ is given by:

$$\log p(x) = \sum_{i=0}^{n} (\log p_i) \delta_i(x) \tag{142}$$

$$= \sum_{i=1}^{n} (\log p_i - \log p_0) \delta_i(x) + (\log p_0) \delta_0(x) \tag{143}$$

$$= \sum_{i=1}^{n} \log \left(\frac{p_i}{p_0} \right) \delta_i(x) + \log p_0. \tag{144}$$

Here, we have introduced a measure $\delta_i(x)$ for the discrete space X and have shown that the probability mass function for the discrete distribution can be expressed in the exponential family form.

We introduce new random variables X_i, where $X_i = h_i(x) = \delta_i(x)$ for $i = 1, \ldots, n$, and new parameters,

$$\theta^i = \log \frac{p_i}{p_0}.$$

So, we can write p as,

$$p(x; \theta) = \exp \left(\sum_{i=1}^{n} \theta^i X_i - \Psi(\theta) \right).$$

The cumulant generating function is

$$\Psi(\theta) = -\log p_0 = \log \left(1 + \sum_{i=1}^{n} \exp(\theta^i) \right).$$

The dual affine coordinates are,

$$\eta_i = \mathbb{E}[h_i(X)] - p_i.$$

The dual convex function, which is the negative entropy, is given by

$$\Phi(\eta) = \sum_{i=1}^{n} \eta_i \log \eta_i + (1 - \sum_{i=1}^{n} \eta_i) \log(1 - \sum_{i=1}^{n} \eta_i).$$

As we expect, the natural parameters θ can be expressed as the gradient of the dual potential $\Phi(\eta)$,

$$\theta^i = \log \frac{\eta_i}{1 - \sum_i \eta_i}.$$

A.20 Mixture Family of Probability Distributions

A mixture family is in general different from an exponential family, but the family of discrete distributions S_n is both an exponential family and a mixture family. These two families play a dual role.

Given n probability distributions $p_0(x), \ldots, p_n(x)$ which are linearly independent, we can compose a family of probability distributions given by,

$$p(x;\eta) = \sum_{i=0}^{n} \eta_i q_i(x), \tag{145}$$

where η satisfies the conditions $\sum_{i=0}^{n} \eta_i = 1$, $\eta_i \geq 0$.

This is a statistical model called a mixture family, where $\eta = (\eta_0, \ldots, \eta_n)$ is a coordinate system. Here, $\eta_n = 1 - \sum_{i=1}^{n-1} \eta_i$.

A.21 Discrete Distributions as Mixture Families

Clearly, the discrete distributions form a mixture family (as well as an exponential family). The parameters η_i are given by $\eta_i = p_i$, and the functions $q_i(x) = \delta_i(x)$, for $i = 0, \ldots, n$.

The η parameters constitute a dual affine coordinate system for the exponential family of discrete distributions.

Now, consider a general mixture family, which is not an exponential family. Even then, the negative entropy

$$\Phi(\eta) = \int p(x;\eta) \log p(x;\eta)\, dx \tag{146}$$

is a convex function of η. We can consider it as a dual convex function and define a dually flat structure to $M = \{p(x;\eta)\}$, where η is the dual affine coordinate system.

The primal affine coordinates are,

$$\Theta = \nabla\Phi(\eta), \tag{147}$$

which defines a primal affine structure, but Θ is not the natural parameter of an exponential family except for the case of discrete distributions (Bregman). The divergence given by the negative entropy $\Phi(\eta)$ is the Kullback-Leibler divergence,

$$D_\Phi[\eta : \eta'] = \int p(x;\eta) \log \frac{p(x;\eta)}{p(x;\eta')}\, dx. \tag{148}$$

A.22 Flat Structure e-flat and m-flat

The manifold M of the exponential family is dually flat. The primal affine coordinates are the natural parameters θ in the exponential family. Consider an e-geodesic connecting $p(x;\theta_1)$ to $p(x;\theta_2)$. In the θ-coordinates,

$$\theta(t) = (1-t)\theta_1 + t\theta_2, \tag{149}$$

then the associated probability distribution,

$$p(x;\theta(t)) = p(x;(1-t)\theta_1 + t\theta_2), \tag{150}$$

$$= \exp\left(t(\theta_2-\theta_1)x + \theta_1 x - \psi(\theta(t))\right) \tag{151}$$

The geodesic is a one-parameter exponential family where t is the natural parameter. it is the linear interpolant in the logarithmic scale.

More generally, a submanifold which is defined by linear constraints on θ is said to be e-flat. The affine parameter θ is called the e-affine parameter.

The dual affine coordinates are η and define a dual flat structure. The dual geodesic (or m-geodesic) connecting two distributions with coordinates η_1, η_2 is,

$$\eta(t) = (1-t)\eta_1 + t\eta_2. \tag{152}$$

Along a dual geodesic, the expectation of x is linearly interpolated,

$$E_{\eta(t)}[x] = (1-t)E_{\eta_1}[x] + tE_{\eta_2}[x]. \tag{153}$$

For discrete probability distributions,

$$p(t) = (1-t)p_1 + tp_2, \tag{154}$$

which is a mixture of the two distributions p_1 and p_2. So in this case, the dual geodesic is a mixture of two probability distributions, so we call it an m-geodesic, where m stands for mixture. A submanifold defined by linear constraints in η is m-flat.

The linear mixture

$$(1-t)p(x,\eta_1) + tp(x,\eta_2) \tag{155}$$

is not included in M in general, but

$$p(x;(1-t)\eta_1 + t\eta_2) \tag{156}$$

is in M, and we refer to this "nonlinear" mixture as an m-geodesic even in this case.

A.23 Infinite-dimensional Manifold of Probability Distributions

Recall that the discrete probability distributions are both an exponential family and a mixture family. And any statistical model of a discrete random variable embeds into this space.

We want something analogous for statistical models of continuous random variables. To do this we have to consider an infinite-dimensional function space.

Let $p(x)$ be a probability density function of a real random variable $x \in \mathbb{R}$, which is mutually absolutely continuous with Lebesgue measure. We put,

$$F = \{p(x) \mid p(x) > 0, \int p(x)dx = 1\}$$

Then F is a function space consisting of positive L^1 functions.

For two distributions $p_1(x)$ and $p_2(x)$, the exponential family connecting them is given by,

$$p_{\exp}(x;t) = \exp\left\{(1-t)\log p_1(x) + t\log p_2(x) - \psi(t)\right\},$$

provided it exists in F. Also, the mixture family connecting them is,

$$p_{\min}(x;t) = (1-t)p_1(x) + tp_2(x),$$

which is assumed to be in F.

Then F is regarded as an exponential and mixture family, which is analogous to the case for discrete probability distributions.

The subtle is the issue of topology which you endow F with, L^1, L^2 norms induce different topologies, $p(x)$ vs. $\log p(x)$ induce different topologies. The significance of this can be observed in basic issues like tightness, convergence, etc.

Ignore the mathematical subtleties for now, and consider a discretization of $\mathbb{R}$ into $n+1$ intervals, $I_0, \ldots, I_n$. Then, the discretized version of $p(x)$ is given by, $\mathbf{p} = (p_0, \ldots, p_n)$.

Where p_i is defined as:

$$p_i = \int_{I_i} p(x)\,dx, \quad i = 0, \ldots, n.$$

This gives a projection from F to S_n, and which approximates $p(x)$ by $\mathbf{p}$ in S_n.

We denote:

$$\hat{p} \to \frac{1}{n}\sum_{i=0}^{n} \frac{p_i}{|I_i|}\chi_{I_i}(x), \quad \text{in } F.$$

There is a sense in which if $p(x)$ is regular enough, and $I_0, \ldots, I_n$ is chosen appropriately, and $n \to \infty$, there is a sense in which this approximation converges. And this endows F with some geometry. The geometry induced when $n \to \infty$ depends on the discretization.

Let us introduce a family of random variables, $\delta(s-x)$, indexed by a real parameter s, which plays the role of the index i in $S_i(x)$ in S_n.

For continuous $p(x)$:

$$p(x) = \int p(s)\delta(s-x)\,ds.$$

For discrete $p(x)$:

$$p(x) = \sum_{i=0}^{n} p_i\delta_i(x).$$

This shows that F is a mixture family, generated by Dirac delta distributions $\delta(s-x)$, $s \in \mathbb{R}$. $p(s)$ are the mixing coefficients.

We can also write,

$$p(x) = \exp\left\{\int \theta(s)\delta(s-x)\,ds - \psi\right\},$$

where $\theta(s) = \log p(s) + \gamma$, and

$$\psi(\theta(s)) = \int \exp(\theta(s))\delta(s-x)\,ds.$$

Hence, F is an exponential family, where $\theta(s) = \log p(s) + \psi$ is the affine coordinate, and $\eta(s) = p(s)$ is the dual affine coordinate.

The dual convex function is

$$\phi(\eta(s)) = \int \eta(s)\log\eta(s)\,ds.$$

We can check that the dual coordinates are given by,

$$\eta(s) = \mathbb{E}_p[\delta(s-x)] = p(s),$$

and

$$\nabla\psi(\theta(s)) = \nabla\theta(s) = \nabla\log p(s) + \nabla\psi.$$

Here, ∇ is the Fréchet derivative with respect to $\theta(s)$.

We've already discussed e-geodesics and m-geodesics.

For the e-geodesic, we have:

$$p_{\exp}(x;t) = \exp\left((1-t)\log p_1(x) + t\log p_2(x) - \psi(t)\right)$$

The tangent vector is given by:

$$\left.\frac{d}{dt}\right|_{t=0} \log p(x;t) = \log q(x) - \log p(x)$$

For the m-geodesic, we have:

$$p_{\text{mix}}(x;t) = (1-t)p_1(x) + tp_2(x)$$

The tangent vector is given by:

$$\dot{p}(x;t) = q(x) - p(x)$$

The KL-divergence is:

$$D_{KL}[p(x) : q(x)] = \int p(x)\log\frac{p(x)}{q(x)}\,dx,$$

which is the Bregman divergence derived from $\psi(\theta)$, and gives F a dually flat structure.

The generalized Pythagorean theorem is:

$$D_{KL}[p(x) : r(x)] = D_{KL}[p(x) : q(x)] + D_{KL}[q(x) : r(x)],$$

when the m-geodesic connecting p and q is orthogonal to the e-geodesic connecting q and r.

which reads:

$$\int (p(x) - q(x)) \cdot (\log r(x) - \log q(x))\, dx = 0.$$

Then the projection theorem follows

The KL-divergence between two nearby distributions, $p(x)$ and $p(x) + \delta p(x)$, is expanded as,

$$D_{KL}[p(x) : p(x) + \delta p(x)] = \int p(x) \log \left(1 - \frac{\delta p(x)}{p(x)}\right) dx.$$

This approximates to

$$\approx \frac{1}{2} \int \frac{(\delta p(x))^2}{p(x)} dx.$$

The squared distance of an infinitesimal deviation δp is,

$$ds^2 = \int \frac{(\delta p(x))^2}{p(x)} dx,$$

which is the Riemannian metric given by the Fisher information.

What can go wrong in infinite dimensions?

We can define a quasi-e-neighborhood of $p(x)$ using the KL-divergence,

$$N_\varepsilon = \{q(x) \mid D_{KL}[p(x) : q(x)] < \varepsilon\}.$$

The set of quasi-e-neighborhoods do not satisfy the axioms for a topological space. So, we cannot use KL to define a topology.

It can be shown that the entropy functional,

$$\phi(p(x)) = \int p(x) \log p(x)\, dx,$$

is not continuous in F (but it is continuous and differentiable in S_n).

A.24 Kernel Exponential Family

Given a kernel function $k(x, y)$ satisfying a positivity condition,

$$\int k(x, y) f(x) f(y)\, dx\, dy > 0$$

for any $f(x)$ which is not identically zero.

A typical example is the Gaussian kernel,

$$k(x,y) = \frac{1}{\sqrt{2\pi\sigma^2}} \exp\left(-\frac{1}{2\sigma^2}(x-y)^2\right),$$

where σ is a free parameter.

Then a kernel exponential family

$$p(x;\Theta) = \exp\left\{\int \Theta(y)k(x,y)\,dy - \psi(\Theta)\right\}$$

and this is with respect to a suitable measure,

$$d\mu(y) = \exp\left(-\frac{y^2}{2\sigma^2}\right)\frac{dy}{\sqrt{2\pi\sigma^2}}.$$

The natural or canonical parameter is a function $\Theta(y)$ which is indexed by y instead of θ, and the dual parameter is

$$\eta(y) = \mathbb{E}[k(x,y)].$$

As before, $\psi(\Theta)$ is a convex functional of $\Theta(y)$.

We can think of the naive treatment from before as the case where

$$k(x,y) = \delta(x-y).$$

A.25 Bregman Divergence and Exponential Family

In an exponential family, the normalization factor $\psi(\Theta)$ is convex, which induces a Bregman divergence $D_\psi[\Theta : \Theta']$.

It is natural to ask the converse, i.e., given a Bregman divergence $D_\psi[\Theta : \Theta']$, is there a corresponding exponential family?

Consider a random variable x, that defines a point $\eta' = x$ in the η-coordinates of a dually flat manifold given by ψ. Let Θ' be its Θ-coordinates.

The ψ-divergence from Θ to Θ' is as follows,

$$D_\psi[\Theta : \Theta'](x) = \psi(\Theta') + \psi(\Theta) - \Theta' \cdot x.$$

With this, we can define a probability density function.

The probability density function is given by:

$$p(x;\Theta') = \exp\left\{\Theta' \cdot x - \psi(\Theta')\right\},$$

where Θ' is determined from x as the Θ-coordinate associated with $\eta' = x$. So it is clear that we have an exponential family derived from the Bregman divergence.

Given a convex function $\psi(\Theta)$, find a measure $d\mu(x)$ such that

$$\psi(\Theta) = \log \int \exp(\Theta \cdot x)\,d\mu(x)$$

or equivalently,

$$\exp\{\psi(\Theta)\} = \int \exp(\Theta \cdot x)\, d\mu(x).$$

This is the inverse of the laplace transform

Theorem 7. *There is a bijection between regular exponential families and regular Bregman divergences.*

Remark 1. *Given a Bregman divergence, there is a corresponding family of probability distributions for which the Bregman divergence is the KL-divergence for that family.*

A.26 Maximum Entropy Principle

Consider discrete probability distributions $S_n = \{p(x)\}$, but this argument extends to the case where x is a continuous random variable.

Let $c_1(x), \ldots, c_k(x)$ be k random variables, k functions of x, then the expectations are,

$$E\left[c_i(x)\right] = \sum_x p(x) c_i(x), \quad i = 1, \ldots, k.$$

Consider a probability distribution $p(x)$ for which the expectations of $c_i(x)$ are given by $\mathbf{a} = (a_1, \ldots, a_k)$.

$$E\left[c_i(x)\right] = a_i.$$

There are many such distributions, and they form a $(n-k)$-dimensional submanifold. $M_{n-k}(\mathbf{a}) \subseteq S_n$. This submanifold M_{n-k} is m-flat, because it is closed under mixtures.

When choosing a distribution from M_{n-k}, when there are no other considerations, one chooses the distribution that maximizes the entropy. Let P_0 be the uniform distribution that maximizes entropy in S_n. The dual divergence between $P \in S_n$ and P_0 is given by:

$$D_\psi[P_0 : P] = \psi(\boldsymbol{\theta}_0) + \psi(\boldsymbol{\eta}) - \boldsymbol{\theta}_0 \boldsymbol{\theta}.$$

Here $\boldsymbol{\theta}_0$ is the e-coordinates of P_0, $\boldsymbol{\eta}$ is the m-coordinates of P, and $\psi(\boldsymbol{\theta})$ is the negative entropy. This is the KL-divergence $D_{KL}[P_0 : P]$.

Since P_0 is the uniform distribution, $\boldsymbol{\theta}_0 = \mathbf{0}$.

So minimizing the divergence is equivalent to maximizing the entropy.

Let $\hat{P} \in M_{n-k}$ be the point that maximizes the entropy. Then, $P \perp P_0$ is orthogonal and we can apply the Pythagorean relationship,

$$D_{KL}[P : P_0] = D_{KL}[P : \hat{P}] + D_{KL}[\hat{P} : P_0].$$

The upshot is that the maximizing entropy point $\hat{P} \in M_{n-k}$ is the e-projection of P_0 onto M_{n-k}.

Mutual Information

Consider two random variables X, Y, and the manifold M consists of all $p(x, y)$. When X, Y are independent then

$$p(x, y) = p_X(x) \cdot p_Y(y),$$

where $p_X(x)$, $p_Y(y)$ are the marginal distributions.

Let M_I denote the family of all independent distributions. Observe that the exponential family connecting two independent distributions is again independent. So, M_I is an e-flat submanifold. Given a non-independent distribution $p(x, y)$, we want to find the closest independent distribution in the sense of KL-divergence. This corresponds to m-projection of $p(x, y)$ to M_I. This projection is unique, and it is given by

$$\hat{p}(x, y) = p_X(x) \cdot p_Y(y).$$

The KL-divergence between $p(x, y)$ and its projection is,

$$D_{KL}[p(x, y) : \hat{p}(x, y)] = \int p(x, y) \log \frac{p(x, y)}{\hat{p}(x, y)} dxdy,$$

which is the mutual information of the two random variables x, y. So, mutual information is a measure of the discrepancy of $p(x, y)$ from independence.

One can ask the reverse question. Given an independent distribution $\hat{p}$, find the distribution $p(x, y)$ which maximizes $D_{KL}[p : \hat{p}]$ over the class of distributions with the same marginal distributions as $\hat{p}$. These are the inverse image of the m-projection.

A.27 Repeated Observations and Maximum Likelihood Estimators

Consider independently observed data $X_1, \ldots, X_N$ from the same probability distribution $P(X; \theta)$ in an exponential family, with a view towards estimating θ. The joint probability density is given by,

$$p(x_1, \ldots, x_N; \theta) = \prod_{i=1}^{N} p(x_i; \theta).$$

How does the geometry of M change upon repeated observations? Consider

$$\bar{X} = \frac{1}{N} \sum_{i=1}^{N} X_i.$$

Then,

$$P_N(\bar{X}; \theta) = p(x_1, \ldots, x_N; \theta) = \exp\{N[\bar{X} \cdot \theta - \psi(\theta)]\},$$

the probability density at $\bar{X}$ has the same form as $p(x; \theta)$, except that x is replaced by $\bar{X}$ and the term $\theta \cdot \theta$ becomes N times as large.

- The convex function becomes N times as large.
- KL-divergence, Riemannian metric also become N times larger.
- Dual affine structure of M does not change.
  - So, we can use the same coordinates θ.
- Binomial and multinomial distributions are exponential families derived from S_2 and S_n by multiple observation.

Let M be an exponential family, and consider a statistical model, $S : \{p(x,u)\} \subset M$ submanifold of parameters $u = (u_1, \ldots, u_k), k \leq n$. Since $S \subset M$, the e-coordinates of $P(x;u)$ in M are determined by u, i.e., $\theta(u)$.

Given N independent observations $x_1, \ldots, x_N$, want to estimate u based on them.

The observed data specifies a distribution on M, such that its m-coordinates are given by,

$$\bar{\boldsymbol{\xi}} = \frac{1}{N}\sum_{i=1}^{N} \boldsymbol{\xi}_i = \bar{\boldsymbol{x}}.$$

This is the observed point. The KL-divergence from the observed $\bar{\boldsymbol{\xi}}$ to a distribution $p(x;u)$ in S is given by

$$D_{KL}[\bar{\boldsymbol{\xi}} : \boldsymbol{\theta}(u)].$$

$\boldsymbol{\theta}$ is the Θ-coordinate corresponding to the dual coordinate $\bar{\boldsymbol{x}} = \bar{\boldsymbol{\xi}}$.

Consider the simple case of S_n, where the observed point is given by

$$\hat{p}(x) = \frac{1}{N}\sum_{i=1}^{N} \delta(x - x_i).$$

Modulo a constant term, minimizing KL-divergence is equivalent to maximizing the log likelihood,

$$L = \sum_{i=1}^{N} \log p(x_i;u).$$

So, the maximum likelihood estimator corresponds to minimizing the divergence by m-projection of $\hat{p}(x)$ to S.

A.28 Dual Connections

The Levi-Civita connection is the only affine connection that is torsion free and metric compatible. What that means is that it preserves the metric under parallel transport.

Consider a pair of symmetric affine connections Γ and Γ^*, and we denote the associated parallel transport by Π and Π^*, respectively. These affine connections are dually coupled when,

$$\langle A, B\rangle = \langle \Pi A, \Pi^* B\rangle$$

When the two connections are the same, this reduces to the usual notion of metric compatibility. And the Levi-Civita connection is self-dual.

Characterizing Dual Connections Is there a way to characterize dual connections? Consider the basis vectors, e_i, e_j at the point $\xi + d\xi$.

We want to parallel transport them to ξ using Γ and Γ^*.

Parallel Transport and the Inner Product We express the parallel transport of basis vectors as:

$$e_i + de_i = e_i + \Gamma^k{}_{ki} e_j d\xi^k,$$
$$e_j + de_j^* = e_j + \Gamma^{*k}{}_{kj} e_i d\xi^k.$$

From the preservation of the inner product, we have:

$$\langle \tilde{e}_i, \tilde{e}_j \rangle_{\xi + d\xi} = \langle e_i + de_i, e_j + d^* e_j \rangle_\xi.$$

Expanding the metric coefficients at $\xi + d\xi$, we get:

$$g_{ij}(\xi + d\xi) = g_{ij}(\xi) + \langle de_i, e_j \rangle_\xi + \langle e_i, d^* e_j \rangle_\xi.$$

Where higher-order terms in $d\xi$ are neglected. By Taylor expanding the left-hand side and ignoring higher-order terms, we obtain:

$$\partial_i g_{jk} = \Gamma^l{}_{ijk} + \Gamma^{*l}{}_{ikj}.$$

And for the self-dual case:

$$\partial_i g_{jk} = \Gamma^l{}_{ijk} + \Gamma^l{}_{ikj}.$$

This can be written in terms of covariant derivatives as:

$$\langle X, Y \rangle_Z = \langle \nabla_Z X, Y \rangle + \langle X, \nabla_Z Y \rangle, \tag{157}$$

where X, Y, Z are vector fields. We can verify this by considering $X = e_i$, $Y = e_j$, $Z = e_k$, and observing that:

$$e_i \langle e_j, e_k \rangle = \langle \nabla_{e_i} e_j, e_k \rangle + \langle e_j, \nabla^*_{e_i} e_k \rangle.$$

The average of the two dual connections is given by:

$$\Gamma^0_{ijk} = \frac{1}{2} \left(\Gamma_{ijk} + \Gamma^*_{ijk} \right).$$

The associated covariant derivative is:

$$\nabla^{(0)} = \frac{1}{2} \left(\nabla + \nabla^* \right).$$

From equation (157), we see that $\nabla^{(0)}$ satisfies the condition for the covariant derivative associated with the Levi-Civita connection, and Γ^0_{ijk} is the Levi-Civita connection.

Let us define

$$T_{ijk} = \Gamma^*_{ijk} - \Gamma_{ijk}.$$

Then, the dual connections can be written as:

$$\Gamma^*_{ijk} = \Gamma^0_{ijk} + \frac{1}{2}T_{ijk}, \quad \Gamma_{ijk} = \Gamma^0_{ijk} - \frac{1}{2}T_{ijk}.$$

Theorem 8. *When Γ and Γ^* are dual affine connections, T is a symmetric tensor, given by,*

$$\nabla_i g_{jk} = T_{ijk}, \quad \nabla_i g^{jk} = -T^{ijk}.$$

Metric and Cubic Tensor Derived from Divergence

Given a divergence $D[\xi;\xi']$ defined on M, we obtain two tensors, g^D_{ij} and T^D_{ijk}, which are induced by D. Since D has two arguments, we will introduce notation that specifies which argument we are differentiating with respect to,

$$D_i = \frac{\partial}{\partial \xi^i} D[\xi;\xi']\Big|_{\xi'=\xi}, \quad D_{;j} = \frac{\partial}{\partial \xi'^j} D[\xi;\xi']\Big|_{\xi'=\xi}.$$

Extends naturally to multiple derivatives,

$$D_{ij;k} = \frac{\partial^2}{\partial \xi^i \partial \xi^j} \frac{\partial}{\partial \xi'^k} D[\xi;\xi']\Big|_{\xi'=\xi}.$$

With this, we define,

$$g^D_{ij} = -D_{i;j}, \quad \Gamma^D_{ijk} = -D_{ij;k}, \quad \Gamma^{*D}_{ijk} = -D_{ik;j}.$$

We can check that the Γ, Γ^* are indeed affine connections

Theorem 9. *The two affine connections Γ^D and Γ^{*D} are dual with the Riemannian metric g^D.*

When you have a dual pair of convex functions, $\Phi(\theta)$ and $\phi(\gamma)$, where θ and γ are connected by Legendre transforms, we have a Bregman divergence:

$$D_\Phi[\theta;\theta'] = \Psi(\theta) + \Phi(\theta') - \langle \theta, \eta' \rangle,$$

where θ' is the Legendre dual of θ.

The metric and affine connection coefficients induced by Φ are given by:

$$g_{ij}(\theta) = \partial_i \partial_j \Psi(\theta), \quad g^{ij}(\eta) = \partial^i \partial^j \Phi(\eta).$$

Consequently, the connections $\Gamma_{ijk}(\theta)$ and $\Gamma^*_{ijk}(\gamma)$ satisfy:

$$\Gamma_{ijk}(\theta) = \Gamma^{*ijk}(\eta) = 0.$$

This implies that the geometry derived from a convex function or the related Bregman divergence is dually flat, and the affine coordinates are θ, η .

We have previously defined the tensor $T^D_{ijk} = \Gamma^{D*}_{ijk} - \Gamma^D_{ijk}$.

The cubic tensor is given by:

$$T_{ijk} = \partial_i \partial_j \partial_k \Psi(\theta), \quad T^*_{ijk} = \partial^i \partial^j \partial^k \Phi(\eta).$$

A.29 Dually Flat Manifolds

Theorem 10. *When the RC curvature R vanishes with one of the affine connections, then the RC curvature R^* with respect to the dual connection vanishes as well, and vice versa.*

Proof. When the RC curvature vanishes, $R = 0$, then the round-the-world parallel transport does not change a vector A, i.e., $A = \Pi A$. We also know that

$$\langle A, B \rangle = \langle \Pi A, \Pi^* B \rangle.$$

When $(*)$ holds, this implies

$$\langle A, B \rangle = \langle A, \Pi^* B \rangle,$$

for any vectors A, B. This leads to $B = \Pi^* B$ and consequently, the RC curvature for the dual connection, R^*, vanishes.

A manifold is always dually flat when it is flat with one connection. □

When M is dually flat, there is always an affine coordinate system θ for which

$$\Gamma_{ijk}(\theta) = 0.$$

θ induces a basis for $TM : \{e_i\}$

Similarly, there exists a dual affine coordinate system η such that

$$\Gamma^*_{ijk}(\eta) = 0.$$

η induces a basis for $TM : \{e^i\}$

The Jacobian for the coordinate transformations are,

$$g_{i;j} = \frac{\partial \theta_i}{\partial \theta^j}, \quad g^i{}_j = \frac{\partial \eta^i}{\partial \eta_j}.$$

This implies that,

$$e_i = g_{i;j} e^j = \frac{\partial \eta_i}{\partial \theta^j} e^j, \quad e^i = g^i{}_j e_j = \frac{\partial \theta^i}{\partial \eta_j} e_j.$$

Theorem 11. *In a dually flat manifold, there exist affine coordinates θ, and dual affine coordinates γ such that their tangent vectors are reciprocally orthogonal, i.e.,*

$$\langle e_i, e^j \rangle = \langle \partial_i, \partial^j \rangle = \delta^j_i,$$

where δ^j_i is the Kronecker delta.

Proof. We have that

$$\langle e_i, e^j \rangle = \langle e_i, g^{jk} e_k \rangle = g_{ik} g^{jk} = \delta_i^k,$$

which establishes the reciprocal orthogonality of the basis vectors. □

A.30 Canonical Divergences in Dually Flat Manifolds

We have seen that given a divergence function, we can obtain a Riemannian metric and a pair of dual affine connections.

Question: Given a Riemannian metric, and a dual pair of affine connections, can we find a divergence function that induces those given geometric structures?

Answer: With regards to the uniqueness, many divergence functions induce the same dual structure. This is because the dual structure only depends locally on the divergence function in a neighborhood at the diagonal.

Given $D[\xi; \xi']$, we can add a term $d(\xi, \xi')$, without changing the dual structure, so long as

$d(\xi, \xi) = 0$, $\frac{\partial}{\partial \xi^i} d(\xi, \xi') \Big|_{\xi'=\xi} = 0$, and $\frac{\partial}{\partial \xi'^i} d(\xi, \xi') \Big|_{\xi'=\xi} = 0$.

Additionally, the second derivatives must vanish at the diagonal.

$$\frac{\partial^2}{\partial \xi^i \partial \xi^j} d(\xi, \xi') \Big|_{\xi'=\xi} = 0 \quad \frac{\partial^2}{\partial \xi'^i \partial \xi'^j} d(\xi, \xi') \Big|_{\xi'=\xi} = 0.$$

and , the third derivatives at the diagonal must also vanish:

$$\frac{\partial^3}{\partial \xi^i \partial \xi^j \partial \xi'^k} d(\xi, \xi') \Big|_{\xi'=\xi} = 0, \quad \frac{\partial^3}{\partial \xi'^i \partial \xi'^j \partial \xi^k} d(\xi, \xi') \Big|_{\xi'=\xi} = 0.$$

But, on a dually flat manifold, we can obtain a unique canonical divergence, up to affine transformations.

Lemma 1. *If M is dually flat, there are a pair of dual coordinate systems θ, η and a pair of Legendre-dual convex functions $\Psi(\theta)$, $\Phi(\eta)$ satisfying*

$$\Psi(\theta) + \Phi(\eta) - \langle \theta, \eta \rangle = 0,$$

and the metric is given by

$$g_{ij}(\theta) = \frac{\partial^2 \Psi}{\partial \theta^i \partial \theta^j}, \quad g^{ij}(\eta) = \frac{\partial^2 \Phi}{\partial \eta^i \partial \eta^j},$$

and the cubic tensor by

$$T_{ijk}(\theta) = \frac{\partial^3 \Psi}{\partial \theta^i \partial \theta^j \partial \theta^k}, \quad T^*_{ijk}(\eta) = \frac{\partial^3 \Phi}{\partial \eta^i \partial \eta^j \partial \eta^k}.$$

Proof. We start with an affine coordinate system θ, for which $\Gamma_{ijk}(\theta) = 0$. We use the definition of dual metric compatibility,

$$\langle v, w \rangle = \langle \Pi v, \Pi^* w \rangle,$$

which in coordinates is given by

$$\partial_i g_{jk} = \Gamma_{ijk} + \Gamma^*_{ikj}$$

but

$$\Gamma_{ijk} = 0$$

so

$$\partial_i g_{jk} = \Gamma^*_{ijk}$$

Use the fact that the connections are symmetric, $\partial_i g_{jk} = \partial_k g_{ji}$. Fix index j, denoted by "."

$$\partial_i g_{k.} = \partial_k g_{i.}.$$

Then, we can find a function Ψ, such that

$$g_{i.} = \partial_i \Psi$$

Or for each j,

$$g_{ij} = \partial_i \Psi_j$$

But g_{ij} is symmetric, thus

$$\partial_i \Psi_j = \partial_j \Psi_i.$$

This implies that there exists a Ψ such that,

$$\Psi_{,i} = \partial_i \Psi$$

and therefore,

$$g_{ij} = \partial_i \partial_j \Psi,$$

which is convex because (g_{ij}) is positive-definite.

For θ-coordinates, since $T_{ijk}(\theta) = 0$, we have,

$$\nabla_i = \partial_i,$$

so,

$$T_{ijk} = \partial_i \partial_j \partial_k \Psi(\theta).$$

Similarly, for the dual convex function $\Phi(\eta)$, we need to show they are related by Legendre transforms.

□

Theorem 12. *When M is dually flat, there exists a Legendre pair of convex functions $\Phi(\theta)$, $\phi(\eta)$ and a canonical divergence given by the Bregman divergence,*

$$D[\theta : \eta^{'}] = \Psi(\theta) + \Phi(\eta^{'}) - \langle \theta, \eta^{'} \rangle.$$

Remark 2. *This canonical divergence is unique up to affine transformations. Conversely, the canonical divergence induces the dually flat structure.*

That we can summarize by :

Theorem 13. *The KL-divergence is the canonical divergence of an exponential family of probability distributions, which is invariant and dually flat.*

A.31 Estimation

$M = \{p(x;\xi)\}$ is a statistical model specified by a parameter ξ, which we wish to estimate. When we make N independent observations $D : \{x_1, x_2, \ldots, x_N\}$ generated from $p(x;\xi)$, we wish to estimate ξ. This is the problem of estimation, and an estimator,

$$\hat{\xi} = f(x_1, x_2, \ldots, x_N),$$

is a function of D. The estimation error is given by,

$$e = \hat{\xi} - \xi,$$

where ξ is the true value. The bias of the estimator is,

$$b(\xi) = E[\hat{\xi}] - \xi,$$

where the expected value is with respect to $p(x;\xi)$. An estimator is unbiased when $b(\xi) = 0$. The asymptotic theory studies the behavior of an estimator when N is large. When the bias satisfies,

$$\lim_{N\to\infty} b(\xi) = 0,$$

it is asymptotically unbiased. It is desirable for a good estimator to converge to the true parameter as $N \to \infty$,

$$\lim_{N\to\infty} \hat{\xi} = \xi.$$

When this holds, the estimator is consistent. One can measure the accuracy of an estimator by the error covariance matrix, $V = (V_{ij})$,

$$V_{ij} = E\left[(\hat{\xi}_i - \xi_i)(\hat{\xi}_j - \xi_j)\right].$$

This decreases in general in proportion to $1/N$. The estimator $\hat{\xi}$ becomes sufficiently accurate when N increases

Theorem 14. *For an asymptotically unbiased estimator $\hat{\xi}$, the Cramér-Rao theorem gives a bound on accuracy,*

$$V \geq \frac{1}{N} G^{-1}$$

which means that :

$$(V - \frac{1}{N} G^{-1}) \text{ is positive semi-definite.}$$

where $V = (V_{ij})$ is positive semi-definite, and $G = (g^{ij})$ is the Fisher information matrix,

$$V_{ij} = E[(\hat{\xi}_i - \xi_i)(\hat{\xi}_j - \xi_j)] \geq \frac{1}{N} g^{ij},$$

and $G^{-1} = (g_{ij})$ is its inverse.

The maximum likelihood estimation (MLE) is the maximizer of the likelihood,

$$\hat{\xi}_{MLE} = \arg\max_{\xi} \prod_{i=1}^{N} p(x_i|\xi),$$

or in the log space

$$\hat{\xi}_{MLE} = \arg\max_{\xi} \frac{1}{N} \sum_{i=1}^{N} \log p(x_i|\xi),$$

and the MLE is asymptotically unbiased, and its error covariance satisfies

$$V_{MLE} = NG^{-1} + O\left(\frac{1}{N}\right).$$

It achieves the Cramér-Rao bound asymptotically. This is referred to as Fisher-efficient.

A.32 Estimation in the Exponential Family

Estimation in the Exponential Family is given by

$$p(x;\theta) = \exp(\theta \cdot x - \psi(\theta))$$

Given data D, the joint probability distribution is written as,

$$p(D;\theta) = \exp(N(\bar{X} \cdot \theta) - N\psi(\theta))$$

where $\bar{X}$ is the arithmetic mean of the observed data,

$$\bar{X} = \frac{1}{N} \sum_{i=1}^{N} x_i,$$

which is a sufficient statistic. The MLE $\hat{\theta}_{MLE}$ is given by differentiating ψ and is given by,

$$\hat{\theta}_{MLE} = \nabla\psi(\theta) = \bar{X}$$

Using the η-coordinates, this is written as,

$$\eta = \hat{\theta}_{MLE} = \bar{X}$$

So, the observed data defines a point $\hat{\gamma}$ in M with coordinates $\hat{\gamma} = \bar{X}$ which is the observed point from the data D.

Theorem 15. *The MLE is unbiased and efficient, i.e.,*

$$E[\hat{\theta}_{MLE}] = \theta, \quad V = \frac{1}{N} G^{-1}.$$

Proof. Invoke the central limit theorem and conclude that $\hat{\theta}$ is asymptotically described by a Gaussian distribution with mean θ and covariance G^{-1}/N. Since the MLE attains the Cramér-Rao bound, it is the best estimator in an exponential family. □

Remark 3. *The MLE $\hat{\theta}_{MLE}$ expressed in η-coordinates is asymptotically unbiased and asymptotically efficient, but it is not unbiased nor does it attain the Cramér-Rao bound exactly. This is because the bias and covariance matrix are not tensors, so their properties depend on the choice of coordinates.*

A.33 Estimation in a Curved Exponential Family

Consider a submanifold embedded in an exponential family,

$$p(x;u) = \exp(\langle \theta(u), x\rangle - \psi(\theta(u)))$$

where $S = \{p(x;u)\}$ is a submanifold of an exponential family $\mathcal{E} = \{p(x;\theta)\}$ where u is a coordinate system of S.

Given observed data D, this specifies an observed point $\hat{u}$ which is in the ambient space M, but not on S in general. An estimated value of u can be determined by mapping the observed point $\hat{u}$ to S.

Let us consider a map $\hat{S} : M \to S$ such that $\hat{u} = f(\hat{y})$.

We know that $\hat{y}$ converges to the true value y as $N \to \infty$. So, a consistent estimator $\hat{y}$ satisfies

$$\lim_{N\to\infty} \hat{u} = f(y(u)).$$

Let us consider the set of points h in M which are mapped to u by the estimator $f(y)$. This is an inverse image of an estimator f,

$$A(u) = \{h \in M | f(y(h)) = u\}.$$

This forms an $(n-m)$-dimensional submanifold passing through u in M, which is the ancillary submanifold associated with the estimator f.

$A(u)$ is defined for every $u \in S$, and this gives at least a local foliation of M in a neighborhood of S. The foliation $A(u)$ locally partitions M into disjoint subsets around S.

$$A(u) \cap A(u') = \emptyset \text{ for } u \neq u', \quad \bigcup_{u\in S} A(u) \supseteq U,$$

When $A(u) = f(u)$, $A(u)$ gives a consistent estimator.

An estimator defines an ancillary family A, and conversely, if $\lim_{N\to\infty} \hat{u} = f(u)$, then the family A defines a consistent estimator.

Question: How does the geometry of S relate to the performance of the estimator?

Let us define a coordinate system v inside each $A(u)$ such that $v = 0$ at $\eta(u)$ which is the intersection of $A(u)$ and S. We denote coordinates of S by,

$$u = f(u^{(1)}, \ldots, u^{(k)}),$$

and coordinates on $A(u)$ by $v = (v^{(k+1)}, \ldots, v^{(n)})$. Together, we get a coordinate system for the tubular neighborhood U of S, $w = (u, v) = (u^{(1)}, \ldots, u^{(k)}, v^{(k+1)}, \ldots, v^{(n)})$.

We can consider the associated θ, η coordinates,

$$\theta = \theta(w) = \theta(u, v), \quad \eta = \eta(w) = \eta(u, v).$$

Any point in S satisfies $\eta = 0$, so S is represented by,

$$S = \{\eta(u, v) | v = 0\}.$$

The Jacobian matrices of the coordinate transformation between w and θ, and w and η are,

$$B^i{}_j = \frac{\partial \theta^i}{\partial w^j}, \quad B_i{}^j = \frac{\partial \eta_i}{\partial w^j}.$$

and these are decomposed into,

$$B^i{}_a = \frac{\partial \theta^i}{\partial u^a}, \quad B^i{}_k = \frac{\partial \theta^i}{\partial v^k},$$

$$B_{ai} = \frac{\partial \eta_a}{\partial u^i}, \quad B_{ki} = \frac{\partial \eta_k}{\partial v^i}.$$

In terms of (u, v) coordinates, the Fisher information in w-coordinates are,

$$g_{ab} = B^i{}_a g_{ij} B^j{}_b,$$

and can be decomposed as

$$G = \begin{bmatrix} g_{ab} & g_{ak} \\ g_{kb} & g_{kk} \end{bmatrix}.$$

Given the data D, the u, v coordinates of the observed point $\bar{u}$ is given by $\hat{u} = f(\hat{y}(u, v))$ and the estimator associated with the ancillary family $\hat{u}$ is $\hat{u} = \hat{u}$.

Given the data D, the u, v coordinates $(\bar{u}, \bar{v})$ of the observed point $\bar{\eta}$ is given by

$$\bar{\eta} = \eta(\bar{u}, \bar{v})$$

and the estimator associated with the ancillary family A is $\hat{u} = \bar{u}$.

B Understanding a few Projection Algorithms

B.1 Iterative Proportional Fitting (IPF) via Alternating e-Projections

Iterative Proportional Fitting (IPF), also known as the Sinkhorn algorithm, is an iterative method to solve for optimal transport plans that satisfy marginal constraints. The algorithm employs alternating e-projections to minimize Kullback-Leibler (KL) divergence between measures.

1. **Initialization**: Start with an initial guess for the transport plan $Q_{0,T}$ that is feasible, meaning it satisfies the marginal constraints.

2. **Marginal Constraints**: Define the marginal constraints for the transport plan. These are distributions μ_0 and μ_T at the initial and terminal times, respectively. The set of all measures with these marginals is convex.

3. **e-Projection onto** $\Pi(\mu_0, \cdot)$:

   (a) Consider the current estimate of the transport plan $Q_{0,T}^{(n)}$.

   (b) Perform the e-projection by solving the following optimization problem:
   $$Q_{0,T}^{(n+1)} = \arg \min_{Q_{0,T} \in \Pi(\mu_0, \cdot)} D_{KL}[Q_{0,T} : Q_{0,T}^{(n)}]. \tag{158}$$

   (c) Update the transport plan using the result of the projection.

4. **e-Projection onto** $\Pi(\cdot, \mu_T)$:

   (a) Consider the updated estimate $Q_{0,T}^{(n+1)}$.

   (b) Perform the e-projection onto the set of measures with marginal μ_T:
   $$Q_{0,T}^{(n+2)} = \arg \min_{Q_{0,T} \in \Pi(\cdot, \mu_T)} D_{KL}[Q_{0,T} : Q_{0,T}^{(n+1)}]. \tag{159}$$

   (c) Update the transport plan again with the new projection.

5. **Iteration and Convergence**: Alternate between the two e-projections, incrementing n by 2 after each full cycle (i.e., after each pair of projections). Check for convergence, typically by looking at the stability of the KL divergence or the changes in the transport plan. If convergence criteria are met, terminate the algorithm.

6. **Output**: The resulting transport plan $Q_{0,T}$ approximates the solution to the entropy-regularized optimal transport problem and should satisfy the marginal constraints given by μ_0 and μ_T.

Remarks

- The IPF algorithm is guaranteed to converge under certain conditions. The Pythagorean relation helps in establishing monotonicity in the KL divergence during the projections.

- In practice, IPF can be computationally efficient and has been successfully applied in various domains where optimal transport is relevant.

B.2 Markov Projection algorithm

The Markov Projection algorithm is a key step within the Iterative Markovian Fitting (IMF) method, which refines a stochastic process to fit a target Markov process. Below are the steps involved in the Markov m-Projection:

1. **Objective**: Approximate the current estimate of the process $Q_{0,T}^{(n)}$ by finding a probability measure $Q_{0,T}^{*}$ that minimizes the KL divergence to a reference measure, constrained by the Markov property.

2. **KL Divergence Minimization**: Define the measure of similarity between two probability distributions using KL divergence. Minimizing this divergence aligns the current estimate of the process closer to the reference measure.

3. **Markov Property**: Ensure that the future states of the process depend only on the current state, not on the history of states, adhering to the space of Markov processes denoted by M.

4. **Vector Field** $v(x,t)$: Introduce a vector field $v(x,t)$ that potentially modifies the drift term in the stochastic differential equation of the process. This field is adjusted iteratively.

5. **Girsanov Theorem Application**: Use the Girsanov theorem to adjust the measure of the stochastic process, thereby transforming the original process $Q_{0,T}^{(n)}$ to resemble the desired Markov process $Q_{0,T}^{*}$.

6. **Optimization Problem**: Solve the following optimization problem to determine the best-fit vector field:

$$v^{(n+1)}(x,t) = \arg\min_{v_0} \int_0^T \mathbb{E}_{Q_{0,T}^{(n)}} \left[\frac{1}{2\sigma^2} \left\| \frac{dx_t}{dt} - v_0(x_t,t) \right\|^2 \right] dt. \tag{160}$$

7. **Update Process**: Use the computed vector field $v^{(n+1)}(x,t)$ to update the drift term of the stochastic process:

$$dx_t = (b(x_t,t) + v^{(n+1)}(x_t,t))dt + \sigma dB_t, \quad x_0 \sim \mu_0. \tag{161}$$

8. **Marginal Distribution Preservation**: Check that the update preserves the marginal distributions of the process at all times.

9. **Iterate and Converge**: Repeat the steps iteratively until the process converges to the optimal measure $Q_{0,T}^{*}$ that lies within the desired constraints.

B.3 Iterative Markovian Fitting and Exact Marginal Fitting

The Iterative Markovian Fitting algorithm refines a stochastic process to match a target Markovian property and a given reciprocal class constraint.

Algorithm 1: Iterative Markovian Fitting

The Iterative Markovian Fitting algorithm refines a stochastic process to match a target Markovian property and a given reciprocal class constraint.

Algorithm 1 Iterative Markovian Fitting

Input: Reference bridge process $Q^{\text{ref}}_{0,T}$
Input: Initial coupling $Q^{(0)}_{0,T} \in \Pi(\mu_0, \nu)$
Initialize: $Q^{(0)}_{0,T} = Q^{\text{ref}}_{0,T} \oslash Q^{(0)}_{0,T}$
while not converged **do**
    Markov m-Projection (Flow Matching):
    Sample $Q^{(n)}_{0,T} \oslash Q^{\text{ref}}_{0,T}$
    $v_t^{(n+1)} \leftarrow \arg\min_{v_t} \mathbb{E}_{Q^{(n)}_{0,T}} \left\| x_t^{(n)} - v_t \right\|^2$
    $Q^{(n+1)}_{0,T} \leftarrow \text{Law}(\text{SDE}(b_t, v_t^{(n+1)}, \sigma_t))$
    $Q^{(n+1)}_{0,T} \leftarrow \arg\min_{P \in MLC} D_{KL}(Q^{(n)}_{0,T} \parallel P_{0,T})$

    Reciprocal m-Projection (Rectification):
    $Q^{(n+2)}_{0,T} \leftarrow Q^{(n+1)}_{0,T} \oslash Q^{\text{ref}}_{0,T}$
    $Q^{(n+2)}_{0,T} \leftarrow \arg\min_{P \in RLC} D_{KL}(Q_{0,T} \parallel P_{0,T})$
    $n \leftarrow n + 2$
end while
return $Q^{(n)}_{0,T} \in MLC \cap RLC \cap \Pi(\mu_0, \nu_T)$

Algorithm 2: Exact Bridge Matching (EM)

The EM algorithm alternates between exact e-projections and m-projections to match a stochastic bridge to given marginal constraints, minimizing the KL divergence in the process.

Algorithm 2 Exact Bridge Matching

Input: Reference bridge process $Q^{\text{ref}}_{0,T}$
Input: Initial coupling $Q^{(0)}_{0,T} \in \Pi(\mu_0, \nu)$
Initialize: $Q^{(0)}_{0,T} = Q^{\text{ref}}_{0,T} \oslash Q^{(0)}_{0,T}$, $n = 0$
while not converged **do**
    Markov m-Projection (Flow Matching):
    $P^{(n+1)}_{0,T} \leftarrow \arg\min_{P \in MLC} D_{KL}(Q^{(n)}_{0,T} \parallel P_{0,T})$
    Reciprocal e-Projection:
    $Q^{(n+2)}_{0,T} \leftarrow \arg\min_{Q \in RLC} D_{KL}(Q_{0,T} \parallel P^{(n+1)}_{0,T})$
    Initialize $i = 0$, $P^{(i+n+2)}_{0,T} = Q^{(n+2)}_{0,T}$
    while not converged **do**
        e-Projection onto $\Pi(\cdot, \nu_T)$:
        $P^{(i+n+2)}_{0,T} \leftarrow \arg\min_{P \in \Pi(\cdot, \nu_T)} D_{KL}(Q_{0,T} \parallel P^{(i+n+2)}_{0,T})$
        e-Projection onto $\Pi(\mu_0, \cdot)$:
        $P^{(i+n+2)}_{0,T} \leftarrow \arg\min_{P \in \Pi(\mu_0, \cdot)} D_{KL}(Q_{0,T} \parallel P^{(i+n+1)}_{0,T})$
        $i \leftarrow i + 2$
    end while
    $n \leftarrow n + 2$, $Q^{(n)}_{0,T} \leftarrow P^{(i+n)}_{0,T}$
end while
return $Q^{(n)}_{0,T} \in MLC \cap RLC \cap \Pi(\mu_0, \nu_T)$

C Optimal Transport

C.1 The Monge Problem

We are given two distributions: one representing mines and one representing factories. The goal is to minimize the cost of transporting goods from the mines to the factories. Mathematically, let:

$$T : \mathbb{R}^n \to \mathbb{R}^n \quad \text{be a mapping from source to target locations}$$

The cost function is given by:

$$\int |x - T(x)| f(x)\, dx$$

where f is a given source density.

Example

- Mines and factories

C.1.1 Other Cost Functions

We can consider other cost functions $c(x, y)$.

The optimization problem becomes:

$$\min_T \int c(x, T(x)) f(x)\, dx$$

where:

- We want to work with measures.
- We have a source measure μ and a target measure ν.
- $\mu(E)$ tells us how much mass is in the set E.

Mass Balance

To ensure mass balance, we require:

$$\mu(\mathbb{R}^n) = \nu(\mathbb{R}^n)$$

Transport Map $T(x)$

We seek a transport map $T(x)$ such that:

$$T : X \to Y$$

where: - The source is supported on X. - The target is supported on Y.

We want to conserve mass:

$$\mu(T^{-1}(A)) = \nu(A), \quad \forall A \subseteq Y$$

Pushforward of μ

$\mu(T^{-1}(A))$ is called the pushforward of μ through T, denoted $T_{\#}\mu$.

Mass conservation:

$$T_{\#}\mu = \nu$$

The Monge formulation of optimal transport (OT) is:

$$\min \left\{ \int_{\mathbb{R}^n} c(x, T(x))\, d\mu(x) \mid T_{\#}\mu = \nu \right\}$$

Special Cases of Optimal Transport

- **Discrete OT**: (Dirac masses $\to$ Dirac masses)
- **Continuous OT**: μ and ν are absolutely continuous with densities f and g.
- **Semi-discrete OT**: μ is absolutely continuous, and ν consists of Diracs.

Formulating an Optimization Problem

Let's start in $\mathbb{R}^n$ and assume things are "nice enough."

C.1.2 The Transportation Problem in $\mathbb{R}$

Goal: Find $T(x)$ to minimize:

$$\frac{1}{2}\int_{\mathbb{R}^n}(x-T(x))^2 f(x)\,dx$$

subject to the constraint:

$$\int_{T^{-1}(A)} f(x)\,dx = \int_A g(y)\,dy, \quad \forall A \subseteq \mathbb{R}^n$$

Alternatively, this can be stated as:

$$\int_{\mathbb{R}^n} h(T(x))f(x)\,dx = \int_{\mathbb{R}^n} h(y)g(y)\,dy, \quad \forall h \in C(\mathbb{R}^n)$$

Monotony of the transport map

Let's pick two points $x_1 < x_2$ and $\epsilon > 0$, and make two little open intervals $x_1 \in I_1$ and $x_2 \in I_2$ such that:

$$\int_{I_1} f(x)\,dx = \int_{I_2} f(x)\,dx = \epsilon$$

with:

$$\int_{I_1} f(x)\,dx = \int_{J_1} g(y)\,dy, \quad \int_{I_2} f(x)\,dx = \int_{J_2} g(y)\,dy$$

Under the transport map T:

$$y_i = T(x_i), \quad J_i = T(I_i)$$

Let's "permute" part of the map and create a new measure-preserving map $\tilde{T}$ such that:

$$\begin{aligned}\tilde{T}(x_1) = y_2, \quad \tilde{T}(x_2) = y_1\\ \tilde{T}(I_1) = J_2, \quad \tilde{T}(I_2) = J_1\\ \tilde{T}(x) = T(x) \quad \text{if } x \in I_1 \cup I_2\end{aligned}$$

Since T was optimal:

$$\frac{1}{2}\int_{\mathbb{R}^n}(x-T(x))^2 f(x)\,dx \leq \frac{1}{2}\int_{\mathbb{R}^n}(x-\tilde{T}(x))^2 f(x)\,dx$$

$$\Rightarrow -\int_{I_1} xT(x)f(x)\,dx - \int_{I_2} xT(x)f(x)\,dx \leq -\int_{I_1} x\tilde{T}(x)f(x)\,dx - \int_{I_2} x\tilde{T}(x)f(x)\,dx$$

$$\Rightarrow \frac{1}{\epsilon}\int_{I_1} x(\tilde{T}(x)-T(x))f(x)\,dx + \frac{1}{\epsilon}\int_{I_2} x(\tilde{T}(x)-T(x))f(x)\,dx \leq 0$$

As $\epsilon \to 0$:

$$x_1(y_2-y_1)+x_2(y_1-y_2)\leq 0$$
$$\Rightarrow (y_2-y_1)(x_2-x_1)\geq 0$$

Conclusion: The map is monotone.

Use of Cumulative Distribution Functions

We consider the use of cumulative distribution functions to analyze a monotone solution. The question arises, can we construct it? To explore this, we look at the mathematical foundation provided by these functions.

Let f be a function represented graphically, and consider its integration over a domain to define the cumulative distribution function F:

$$F(x)=\int_{-\infty}^{x} f(t)\,dt$$

Furthermore, we can define another function G as:

$$G(y)=\int_{-\infty}^{y} g(t)\,dt$$

We expect

$$F(x)=G(T(x))$$

To derive an exact solution, we consider the inverse transformation G^{-1}, leading us to express $T(x)$ as:

$$T(x)=G^{-1}(F(x))$$

This relationship provides a method to retrieve $T(x)$ explicitly, assuming the invertibility of G.

C.1.3 The Transportation Problem in $\mathbb{R}^n$

The goal of the transportation problem in $\mathbb{R}^n$ is to find a map $T(x)$ that minimizes the following objective function:

$$\frac{1}{2}\int_X |x-T(x)|^2 f(x)\,dx$$

subject to the constraint that the integral of f over any transformed region $T^{-1}(A)$ matches the integral of g over A:

$$\int_{T^{-1}(A)} f(x)\,dx = \int_A g(y)\,dy \quad \forall A$$

To address this, a change of variables $y = T(x)$ is performed, leading to the equality:

$$\int_{T^{-1}(A)} f(x)\,dx = \int_{T^{-1}(A)} g(T(x))\det(\nabla T(x))\,dx \quad \forall A$$

This transformation utilizes the determinant of the Jacobian matrix ($\nabla T(x)$ to adjust for the change in volume caused by the map T.

C.1.4 Optimality and cyclical monotonicity

We expect the transformation T to satisfy the following condition:

$$g(T(x_i))\det(DT(x_i)) = f(x_i)$$

for chosen points $x_1, x_2, \ldots, x_N \in X$.

Assuming that T is optimal, we consider the transformation at selected points $y_i = T(x_i)$. For each x_i, let E_i be a small neighborhood (a ball centered at x_i) such that:

$$\int_{E_i} f(x)\,dx < \epsilon$$

where ϵ is a small positive number.

We then define $F_i = T(E_i)$

Let's define a new map $\tilde{T}$ that is measure-preserving with specific properties. We want:

$$\begin{aligned}
\tilde{T}(x_i) &= y_{i+1}, \\
\tilde{T}(E_i) &= F_{i+1}, \\
\tilde{T}(x) &= T(x) \quad \text{if } x \notin \bigcup_{i=1}^{N} E_i.
\end{aligned}$$

This formulation ensures that $\tilde{T}$ modifies the behavior of T at specific points x_i and on specific sets E_i, while retaining the original mapping T elsewhere.

Given that T is optimal, we establish the following inequality for the transformation:

$$\frac{1}{2}\int_X |x - T(x)|^2 f(x)\,dx \leq \frac{1}{2}\int_X |x - \tilde{T}(x)|^2 f(x)\,dx$$

As in a one-dimensional scenario, we consider:

$$\frac{1}{\epsilon}\sum_{i=1}^{N}\int_{E_i} x \cdot (\tilde{T}(x) - T(x)) f(x)\,dx \leq 0$$

Taking $\epsilon \to 0$, this implies:

$$\sum_{i=1}^{N} x_i \cdot (y_{i+1} - y_i) \leq 0$$

This condition, known as *cyclical monotonicity*, is crucial for verifying the optimality of T in transport and allocation problems.

Cyclical Monotonicity for $N = 2$

For the case where $N = 2$, consider two points x_1 and x_2 with corresponding images y_1 and y_2 under a transformation. The cyclical monotonicity condition is expressed as:

$$x_1 \cdot (y_2 - y_1) + x_2 \cdot (y_1 - y_2) \leq 0$$

which simplifies to:

$$(x_2 - x_1) \cdot (y_2 - y_1) \geq 0$$

This condition suggests that the vectors $(x_2 - x_1)$ and $(y_2 - y_1)$ form an acute angle, indicating a kind of alignment between the increments in the domain and the image under the transformation, which aligns with the theory of optimal transport.

The cyclical monotonicity condition discussed must not only hold for $N = 2$ but for any arbitrary N. This universality ensures the condition's robustness in describing the optimality of transport maps. Mathematically, we express this necessity as:

$$\sum_{i=1}^{N} x_i \cdot (y_{i+1} - y_i) \leq 0 \quad \text{(with cyclic indexing)}$$

This condition fundamentally restricts our ability to arbitrarily "twist" mass in the domain, aligning the transportation with geometrically coherent paths.

Cyclical monotonicity is not just a geometric constraint; it represents a stronger condition than being irrotational. According to the theorem (often attributed to Rockafellar), a cyclically monotone map can be expressed as the gradient of a convex function. This assertion bridges the concept of optimality in transport to convex analysis.

Theorem 16. ***(Rockafellar):*** *A map T is cyclically monotone if and only if there exists a convex function f such that $T = \nabla f$. Convexity is defined by the inequality:*

$$f(\lambda x + (1 - \lambda)y) \leq \lambda f(x) + (1 - \lambda) f(y)$$

for all x, y in the domain of f and $\lambda \in [0, 1]$.

This result implies that the gradient vector field induced by f is such that the transportation along the vector field minimizes the transport cost, adhering to the optimality conditions imposed by cyclical monotonicity.

This representation is significant due to the following mass-preservation condition that we saw derived from transport theory:

$$\det(\nabla T(x)) = \frac{f(x)}{g(T(x))}$$

Since $T(x) = \nabla u(x)$, the Jacobian matrix $\nabla T(x)$ becomes $D^2 u(x)$, the Hessian matrix of u. Therefore, the mass-preservation condition can be reformulated as:

$$\det(D^2 u(x)) = \frac{f(x)}{g(\nabla u(x))}$$

This equation is a form of the **(Monge-Ampère equation)**, linking the geometric properties of the map T with differential properties of the function u, under constraints imposed by the densities f and g.

C.2 The Kantorovich Problem

Need for a more general formulation

We seek a transport plan that allows mass to split.

Again, we have a source measure μ supported on X and a target measure ν supported on Y.

We want to know how much mass gets moved from x to y. We store this in a measure π defined on $X \times Y$.

Example of a Transport Plan

Consider a mine at $x = 0$ with 1 unit of resource and factories at $y = 0, 1$ with $\frac{1}{3}$ and $\frac{2}{3}$ units respectively.

The transport plan π is defined as follows:

$$\pi(0,0) = \frac{1}{3}, \quad \pi(0,1) = \frac{2}{3}$$

$$\pi(0, \mathbb{R}) = 1$$

In general, if $A \subseteq X$ and $B \subseteq Y$, then $\pi(A, B)$ tells us how much mass is transported from A to B.

We need to conserve mass.

Choose some $x \in X$, then:

$$\pi(x, Y) = \mu(x)$$

which represents the total mass coming from X.

More generally, if $A \subseteq X$:

$$\pi(A, Y) = \mu(A)$$

We say that μ is the marginal of π on X. Also, we need ν to be the marginal of π on Y.

If $B \subseteq Y$, then:

$$\pi(X, B) = \nu(B)$$

How do we measure cost?

The cost function $c(x, y)$ is weighted by the amount of mass moving from x to y.

$$\inf \left\{ \int_{X \times Y} c(x, y)\, d\pi(x, y) \mid \pi \in \Pi(\mu, \nu) \right\}$$

where:

$$\Pi(\mu, \nu)$$

consists of measures whose marginals on X and Y are μ and ν, respectively.

The Kantorovich problem is a classical problem in the theory of optimal transport. It can be formulated as follows:

Problem: Given two probability measures μ on X and ν on Y, the goal is to minimize the total cost of transporting mass from X to Y using a transportation plan π. The mathematical formulation is:

$$\inf \left\{ \int_{X \times Y} c(x, y) \, d\pi(x, y) \mid \pi \in \Pi(\mu, \nu) \right\}$$

where $c(x, y)$ represents the cost of transporting mass from x to y, and $\Pi(\mu, \nu)$ is the set of all measures on $X \times Y$ with marginals μ on X and ν on Y.

Feasibility: A plan π is feasible if it respects the mass balance between μ and ν, meaning that the total mass sent from X equals the total mass received in Y.

Existence of a Solution: As long as the cost function c is bounded below and both X and Y are bounded spaces, there exists an infimum that is finite.

Question: The main question remains, can we find a minimizer for this infimum?

C.2.1 Existence of a Minimum in the Kantorovich Problem

We approach the existence of a minimum for the Kantorovich problem through compactness and continuity arguments.

Theorem 17. ***Weierstrass:*** *If $f : U \to \mathbb{R}$ is continuous and U is compact, then f attains a minimum on U. This theorem is fundamental in analysis and applicable in many areas of optimization.*

Applying this to the Kantorovich problem, consider the following:

Theorem 18. *Suppose $X, Y \subseteq \mathbb{R}^n$ are compact and that the cost function $c(x, y)$ is continuous. Then the Kantorovich problem has a minimum.*

Proof. Since X and Y are compact, the product space $X \times Y$ is also compact. The continuity of $c(x, y)$ ensures that the functional

$$\int_{X \times Y} c(x, y) \, d\pi(x, y)$$

is well-defined and continuous under the weak topology of probability measures. By the Weierstrass theorem, since the set of all transportation plans $\Pi(\mu, \nu)$ is non-empty and compact in the weak topology, there exists a minimizer for the Kantorovich problem.

Convergence in the Space of Probability Measures

Before discussing compactness, it is essential to establish a notion of convergence. We consider the space $U = \Pi(\mu, \nu)$ where, without loss of generality, these are probability measures.

Definition of Convergence: We say that a sequence of measures γ_n converges to γ in U if for every continuous bounded function g on $X \times Y$, the following holds:

$$\int_{X\times Y} g(x,y)\, d\gamma_n(x,y) \to \int_{X\times Y} g(x,y)\, d\gamma(x,y) \text{ as } n \to \infty.$$

$$\forall g \in C_b(X \times Y)$$

Here, $C_b(X\times Y)$ represents the space of all bounded continuous functions defined on the Cartesian product $X \times Y$.

This type of convergence is often referred to as weak* convergence in the space of measures.

This setup is crucial for applying compactness arguments in proving the existence of a minimizer in the Kantorovich problem, as continuity and boundedness of the cost function along with the weak* convergence ensure that the functional being minimized is well-behaved. We now demonstrate the compactness of the set $\Pi(\mu, \nu)$ in the weak* topology, which is instrumental in proving the existence of a minimizer for the Kantorovich problem.

Step 1: Choosing a Measure. Begin by selecting any probability measure π_0 from $\Pi(\mu, \nu)$.

Step 2: Subsequence Extraction. Given a sequence of probability measures $\{\pi_n\}$, we need to show that it is possible to extract a convergent subsequence. Since π_n are all probability measures, and assuming the space $X \times Y$ is Polish (complete and separable), by Prokhorov's theorem, which states that a tight family of probability measures on a Polish space is relatively compact, we can extract a convergent subsequence:

$$\pi_{n_k} \to \pi \text{ in the weak* topology as } k \to \infty.$$

This convergence implies that the limit π is also a probability measure.

Implication of Convergence. This convergence is critical because it ensures that every sequence of measures in $\Pi(\mu, \nu)$ has a convergent subsequence, thereby establishing the compactness of $\Pi(\mu, \nu)$ under the weak* topology. Compactness, combined with the lower semicontinuity of the cost function, ensures the existence of a minimizer for our Kantorovich problem.

Checking the Marginals: To verify this, consider a measure π in the limit of a sequence $\{\pi_n\}$ converging to π within the set $\Pi(\mu, \nu)$. For each measure π_n, the marginals over X and Y match μ and ν respectively. We must show that this property holds for π as well.

For any function g in $C(X)$ (the space of continuous functions on X), the integral of g over X with respect to the measure π_n converges to the integral with respect to π:

$$\int_{X\times Y} g(x)\, d\pi(x,y) = \lim_{k\to\infty} \int_{X\times Y} g(x)\, d\pi_{n_k}(x,y)$$

This convergence ensures that:

$$\int_X g(x)\, d\mu(x) = \int_{X\times Y} g(x)\, d\pi(x,y)$$

implying that the marginal of π over X is indeed μ, and a similar argument holds for ν over Y.

Conclusion: compactness of $\Pi(\mu,\nu)$ Since π_{n_k} converges to π and all π_{n_k} are in $\Pi(\mu,\nu)$, the limit measure π also respects the marginal conditions, and thus, $\pi \in \Pi(\mu,\nu)$.

Now that we have established that $\Pi(\mu,\nu)$ is compact, let's look at the continuity of the functional F over this set.

Continuity of F: The functional F applied to a transportation plan π is defined by:

$$F(\pi) = \int_{X\times Y} c(x,y)\, d\pi(x,y)$$

where $c(x,y)$ represents the cost of transporting mass from x to y.

To confirm the continuity of the functional F, consider a sequence of transportation plans $\{\pi_n\}$ in $\Pi(\mu,\nu)$ converging to some π in the same set. We need to show that $F(\pi_n)$ converges to $F(\pi)$.

Functional Formulation: The functional F for any measure π is defined as:

$$F(\pi) = \int_{X\times Y} c(x,y)\, d\pi(x,y)$$

where $c(x,y)$ is the cost function.

Since π_n converges to π in the weak* sense, and given that c is a continuous and bounded function, we apply the definition of weak* convergence:

$$\int_{X\times Y} c(x,y)\, d\pi_n(x,y) \to \int_{X\times Y} c(x,y)\, d\pi(x,y)$$

as $n \to \infty$. This implies that $F(\pi_n)$ converges to $F(\pi)$.

The convergence of $F(\pi_n)$ to $F(\pi)$ under weak* convergence of π_n to π establishes that F is continuous on $\Pi(\mu,\nu)$.

Final conclusion: The Kantorovich problem, a fundamental question in optimal transport theory, involves minimizing a real-valued, continuous function over a compact set. This setup is ideal for applying classical results from real analysis.

The problem seeks to minimize:

$$F(\pi) = \int_{X\times Y} c(x,y)\, d\pi(x,y)$$

over the set $\Pi(\mu,\nu)$, which is compact by previous discussions. According to the Weierstrass Extreme Value Theorem, every continuous function on a compact set attains its minimum. Therefore:

The Kantorovich problem admits a minimizer.

This conclusion hinges on the compactness of $\Pi(\mu, \nu)$ and the continuity of the cost function $c(x, y)$, ensuring the existence of an optimal transport plan that minimizes the transportation cost.

□

C.3 Dual Problem: Discrete Case

Consider the discrete case:

$$\mu(x) = \sum_{i=1}^{n} u_i \delta_{x_i}(x) \quad \text{and} \quad \nu(y) = \sum_{j=1}^{m} v_j \delta_{y_j}(y)$$

Π is also finite-dimensional. Π_{ij} tells us how much mass moves from x_i to y_j.

Constraints:

$$\sum_{j=1}^{m} \Pi_{ij} = \mu_i \quad \forall i$$

$$\sum_{i=1}^{n} \Pi_{ij} = \nu_j \quad \forall j$$

$$\Pi_{ij} \geq 0$$

Objective function:

$$\sum_{i=1}^{n} \sum_{j=1}^{m} C_{ij} \Pi_{ij}$$

C.3.1 Discrete Optimization Problem

The discrete optimization problem is to minimize:

$$\sum_{i=1}^{n} \sum_{j=1}^{m} C_{ij} \Pi_{ij}$$

Subject to:

$$\sum_{j=1}^{m} \Pi_{ij} = \mu_i \quad i = 1, \ldots, n$$

$$\sum_{i=1}^{n} \Pi_{ij} = \nu_j \quad j = 1, \ldots, m$$

$$\Pi_{ij} \geq 0 \quad i = 1, \ldots, n, \ j = 1, \ldots, m$$

This is a linear program ! So we can write a dual linear program

C.3.2 Linear Program Duality

L.P. have a dual problem.

The primal problem is to minimize:

$$\min \mathbf{b}^T \mathbf{y}$$

Subject to:

$$A\mathbf{y} = \mathbf{c}$$

$$\mathbf{y} \geq 0$$

The dual problem is to maximize:

$$\max \mathbf{c}^T \mathbf{x}$$

Subject to:

$$A\mathbf{x} \leq \mathbf{b}$$

The dual formulation for our problem is:

The role of x is played by $u_1, \ldots, u_n, v_1, \ldots, v_m$.

Maximize:

$$\sum_{i=1}^{n} u_i \mu_i + \sum_{j=1}^{m} v_j \nu_j$$

Subject to:

$$u_i + v_j \leq C_{ij} \quad \forall i = 1, \ldots, n,\ j = 1, \ldots, m$$

Moreover, the max of the dual is equal to the min of the primal.

C.3.3 ContinuousMeasures

Can we write down something like this for more general measures μ and ν? Propose to study: Maximize:

$$\int_X u(x)\, d\mu(x) + \int_Y v(y)\, d\nu(y)$$

Subject to:

$$u(x) + v(y) \leq C(x, y) \quad \forall (x, y) \in X \times Y$$

Let

$$\Phi = \{(u, v) \in C^0(X) \times C^0(Y) \mid u(x) + v(y) \leq C(x, y)\}$$

$$J[u, v] = \int_X u(x)\, d\mu(x) + \int_Y v(y)\, d\nu(y)$$

Let

$$I[\pi] = \int_{X \times Y} C(x, y)\, d\pi(x, y)$$

Make the observation:

$$J[u,v] = \int_X u(x)\,d\mu(x) + \int_Y v(y)\,d\nu(y)$$

$$= \int_{X\times Y} u(x)\,d\pi(x,y) + \int_{X\times Y} v(y)\,d\pi(x,y)$$

$$= \int_{X\times Y} (u(x)+v(y))\,d\pi(x,y)$$

$$\leq \int_{X\times Y} C(x,y)\,d\pi(x,y) = I[\pi]$$

This is weak duality.

Could we get equality using optimal values of u, v, π?

$$\inf_{\pi\in\Pi(\mu,\nu)} I[\pi] = \inf_{\pi}\left\{ I[\pi] + \begin{cases} 0 & \pi\in\Pi(\mu,\nu) \\ +\infty & \text{o.w.} \end{cases} \right\}$$

$$= \inf_{\pi} I[\pi] + \sup_{u,v}\left[\int_X u(x)\,d\mu(x) + \int_Y v(y)\,d\nu(y) - \int_{X\times Y} (u(x)+v(y))\,d\pi(x,y) \right]$$

Why does this work?

Suppose $\pi \notin \Pi(\mu,\nu)$. Then we can certainly find u, v such that:

$$\int_X u(x)\,d\mu(x) + \int_Y v(y)\,d\nu(y) - \int_{X\times Y} (u(x)+v(y))\,d\pi(x,y) = K \neq 0$$

Then inputting $\pm Mu, \pm Mv$

$$\Rightarrow \text{get value of } \pm MK \text{ which is unbounded}$$

$$\Rightarrow \text{supremum is infinite}$$

$$\inf_{\pi\in\Pi(\mu,\nu)} I[\pi] = \inf_{\pi}\sup_{u,v}\left\{ I[\pi] + \int_X u(x)\,d\mu(x) + \int_Y v(y)\,d\nu(y) - \int_{X\times Y} (u(x)+v(y))\,d\pi(x,y) \right\}$$

$$= \sup_{u,v}\inf_{\pi}\{\ldots\}$$

$$= \sup_{u,v}\left\{ \int_X u(x)\,d\mu(x) + \int_Y v(y)\,d\nu(y) \right\}$$

$$+ \inf_{\pi}\left\{ \int_{X\times Y} C(x,y)\,d\pi(x,y) - \int_{X\times Y} (u(x)+v(y))\,d\pi(x,y) \right\}$$

Suppose $u + v \leq C$ everywhere.

$$\int_{X\times Y} (C(x,y) - (u(x) + v(y)))\, d\pi(x,y) \geq 0$$

And the infimum is 0 since π is a positive measure. Suppose $u(x) + v(y) > C(x^*, y^*)$.

For example: $\pi(x,y) = M\delta_{x^*,y^*}$.

Taking $M \to \infty$,

$$\int_{X\times Y} (C(x,y) - (u(x) + v(y)))\, d\pi(x,y) \to -\infty$$

$$\Rightarrow \text{The infimum is } -\infty$$

$$\inf_{\pi\in\Pi(\mu,\nu)} I[\pi] = \inf_{\pi} \sup_{u,v} \left\{ I[\pi] + \begin{cases} J[u,v] & (u,v) \in \Phi \\ -\infty & \text{o.w.} \end{cases} \right\}$$

$$= \sup_{(u,v)\in\Phi} J[u,v]$$

It's reasonable (maybe) to expect no duality gap.

Refer to Villani (1.1.6, p.23) for the mini-max principle that allows this.

For now we work with quadratic cost:

$$C(x,y) = \frac{1}{2}\|x-y\|^2$$

We need tools from convex analysis.

C.4 Convex Sets and Convex Functions

Definition: A set E is convex if whenever $x, y \in E$ and $\lambda \in [0,1]$,

$$\lambda x + (1-\lambda)y \in E.$$

Definition: A function f defined on a convex set E is convex if $\forall x, y \in E$ and $\lambda \in [0,1]$,

$$f(\lambda x + (1-\lambda)y) \leq \lambda f(x) + (1-\lambda) f(y).$$

Properties of convex functions:

- A convex function is locally Lipschitz on the interior of its domain.
- A convex function is differentiable almost everywhere on its domain.

- If $\mathbf{v} \in \mathbb{R}^n$ with $\|\mathbf{v}\| = 1$, the directional derivative of f in the direction $\mathbf{v}$ is defined for $x \in E^\circ$:

$$\frac{\partial f}{\partial \mathbf{v}}(x) = \lim_{h\to 0^+} \frac{f(x+h\mathbf{v}) - f(x)}{h}$$

- If $f \in C^2$, then it is convex if and only if:

$$D^2 f(x) \geq 0 \quad \forall x \in E$$

C.4.1 Subgradient

- We can generalize the gradient to the subgradient.

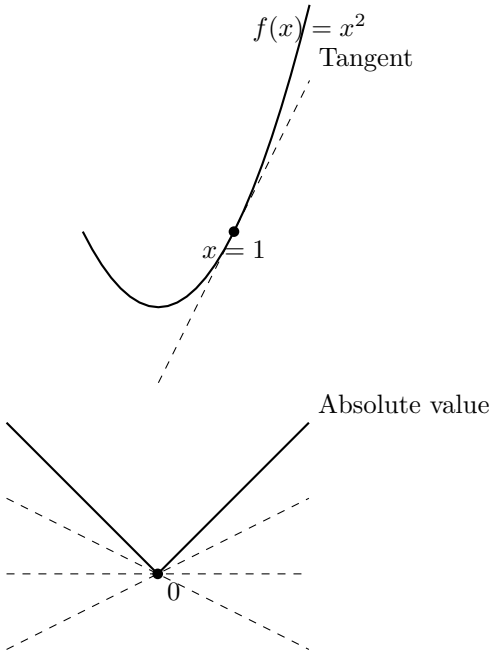

The subdifferential consists of a set of slopes of *all tangent lines* to f.
We need to decide on admissible slopes.
Let ρ be such a slope for f at the point x_0.
The tangent line is given by:

$$L(x) = f(x_0) + \rho \cdot (x - x_0)$$

We require $L(x) \leq f(x)$ for all x.
The subgradient of f at a point $x \in E$ is:

$$\partial f(x) = \{\rho \mid f(y) \geq f(x) + \rho \cdot (y - x) \quad \forall y \in E\}$$

The subgradient of f over a set U is:

$$\partial f(U) = \bigcup_{x \in U} \partial f(x)$$

Exemple: $f(x) = |x|$

$$\partial f(0) = [-1, 1]$$

$$\partial f(1) = \{1\}$$

Exemple: $u(x_1, x_2) = \sqrt{x_1^2 + x_2^2}$**)**

We want to find $\partial u(\vec{x})$

At $x = \vec{0}$, we need ρ such that:

$$|y| = \sqrt{y_1^2 + y_2^2} \geq \rho \cdot y$$

If $y = 0$, this always holds.

At $y \neq 0$, we need $\rho \cdot y \leq \sqrt{y_1^2 + y_2^2}$.

$$\rho \cdot y \leq \frac{|\rho||y|}{|y|} = |\rho|$$

This always holds for $|\rho| \leq 1$.

If $\rho = \frac{y}{|y|}$, we get equality, i.e., if $|\rho| > 1$, we can find y to violate $\frac{\rho \cdot y}{|y|} \leq 1$.

$$\partial u(\vec{0}) = \{\rho \in \mathbb{R}^2 \mid |\rho| \leq 1\} = \overline{B(\vec{0}, 1)}$$

$$\therefore \partial u(\vec{x}) = \begin{cases} \overline{B}(\vec{0}, 1) & \text{if } \vec{x} = \vec{0} \\ \frac{\vec{x}}{|\vec{x}|} & \text{o.w.} \end{cases}$$

$$\partial u(\mathbb{R}^2) = \overline{B}(\vec{0}, 1)$$

C.4.2 Ligendre Transforms

Suppose f is convex on $\mathbb{R}$.

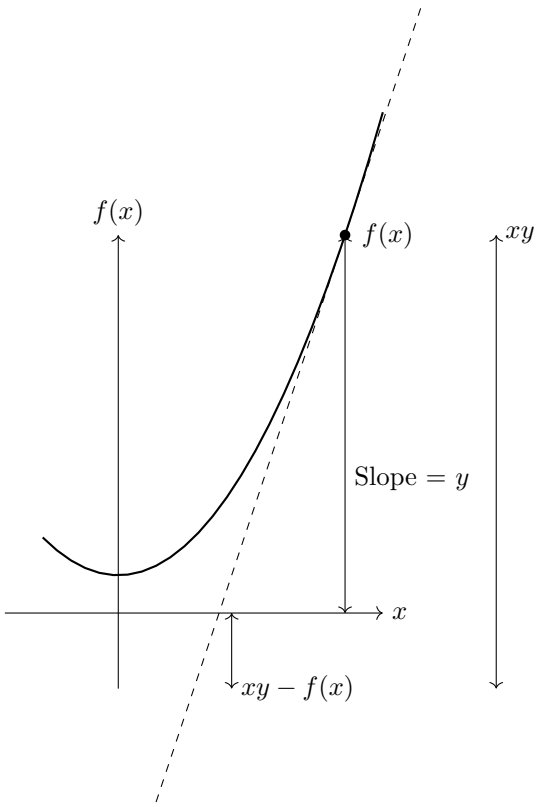

For fixed x, define $g(y) = xy - f(x)$ where $y = f'(x)$.

This extra condition also comes from differentiating g with respect to y and setting it to zero.

This zero derivative evoques an optimization, then maybe

$$g(y) = \max / \min_x \{xy - f(x)\}$$

$f(x)$ is convex.
$xy - f(x)$ is concave.
Makes sense to maximize.
Propose:

$$g(y) = \max_x \{xy - f(x)\}$$

May be interesting.
Define the Legendre-Fenchel transform of f by:

$$f^*(y) = \sup_{x \in E} \{xy - f(x)\}$$

Example 1: $f(x) = 0$, $E = \mathbb{R}$

$$f^*(y) = \sup_{x\in\mathbb{R}}\{xy\} = \begin{cases} 0 & \text{if } y = 0 \\ \infty & \text{if } y \neq 0 \end{cases}$$

$$\text{dom}(f^*) = \{0\}$$

Example 2: $f(x) = 0$, $E = [-1, 1]$

$$f^*(y) = \sup_{x\in[-1,1]}\{xy\} = |y|$$

$$\text{dom}(f^*) = \mathbb{R}$$

Example 3: $f(x) = \rho \cdot x$

$$f^{**}(x) = \rho \cdot x$$

We can take repeated L-F transforms (biconjugate of f).
Property: f^* is convex.
Let $y_1, y_2 \in \text{dom}(f^*)$ and $\lambda \in [0, 1]$:

$$f^*(\lambda y_1 + (1-\lambda)y_2)$$

$$= \sup_x\{\lambda x \cdot y_1 + (1-\lambda)x \cdot y_2 - f(x)\}$$

$$\leq \sup_x\{\lambda x \cdot y_1 - \lambda f(x)\} + \sup_x\{(1-\lambda)x \cdot y_2 - (1-\lambda)f(x)\}$$

$$= \lambda f^*(y_1) + (1-\lambda)f^*(y_2)$$

Property: $\forall x \in \text{dom}(f)$ and $y \in \text{dom}(f^*)$ then:

$$f(x) + f^*(y) \geq x \cdot y$$

with equality if and only if $y \in \partial f(x)$.
Proof:
Inequality is immediate. Let $y \in \partial f(x)$:

$$\begin{aligned} &\Leftrightarrow f(z) \geq f(x) + y \cdot (z - x) \quad \forall z \\ &\Leftrightarrow xy - f(x) \geq zy - f(z) \quad \forall z \\ &\Leftrightarrow xy - f(x) \geq \sup_z\{zy - f(z)\} = f^*(y) \\ &\Leftrightarrow f(x) + f^*(y) \leq xy \end{aligned}$$

Combined with $f(x) + f^*(y) \geq xy \quad \forall x, y$,
we get the equality.
A few propeties:
Property 1: If $f \leq g$ everywhere then $g^* \leq f^*$.
Property 2: If f is convex and lower semi-continuous, then $f^{**}(x) = f(x)$.

First, we know that $f(x) + f^*(y) \geq x \cdot y$.

$$\Rightarrow f^{**}(x) = \sup_y \{x \cdot y - f^*(y)\} \leq f(x)$$

so we get: $f(x)^{**} \leq f(x)$

to obtain the reversed sens of the iniquality, we introduce the representation of a convex function as a supremum of a familly of hyperplans as for exemple:

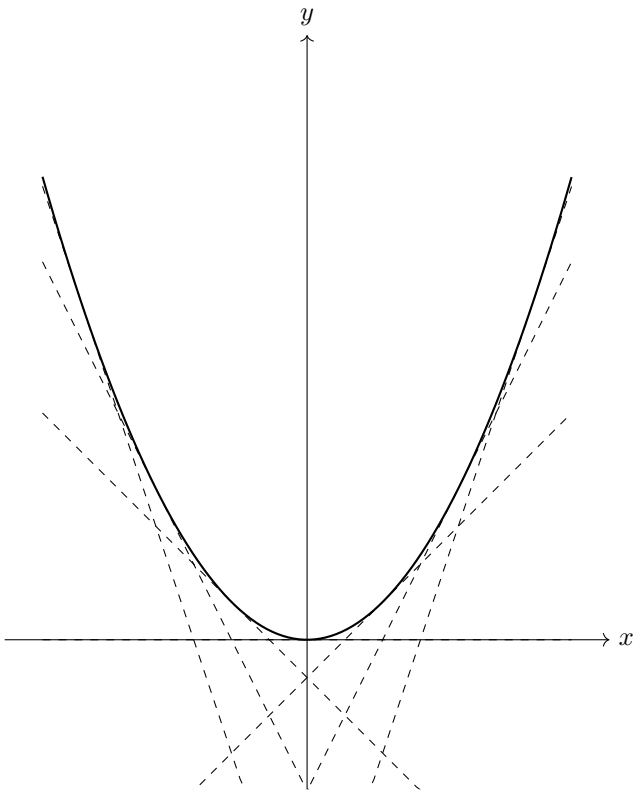

$$f(x) = \sup_{\alpha \in \mathcal{A}} \{L^\alpha(x)\}$$

Choose any $\alpha \in \mathcal{A}$:

$$f(x) \geq L^\alpha(x)$$

$$\Rightarrow f^*(y) \leq (L^\alpha)^*(y)$$

$$\Rightarrow f^{**}(x) \geq (L^\alpha)^{**}(x)$$

$$= L^\alpha(x)$$

Since L^α is affine:

$$\Rightarrow f^{**}(x) \geq \sup_\alpha L^\alpha(x) = f(x)$$

$$\therefore f^{**} = f$$

It's now reasonable to talk about convex L-F dual functions φ, ψ such that:

$$\varphi = \psi^* \quad \text{and} \quad \psi = \varphi^*$$

Property: If $\varphi(x), \psi(y)$ are L-F duals on bounded domains X, Y, then they have uniform Lipschitz bounds.

Proof:

$$\begin{aligned}
\varphi(x_1) - \varphi(x_2) &= \sup_{y\in Y}\{x_1 \cdot y - \psi(y)\} - \sup_{y\in Y}\{x_2 \cdot y - \psi(y)\} \\
&\leq \sup_{y\in Y}\{x_1 \cdot y - \psi(y)\} - (x_2 \cdot y_1 - \psi(y_1)) + \epsilon \quad \forall \epsilon > 0 \\
&\leq (x_1 - x_2) \cdot y_1 + \epsilon \\
&\leq \sup_{y\in Y} |(x_1 - x_2) \cdot y| + \epsilon
\end{aligned}$$

Taking $\epsilon \to 0$:

$$\varphi(x_1) - \varphi(x_2) \leq M|x_1 - x_2|$$

Similarly, we get:

$$|\varphi(x_1) - \varphi(x_2)| \leq M|x_1 - x_2|$$

$\therefore \varphi, \psi$ are uniformly Lipschitz.

C.4.3 Legendre Pairs and Dual Problems

Let's go back to the dual problem (DP) for $c(x, y) = \frac{1}{2}|x - y|^2$.

$$\max_{(u,v)\in\Phi} J[u, v]$$

$$J[u, v] = \int_X u(x)\, d\mu(x) + \int_Y v(y)\, d\nu(y)$$

We want to use tools from convex analysis. Let's transform:

$$\varphi(x) = \frac{1}{2}|x|^2 - u(x), \quad \psi(y) = \frac{1}{2}|y|^2 - v(y)$$

Instead of maximizing J, we minimize $-J$:

$$-J = -\int_X u(x)\,d\mu(x) - \int_Y v(y)\,d\nu(y)$$

$$= \int_X \left(\varphi(x) - \frac{1}{2}|x|^2\right) d\mu(x) + \int_Y \left(\psi(y) - \frac{1}{2}|y|^2\right) d\nu(y)$$

Or just minimize:

$$\int_X \varphi(x)\,d\mu(x) + \int_Y \psi(y)\,d\nu(y)$$

$$\equiv \mathcal{L}[\varphi, \psi]$$

Constraints:

$$\frac{1}{2}|x-y|^2 \geq u(x) + v(y) = \frac{1}{2}|x|^2 - \varphi(x) + \frac{1}{2}|y|^2 - \psi(y)$$

$$\Rightarrow \varphi(x) + \psi(y) \geq x \cdot y$$

$$\Phi^* = \left\{(\varphi, \psi) \in C^0(X) \times C^0(Y) \mid \varphi(x) + \psi(y) \geq x \cdot y \quad \forall x \in X, y \in Y\right\}$$

where

$$C^0(X)$$

means the continuous bounded real function on X

New problem is $(DP)^*$:

$$\min_{(\varphi,\psi)\in\Phi^*} \mathcal{L}[\varphi, \psi]$$

The feasible set is non-empty (large constant functions).

Let's try to understand what feasible pairs actually look like.

Let $(\varphi, \psi) \in \Phi^*$:

$$\Rightarrow \varphi(x) \geq x \cdot y - \psi(y) \quad \forall x, y$$

$$\Rightarrow \varphi(x) \geq \psi^*(x)$$

$$\Rightarrow \psi(y) \geq \psi^{**}(y)$$

$$\Rightarrow \psi^*(x) + \psi^{**}(y) \geq x \cdot y$$

We have a new feasible pair (ψ^*, ψ^{**}), which are L-F duals.

Let's look at the objective function:

$$\mathcal{L}[\psi^*, \psi^{**}] = \int_X \psi^*(x)\, d\mu(x) + \int_Y \psi^{**}(y)\, d\nu(y)$$

$$\leq \int_X \varphi(x)\, d\mu(x) + \int_Y \psi(y)\, d\nu(y)$$

$$= \mathcal{L}[\varphi, \psi]$$

Conclusion:
We can minimize over this set:

$$\Phi^* = \{(\varphi, \psi) \in \Phi^* \mid \varphi = \psi^*,\, \psi = \varphi^*\}$$

C.5 Characterising the Optimal Map

$$\text{minimize } \mathcal{L}[\varphi, \psi] \quad (\text{DP})^*$$
$$\text{subject to } (\varphi, \psi) \in \Phi^*$$

We can assume that:

$$\varphi(x) = \sup_{y \in Y} \{x \cdot y - \psi(y)\}$$

$$\psi(y) = \sup_{x \in X} \{x \cdot y - \varphi(x)\}$$

Both φ and ψ are convex.
Is $\mathcal{L}$ bounded below?

$$\mathcal{L}[\varphi, \psi] = \frac{1}{2}\int_X |x|^2 d\mu(x) + \frac{1}{2}\int_Y |y|^2 d\nu(y) - J[u, v]$$

$$\geq \frac{1}{2}\int_X |x|^2 d\mu(x) + \frac{1}{2}\int_Y |y|^2 d\nu(y) - I[\pi]$$

for any feasible $\pi \in \Pi(\mu, \nu)$.
This is by weak duality.
This RHS is finite. $\mathcal{L}$ is bounded below and the infimum is well-defined.
Is it a minimum?
Note: If $(\varphi, \psi) \in \Phi^*$, then $\forall a \in \mathbb{R}$,

$$(\varphi - a, \psi + a) \in \Phi^*$$

We can restrict to $(\varphi, \psi) \in \Phi^*$ such that

$$\inf_{x \in X} \varphi(x) = 0$$

Let $(\varphi_n, \psi_n) \in \Phi^*$ such that $\mathcal{L}[\varphi_n, \psi_n] \to \inf \mathcal{L}[\varphi, \psi]$.
These are L-F duals and X, Y are bounded.

$$\Rightarrow \text{uniform Lipschitz bounds}$$

$$\Rightarrow \text{equicontinuous}$$

$$0 \leq \varphi_n \leq \text{Lip}(\varphi_n) \cdot \text{diam}(X)$$

$$\leq \sup_{y \in Y} |y| \cdot \text{diam}(X)$$

We can do the same thing for ψ_n.

$$\Rightarrow \text{sequences are uniformly bounded}$$

By Ascoli-Arzelà:

$$\exists \text{ a uniformly convergent subsequence}$$

$$\varphi_{n_k} \to \varphi, \quad \psi_{n_k} \to \psi$$

$$(\varphi, \psi) \in \Phi^*$$

$$\mathcal{L}[\varphi, \psi] = \lim_{k \to \infty} \mathcal{L}[\varphi_{n_k}, \psi_{n_k}]$$

$$= \inf_{(\varphi, \psi) \in \Phi^*} \mathcal{L}[\varphi, \psi]$$

$$\therefore (\varphi, \psi) \text{ are minimizers of (DP)}^*$$

Let's focus on the case where μ and ν are "nice enough" i.e. if $|E| = 0$ then $\mu(E) = \nu(E) = 0$.

We have an optimal pair (φ, ψ) for $(\text{DP})^*$.

They are convex duals and they are differentiable a.e.

We know that $\forall x \in X$ we can choose some $y \in \partial\varphi(x)$ and have

$$x \cdot y = \varphi(x) + \psi(y)$$

For a.e. $x \in X$, this y is unique: $y = \nabla\varphi(x)$.

Let's say $\forall x \in \hat{X}$, φ is differentiable and $|\hat{X}| = |X|$.

We've found a natural relationship between points in X and Y.

Let's define $T(x)$ for $x \in X$ so that

$$T(x) \in \partial\varphi(x)$$

(for $x \in \hat{X}$, $T(x) = \nabla\varphi(x)$).

Does this map solve the Monge formulation?

(Q1): Is T measure-preserving?
Try to show that

$$\int_X h(T(x))\,d\mu(x) = \int_Y h(y)\,d\nu(y) \quad \forall h \in C(\bar{Y})$$

Introduce:

$$\psi_\epsilon(y) = \psi(y) + \epsilon h(y)$$

$$\varphi_\epsilon(x) = \sup_{y\in Y}\{x\cdot y - \psi_\epsilon(y)\} = \sup_{y\in Y}\{x\cdot y - \psi(y) - \epsilon h(y)\}$$

$$(\varphi_\epsilon, \psi_\epsilon) \in \Phi^*$$

Since (φ, ψ) are optimal:

$$0 \le \frac{\mathcal{L}[\varphi_\epsilon, \psi_\epsilon] - \mathcal{L}[\varphi, \psi]}{\epsilon}$$

$$= \int_X \frac{\varphi_\epsilon(x) - \varphi(x)}{\epsilon}\,d\mu(x) + \int_Y h(y)\,d\nu(y)$$

Need to argue about the limiting value. Notice: - We could integrate over $\hat{X}$ instead of X.
For $x \in \hat{X}$,

$$\varphi(x) = \sup_{y\in Y}\{x\cdot y - \psi(y)\}$$

There is a unique maximizer at $y = T(x) = \nabla\varphi(x)$.

$$\varphi(x) = x\cdot T(x) - \psi(T(x))$$

For $x \in \hat{X}$,

$$\varphi_\epsilon(x) = \sup_{y\in Y}\{x\cdot y - \psi(y) - \epsilon h(y)\}$$

This has a maximizer $y_\epsilon = T(x) + o(1)$.

$$\varphi_\epsilon(x) = x\cdot y_\epsilon - \psi(y_\epsilon) - \epsilon h(y_\epsilon)$$

For $x \in \hat{X}$,

$$\varphi_\epsilon(x) - \varphi(x) = x\cdot y_\epsilon - \psi(y_\epsilon) - \epsilon h(y_\epsilon) - \varphi(x)$$

$$\le \varphi(x)$$

$$\varphi_\epsilon(x) - \varphi(x) \le -\epsilon h(y_\epsilon)$$

$$= -\epsilon h(T(x) + o(1)) = -\epsilon h(T(x)) + o(\epsilon)$$

$$\varphi_\epsilon(x) - \varphi(x) \geq x \cdot T(x) - \psi(T(x)) - \epsilon h(T(x)) - \varphi(x)$$

$$= \varphi(x) - \epsilon h(T(x)) - \varphi(x)$$

$$= -\epsilon h(T(x))$$

$$\frac{\varphi_\epsilon(x) - \varphi(x)}{\epsilon} = -h(T(x)) + o(1)$$

If we want to integrate $\frac{\varphi_\epsilon - \varphi}{\epsilon}$,
use the Dominated Convergence Theorem.

$$\frac{\varphi_\epsilon(x) - \varphi(x)}{\epsilon} \leq -h(y_\epsilon) \leq \|h\|_\infty$$

$$\frac{\varphi_\epsilon(x) - \varphi(x)}{\epsilon} \geq -h(T(x)) \geq -\|h\|_\infty$$

$$\Rightarrow \int_X \frac{\varphi_\epsilon(x) - \varphi(x)}{\epsilon}\, d\mu(x) = -\int_X h(T(x))\, d\mu(x)$$

Taking $\epsilon \to 0$ we get:

$$0 \leq -\int_X h(T(x))\, d\mu(x) + \int_Y h(y)\, d\nu(y)$$

Repeat with $-h$:

$$\therefore \int_X h(T(x))\, d\mu(x) = \int_Y h(y)\, d\nu(y)$$

$$\therefore T\#\mu = \nu$$

The cost we want to minimize is

$$\rho(s) = \frac{1}{2}\int_X |x - s(x)|^2\, d\mu(x)$$

Choose any s such that $\int s\, d\mu = \nu$.

$$\rho(s) = \int_X \left(\frac{1}{2}|x|^2 + \frac{1}{2}|s(x)|^2 - x \cdot s(x)\right) d\mu(x)$$

$$s(x) \in \Psi \implies x \cdot s(x) \leq \Phi(x) + \Psi(s(x)) \quad \text{(constraint from DP*)}$$

$$\rho(s) \geq \int_X \left(\frac{1}{2}|x|^2 + \frac{1}{2}|s(x)|^2 - \Phi(x) - \Psi(s(x)) \right) d\mu(x)$$

$$= \int_X \left(\frac{1}{2}|x|^2 - \Phi(x) \right) d\mu(x) + \int_Y \left(\frac{1}{2}|y|^2 - \Psi(y) \right) d\nu(y)$$

$$= \int_X \left(\frac{1}{2}|x|^2 + \frac{1}{2}|T(x)|^2 - \Phi(x) - \Psi(T(x)) \right) d\mu(x)$$

$$= \int_X \left(\frac{1}{2}|x|^2 + \frac{1}{2}|T(x)|^2 - x \cdot T(x) \right) d\mu(x)$$

$$= \rho(T)$$

$$\therefore T \text{ is optimal}$$

We know: $\exists$ convex function Φ such that the optimal map $T(x) = \nabla\Phi(x)$ a.e. $x \in X$.

This was needed to give us the Monge-Ampère equation.

If $d\mu(x) = f(x)\,dx$ and $d\nu(y) = g(y)\,dy$, then mass conservation implies

$$g(T(x)) \det(\nabla T(x)) = f(x)$$

$$\implies \det(\nabla^2\Phi(x)) = \frac{f(x)}{g(\nabla\Phi(x))}$$

where Φ is convex.

C.6 Brenier's Polar Factorisation

Let $\Omega \subseteq \mathbb{R}^n$ be open, bounded with $|\partial\Omega| = 0$. Let $r : \Omega \to \mathbb{R}^n$ be any non-degenerate, L^2 vector-valued mapping,

i.e., if $|N| = 0 \implies |r^{-1}(N)| = 0$.

Then $\exists$ a convex function $\Psi : \Omega \to \mathbb{R}$ (up to additive constants) and a measure-preserving rearrangement $S : \Omega \to \Omega$ such that

$$r(x) = \nabla\Psi(S(x)).$$

Proof

We want to modify $(DP)^*$ to study this:

Minimize

$$\mathcal{L}(\varphi, \psi) = \int_\Omega (\varphi(r(x)) + \psi(x))\,dx$$

subject to

$$\varphi(x) + \psi(y) \geq x \cdot y \quad \forall x, y$$

As before, we can assume that φ, ψ are convex duals.

Is $\mathcal{L}$ bounded below?

$$\hat{\mathcal{L}}(\varphi, \psi) \geq \int_\Omega r(x) \cdot x \, dx$$

$$\geq -\sqrt{\left(\int_\Omega |r(x)|^2 \, dx\right)\left(\int_\Omega |x|^2 \, dx\right)}$$

is finite since $r \in L^2$ and Ω is bounded.

$$\therefore \text{ There is an infimum.}$$

As before, there is a minimum by Ascoli-Arzelà. Can we extract a measure-preserving map S from this?

i.e., find $S(x)$ such that

$$\int_\Omega h(x) \, dx = \int_\Omega h(S(x)) \, dx \quad \forall h \in C(\overline{\Omega})$$

Let's perturb φ, ψ as before:

$$\psi_\epsilon(y) = \psi(y) + \epsilon h(y)$$

$$\varphi_\epsilon(x) = \sup_y \{x \cdot y - \psi_\epsilon(y)\}$$

This is an admissible pair.

$$0 \leq \frac{\hat{\mathcal{L}}[\varphi_\epsilon, \psi_\epsilon] - \hat{\mathcal{L}}[\varphi, \psi]}{\epsilon}$$

$$= \int_\Omega \frac{\varphi_\epsilon(r(x)) - \varphi(r(x))}{\epsilon} \, dx + \int_\Omega h(y) \, dy$$

Note: $x \cdot y - \psi(y)$ is maximized when $y = \nabla\varphi(x)$

$$\varphi(r(x)) = \sup_y \{r(x) \cdot y - \psi(y)\}$$

$$= r(x) \cdot \nabla\varphi(r(x)) - \psi(\nabla\varphi(r(x)))$$

$x \cdot y - \psi(y) - \epsilon h(y)$ is maximized when $y = \nabla\varphi(x) + o(1)$.

$$\varphi_\epsilon(r(x)) = r(x) \cdot (\nabla\varphi(r(x)) + o(1)) - \psi(\nabla\varphi(r(x)) + o(1)) - \epsilon h(\nabla\varphi(r(x)) + o(1))$$

As before, we argue that:

$$\lim_{\epsilon \to 0} \int_\Omega \frac{\varphi_\epsilon(r(x)) - \varphi(r(x))}{\epsilon} \, dx = -\int_\Omega h(\nabla\varphi(r(x))) \, dx$$

Do the same thing with $h \leftarrow -h$:

$$\therefore \int_\Omega h(\nabla\varphi(r(x)))\,dx = \int_\Omega h(y)\,dy$$

$$S(x) = \nabla\Phi(r(x))$$

is measure-preserving.

φ, ψ are Legendre duals.

$$r(x) = \nabla\Psi(S(x))$$

Example: Special Case of Vector Fields Close to Identity

Let m be any "nice enough" vector field and let $r(x) = x + \epsilon m(x)$.

$$= \nabla\Psi(S(x))$$

for some convex Ψ and measure-preserving S.

How would we factor the identity map? Use $S_0(x) = x$, $\Phi_0(x) = \frac{|x|^2}{2}$

$$\nabla\Phi_0(S_0(x)) = x$$

Make the ansatz:

$$S(x) = x + \epsilon S_1(x) + O(\epsilon^2)$$

$$\Psi(x) = \frac{|x|^2}{2} + \epsilon\Psi_1(x) + O(\epsilon^2)$$

From the Polar Factorisation of r:

$$x + \epsilon m(x) = \left(x + \epsilon S_1(x) + O(\epsilon^2)\right) + \epsilon\nabla\Psi_1\left(x + \epsilon S_1(x) + O(\epsilon^2)\right) + O(\epsilon^2)$$

$$= x + \epsilon\left(S_1(x) + \nabla\Psi_1(x)\right) + O(\epsilon^2)$$

$$\implies m(x) = S_1(x) + \nabla\Psi_1(x)$$

We also know that S is measure-preserving:

$$1 = \det(\nabla S(x))$$

$$= \det\left(I + \epsilon\nabla S_1(x) + O(\epsilon^2)\right)$$

$$= 1 + \epsilon\nabla\cdot S_1(x) + O(\epsilon^2)$$

$$\implies \nabla \cdot S_1(x) = 0$$

We found that we can decompose a vector field m into the sum of a gradient and a divergence-free field. (Helmholtz Decomposition Theorem)

This type of decomposition is useful in various fields, including fluid dynamics, electromagnetism, and the study of partial differential equations.

Helmholtz decomposition is a "linearisation" of Polar Factorisation.

Can we work back to relate Polar Fact. to an O-T like minimisation problem?

We solved:

$$\min \int (\varphi(r(x)) + \psi(x))\ dx$$

subject to

$$\varphi(x) + \psi(y) \geq x \cdot y$$

Let's make this look more like $(DP)^*$.

We have freedom to change measures.

- Let ν be the Lebesgue measure. - Want a measure $\mathcal{M}$ such that

$$\int h(r(x))\, dx = \int h(y)\, d\mu(y) \quad \forall h$$

Let $\mathcal{M} = r_{\#}\nu$ (pushforward of Lebesgue through r).

In this notation we are studying:

$$\int \varphi(y)\, d\mu(y) + \int \psi(x)\, d\nu(x)$$

subject to

$$\varphi(x) + \psi(y) \geq x \cdot y$$

This is $(DP)^*$.

Equivalent to quad-cost OT between μ and ν.

We are solving:

$$\min \int |x - T(x)|^2\, d\mu(x)$$

subject to

$$T_{\#}\mu = \nu$$

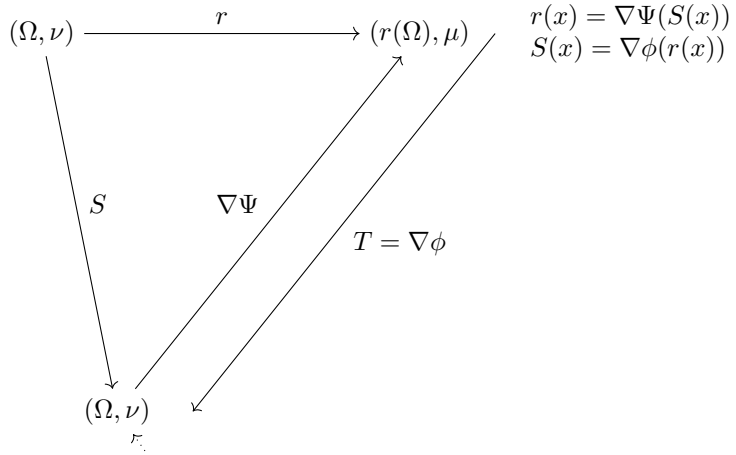

S is a measure-preserving rearrangement

$$\text{Objective function for OT is} \quad \int |x - T(x)|^2 \, d\mu(x)$$

$$= \int |r(x) - T(r(x))|^2 \, dx \quad \text{(Def. of } \mu\text{)}$$

$$= \int |r(x) - S(x)|^2 \, dx$$

We want to minimize this over measure-preserving rearrangements S.
We are looking for S "as close as possible" to r.

measure-preserving

S is the projection of r onto measure-preserving mappings.

C.7 Viscosity Solution of Monge-Ampere

Monge-Ampère Equation

$$\begin{cases} g(\nabla\varphi(x)) \det(D^2\varphi(x)) = f(x), \quad x \in \Omega \\ \varphi \text{ is convex} \end{cases} \tag{162}$$

Observations

- Expect that we need boundary conditions. For now, let's use homogeneous Dirichlet:

$$\varphi = 0 \text{ on } \partial\Omega$$

Remove Convexity Constraint

Suppose φ is any solution of the PDE and BC:

$$\begin{cases} \det(D^2\varphi) = 1 \quad \text{in } \Omega \subset \mathbb{R}^2 \\ \varphi = 0 \quad \text{on } \partial\Omega \end{cases} \tag{163}$$

Then $-\varphi$ is also a solution.

We don't have uniqueness without the convexity condition.

How do solutions behave?

Let's consider the solution of

$$\begin{cases} \varphi_{xx}\varphi_{yy} - \varphi_{xy}^2 = 1 \quad \text{in } [0,1]^2 \\ \varphi = 0 \quad \text{on } \partial[0,1]^2 \\ \varphi \text{ is convex} \end{cases} \tag{164}$$

Let's consider a point $(0, y)$ on the left side of the domain.

$$\varphi_{yy} = 0 \text{ at this point (because of BC)}$$

From the PDE:

$$\varphi_{xy}^2 + 1 = \varphi_{xx}\varphi_{yy} = 0$$

We must not actually have a classical C^2 solution.

We need a concept of weak solution.

Using integration by parts to transfer derivatives to smooth test functions doesn't work for a non-divergence structure operator.

Note: $D^2\varphi$ is a symmetric matrix.

For φ convex, $D^2\varphi \geq 0$.

Rewrite determinant as:

$$\det(D^2\varphi) = \prod_{j=1}^{n} \lambda_j(D^2\varphi)$$

and $\lambda_j(D^2\varphi) \geq 0$ if φ is convex.

Write PDE as:

$$\begin{cases} F(x, \nabla\varphi(x), D^2\varphi(x)) = 0 \\ \text{s.t. } D^2\varphi(x) \geq 0 \end{cases} \tag{165}$$

Where

$$F(x,p,M) = -g(p)\prod_{j=1}^{n}\lambda_j(M) + f(x)$$

$$\lambda_j(M) \geq 0$$

F is a monotone non-increasing function of the $\lambda_1(M),\ldots,\lambda_n(M)$ if we restrict to the constraint set.

This is also true of the Laplacian:

$$-\Delta u = -\mathrm{tr}(D^2u) = -\sum_{j=1}^{n}\lambda_j(D^2u)$$

Def: $F(x,\nabla u(x), D^2u(x),\ldots,D^nu(x))$ is a degenerate elliptic operator if it is a non-increasing function of $\lambda_1,\ldots,\lambda_n$.

- The Laplacian is elliptic.
- Monge-Ampère is elliptic on the space of convex functions.

Think about properties of the Laplacian that hopefully will generalize:

- **Maximum Principle:** If u is subharmonic ($-\Delta u \leq 0$), then

$$\max_{x\in\overline{\Omega}} u(x) = \max_{x\in\partial\Omega} u(x)$$

- **Comparison Principle:** If $-\Delta u \leq -\Delta v$ on Ω and $u \leq v$ on $\partial\Omega$, then $u \leq v$ on $\overline{\Omega}$.
- **Uniqueness**
- **Local extrema:** Let $u \in C^2$ have a local minimum at x_0.
  - 1^{st} Derivative test: $\nabla u(x_0) = 0$
  - 2^{nd} Derivative test: $D^2u(x_0) \geq 0$

$$\implies -\Delta u(x_0) = -\sum_{j=1}^{n}\lambda_j(D^2u(x_0)) \leq 0$$

Let's start by assuming

$$-\Delta u(x) + f(x) \geq 0$$

(u is a supersolution)

Pick any $x_0 \in \Omega$

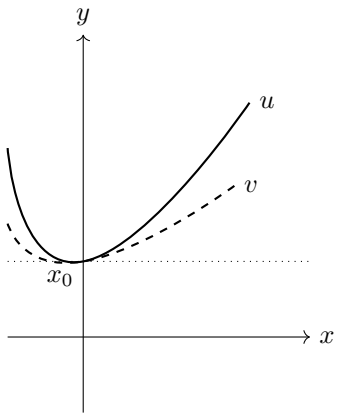

Introduce a smooth test function v.

Suppose $u - v$ has a local minimum at x_0.

$$-\Delta(u-v)(x_0) \leq 0$$

$$\implies -\Delta v(x_0) + f(x_0) \geq -\Delta u(x_0) + f(x_0) \geq 0$$

Eg: u is smooth and let $x_0 \in \Omega$.

Suppose that whenever $v \in C^2$ such that $u - v$ has a local minimum at x_0, then

$$-\Delta v(x_0) + f(x_0) \geq 0$$

Does this imply that $-\Delta u(x_0) + f(x_0) \geq 0$?

Consider

$$V(x) = u(x_0) + \nabla u(x_0) \cdot (x - x_0) + \frac{1}{2}(x - x_0)^T \left(D^2 u(x_0) - \varepsilon I\right)(x - x_0)$$

$$= u(x) + o(|x - x_0|^2) - \frac{\varepsilon}{2}|x - x_0|^2$$

$$\leq u(x) \quad \text{in a neighborhood of } x_0.$$

From our test:

$$\implies -\Delta v(x_0) + f(x_0) \geq 0$$

$$\implies -\Delta u(x_0) + \varepsilon n + f(x_0) \geq 0 \quad \forall \varepsilon > 0$$

$$\implies -\Delta u(x_0) + f(x_0) \geq 0$$

This test for u being a supersolution of Poisson's equation doesn't require derivatives of u.

Definition: We say that u is a viscosity supersolution of

$$F(x, u(x), Du(x), D^2 u(x)) = 0$$

if $\forall \varphi \in C^2$ such that $u - \varphi$ has a local minimum at $x_0 \in \Omega$, then

$$F(x_0, \varphi(x_0), \nabla\varphi(x_0), D^2\varphi(x_0)) \geq 0$$

Definition: We say that u is a viscosity subsolution of

$$F(x, u(x), Du(x), D^2u(x)) = 0$$

if $\forall \varphi \in C^2$ such that $u - \varphi$ has a local maximum at $x_0 \in \Omega$, then

$$F(x_0, \varphi(x_0), \nabla\varphi(x_0), D^2\varphi(x_0)) \leq 0$$

Definition: We say that u is a viscosity solution if it is both a subsolution and a supersolution.

$$|\nabla u(x)| - 1 = 0$$

Example:

$$|u'(x)| - 1 = 0 \quad \text{in } (-1, 1)$$
$$u(\pm 1) = 0$$

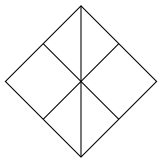

Use vanishing viscosity:

$$|u'| - 1 = \epsilon u''$$

$$|\nabla u(x)| - 1 = 0$$

Example:

$$|u'(x)| - 1 = 0 \quad \text{in } (-1, 1)$$
$$u(\pm 1) = 0$$

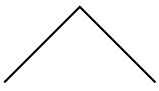

$|u'| - 1 = 0$

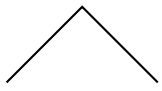

$1 - |u'| = 0$

Use vanishing viscosity:

$$|u'| - 1 = \epsilon u''$$

- For Monge-Ampère, we should only use $\varphi \in C^2$ that are convex (that live in the space where F is elliptic).
- Still need the convexity constraint.

- Regularity?
  - When testing if u is a supersolution, I need to make sense of local mins of $u - \varphi$:

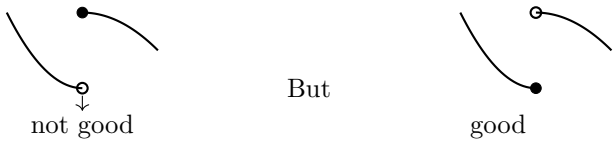

This is lower semi-continuous

We want supersolutions to be LSC:

$$f(x_0) \leq \liminf_{x \to x_0} f(x)$$

We want subsolutions to be USC:

$$f(x_0) \geq \limsup_{x \to x_0} f(x)$$

We expect viscosity solutions to be continuous.
For Monge-Ampere we expect convex and thus locally Lipschitz solutions.

C.8 Viscosity Subsolutions and Solutions

A convex function $u \in USC$ is a viscosity subsolution of the Monge-Ampère equation if for every $\varphi \in C^2$ convex and $x_0 \in \Omega$ such that $u - \varphi$ has a maximum at x_0, then

$$-\det(D^2\varphi(x_0)) + f(x_0) \leq 0.$$

Example:

$$\det(D^2 u) = f$$

where $f(x) = \max\left\{1 - \frac{1}{|x|}, 0\right\}$ with $x \in \mathbb{R}^2$.

Show that $u(x) = \frac{1}{2}\max\{|x| - 1, 0\}$ is a viscosity solution.
Consider a convex function $u \in C^1$ but not C^2.

Note: Along the circle $|x| = 1$, we lose second derivatives, so we cannot interpret in the classical sense. Choose some x_0 such that $|x_0| = 1$.

Question: Is u a subsolution here?

Analysis: Let φ be any convex C^2 function such that $u - \varphi$ has a local maximum at x_0. Then,

$$\det(D^2\varphi(x_0)) \geq 0 = f(x_0)$$

since φ is convex. Therefore, u is a subsolution.

Question: Is u a supersolution here?

Analysis: Let φ be any C^2 convex function such that $u - \varphi$ has a local minimum at x_0. Then,

$$\nabla u(x_0) = \nabla \varphi(x_0).$$

In any neighborhood of x_0, there is an open set on which $u(x) = 0$. Also, we have $\varphi(x) \leq u(x) = 0$ on this set with $\varphi(x_0) = u(x_0) = 0$.

If $\varphi(x) < u(x)$ on this open set (which always contains a line segment in the direction of $-x_0$), then $\varphi(x)$ cannot touch $u(x)$ from below at x_0. Hence, u is a supersolution.

If $\varphi(x_0) \neq 0$, then we have identified a region (this line segment) where $\varphi = 0$.

Further Analysis: In some direction,

$$\frac{\partial^2(\varphi)}{\partial t^2}(x_0) = 0.$$

This implies

$$v^T D^2 \varphi(x_0) v = 0.$$

Since $D^2\varphi(x_0)$ is positive semidefinite but not positive definite, we have

$$-\det(D^2\varphi(x_0)) + f(x_0) = 0 \geq 0.$$

Therefore:

$$u \text{ is a supersolution.}$$

$$u \text{ is a viscosity solution.}$$

C.8.1 General Measures in the Monge-Ampère Equation

What if we want to interpret the Monge-Ampère equation when μ and/or ν are more general measures?

We need to let mass split. The gradient can't do this, but a subgradient might.

Example: Consider $u(x) = |x|$.

What kind of "mapping" can we get from this?

$$\partial u(x) = \begin{cases} -1 & \text{if } x < 0 \\ [-1, 1] & \text{if } x = 0 \\ 1 & \text{if } x > 0 \end{cases}$$

What sort of Monge-Ampère equation might this solve?

Let's start by letting ν be a uniform measure on $[-1,1]$, i.e., ν has density

$$g(y) = \begin{cases} 1 & y \in [-1,1] \\ 0 & \text{otherwise} \end{cases}$$

Let's pick a set A and see where it is mapped to.
If $0 \in A \Rightarrow \partial u(A) = [-1,1]$.
Mass balance suggests that

$$\nu(\partial u(A)) = |\partial u(A)| = 2 = \mu(A) \quad \text{(target mass = source mass)}.$$

If $0 \notin A$,

$$\partial u(A) \subseteq \{-1,1\}$$
$$\nu(\partial u(A)) = |\partial u(A)| = 0 = \mu(A)$$

We conclude

$$\mu(A) = \begin{cases} 2 & 0 \in A \\ 0 & \text{otherwise} \end{cases}$$

$$\mu(x) = 2\delta(x)$$

If $\mu(x) = 2\delta(x)$ and $d\nu(y) = g(y)dy$, then

$$|\partial u(A)| = \mu(A) \quad \forall A$$

We call $|\partial u(A)|$ the Monge-Ampère measure or subgradient measure associated with u.

We can do this in general: let's take

$$g(y) = \begin{cases} 1 & y \in Y \\ 0 & \text{otherwise} \end{cases}$$

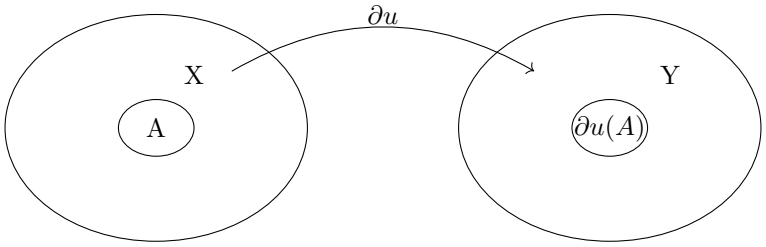

We expect:

$$\mu(A) = |\partial u(A)|$$

C.8.2 Monge-Ampère Measure

Definition 1. Let μ be a measure defined on a convex set $X \subset \mathbb{R}^n$. We say that a convex function u is an **Aleksandrov solution** or **generalized solution** of the Monge-Ampère equation

$$\det(D^2 u) = \mu$$

if

$$\mu(A) = |\partial u(A)|$$

for all $A \subset X$.

The optimal "map" is given by $\partial u(x)$.

C.8.3 Example of a Generalized Solution

For $x \in \mathbb{R}^2$, let $\mu(x) = \pi\delta(x)$.

Show that $u(x) = |x| = \sqrt{x_1^2 + x_2^2}$ is a generalized solution of

$$\det(D^2 u) = \pi\delta(x)$$

$$\partial u(x) = \begin{cases} B(0,1) & x = 0 \\ \frac{x}{|x|} & x \neq 0 \end{cases}$$

Choose some set $A \subset \mathbb{R}^2$.

If $0 \in A \Rightarrow \partial u(A) = B(0,1)$

$$\Rightarrow |\partial u(A)| = \pi$$

If $0 \notin A \Rightarrow \partial u(A) \subset \partial B(0,1)$

$$\Rightarrow |\partial u(A)| = 0$$

$$\Rightarrow \partial u(A) = \pi\delta(A) = \mu(A)$$

Therefore, u solves this Monge-Ampère equation.

C.8.4 Mapping and Gradients

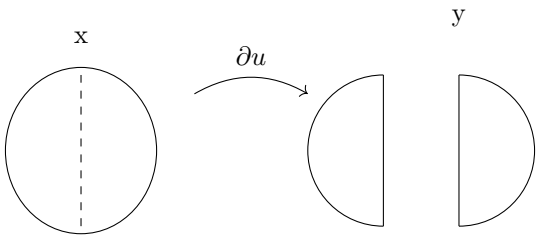

A gradient of u can't do this.
The map is expected to be

$$T(x) = \begin{cases} (x_1 - 1, x_2) & x_1 < 0 \\ (x_1 + 1, x_2) & x_1 > 0 \end{cases}$$

C.8.5 Contributions of Luis A. Caffarelli to Regularity of the Solutions of the Monge-Ampère Equation

Luis A. Caffarelli has made significant contributions to the study of the Monge-Ampère equation, particularly in the context of regularity theory and convex solutions. Some of his notable work includes:

Interior $W^{2,p}$ Estimates: Caffarelli developed interior $W^{2,p}$ estimates for second derivatives of solutions to the Monge-Ampère equation. This result provides important regularity insights for solutions when the right-hand side is positive and continuous (Annals of Mathematics).

$W^{2,1}$ Regularity: He also proved $W^{2,1}$ regularity for strictly convex Alexandrov solutions to the Monge-Ampère equation under certain conditions, which involves higher integrability and a priori estimates for the second derivatives (Annals of Mathematics).

Regularity Theory for Nonlinear PDEs: Caffarelli's broader contributions to regularity theory for nonlinear partial differential equations, including free-boundary problems and the Monge-Ampère equation, have been widely recognized and were part of the reason he was awarded the Abel Prize in 2023 (Annals of Mathematics).

These works are fundamental for understanding the behavior of solutions to the Monge-Ampère equation and have applications in various areas of analysis and geometry.

Being connected is not enough to guarantee "nice" mappings. Still get mass splitting. We need convexity of the target set to get regularity.

Same issue if densities are allowed to vanish:

Letting f vanish is a problem.

For regularity, we need to bound densities away from 0.

Main Results

Let $f, g \in C^{0,\alpha}$ defined on bounded sets X, Y with Y convex. f and g are bounded above and below by positive constants. Consider

$$g(\nabla u(x)) \det(D^2 u(x)) = f(x), \quad x \in X$$

- $u \in C^2(X)$
- If X is convex, we also have $u \in C^{1,\alpha}(\overline{X})$

- If X, Y are uniformly convex and $f \in C^{0,\alpha}(\overline{X})$, $g \in C^{0,\alpha}(\overline{Y})$, then $u \in C^2(\overline{X})$

C.9 Boundary Conditions for the Monge-Ampère Equation

Consider the Monge-Ampère equation with the following boundary conditions. Let X be the domain in which the function u is defined, and let Y be the target domain, which is the image of X under the gradient map ∇u.

- The gradient map ∇u maps points from X to Y.
- The image of X under ∇u is contained within the closure of Y, denoted $\bar{Y}$.

This gives us the second boundary value problem (BVP) for the Monge-Ampère equation:

$$\begin{cases} g(\nabla u(x)) \det(D^2 u(x)) = f(x), \quad x \in X, \\ u \text{ is convex}, \\ \nabla u(X) \subseteq \bar{Y}. \end{cases}$$

where:

- $g(\nabla u(x))$ is a function depending on the gradient $\nabla u(x)$,
- $\det(D^2 u(x))$ is the determinant of the Hessian matrix of u,
- $f(x)$ is a given function defined on X.

The conditions can be summarized as follows:

- For every $x \in X$, $\nabla u(x) \in \bar{Y}$.
- The function u is convex.
- The gradient image $\nabla u(X) \subseteq \bar{Y}$.

The convexity of u ensures that the Hessian $D^2 u(x)$ is positive semi-definite, which is necessary for the determinant to be well-defined and non-negative. The map ∇u sends points in X to $\bar{Y}$, ensuring that the transport map remains within the desired target domain.

The Monge-Ampère equation with the second boundary value problem involves finding a convex function u defined on a domain X such that its gradient map ∇u maps X into the closure of another domain Y. The equation $g(\nabla u(x)) \det(D^2 u(x)) = f(x)$ must be satisfied, where g is a function of the gradient ∇u, and $f(x)$ is a given function.

C.9.1 Uniqueness and Existence for the Monge-Ampère Equation

If $u(x)$ is a solution to the Monge-Ampère equation, then $u(x) + C$ is also a solution for any constant C. To ensure uniqueness, we can add an extra constraint such as:

$$\langle u \rangle = 0$$

This constraint implies that the average value of u over the domain X is zero, which helps in obtaining a unique solution.

To address the existence of solutions, we consider the following boundary value problem:

$$\begin{cases} \Delta u = f, & \text{for } x \in X, \\ \frac{\partial u}{\partial n} = g, & \text{for } x \in \partial X, \end{cases}$$

where:

- Δu is the Laplacian of u,
- f is a given function defined on X,
- $\frac{\partial u}{\partial n}$ denotes the normal derivative of u on the boundary ∂X,
- g is a given function defined on the boundary ∂X.

The existence of solutions to this boundary value problem can be studied using various analytical and numerical techniques.

Solvability Condition for the Monge-Ampère Equation

The data must satisfy a solvability condition for the existence of solutions to the boundary value problem. This condition is derived from integrating both sides of the equation over the domain X.

$$\int_X f(x)\, dx = \int_X \Delta u\, dx$$

Using the divergence theorem, we can transform the volume integral of the Laplacian into a surface integral:

$$\int_X \Delta u\, dx = \int_{\partial X} \frac{\partial u}{\partial n}\, dA$$

Substituting the boundary condition $\frac{\partial u}{\partial n} = g$:

$$\int_{\partial X} \frac{\partial u}{\partial n}\, dA = \int_{\partial X} g\, dA$$

Therefore, the solvability condition is:

$$\int_X f(x)\,dx = \int_{\partial X} g\,dA$$

This condition ensures that the given data f and g are compatible, allowing for the existence of a solution to the boundary value problem.

Mass Balance Condition for the Monge-Ampère Equation

Returning to the Monge-Ampère equation, the integral condition for solvability can be expressed in terms of mass balance. The condition ensures that the total mass is conserved under the mapping defined by the Monge-Ampère equation.

$$\int_X f(x)\,dx = \int_X g(\nabla u(x)) \det(D^2 u(x))\,dx$$

Using the change of variables $y = \nabla u(x)$:

$$\int_X g(\nabla u(x)) \det(D^2 u(x))\,dx = \int_{\nabla u(X)} g(y)\,dy$$

Since $\nabla u(X) = Y$:

$$\int_X f(x)\,dx = \int_Y g(y)\,dy$$

This integral condition is a statement of mass balance. It ensures that the total mass in the source domain X (with density f) matches the total mass in the target domain Y (with density g).

Summary: The mass balance condition for the Monge-Ampère equation is:

$$\int_X f(x)\,dx = \int_Y g(y)\,dy$$

Local Boundary Conditions for the Monge-Ampère Equation

Can we make the boundary conditions (BC) local?

The question of whether the boundary conditions for the Monge-Ampère equation can be made local pertains to the possibility of expressing the boundary conditions in a form that depends only on local properties of the solution and its derivatives at the boundary, rather than on global integral constraints.

To introduce local boundary conditions for the Monge-Ampère equation, we can define a function $H(y)$ for the target domain Y. This defining function helps in formulating conditions that are local but might not directly serve as boundary conditions (BC).

$$H(y) = \begin{cases} < 0 & \text{if } y \in Y, \\ = 0 & \text{if } y \in \partial Y, \\ > 0 & \text{otherwise.} \end{cases}$$

An example of such a function is the signed distance to the boundary ∂Y.

Consider the gradient map $\nabla u(x)$:

$$\nabla u(x) \in Y$$

This implies that:

$$H(\nabla u(x)) \leq 0$$

This condition is local since it depends only on the value of $\nabla u(x)$ at each point $x \in X$. However, it is not a traditional boundary condition but rather a constraint that ensures the image of X under the gradient map ∇u lies within the target domain Y.

Consider the boundary condition for the Monge-Ampère equation by examining points on the boundary of the domain X.

Let $x \in \partial X$. Can we assume that $\nabla u(x) \in \partial Y$?

If we can make this assumption, then:

$$H(\nabla u(x)) = 0, \quad x \in \partial X$$

This assumption provides a condition on the boundary of X that relates the gradient of u to the boundary of the target domain Y. Specifically, it states that if x lies on the boundary of X, then the gradient $\nabla u(x)$ should lie on the boundary of Y, and the defining function H should be zero at these points.

With the assumptions made earlier, we derive a nonlinear Neumann problem for the Monge-Ampère equation:

$$\begin{cases} g(\nabla u(x)) \det(D^2 u(x)) = f(x), & x \in X, \\ u \text{ is convex}, & \\ H(\nabla u(x)) = 0, & x \in \partial X. \end{cases}$$

Convexity Condition for the Monge-Ampère Equation

Question: If I solve this new problem, am I guaranteed that $\nabla u(x) \in \bar{Y}$ for all $x \in X$?

Claim: This works if X and Y are convex.

To ensure that the solution to the Monge-Ampère equation satisfies the condition that the gradient map $\nabla u(x)$ maps the domain X into the closure of the target domain $\bar{Y}$, we need to consider the convexity of X and Y.

is guaranteed to ensure that $\nabla u(x) \in \bar{Y}$ for all $x \in X$, provided that both X and Y are convex sets. The convexity of these sets helps in maintaining the structure needed for the gradient map to map the domain appropriately.

To solve the Monge-Ampère equation, we start with a convex function u such that:

$$\nabla u(x) \in Y \quad \forall x \in \partial X$$

Let's build a cone below u.

By starting with a convex function u and ensuring that the gradient map $\nabla u(x)$ for boundary points $x \in \partial X$ lies within the target domain Y, we lay the foundation for solving the Monge-Ampère equation. The construction of a cone below u is a technique used to establish lower bounds and facilitate the analysis and solution of the equation.

For each $z \in \partial X$, define:

$$V_z(x) = u(z) + \nabla u(z) \cdot (x - z)$$

Then, define:

$$V(x) = \max_{z \in \partial X} V_z(x)$$

Observations

- $V \leq u$
- V is convex
- $\nabla V_z(x) = \nabla u(z)$

1. **Support Functions $V_z(x)$**: - The function $V_z(x)$ represents the support function of u at the point z. It is a linear approximation of u at z.

2. **Maximum Function $V(x)$**: - The function $V(x)$ is constructed as the maximum of all support functions $V_z(x)$ for $z \in \partial X$. This ensures that $V(x)$ is below $u(x)$ and provides a convex approximation.

3. **Convexity**: - $V(x)$ is convex because it is the maximum of linear functions, which are themselves convex.

4. **Gradient Preservation**: - The gradient of $V_z(x)$ at any point x is equal to the gradient of u at z. This preserves the gradient information of u at the boundary points z.

C.9.2 Characterizing the Subdifferential using Danskin's Theorem

We are going to use Danskin's Theorem to characterize the subdifferential ∂V.

Let $\mathcal{Z}(x)$ be the set of maximizers:

$$\mathcal{Z}(x) = \{z \in \partial X \mid V(x) = V_z(x)\}$$

Then:

$$\partial V(x) = \operatorname{conv}\{\nabla V_z(x) \mid z \in \mathcal{Z}(x)\}$$

This can be further related to:

$$\partial V(x) \subseteq \operatorname{conv}\{\nabla u(z) \mid z \in \partial X\}$$

Given that $\nabla u(z) \in \partial Y$, we have:

$$\partial V(x) \subseteq \text{conv}\{\partial Y\} = \bar{Y} \quad \text{since } Y \text{ is convex}$$

Since $V \leq u$ with equality on the boundary, we claim that:

$$\nabla u(X) \subseteq \partial V(X)$$

1. **Set of Maximizers $\mathcal{Z}(x)$**: - The set $\mathcal{Z}(x)$ consists of points $z \in \partial X$ where the support function $V_z(x)$ attains the maximum value $V(x)$.

2. **Subdifferential $\partial V(x)$**: - The subdifferential $\partial V(x)$ is the convex hull of the gradients $\nabla V_z(x)$ for all z in the set of maximizers $\mathcal{Z}(x)$. This is derived using Danskin's Theorem, which provides a way to compute the subdifferential of a pointwise maximum of functions.

3. **Relation to ∂Y**: - Since $\nabla u(z) \in \partial Y$ for all $z \in \partial X$, the convex hull of these gradients is contained within $\bar{Y}$, given that Y is convex.

4. **Gradient Inclusion**: - The inclusion $\nabla u(X) \subseteq \partial V(X)$ follows from the fact that $V \leq u$ with equality on the boundary, ensuring that the gradients of u at points within X are contained within the subdifferential $\partial V(X)$.

Define:

$$a \equiv \max_{x \in \bar{X}} \{u(x_0) + p \cdot (x - x_0) - V(x)\}$$

This can be expressed as:

$$a = u(x_0) + p \cdot (x_1 - x_0) - V(x_1) \quad \text{for some } x_1 \in \bar{X}$$

Given $a \geq 0$ (since $x = x_0$ gives a non-negative value):
Case 1: $a > 0$

$$a = u(x_0) + p \cdot (x_1 - x_0) - V(x_1)$$

This can be expressed as:

$$a \leq u(x_1) - V(x_1) \quad \text{since } u \text{ is convex and } p = \nabla u(x_0)$$

$$a \leq u(x_1) - V(x_1)$$

Since $a > 0$, this implies:

$$u(x_1) \neq V(x_1)$$

Thus:

$$x_1 \notin \partial X$$

$$u(x_0) + p \cdot (x_1 - x_0) - V(x_1) \geq u(x_0) + p \cdot (x - x_0) - V(x) \quad \forall x \in X$$

This implies:

$$V(x) \geq V(x_1) + p \cdot (x - x_1) \quad \forall x \in X$$

Therefore:

$$p \in \partial V(x_1) \subseteq \bar{Y}$$

Thus:

$$\nabla u(x_0) \in \bar{Y}$$

Case 2: $a = 0$
For all x:

$$u(x_0) + p \cdot (x - x_0) - V(x) \leq a = 0$$

This implies:

$$V(x) \geq u(x_0) + p \cdot (x - x_0)$$

and since:

$$V(x_0) \geq u(x_0) + p \cdot (x_0 - x_0)$$

we have:

$$V(x) \geq V(x_0) + p \cdot (x - x_0)$$

Therefore:

$$p \in \partial V(x_0) \subseteq \bar{Y}$$

1. **Non-Positive Condition**: - The condition $a = 0$ implies that $u(x_0) + p \cdot (x - x_0) \leq V(x)$ for all x, making the difference non-positive.

2. **Inequality for V**: - From the non-positive condition, we derive $V(x) \geq u(x_0) + p \cdot (x - x_0)$. Evaluating this at x_0, we get $V(x_0) \geq u(x_0)$.

3. **Gradient Membership**: - The inequality $V(x) \geq V(x_0) + p \cdot (x - x_0)$ for all x implies that p is in the subdifferential $\partial V(x_0)$.

4. **Inclusion in $\bar{Y}$**: - Since $\partial V(x_0) \subseteq \bar{Y}$ by construction, we have that $\nabla u(x_0) = p$ is also contained in $\bar{Y}$.

Thus:

In summary :

$$\nabla u(x_0) \in \bar{Y} \quad \forall x_0 \in X$$

C.9.3 Example: L cost between parallel planes

General Monge-Ampere Equation

$$\det\left(D^2h(\nabla h)^{-1}(\nabla u) - D^2u\right) = \det\left(D^2h(\nabla h)^{-1}(\nabla u)\right)\frac{f}{g(x-(\nabla h)^{-1}(\nabla u))}$$

$$h(z) = \sqrt{|z|^2 + L^2}$$

$$c(x,y) = h(x-y)$$

$$\nabla h(z) = \frac{z}{\sqrt{|z|^2+L^2}}$$

To get $(\nabla h)^{-1}$, set

$$\frac{z}{\sqrt{|z|^2+L^2}} = p$$

$$\Rightarrow \frac{|z|^2}{|z|^2+L^2} = |p|^2$$

$$\Rightarrow |z|^2\left(1-|p|^2\right) = |p|^2L^2$$

$$\Rightarrow |z| = \frac{|p|L}{\sqrt{1-|p|^2}}$$

$$\Rightarrow z = \frac{pL}{\sqrt{1-|p|^2}} = (\nabla h)^{-1}(p)$$

Optimal map has the form

$$T(x,\nabla u) = x - \frac{Lu}{\sqrt{1-|x|^2}}$$

$$(D^2h)_{ij} = \begin{cases} \frac{(1+|z|^2+L^2-z_i^2)}{(|z|^2+L^2)^{3/2}} & i=j \\ \frac{-z_iz_j}{(|z|^2+L^2)^{3/2}} & i\neq j \end{cases}$$

$$(D^2h(\nabla h)^{-1}(p))_{ij} = \begin{cases} \frac{(1-|p|^2)\sqrt{1-|p|^2}}{L} & i=j \\ \frac{-p_ip_j\sqrt{1-|p|^2}}{L} & i\neq j \end{cases}$$

$$D^2h(\nabla h)^{-1}(p) = \frac{\sqrt{1-|p|^2}}{L}\left(I-pp^T\right)$$

$$\det\left(D^2h((\nabla h)^{-1}(p))\right) = \frac{(1-|p|^2)^{n/2+1}}{L^n}$$

The PDE is

$$\det\left(\frac{\sqrt{1-|\nabla u|^2}}{L}\left(I-(\nabla u(\nabla u)^T)\right)-D^2u\right)=\frac{(1-|\nabla u|^2)^{n/2+1}}{L^n}\cdot\frac{f}{g\left(x-\frac{L\nabla u}{\sqrt{1-|\nabla u|^2}}\right)}$$

$$\det\left(D^2h((\nabla h)^{-1}(p))\right)=\frac{(1-|p|^2)^{n/2+1}}{L^n}$$

The PDE is

$$\det\left(\frac{\sqrt{1-|\nabla u|^2}}{L}\left(I-(\nabla u(\nabla u)^T)\right)-D^2u\right)=\frac{(1-|\nabla u|^2)^{n/2+1}}{L^n}\cdot\frac{f}{g\left(x-\frac{L\nabla u}{\sqrt{1-|\nabla u|^2}}\right)}$$

All this can be done rigorously for costs satisfying MTW conditions (Ma-Trudinger-Wang)

- $h\in C^4$
- ∇h is invertible
- $\det(D^2h(z))\neq 0$
- Technical condition satisfied by higher derivatives of cost.

C.10 Wasserstein Metric

Do OT with cost c between probability measures μ, ν with $c=|x-y|^p$

$$\inf_{T_{\#}\mu=\nu}\int_X c(x,T(x))\,d\mu(x)$$

or

$$\inf_{\pi\in\Pi(\mu,\nu)}\int_{X\times Y}c(x,y)\,d\pi(x,y)$$

If $\mu=\nu$, the cost is 0.
The transport cost gives notion of "distance" between μ and ν.
For $p\in[1,\infty)$, we define the Wasserstein-p distance as

$$W_p(\mu,\nu)=\left(\inf_{\pi\in\Pi(\mu,\nu)}\int_{X\times Y}c(x,y)\,d\pi(x,y)\right)^{1/p}$$

Theorem 19. *W_p defines a metric on the space of probability measures.*

Need to show:

(1) Triangle inequality

$$W_p(\mu,\nu)\leq W_p(\mu,\sigma)+W_p(\sigma,\nu)$$

(2) Symmetry

$$W_p(\mu,\nu) = W_p(\nu,\mu)$$

(3) Positivity: $W_p(\mu,\nu) \geq 0$ with equality iff $\mu = \nu$

Proof of (2): Immediate.
Proof of (3):

$$W_p(\mu,\nu) \geq 0 \quad \text{and} \quad W_p(\mu,\mu) = 0$$

Suppose $W_p(\mu,\nu) = 0$. Then $\exists \pi \in \Pi(\mu,\nu)$ such that

$$\int_{X\times Y} |x-y|^p \, d\pi(x,y) = 0$$

Proof of (1): When μ, σ, ν do not give mass to small sets.

$$\begin{array}{ccc} \mu & \xrightarrow{T_1} & \sigma \\ & T_2 \downarrow & \\ & \nu & \end{array}$$

Let $T_1 \# \mu = \sigma$, $T_2 \# \sigma = \nu$ be optimal.
Define $T = T_2 \circ T_1$
$T \# \mu = \nu$ but may not be optimal.

$$\Rightarrow W_p(\mu,\nu) \leq \left(\int_X |x - T(x)|^p \, d\mu(x) \right)^{1/p}$$

$$= \|I - T\|_{L^p(\mu)} \quad \text{where} \quad I(x) = x$$

$$W_p(\mu,\nu) \leq \|I - T\|_{L^p(\mu)} + \|T_1 - T\|_{L^p(\mu)}$$

$$\|I - T\|_{L^p(\mu)} = \left(\int_X |x - T_1(x)|^p \, d\mu(x) \right)^{1/p} = W_p(\mu,\sigma)$$

$$\|T_1 - T\|_{L^p(\mu)} = \left(\int_X |T_1(x) - T_2(T_1(x))|^p \, d\mu(x) \right)^{1/p} = \left(\int_Y |y - T_2(y)|^p \, d\sigma(y) \right)^{1/p} = W_p(\sigma,\nu)$$

$$\therefore W_p(\mu,\nu) \leq W_p(\mu,\sigma) + W_p(\sigma,\nu)$$

More generally (i.e., Kantorovich formulation)
Suppose $\mu \in \mathcal{P}(X)$, $\sigma \in \mathcal{P}(Y)$, $\nu \in \mathcal{P}(Z)$

$$\begin{array}{ccc} \mu & \xrightarrow{\pi_{xy}} & \sigma \\ & \xrightarrow{\pi_{yz}} & \nu \end{array}$$

We find optimal transport plans π_{xy} (between μ and σ) and π_{yz} (between σ and ν).

We want to find a feasible plan between μ and ν.
We need the Gluing Lemma

Lemma 2 (Gluing Lemma)**.** *Suppose $\pi_{xy} \in \Pi(\mu_x, \mu_y)$ and $\pi_{yz} \in \Pi(\mu_y, \mu_z)$ (They share a common marginal)*

$\exists$ a measure $\pi \in \mathcal{P}(X \times Y \times Z)$ such that π_{xy} and π_{yz} are the marginals of π on $X \times Y$ and $Y \times Z$ respectively.

We need the concept of disintegration of measure.

C.10.1 Desintegration of Measures

Given a measure Π on $X \times Y$, we can characterize it as an "average" of many measures on Y.

$$\forall x \in X \quad \exists \Pi_x \in \mathcal{P}(Y) \text{ s.t. } \forall \varphi$$

$$\int_{X\times Y} \varphi(x,y)\, d\Pi(x,y) = \int_X \left(\int_Y \varphi(x,y)\, d\Pi_x(y) \right) d\mu(x)$$

We write $\Pi = \mu \otimes \Pi_x$

Proof of Gluing Lemma

Disintegrate π_{xy} and π_{yz}:

$$\pi_{xy} = \pi_{xy,y} \otimes \mu_y$$

$$\pi_{yz} = \mu_y \otimes \pi_{yz,y}$$

Define a measure π via

$$\int_{X\times Y\times Z} \varphi(x,y,z)\, d\pi = \int_Y \left(\int_X \left(\int_Z \varphi(x,y,z)\, d\pi_{yz,y} \right) d\pi_{xy,y} \right) d\mu_y$$

$$\begin{aligned}
\int_{X\times Y\times Z} \varphi(x,y)\, d\pi &= \int_Y \left(\int_X \varphi(x,y)\, d\pi_{xy,y} \right) \left(\int_Z d\pi_{yz,y} \right) d\mu_y \\
&= \int_Y \left(\int_X \varphi(x,y)\, d\pi_{xy,y} \right) d\mu_y \\
&= \int_{X\times Y} \varphi(x,y)\, d(\pi_{xy,y} \otimes \mu_y) \\
&= \int_{X\times Y} \varphi(x,y)\, d\pi_{xy}
\end{aligned}$$

Similarly, the marginal on $Y \times Z$ is π_{yz}.

Triangle Inequality

Let $\pi_{xy} \in \Pi(\mu, \sigma)$, $\pi_{yz} \in \Pi(\sigma, \nu)$ be optimal.

Construct $\pi \in \mathcal{P}(X \times Y \times Z)$ as in the Gluing Lemma.

Define π_{xz} to be the marginal of π on $X \times Z$.

Check the marginals on X:

Given $A \subseteq X$

$$\pi_{xz}(A \times Z) = \pi(A \times Y \times Z)$$

$$= \pi_{xy}(A \times Y) = \mu(A)$$

and $\pi_{xz}(X \times B) = \nu(B)$

$$\Rightarrow \pi_{xz} \in \Pi(\mu, \nu)$$

$$W_p(\mu, \nu) \leq \left(\int_{X \times Z} |x - z|^p \, d\pi_{xz} \right)^{1/p}$$

$$= \left(\int_{X \times Y \times Z} |x - z|^p \, d\pi \right)^{1/p}$$

$$= \|x - z\|_{L^p(\pi)}$$

$$\leq \|x - y\|_{L^p(\pi_{xy})} + \|y - z\|_{L^p(\pi_{yz})}$$

$$= \left(\int_{X \times Y \times Z} |x - y|^p \, d\pi \right)^{1/p} + \left(\int_{Y \times Z} |y - z|^p \, d\pi \right)^{1/p}$$

$$= \left(\int_{X \times Y} |x - y|^p \, d\pi_{xy} \right)^{1/p} + \left(\int_{Y \times Z} |y - z|^p \, d\pi_{yz} \right)^{1/p}$$

$$= W_p(\mu, \sigma) + W_p(\sigma, \nu)$$

C.11 Benamou-Brenier Formulation

Let's consider a density $(\rho(t, x))$, $x \in \mathbb{R}^d$, $0 < t < 1$

We want

$$\rho(0, x) = f(x)$$

$$\rho(1, x) = g(x)$$

Introduce velocity field $V(t, x)$

Describe a mass-preserving flow via the continuity equation:

$$\partial_t \rho + \nabla \cdot (V\rho) = 0$$

Introduce Lagrangian coordinates $X(t, x)$ to "follow" a particle through the flow:

$$\begin{cases} \frac{\partial X}{\partial t}(t, x) = V(t, X(t, x)) \\ X(0, x) = x \end{cases}$$

Mass in E at $t = 0$ = Mass in $X(t, E)$ at time t

$$\Rightarrow \int_E f(x)\,dx = \int_{X(t,E)} \rho(t,x)\,dx \quad \forall\ 0 < t \leq 1$$

This is the statement:

$$X(t,\cdot)\#f = \rho(t,\cdot)$$

and

$$X(1,\cdot)\#f = g$$

$$W_2^2(f,g) \leq \int_{\mathbb{R}^n} f(x)|X(1,x) - x|^2\,dx$$

$$= \int_{\mathbb{R}^n} f(x)\,|X(1,x) - X(0,x)|^2\ dx$$

$$= \int_{\mathbb{R}^n} f(x) \left| \int_0^1 \frac{\partial X}{\partial t}(t,x)\,dt \right|^2 dx$$

$$\leq \int_{\mathbb{R}^n} f(x) \int_0^1 \left| \frac{\partial X}{\partial t}(t,x) \right|^2 dt\,dx$$

$$= \int_0^1 \int_{\mathbb{R}^n} f(x)\,|V(t, X(t,x))|^2\ dx\,dt$$

Fix t

Define $S(x) = X(t,x)$

$$S\#f = \rho(t,x)$$

$$\varphi(y) = |V(t,y)|^2$$

$$\int_{\mathbb{R}^n} f(x)|V(t,X(t,x))|^2\,dx = \int_{\mathbb{R}^n} f(x)\varphi(S(x))\,dx = \int_{\mathbb{R}^n} \rho(t,y)\varphi(y)\,dy = \int_{\mathbb{R}^n} \rho(t,y)|V(t,y)|^2\,dy$$

$$W_2^2(f,g) \leq \int_0^1 \int_{\mathbb{R}^n} \rho(t,y)|V(t,y)|^2\,dy\,dt$$

for every ρ, V satisfying

$$\begin{cases} \partial_t \rho + \nabla \cdot (\rho V) = 0 \\ \rho(0,x) = f(x) \\ \rho(1,x) = g(x) \end{cases}$$

Can we achieve equality? Need $X(1,x) = T(x)$, the optimal map from f to g.

Need

$$\int_0^1 \left|\frac{\partial X}{\partial t}(t,x)\right|^2 dt = \int_0^1 \left|\frac{\partial X}{\partial t}(t,x)\right|^2 dt$$

This holds if $\frac{\partial X}{\partial t}(t,x) = U(x)$ is constant in time.
Recall: $X(0,x) = x$

$$\Rightarrow X(t,x) = x + U(x)t$$

$$X(1,x) = x + U(x) = T(x)$$

$$\Rightarrow U(x) = T(x) - x$$

$$X(t,x) = x + (T(x) - x)t = x(1-t) + tT(x)$$

Our velocity field should satisfy:

$$V(t, X(t,x)) = U(x) = T(x) - x = (T - I)(x)$$

Let $y = X(t,x) = [(1-t)I + tT](x)$

$$\Rightarrow V(t,y) = (T - I)[(1-t)I + tT]^{-1}(y)$$

achieves the optimum (if f and g are nice).

Otherwise, we do "smoothed" approximations to get arbitrarily close to the infimum.

in summary we have shown that the optimal transport is equivalent to :

$$W_2^2(f,g) = \inf_{\rho,V} \int_0^1 \int_{\mathbb{R}^n} \rho(t,x)|V(t,x)|^2 \, dx \, dt$$

subject to:

$$\begin{cases} \partial_t \rho + \nabla \cdot (\rho V) = 0 \\ \rho(0,x) = f(x) \\ \rho(1,x) = g(x) \end{cases}$$

C.11.1 lagrangian point of view

Example:

$$\min f(x)$$

subject to:

$$Ax = b$$

Could write down Lagrangian:

$$L(x,\lambda) = f(x) + \lambda \cdot (Ax - b)$$

Seek saddle points of this:

$$\min_x \left\{ f(x) + \sup_\lambda \lambda \cdot (Ax - b) \right\}$$

We try to write down a Lagrangian for our flow problem.
Let $\varphi(t, x)$ be the Lagrange multiplier.
The continuity equation gives us a term:

$$\int_0^1 \int_{\mathbb{R}^n} (\partial_t \rho + \nabla \cdot (\rho V))\varphi \, dx \, dt$$

$$= \int_{\mathbb{R}^n} (\rho(1, x)\varphi(1, x) - \rho(0, x)\varphi(0, x)) \, dx - \int_0^1 \int_{\mathbb{R}^n} (\rho \partial_t \varphi + \rho V \cdot \nabla \varphi) \, dx \, dt$$

Lagrangian:

$$L = \int_0^1 \int_{\mathbb{R}^n} \left(\frac{\rho |V|^2}{2} - \rho \partial_t \varphi - \rho V \cdot \nabla \varphi \right) dx \, dt + \int_{\mathbb{R}^n} (g(x)\varphi(1, x) - f(x)\varphi(0, x)) \, dx = G(\varphi)$$

Letting $m = \rho V$

$$L(\varphi, \rho, m) = \int_0^1 \int_{\mathbb{R}^n} \left(\frac{|m|^2}{2\rho} - \rho \partial_t \varphi - m \cdot \nabla \varphi \right) dx \, dt + G(\varphi)$$

We want to solve:

$$\inf_{\rho, m} \sup_\varphi L(\varphi, \rho, m)$$

Let $h(\rho, m) = \frac{|m|^2}{2\rho}$
Claim:

$$h(\rho, m) = \sup_{(a,b) \in K} (a\rho + b \cdot m)$$

where $K = \{(a, b) \in \mathbb{R} \times \mathbb{R}^n \mid a + \frac{|b|^2}{2} \leq 0\}$
Proof:
Let (a^*, b^*) achieve the supremum.
Since $a \leq 0$ we want a to be as big as possible:

$$\Rightarrow a^* = -\frac{|b|^2}{2}$$

$$\sup_{(a,b) \in K} (a\rho + b \cdot m) = \sup_{b \in \mathbb{R}^n} \left(-\frac{|b|^2}{2}\rho + b \cdot m \right)$$

This is concave $\Rightarrow$ set gradient to 0.

$$-\rho b + m = 0 \Rightarrow b^* = \frac{m}{\rho}$$

$$\sup_{(a,b)\in K}(a\rho + b\cdot m) = -\frac{|m|^2}{2\rho} + \frac{|m|^2}{\rho}$$

$$= \frac{|m|^2}{2\rho}$$

$$= h(\rho, m)$$

The saddle point problem is:

$$\inf_{\rho,m}\sup_{\varphi}\int_0^1\int_{\mathbb{R}^n}\left(\frac{|m|^2}{2\rho} + \rho(\partial_t\varphi + m\cdot\nabla\varphi)\right)dx\,dt + G(\varphi)$$

$$= \inf_{\rho,m}\sup_{\varphi}\int_0^1\int_{\mathbb{R}^n}\left(\left(\frac{|m|^2}{2\rho} - \rho\partial_t\varphi\right) + (-\rho V\cdot\nabla\varphi)\right)dx\,dt + G(\varphi)$$

Let $r = (\rho, m)$, $\xi = (a, b)$, $\nabla_{t,x}\varphi = (\partial_t\varphi, \nabla\varphi)$

$$\Rightarrow \inf_r\sup_{\varphi}\langle\xi - \nabla_{t,x}\varphi, r\rangle + G(\varphi)$$

Let's let $\epsilon > 0$ be small to regularize the max.

$$\inf_r\sup_{\varphi}\langle\xi - \nabla_{t,x}\varphi, r\rangle + G(\varphi) - \frac{\epsilon}{2}\|\xi - \nabla_{t,x}\varphi\|^2$$

Optimize these three unknowns independently.
Given $\xi_k, \bar{\xi_k}$, find optimal φ_k:

$$\varphi_k = \arg\max_{\varphi}\left(\langle\nabla_{t,x}\varphi, r\rangle + G(\varphi) - \frac{1}{2}\|\bar{\xi} - \nabla_{t,x}\varphi\|^2\right)$$

Quadratic, unconstrained

$$\Rightarrow \text{Gradient} = 0$$

$$\Rightarrow \text{Linear problem}$$

Computing 1^{st} variation

$$\Rightarrow \text{Poisson equation with Neumann boundary conditions}$$

(homogeneous in space and non-homogeneous in time)

$$\Delta_x\varphi_{k+1} = \nabla\cdot\left(\frac{\bar{\xi_k} - r_k}{\epsilon}\right)$$

Given r_k, φ_{k+1}, optimize for $\bar{\xi_{k+1}}$:

$$\bar{\xi_{k+1}} = \arg\max_{\bar{\xi}\in K}\left(\langle\bar{\xi}, r\rangle - \frac{\epsilon}{2}\|\bar{\xi} - \nabla_{t,x}\varphi\|^2\right)$$

Do this pointwise (geodesic optimization)

- Given $\varphi_{k+1}, \bar{\xi}_{k+1}$

  Do gradient descent in r

$$r_{k+1} = r_k - \gamma \left(\bar{\xi}_{k+1} - \nabla_{t,x} \varphi_{k+1} \right)$$

- Iterate

C.12 Gradient Flow in the Wasserstein metric

C.12.1 JKO Flows

Jordan, Kinderlehrer, Otto 1998

Let $F : \mathbb{R}^n \to \mathbb{R}$ be convex. We want to minimize $F(x)$.

Gradient Flow

$$\begin{cases} \frac{dX(t)}{dt} = -\nabla F(X(t)) \\ X(0) = X_0 \end{cases}$$

Discretization in Time via Backward Euler

$$\frac{X^{n+1} - X^n}{\tau} = -\nabla F(X^{n+1})$$

$$\Rightarrow X^{n+1} - X^n + \tau \nabla F(X^{n+1}) = 0$$

$$\Rightarrow \nabla \left(\frac{1}{2\tau} \|X - X^n\|^2 + F(X) \right) \Big|_{X = X^{n+1}} = 0$$

$$\Rightarrow X^{n+1} \in \arg\min \left\{ \frac{1}{2\tau} \|X - X^n\|^2 + F(X) \right\}$$

Can define a scheme like this in a metric space (X, d)

Let $F : X \to \mathbb{R}$ be l.s.c. and bounded below

$$X^{n+1} \in \arg\min \left\{ F(x) + \frac{d(x, X^n)^2}{2\tau} \right\}$$

Interpolate to all t: e.g., $X_\tau(t) = X^n$ if $t \in ((n-1)\tau, n\tau]$

Study limit as $\tau \to 0$. Consider $F : \mathcal{P}(\Omega) \to \mathbb{R}$, $d = W_2$

- Ω compact
- F is l.s.c. and bounded below

We previously used the continuity equation

$$\partial_t \rho + \nabla \cdot (\rho V) = 0$$

to "flow" densities.

Goal: Find velocity field V such that this flow agrees with $\lim_{\tau \to 0} X_\tau(t)$. Investigate optimality condition in the JKO scheme.

We need to compute the 1st variation. We need to perturb $\rho \in \mathcal{P}(\Omega)$ to $\rho + \epsilon\chi$.

Need $\rho + \epsilon\chi \in \mathcal{P}(\Omega)$ so that $F(\rho + \epsilon\chi)$ is well-defined.

Restrict to χ such that $\overline{\rho} = \rho + \epsilon\chi \in \mathcal{P}(\Omega)$ for all small $\epsilon > 0$.

$$\begin{aligned} \rho + \epsilon\chi &= \rho + \epsilon(\sigma - \rho) \\ &= \rho(1 - \epsilon) + \epsilon\sigma \\ &\in \mathcal{P}(\Omega) \end{aligned}$$

as long as $\rho, \sigma \in \mathcal{P}(\Omega)$

$$\forall \sigma \in \mathcal{P}(\Omega) \cap L^\infty(\Omega)$$

The first variation of F, $\frac{\delta F}{\delta \rho}(\rho)$, is such that

$$\left.\frac{d}{d\epsilon} F(\rho + \epsilon\chi)\right|_{\epsilon=0} = \int \frac{\delta F}{\delta \rho}(\rho)\chi \, dx \quad \forall \chi = \sigma - \rho,\ \sigma \in \mathcal{P}(\Omega) \cap L^\infty(\Omega)$$

$$\int \left(\frac{\delta F}{\delta \rho} + C\right) \chi(x) \, dx = \int \frac{\delta F}{\delta \rho} \chi(x) \, dx + C \int \chi(x) \, dx \to 0$$

The 1st variation is defined only up to additive constants.

Come back to

$$G(\rho) = F(\rho) + \frac{W_2^2(\rho, \rho^\tau)}{2\tau}$$

We need

$$\frac{\delta G}{\delta \rho}(\rho) = \frac{\delta F}{\delta \rho}(\rho) + \frac{1}{2\tau} \frac{\delta W_2^2}{\delta \rho}(\rho, \rho^\tau)$$

Use the dual formulation:

$$\begin{aligned} W_2^2(\rho, \sigma) &= 2 \max_{\pi \in \Pi(\rho, \sigma)} \int \left(u(x) + v(y) - \frac{|x - y|^2}{2}\right) d\pi(x, y) \\ &= 2 \max_{u, v} \left\{ \int u \, d\rho + \int v \, d\sigma \mid u(x) + v(y) \leq \frac{|x - y|^2}{2} \right\} \\ &= 2 \max_{u} \left\{ \int u \, d\rho + \int u^* \, d\sigma \right\} \end{aligned}$$

$$\frac{d}{d\epsilon} W_2^2(\rho + \epsilon\chi, \sigma)\bigg|_{\epsilon=0}$$

$$= 2\frac{d}{d\epsilon} \max_u \left\{ \int u \, d(\rho + \epsilon\chi) + \int u^* \, d\sigma \right\} \bigg|_{\epsilon=0}$$

$$= 2\frac{d}{d\epsilon} \max_u \left\{ \int u(\rho + \epsilon\chi) \, dx + \int u^* \, d\sigma \right\} \bigg|_{\epsilon=0}$$

$$= 2 \int u\chi \, dx$$

Where u^* achieves the max in the previous line.
i.e., u^* is the potential associated with the cost $\frac{1}{2}|x-y|^2$.
When we do OT, the optimal map is $T(x)$:

$$T(x) = x - \nabla u^*(x)$$
$$= (\nabla h)^{-1}(\nabla u^*(x))$$

where $h(z) = \frac{1}{2}|z|^2$

$$\Rightarrow \frac{\delta W_2^2}{\delta \rho}(\rho, \rho_\tau^n) = 2u^*$$

$T(x) = x - \nabla u^t(x)$ is the optimal map from ρ to ρ_τ^n.
The JKO scheme is

$$\rho_\tau^{n+1} = \arg\min_\rho \left\{ F(\rho) + \frac{W_2^2(\rho, \rho_\tau^n)}{2\tau} \right\}$$

$$= \arg\min G(\rho)$$

$$\Rightarrow \frac{\delta G}{\delta \rho}(\rho_\tau^{n+1}) + C = 0$$

$$\Rightarrow \frac{\delta F}{\delta \rho}(\rho_\tau^{n+1}) + \frac{u^*}{\tau} = \text{constant}$$

$$0 = \nabla \left(\frac{\delta F}{\delta \rho} \right) + \frac{u^t}{\tau}$$

$$= \nabla \left(\frac{\delta F}{\delta \rho} \right) + \frac{x - T(x)}{\tau}$$

$$\Rightarrow \frac{T(x) - x}{\tau} = \nabla \left(\frac{\delta F}{\delta \rho} \right)$$

velocity!

$$\text{of a flow from } \rho_\tau^{n+1} \text{ to } \rho^t$$

The flow we want should have velocity

$$V(x) := -\frac{T(x) - x}{\tau} = -\nabla\left(\frac{\delta F}{\delta \rho}\right)$$

This is the velocity associated with our time-discrete scheme.

If everything works out as $\tau \to 0$, we expect our JKO scheme to limit to this flow

$$\partial_t \rho + \nabla \cdot (\rho V) = 0$$

or

$$\partial_t \rho - \nabla \cdot \left(\rho \nabla \left(\frac{\delta F}{\delta \rho}\right)\right) = 0$$

This is the PDE associated with gradient flows of F in the W_2 metric.

C.12.2 Exemple: Link between entropy and heat equation

$F(\rho) = \int \rho \log \rho \, dx$ (negative entropy)

We want a flow that maximizes entropy.

$$\frac{d}{d\epsilon} F(\rho + \epsilon\chi)\Big|_{\epsilon=0}$$

$$= \frac{d}{d\epsilon} \int (\rho + \epsilon\chi) \log(\rho + \epsilon\chi) \, dx \Big|_{\epsilon=0}$$

$$= \int (\chi \log \rho + \chi) \, dx$$

$$\Rightarrow \frac{\delta F}{\delta \rho} = \log \rho + 1$$

$$\nabla\left(\frac{\delta F}{\delta \rho}\right) = \nabla(\log \rho + 1) = \frac{1}{\rho}\nabla\rho$$

$$\Rightarrow \text{The Gradient Flow is}$$

$$0 = \partial_t \rho - \nabla \cdot \left(\rho \frac{1}{\rho} \nabla \rho\right)$$

$$= \partial_t \rho - \nabla \cdot (\nabla \rho)$$

$$= \partial_t \rho - \Delta \rho$$

$$\Rightarrow \partial_t \rho = \Delta \rho \quad \text{(heat equation)}$$

C.12.3 Exemple: Link between entropy plus potential

Eg: $F(\rho) = \int \rho \log \rho \, dx + \int V(x) \rho \, dx$

$$\Rightarrow \partial_t \rho - \Delta \rho - \nabla \cdot (\rho \nabla V) = 0$$

(Fokker-Planck)

C.12.4 Exemple: porous medium

Eg: $F(\rho) = \frac{1}{m-1} \int \rho^m \, dx$

$$\Rightarrow \partial_t \rho - \Delta(\rho^m) = 0$$

C.12.5 Exemple: Renyi entropy

The Rényi entropy of order α, for a probability density ρ on a domain Ω, is defined as:

$$H_\alpha(\rho) = \frac{1}{1-\alpha} \log \int_\Omega \rho(x)^\alpha \, dx, \tag{166}$$

where $\alpha > 0$ and $\alpha \neq 1$. This generalizes to the Shannon entropy as $\alpha \to 1$.

Derivation of the PDE for $\rho(t)$

Given the Rényi entropy of order α for a probability density ρ on a domain Ω, defined as:

$$H_\alpha(\rho) = \frac{1}{1-\alpha} \log \int_\Omega \rho(x)^\alpha \, dx, \tag{167}$$

where $\alpha > 0$ and $\alpha \neq 1$. The functional derivative of the Rényi entropy with respect to the density ρ is computed as follows:

$$\frac{\delta H_\alpha}{\delta \rho} = \alpha \rho^{\alpha - 1}. \tag{168}$$

Using this functional derivative, the gradient flow of ρ in the space of probability measures, endowed with the Wasserstein metric, is described by the following partial differential equation:

$$\partial_t \rho = \nabla \cdot (\rho \nabla \phi), \tag{169}$$

where $\phi = -\alpha \rho^{\alpha - 1}$ is the potential function influenced by the functional derivative.

Substituting ϕ into the gradient flow equation, we obtain:

$$\partial_t \rho = \nabla \cdot \left(\rho \nabla (-\alpha \rho^{\alpha-1}) \right). \tag{170}$$

Expanding this via the product rule, we can further simplify:

$$\partial_t \rho = -\alpha \left((\nabla \rho) \cdot (\nabla \rho^{\alpha-1}) + \rho \Delta (\rho^{\alpha-1}) \right). \tag{171}$$

Utilizing the chain rule for derivatives, $\nabla \rho^{\alpha-1} = (\alpha-1)\rho^{\alpha-2}\nabla\rho$, we rewrite the equation as:

$$\partial_t \rho = -\alpha(\alpha-1) \left(\rho^{\alpha-2} (\nabla \rho) \cdot (\nabla \rho) + \rho \Delta (\rho^{\alpha-1}) \right), \tag{172}$$

which characterizes the evolution of the density ρ under the influence of Rényi entropy. This equation reflects complex diffusion and drift processes driven by the entropy gradient in the Wasserstein space.

C.12.6 Exemple: Keller-Segel, chemotaxis

JKO Scheme Applied to the Keller-Segel Model

The Keller-Segel model, a fundamental mathematical model for chemotaxis, describes the movement of cells in response to a chemical stimulus. The Jordan-Kinderlehrer-Otto (JKO) scheme, traditionally used for Wasserstein gradient flows, can be innovatively applied to this model to explore the dynamics under a gradient flow formulation in the space of probability measures.

Energy Functional of Keller-Segel

To apply the JKO scheme, we first identify a suitable energy functional for the Keller-Segel system:

$$\mathcal{E}(u, c) = \int \left(\frac{D_u}{2} |\nabla u|^2 + \frac{D_c}{2} |\nabla c|^2 - u \log c \right) dx, \tag{173}$$

where u represents the cell density, c the chemoattractant concentration, and D_u, D_c are the respective diffusion coefficients. The term $u \log c$ models the chemotactic attraction to the chemoattractant.

Formulation of the JKO Scheme

The JKO scheme approximates the evolution of the system by solving a series of minimization problems:

$$(u^{k+1}, c^{k+1}) = \arg\min_{u,c} \left\{ \frac{1}{2\tau} W_2^2((u^k, c^k), (u, c)) + \mathcal{E}(u, c) \right\}, \tag{174}$$

where τ is the time step size, and W_2 denotes the Wasserstein distance. This iterative minimization seeks to balance the diffusion and chemotactic effects to simulate the dynamics of chemotaxis.

Insights and Applications

The application of the JSE scheme provides a new perspective on the Keller-Segel model:

- **Regularization Effects:** Incorporating the Wasserstein distance introduces a smoothing effect, which can help prevent the blow-up phenomena often seen in the Keller-Segel model.
- **Numerical Implementation:** The scheme offers a structured approach for numerical simulations, ensuring mass conservation and non-negativity of the density functions.
- **Theoretical Implications:** The framework facilitates deeper theoretical analysis regarding the existence, uniqueness, and stability of solutions.

While promising, applying the JKO scheme to the Keller-Segel model presents computational challenges, particularly in calculating Wasserstein distances for coupled systems. Future research could focus on developing efficient algorithms to overcome these challenges and further explore the implications of this approach in biological systems.

Simplified version

$F(\rho) = \int \rho \log \rho \, dx - \frac{1}{2} \int |\nabla \psi_\rho|^2 \, dx$
where $-\Delta \psi_\rho = \rho$

$$\Rightarrow \begin{cases} \partial_t \rho + \nabla \cdot (\rho \nabla u) - \Delta \rho = 0 \\ -\Delta u = \rho \end{cases}$$

C.12.7 Exemple: aggregation model

Eg: $F(\rho) = \frac{1}{2} \iint W(x-y) \, d\rho(x) \, d\rho(y)$

$$\Rightarrow \partial_t \rho - \nabla \cdot (\rho(\nabla W * \rho)) = 0$$

C.13 OT with non-quadratic costs

$$\begin{aligned} \text{(DP)} \quad & \sup J[u, v] \\ \text{s.t.} \quad & u(x) + v(y) \leq c(x, y)^p \end{aligned}$$

where the functional J is given by

$$J[u, v] = \int_X u(x) \, d\mu(x) + \int_Y v(y) \, d\nu(y)$$

and the cost function $c(x, y)$ is defined by

$$c(x, y) = \frac{1}{2}|x - y|^2$$

with the transformations applied to the coordinates

$$\varphi(x) = \frac{1}{2}|x|^2 - u(x), \quad \psi(y) = \frac{1}{2}|y|^2 - v(y)$$

and φ, ψ are convex duals.

The expression for $u(x)$ in terms of L-F duals is derived as follows:

$$\begin{aligned}\frac{1}{2}|x|^2 - u(x) = \varphi(x) &= \sup_y \{x \cdot y - \psi(y)\} \\ &= \sup_y \left\{x \cdot y - \frac{1}{2}|y|^2 + v(y)\right\}\end{aligned}$$

$$\begin{aligned}u(x) = \inf_y \left\{\frac{1}{2}|x|^2 + \frac{1}{2}|y|^2 - x \cdot y - v(y)\right\} & \\ &= \inf_y \left\{\frac{1}{2}|x - y|^2 - v(y)\right\} \\ &= \inf_y \{c(x, y) - v(y)\}\end{aligned}$$

where $c(x, y) = \frac{1}{2}|x - y|^2$ denotes the cost function.

C.13.1 Definitions and Properties of C-transforms

Definition 2. We say that u is C-concave if there exists v such that

$$u(x) = \inf_y \{C(x, y) - v(y)\}$$

Definition 3. The C-transform of u is given by

$$u^c(y) = \inf_x \{C(x, y) - u(x)\}$$

Properties of C-transforms:

- $u^{cc}(x) \geq u(x)$

Proof:

$$u^{cc}(x) = \inf_y \{C(x, y) - \inf_z \{C(y, z) - u(z)\}\} \geq \inf_y \{C(x, y) - C(y, x) + u(x)\} = u(x)$$

Where we used the symmetry of C(x,y)

- u^c is C-concave

- $u^{ccc}(y) = u^c(y)$

Proof:

$$\begin{aligned} u^{ccc}(y) &= \inf_x\{C(x,y) - \inf_w\{C(x,w) - \inf_z\{C(w,z) - u(z)\}\}\} \\ &\leq \inf_x \sup_w\{C(x,y) - C(x,w) + C(w,x) - u(x)\} \\ &= \inf_x\{C(x,y) - u(x)\} \\ &= u^c(y) \end{aligned}$$

Observations:

- We always have $u^{ccc} \geq u^c$
- Therefore, $u^{ccc} = u^c$
- If u is C-concave, then $u^{cc} = u$.

C.13.2 Generalization of Subgradient for Quadratic Cost

How does the subgradient generalize?

In the normal case with a quadratic cost:

$$\begin{aligned} & P \in \partial\varphi(x) \\ \implies & \varphi(y) \geq \varphi(x) + P \cdot (y - x) && \text{for all } y \\ \implies & |y|^2 - |\varphi(y)| \geq |x|^2 - |\varphi(x)| + P \cdot (y - x) && \text{for all } y \\ \implies & u(y) = \frac{1}{2}|y|^2 - \frac{1}{2}|x|^2 - P \cdot (y - x) + u(x) && \text{for all } y \\ & = u(x) + \frac{1}{2}|y - P|^2 - \frac{1}{2}|x - P|^2 && \text{for all } y \\ & = u(x) + C(P, y) - C(P, x) && \text{for all } y \end{aligned}$$

This derivation shows the generalization of the subgradient in the context of a quadratic cost function.

C.13.3 Definition and Properties of the C-superdifferential

Definition 4. We say that $p \in \partial^c u(x)$ (the C-superdifferential) if

$$u(y) \leq u(x) - C(x,p) + C(y,p) \quad \text{for all } y$$

We consider the optimization problem:

$$\sup\left\{\int_X u(x)\, d\mu(x) + \int_Y v(y)\, d\nu(y)\right\}$$

subject to the constraint:

$$u(x) + v(y) \leq C(x, y)$$

Observation: As before, it's sufficient to focus on (u, v) that are C-concave duals, where:

$$u(x) = \inf_y \{C(x, y) - v(y)\}, \quad v(y) = \inf_x \{C(x, y) - u(x)\}$$

As before, the minimum is attained. Let's characterize u a bit more.

Choose any $x_0 \in X$. Suppose the minimum is attained when $y = T(x_0)$:

$$\begin{aligned} u(x_0) &= c(x_0, T(x_0)) - v(T(x_0)) \\ &= c(x_0, T(x_0)) - \inf_z \{c(T(x_0), z) - u(z)\} \\ &\geq c(x_0, T(x_0)) - c(T(x_0), z) + u(z) \quad \text{for all } z \end{aligned}$$

This implies:

$$T(x) \in \partial^c u(x)$$

We know from earlier conditions:

$$u(x_0) = c(x_0, T(x_0)) - v(T(x_0)) \quad \text{and} \quad u(x) \leq c(x, T(x_0)) - v(T(x_0)) \quad \text{for all } x$$

This implies that the function:

$$c(x, T(x_0)) - v(T(x_0)) - u(x) \geq 0$$

achieves equality when $x = x_0$, indicating it is minimized at x_0.

To further explore, the first derivative test gives us:

$$\nabla_x c(x_0, T(x_0)) - \nabla u(x_0) = 0$$

This result tells us that at x_0, the gradient of the cost function c with respect to x, evaluated at $x_0, T(x_0)$, equals the gradient of u at x_0. This is a critical point indicating where the function u attains its minimum relative to the cost function and transportation plan T.

For the second derivative test, we need:

$$D^2_{xx} c(x_0, T(x_0)) - D^2 u(x_0) \geq 0$$

Let's consider costs of the form:

$$c(x, y) = h(x - y)$$

where h is a function defining the cost based on the distance between x and y.

Our conditions for the map then become:

$$\begin{aligned} \nabla h(x - T(x)) &= \nabla u(x), \\ D^2 h(x - T(x)) - D^2 u(x) &\geq 0 \end{aligned}$$

If ∇h is invertible, this implies:

$$T(x) = x - (\nabla h)^{-1}(\nabla u(x))$$

C.13.4 Analysis of the Optimal Transport Solution

Question 1: Does this $T(x)$ solve the OT problem? Is T measure-preserving?

As before, we define:

$$v_\epsilon(y) = v(y) + \epsilon r(y), \quad u_\epsilon(x) = \inf_y \{c(x,y) - v(y) - \epsilon r(y)\}$$

Thus,

$$u_\epsilon(x) = u(x) - \epsilon r(T(x)) + o(\epsilon)$$

and the change in the functional J is given by:

$$0 \leq J[u_\epsilon, v_\epsilon] - J[u,v]$$

$$= \int_X r(T(x)) d\mu(x) - \int_Y r(y) d\nu(y) + o(\epsilon)$$

To ensure the map T is measure-preserving, we must have:

$$\int_X r(T(x)) d\mu(x) = \int_Y r(y) d\nu(y)$$

This condition implies that the transformed measure $T_{\#}\mu$ must equal ν, ensuring that T indeed preserves measure and satisfies the conditions of the optimal transport problem.

Question 2: Is T optimal?

Consider any transformation S preserving measure μ, the optimal transport (OT) cost for S is given by:

$$C(S) = \int_X c(x, S(x))\, d\mu(x)$$

Recall that the solution to the dual problem satisfies:

$$u(x) + v(y) \leq c(x,y)$$

This implies:

$$C(S) \geq \int_X \left(u(x) + v(S(x))\right)\, d\mu(x)$$

This inequality shows that any transformation S satisfying the measure-preserving condition will have a cost $C(S)$ that is at least as much as the cost derived from the sum of the dual potentials u and v. Therefore, if T satisfies this with equality, it would indeed be optimal.

Continuing the optimality check:

$$= \int_X \left(\inf_y \{c(x,y) - v(y)\} + v(S(x)) \right) d\mu(x)$$

$$= \int_X \left(c(x, T(x)) - v(T(x)) + v(S(x))\right) d\mu(x)$$

$$= \int_X c(x, T(x)) d\mu(x)$$

$$= C(T)$$

This shows that the integral of the cost function over X with respect to $T(x)$ indeed equals the cost $C(T)$, and therefore:

$$T \text{ is optimal}$$

This calculation confirms that T minimizes the transportation cost, thereby fulfilling the criteria for optimality in the context of the optimal transport problem.

Differentiation and Conditions for Optimality

Given the mapping:

$$T(x) = x - (\nabla h)^{-1}(\nabla u(x))$$

We have the conditions:

$$D^2h(x - T(x)) - D^2u(x) \geq 0$$

and the gradient:

$$\nabla u = \nabla h(x - T(x))$$

Differentiating the equation for ∇u yields:

$$D^2u(x) = D^2h(x - T(x))(I - \nabla T(x))$$

This leads to:

$$D^2h(x - T(x)) - D^2u(x) = D^2h(x - T(x))\nabla T(x)$$

To further investigate the stability of this setup, we take the determinant of both sides:

$$\det(D^2h(x - T(x)) - D^2u(x)) = \det(D^2h(x - T(x))\nabla T(x))$$

This determinant condition checks for the stability and injectivity of the transformation T based on the second derivative of h and u.

Continuing the analysis, we explore the determinant conditions:

$$\det(D^2h(x - T(x)) - D^2u(x)) = \det(D^2h(x - T(x))) \cdot \det(I - \nabla T(x))$$

For T defined as:

$$T(x) = x - (\nabla h)^{-1}(\nabla u(x))$$

we derive that:

$$\det(D^2h((\nabla h)^{-1}(\nabla u(x))) - D^2u(x)) = \det(D^2h((\nabla h)^{-1}(\nabla u(x)))) \cdot f(x) \cdot g(T(x))$$

where $f(x)$ and $g(T(x))$ represent additional scalar functions involved in the transformation process, potentially affecting the stability and conditions of T.

This results in:

$$D^2h((\nabla h)^{-1}(\nabla u(x))) - D^2u(x) \geq 0$$

This inequality ensures that the transformation T is stable and injective over the set X, assuming $(\nabla h)^{-1}$ and $\nabla u(x)$ behave regularly across the domain.

C.13.5 Exemple: Recovering the euclidian distance squared for the cost

Given the cost function:

$$h = \frac{1}{2}|x - y|^2$$

We analyze the determinant related to the transformation:

$$\det(I - D^2 u(x)) = \frac{f(x)}{g(x - \nabla u(x))}$$

This equation relates the second derivative of u with functions f and g, which adjust the determinant calculation.

It's noted that:

$$I - D^2 u \geq 0$$

which implies the transformation is stable.

If we define:

$$\varphi(x) = \frac{|x|^2}{2} - u(x)$$

Then, the determinant can be expressed as:

$$\det(D^2 \varphi(x)) = \frac{f(x)}{g(\nabla \varphi(x))}$$

This expression shows how the determinants, involving transformations and potential fields, are adjusted by functions f and g, which may represent scaling factors or corrections to ensure the integrity of physical or mathematical properties in the system. This is the Monge-Ampere equation we saw before.

C.13.6 Exemple: L1 cost between two parallel plan

Consider two parallel planes represented by distributions f and g, separated by a distance L. The L^1 cost between a point on one plane to a point on the other is modeled by the function:

$$h(z) = \sqrt{|z|^2 + L^2}$$

where z represents the horizontal component of the displacement between points on the two planes.

The cost function $c(x, y)$ for transporting a unit mass from point x on the first plane to point y on the second plane is given by:

$$c(x, y) = h(x - y)$$

This represents the Euclidean distance between points, taking into account the fixed vertical separation L.

Given the function:

$$h(z) = \sqrt{|z|^2 + L^2}$$

The gradient of h with respect to z is:

$$\nabla h(z) = \frac{z}{\sqrt{|z|^2 + L^2}}$$

To find the inverse function $(\nabla h)^{-1}$, set:

$$\frac{z}{\sqrt{|z|^2 + L^2}} = p$$

Squaring both sides and solving for $|z|^2$, we have:

$$|z|^2 + L^2 = |p|^2 \Rightarrow |z|^2(1 - |p|^2) = |p|^2 L^2$$

$$\Rightarrow |z|^2 = \frac{|p|^2 L^2}{1 - |p|^2}$$

This leads to:

$$|z| = \frac{|p|L}{\sqrt{1 - |p|^2}}$$

Thus, the component z in terms of p is:

$$z = \frac{pL}{\sqrt{1 - |p|^2}}$$

This relationship provides the inverse gradient $(\nabla h)^{-1}(p)$:

$$(\nabla h)^{-1}(p) = \frac{pL}{\sqrt{1 - |p|^2}}$$

This derivation finds z such that the gradient of h at z equals a given vector p, useful in contexts where distances and gradients need to be mapped inversely, such as in some optimization problems or geometric transformations.

The optimal map has the form:

$$T(x, w) = x - \frac{Lw}{\sqrt{1 - |w|^2}}$$

The Hessian $(D^2 h)$ of h at point y is given by:

$$(D^2 h)_{ij} = \begin{cases} \left(|z|^2 + L^2 - 2z_i^2\right) / \left(|z|^2 + L^2\right)^{3/2} & \text{if } i = j \\ -z_i z_j / \left(|z|^2 + L^2\right)^{3/2} & \text{if } i \neq j \end{cases}$$

Applying $(D^2 h)$ to $(\nabla h)^{-1}(p)$ results in:

$$(D^2 h((\nabla h)^{-1}(p)))_{ij} = \begin{cases} (1 - p_i^2)\sqrt{1 - |p|^2}/L & \text{if } i = j \\ -p_i p_j \sqrt{1 - |p|^2}/L & \text{if } i \neq j \end{cases}$$

The product of D^2h with the matrix $I - pp^T$ gives:

$$D^2h((\nabla h)^{-1}(p)) = \frac{\sqrt{1-|p|^2}}{L}(I - pp^T)$$

These expressions calculate the second derivatives and apply them to transformations involving the gradient and its inverse, illustrating the interplay between geometry and the applied transformation forces in the optimal map setting.

The determinant of the Hessian matrix after transformation is calculated as:

$$\det(D^2h((\nabla h)^{-1}(p))) = \left(\frac{(1-|p|^2)^{n/2+1}}{L^n}\right)$$

This expression reflects how the determinant scales with respect to the parameter p and the dimension n.

The partial differential equation (PDE) involved here is represented by the determinant:

$$\det\left(\frac{\sqrt{1-|\nabla u|^2}}{L}(I - \nabla u \nabla u^T) - D^2u\right) = \left(\frac{(1-|\nabla u|^2)^{n/2+1}}{L^n}\right)\frac{f}{g\left(x - \frac{L\nabla u}{\sqrt{1-|\nabla u|^2}}\right)}$$

These computations are crucial in solving or analyzing the behavior of the system under transformations dictated by the functions u and h, particularly in contexts like geometric transformations or in the study of material behavior under certain constraints.

Generalization to MTW Conditions

The procedures and calculations described can be rigorously applied to costs that satisfy the Ma-Trudinger-Wang (MTW) conditions. These conditions are pivotal in optimal transport theory for ensuring regularity and curvature constraints which facilitate unique and stable solutions. Specifically, the cost function h must meet the following criteria:

- $h \in C^4$ indicating that h is continuously differentiable up to the fourth order.
- ∇h is invertible, ensuring that there is a well-defined and unique gradient at every point, which is crucial for the transformations to be reversible.
- $\det(D^2h(z)) \neq 0$, which implies that the Hessian of h is non-degenerate, maintaining a certain level of convexity or concavity needed for optimal mappings.
- Technical conditions satisfied by higher derivatives of cost, ensuring that more nuanced geometric and analytical properties hold, which are often required for deeper theoretical results in optimal transport.

These conditions ensure that the cost function and the transformations it induces are well-behaved and suitable for sophisticated analysis in the optimal transport framework.

C.13.7 Ma-Trudinger-Wang (MTW) Conditions

The Ma-Trudinger-Wang (MTW) conditions are vital in the theory of optimal transportation, particularly in relation to the regularity and uniqueness of solutions to the Monge-Ampère equation associated with cost functions $c(x, y)$. These conditions are named after mathematicians Xi-Nan Ma, Neil Trudinger, and Xu-Jia Wang and impose stringent requirements on the curvature properties of the cost function to ensure the smoothness of the optimal transport map.

Cross-Curvature Condition

The MTW tensor, which measures the cross-curvature of the cost function, is defined for vectors ξ and η at points x and y respectively as:

$$\text{MTW}(x, y, \xi, \eta) = -\frac{3}{4} \frac{\partial^3 c}{\partial x^i \partial y^j \partial y^k}(x, y) \xi^i \eta^j \eta^k + \frac{3}{4} \frac{\partial^3 c}{\partial x^i \partial x^j \partial y^k}(x, y) \eta^i \eta^j \xi^k$$

This tensor should not change sign across the domain of the cost function, ensuring a consistent behavior in terms of the geometry defined by the cost function.

Smoothness and Regularity

The cost function $c(x, y)$ should be sufficiently smooth, typically requiring C^4 smoothness (four times continuously differentiable). This level of differentiability ensures that all necessary derivatives used in the MTW tensor and other analytical constructs are well-defined and behave continuously.

Global Curvature Conditions

These conditions require the curvature defined by the cost function to behave consistently on a global scale, aiding in proving global regularity results for the optimal transport map. This is crucial for preventing singularities and ensuring the stability and uniqueness of solutions to the optimal transport problem.

These MTW conditions are integral in proving that the optimal transport map is not only well-defined but also smooth and unique, particularly in more complex or higher-dimensional transport scenarios.

C.14 divergence of divergences

Radon-Nikodym Derivative

For two equivalent Gaussian measures $\nu = N(m, C)$ and $\mu = N(m_0, C_0)$ on a Hilbert space H, the Radon-Nikodym derivative $\frac{d\nu}{d\mu}$ expresses the density of one

measure with respect to the other. This derivative is crucial for calculating the divergences between the measures. The Girsanov theorem provides the Radon-Nikodym derivative for Gaussian measures as:

$$\frac{d\nu}{d\mu}(x) = \exp\left(\langle x, h\rangle - \frac{1}{2}\|h\|^2\right),$$

where $h = C_0^{-1/2}(m - m_0)$.

Kullback-Leibler Divergence

The Kullback-Leibler (KL) divergence between two probability distributions measures the information loss when μ is used to approximate ν. For two Gaussian measures $\nu = N(m, C)$ and $\mu = N(m_0, C_0)$, the explicit formula for the KL divergence is derived as follows:

$$D_{\mathrm{KL}}(\nu\|\mu) = \frac{1}{2}\left(\langle m - m_0, C_0^{-1}(m - m_0)\rangle + \mathrm{tr}(C_0^{-1}C - I) - \log\det(C_0^{-1}C)\right).$$

However, in infinite dimensions, regularization is necessary. The regularized KL divergence $D_{\mathrm{KL}}^{\gamma}(\nu\|\mu)$ is defined and shown to converge to the true KL divergence as the regularization parameter γ approaches zero:

$$D_{\mathrm{KL}}^{\gamma}(N(m, C)\|N(m_0, C_0)) = \frac{1}{2}\left(\langle m - m_0, (C_0 + \gamma I)^{-1}(m - m_0)\rangle + d_{\mathrm{logdet}}^{\gamma}(C, C_0)\right),$$

where

$$d_{\mathrm{logdet}}^{\gamma}(C, C_0) = \mathrm{tr}[(C_0 + \gamma I)^{-1}(C + \gamma I) - I] - \log\det[(C_0 + \gamma I)^{-1}(C + \gamma I)].$$

Rényi Divergence

The Rényi divergence generalizes the KL divergence and provides a parameterized family of divergences. For two Gaussian measures $\nu = N(m, C)$ and $\mu = N(m_0, C_0)$, the explicit formula for the Rényi divergence of order r is given by:

$$D_{\mathrm{R},r}(\nu\|\mu) = \frac{1}{2}\left(\frac{1}{1 - r}\log\mathbb{E}_{\mu}\left[\left(\frac{d\nu}{d\mu}\right)^{r}\right]\right).$$

The regularized Rényi divergence $D_{\mathrm{R},r}^{\gamma}(\nu\|\mu)$ is defined similarly to the regularized KL divergence and shown to converge to the true Rényi divergence as $\gamma \to 0$:

$$D_{\mathrm{R},r}^{\gamma}(N(m, C)\|N(m_0, C_0)) = \frac{1}{2}\left(\langle m - m_0, [(1 - r)(C + \gamma I) + r(C_0 + \gamma I)]^{-1}(m - m_0)\rangle\right.$$
$$\left. + \frac{1}{r(1 - r)}\log\det[(1 - r)(C + \gamma I) + r(C_0 + \gamma I)]\right).$$

Key Results

1. **Convergence of Regularized Divergences**: The regularized KL and Rényi divergences between two equivalent Gaussian measures converge to the true divergences as the regularization parameter γ approaches zero.

2. **Explicit Formulas**: The paper provides explicit formulas for the Radon-Nikodym derivative, KL divergence, and Rényi divergence between two equivalent Gaussian measures, extending existing results to the most general Gaussian settings.

3. **Applications**: These formulas are applied to problems such as Bayesian inverse problems on Hilbert spaces, demonstrating their practical utility in computing divergences between posterior and prior probability measures.

C.15 ultra-violet divergence

The term "ultra-violet divergence" is often used in the context of quantum field theory and statistical mechanics to describe divergences that occur at high frequencies or short wavelengths. This term is indeed appropriate for the type of divergences encountered in computing the KL divergence and differential entropy of infinite-dimensional Gaussian measures, especially when these measures are analyzed in the Fourier domain.

Ultra-Violet Divergence in Infinite-Dimensional Gaussian Measures

In the context of infinite-dimensional Gaussian measures, the covariance operator often has eigenvalues that decay to zero, corresponding to the high-frequency components in the Fourier analysis. The challenge in computing quantities like the KL divergence and differential entropy arises from these high-frequency components, leading to divergences that can be thought of as "ultra-violet" in nature.

Fourier Analysis and High Frequencies

When analyzing Gaussian measures on a Hilbert space, Fourier analysis can be a powerful tool. In this setting, the covariance operator's eigenfunctions can be viewed as Fourier modes, with corresponding eigenvalues indicating the contribution of each mode. The high-frequency modes (or ultra-violet components) have smaller eigenvalues, and their accumulation at zero leads to the divergences observed.

Regularization as Handling Ultra-Violet Divergences

Regularization techniques, such as adding a small positive parameter γ to the covariance operator, can be seen as a way to tame these ultra-violet divergences. By shifting the spectrum away from zero, regularization effectively dampens the

contribution of high-frequency components, making the necessary operations (like taking logarithms and traces) well-defined.

Summary

- **Ultra-Violet Divergence**: The divergences encountered in the KL divergence and differential entropy of infinite-dimensional Gaussian measures can be aptly termed "ultra-violet divergences" because they are linked to high-frequency components in Fourier analysis.
- **Fourier Analysis**: In this framework, the eigenvalues of the covariance operator correspond to the contributions of different Fourier modes. The high-frequency modes, with eigenvalues close to zero, are the source of the divergences.
- **Regularization**: Techniques such as adding a parameter γ to the covariance operator serve to regularize these ultra-violet divergences, ensuring that the mathematical expressions are well-defined and finite.

Renormalizable and Non-Renormalizable Theories in High Energy Physics

In theoretical physics, particularly in high energy physics, the concepts of renormalizable and non-renormalizable theories play a crucial role.

Renormalizable Theories

Definition: Renormalizable theories are those in which the infinities that arise in quantum field theory calculations can be managed by introducing a finite number of counterterms. These counterterms are added to the Lagrangian to cancel out the divergences, making the physical predictions finite and well-defined.

Key Points:

- **Counterterms:** In renormalizable theories, only a finite number of counterterms are needed to absorb the infinities in all orders of perturbation theory.
- **Dimensional Analysis:** These theories typically involve interactions with mass dimensions less than or equal to four (in four-dimensional spacetime). This is because interactions with higher mass dimensions lead to non-renormalizable terms.
- **Physical Predictability:** Renormalizable theories allow for a finite set of physical parameters (like masses and coupling constants) to be experimentally measured and used to predict other observables.

- **Examples:** Quantum Electrodynamics (QED), Quantum Chromodynamics (QCD), and the Standard Model of particle physics are all renormalizable theories.

Process:

- **Regularization:** Introduce a regularization scheme (such as dimensional regularization) to systematically handle the infinities.
- **Renormalization:** Adjust the parameters (masses, coupling constants) in the Lagrangian by adding counterterms.
- **Renormalization Group:** Use renormalization group equations to study how physical parameters change with energy scale.

Non-Renormalizable Theories

Definition: Non-renormalizable theories are those where an infinite number of counterterms would be needed to cancel all the infinities that arise in quantum field theory calculations. These theories contain interactions with mass dimensions greater than four in four-dimensional spacetime.

Key Points:

- **Infinite Counterterms:** Non-renormalizable theories require an infinite number of counterterms, making them impractical for predictive calculations.
- **Effective Field Theories:** Often, non-renormalizable theories are treated as effective field theories that are valid up to a certain energy scale. Beyond this scale, a more fundamental theory is needed.
- **Examples:** Gravity, when described by General Relativity, is non-renormalizable. At high energies, quantum gravitational effects become significant, requiring a more fundamental theory like string theory or loop quantum gravity.

Process:

- **Effective Theories:** Use the theory as an effective field theory valid up to a certain energy scale.
- **Higher-Order Terms:** Include higher-order terms with higher mass dimensions, acknowledging that these terms become important at higher energies.

Renormalization and Regularization in High Energy Physics

Renormalization:

- A process to remove infinities by redefining the parameters of the theory (masses, coupling constants).

- Ensures finite, physically meaningful predictions.

Regularization:

- A mathematical technique to handle infinities. Common methods include:
  - **Dimensional Regularization:** Continue the number of spacetime dimensions to a non-integer value to control divergences.
  - **Cut-off Regularization:** Introduce a cut-off parameter to limit the maximum energy/momentum.

Example - Quantum Electrodynamics (QED):

- **Lagrangian:** The QED Lagrangian involves terms like $\bar{\psi}(i\gamma^\mu\partial_\mu - m)\psi - e\bar{\psi}\gamma^\mu A_\mu\psi$, where ψ is the electron field, A_μ is the photon field, and e is the electric charge.
- **Divergences:** Loop diagrams in QED lead to infinities.
- **Counterterms:** Introduce counterterms in the Lagrangian to cancel these infinities.
- **Renormalized Quantities:** Define renormalized masses and charges that are finite and measurable.

In summary

Renormalizable theories provide a framework for making finite, predictive calculations in quantum field theory by introducing a finite number of counterterms. Non-renormalizable theories, while challenging due to the infinite counterterms required, are often treated as effective field theories valid up to a certain energy scale. The process of renormalization ensures that physical quantities remain finite and measurable, allowing for meaningful comparisons with experimental data.

C.16 Renormalizable and Non-Renormalizable Theories in High Energy Physics

In theoretical physics, particularly in high energy physics, the concepts of renormalizable and non-renormalizable theories play a crucial role.

Renormalizable Theories

Definition: Renormalizable theories are those in which the infinities that arise in quantum field theory calculations can be managed by introducing a finite number of counterterms. These counterterms are added to the Lagrangian to cancel out the divergences, making the physical predictions finite and well-defined.

Key Points:

- **Counterterms:** In renormalizable theories, only a finite number of counterterms are needed to absorb the infinities in all orders of perturbation theory.
- **Dimensional Analysis:** These theories typically involve interactions with mass dimensions less than or equal to four (in four-dimensional spacetime). This is because interactions with higher mass dimensions lead to non-renormalizable terms.
- **Physical Predictability:** Renormalizable theories allow for a finite set of physical parameters (like masses and coupling constants) to be experimentally measured and used to predict other observables.
- **Examples:** Quantum Electrodynamics (QED), Quantum Chromodynamics (QCD), and the Standard Model of particle physics are all renormalizable theories.
- **Additional Examples:** Gauge theories and supersymmetric theories are also renormalizable. Gauge theories include the electroweak theory and quantum chromodynamics. Supersymmetric theories, which extend the Standard Model by introducing supersymmetry, are designed to be renormalizable.

Process:

- **Regularization:** Introduce a regularization scheme (such as dimensional regularization) to systematically handle the infinities.
- **Renormalization:** Adjust the parameters (masses, coupling constants) in the Lagrangian by adding counterterms.
- **Renormalization Group:** Use renormalization group equations to study how physical parameters change with energy scale.

Non-Renormalizable Theories

Definition: Non-renormalizable theories are those where an infinite number of counterterms would be needed to cancel all the infinities that arise in quantum field theory calculations. These theories contain interactions with mass dimensions greater than four in four-dimensional spacetime.

Key Points:

- **Infinite Counterterms:** Non-renormalizable theories require an infinite number of counterterms, making them impractical for predictive calculations.
- **Effective Field Theories:** Often, non-renormalizable theories are treated as effective field theories that are valid up to a certain energy scale. Beyond this scale, a more fundamental theory is needed.

- **Examples:** Gravity, when described by General Relativity, is non-renormalizable. At high energies, quantum gravitational effects become significant, requiring a more fundamental theory like string theory or loop quantum gravity.

Process:

- **Effective Theories:** Use the theory as an effective field theory valid up to a certain energy scale.
- **Higher-Order Terms:** Include higher-order terms with higher mass dimensions, acknowledging that these terms become important at higher energies.

Renormalization and Regularization in High Energy Physics

Renormalization:

- A process to remove infinities by redefining the parameters of the theory (masses, coupling constants).
- Ensures finite, physically meaningful predictions.

Regularization:

- A mathematical technique to handle infinities. Common methods include:
  - **Dimensional Regularization:** Continue the number of spacetime dimensions to a non-integer value to control divergences.
  - **Cut-off Regularization:** Introduce a cut-off parameter to limit the maximum energy/momentum.

Example - Quantum Electrodynamics (QED):

- **Lagrangian:** The QED Lagrangian involves terms like $\bar{\psi}(i\gamma^\mu\partial_\mu - m)\psi - e\bar{\psi}\gamma^\mu A_\mu\psi$, where ψ is the electron field, A_μ is the photon field, and e is the electric charge.
- **Divergences:** Loop diagrams in QED lead to infinities.
- **Counterterms:** Introduce counterterms in the Lagrangian to cancel these infinities.
- **Renormalized Quantities:** Define renormalized masses and charges that are finite and measurable.

Link Between Losses and Action-Based Dynamics

The link between losses, including KL-divergences, and action-based dynamics in theoretical physics allows us to predict that the results of the paper can be extended to non-Gaussian situations based on the renormalizable examples.

Key Points:

- **KL-Divergence and Action:** In theoretical physics, the KL-divergence is analogous to the action in a field theory, where minimizing the action corresponds to finding the most probable configurations of the field.
- **Extension to Non-Gaussian Situations:** Given that renormalizable theories successfully handle infinities by adding counterterms, we can extend this approach to non-Gaussian measures. Non-Gaussian situations can be treated by introducing appropriate counterterms to manage divergences.
- **Predictive Power:** This analogy suggests that we can use the techniques developed for renormalizable theories to predict and handle divergences in more complex, non-Gaussian systems.

Conclusion: The results from the paper on Gaussian measures and divergences can be extended to non-Gaussian situations by leveraging the principles of renormalization and regularization from action-based dynamics in theoretical physics. This approach underscores the deep connection between field theory techniques and statistical methods for managing divergences in high-dimensional spaces.

Example - Quantum Electrodynamics (QED)

Quantum Electrodynamics (QED) is a prime example of a renormalizable theory. The QED Lagrangian is given by:

$$\mathcal{L}_{\text{QED}} = -\frac{1}{4}F_{\mu\nu}F^{\mu\nu} + \bar{\psi}(i\gamma^\mu D_\mu - m)\psi,$$

where

- $F_{\mu\nu} = \partial_\mu A_\nu - \partial_\nu A_\mu$ is the field strength tensor of the electromagnetic field A_μ.
- ψ is the Dirac spinor field representing the electron.
- $D_\mu = \partial_\mu + ieA_\mu$ is the covariant derivative.
- m is the mass of the electron.
- e is the electric charge.

Divergences: Loop diagrams in QED lead to infinities. For example, the self-energy of the electron and the vacuum polarization lead to divergent integrals.

Counterterms: To address these divergences, counterterms are added to the Lagrangian. These counterterms adjust the parameters m and e to absorb the infinities and yield finite results for observable quantities.

Renormalized Quantities: After introducing the counterterms, the renormalized mass m_r and charge e_r are finite and measurable. The renormalization procedure ensures that physical predictions match experimental observations.

Link Between Losses and Action-Based Dynamics

The link between losses, including KL-divergences, and action-based dynamics in theoretical physics allows us to predict that the results of the paper can be extended to non-Gaussian situations based on the renormalizable examples.

Key Points:

- **KL-Divergence and Action:** In theoretical physics, the KL-divergence is analogous to the action in a field theory, where minimizing the action corresponds to finding the most probable configurations of the field.
- **Extension to Non-Gaussian Situations:** Given that renormalizable theories successfully handle infinities by adding counterterms, we can extend this approach to non-Gaussian measures. Non-Gaussian situations can be treated by introducing appropriate counterterms to manage divergences.
- **Predictive Power:** This analogy suggests that we can use the techniques developed for renormalizable theories to predict and handle divergences in more complex, non-Gaussian systems.

Key Points:

- **Action Minimization:** In theoretical physics, the action S is obtained by integrating the Lagrangian $\mathcal{L}$ over all spacetime:

  $$S = \int_{-\infty}^{+\infty} \mathcal{L}\, d^4x.$$

  Minimizing the action corresponds to finding the most probable configurations of the field.
- **KL-Divergence and Action:** The KL-divergence in probability theory can be seen as analogous to the action in field theory. Both involve an integral over a space (parameter space for KL-divergence and spacetime for the action) and measure the "distance" from a reference configuration (or measure).
- **Extension to Non-Gaussian Situations:** Given that renormalizable theories successfully handle infinities by adding counterterms, we can extend this approach to non-Gaussian measures. Non-Gaussian situations can be treated by introducing appropriate counterterms to manage divergences.
- **Predictive Power:** This analogy suggests that we can use the techniques developed for renormalizable theories to predict and handle divergences in more complex, non-Gaussian systems.

C.17 Formulations of Quantum Field Theory Using Divergences

In theoretical physics, particularly in high energy physics, divergences such as the Kullback-Leibler (KL) divergence and other related measures are used in various formulations of quantum field theory (QFT). These formulations are especially relevant in contexts such as the path integral formulation, the holographic principle, and the study of entanglement entropy.

Path Integral Formulation and Statistical Mechanics

In the path integral formulation of QFT, the action S plays a central role. The path integral formulation can be seen as an extension of statistical mechanics to quantum fields, where the connection to divergences such as the KL-divergence becomes apparent.

Action Minimization and KL-Divergence: The action S is minimized in the classical limit, and this minimization is analogous to minimizing the KL-divergence in statistical mechanics. This analogy is often drawn in the study of statistical field theory, where one uses a free energy functional that includes entropy terms, leading to expressions that resemble the KL-divergence.

Holographic Principle and Entanglement Entropy

The holographic principle and the AdS/CFT (Anti-de Sitter/Conformal Field Theory) correspondence provide another framework where divergences are studied.

Entanglement Entropy: In QFT, the entanglement entropy of a subsystem A is given by the von Neumann entropy $S = -\mathrm{Tr}(\rho_A \log \rho_A)$, where ρ_A is the reduced density matrix of A. This entropy can be related to divergences such as the Rényi divergence, and these concepts are deeply connected in the context of holography and black hole thermodynamics.

Relative Entropy and Modular Hamiltonian

Relative Entropy: The relative entropy, which is a generalization of the KL-divergence, is used in QFT to measure the distinguishability between two quantum states. The relative entropy $S(\rho\|\sigma) = \mathrm{Tr}(\rho \log \rho) - \mathrm{Tr}(\rho \log \sigma)$ can be interpreted in terms of the modular Hamiltonian, and it plays a crucial role in understanding the stability of quantum systems and the dynamics of entanglement.

Examples and Applications

Quantum Statistical Mechanics: In quantum statistical mechanics, the KL-divergence is used to study the thermodynamics of quantum systems. The connection between the free energy functional and the KL-divergence is often explored to understand phase transitions and critical phenomena.

Quantum Information Theory: In the context of quantum information theory, divergences such as the KL-divergence, Rényi divergence, and relative entropy are used to quantify information and entanglement in quantum systems. These measures are essential for understanding quantum communication and error correction.

Holography and AdS/CFT: The AdS/CFT correspondence uses concepts from information theory, such as relative entropy and entanglement entropy, to explore the duality between gravitational theories in AdS space and conformal field theories on the boundary. These concepts help in understanding the emergence of spacetime and the behavior of black holes.

In summary

The use of divergences such as the KL-divergence in quantum field theory is rich and multifaceted. These divergences provide deep insights into the behavior of quantum systems, the dynamics of entanglement, and the connection between quantum information and spacetime geometry. The path integral formulation, holographic principle, and the study of entanglement entropy are key areas where these concepts are applied.

Holographic Principle and Entanglement Entropy

The holographic principle and the AdS/CFT (Anti-de Sitter/Conformal Field Theory) correspondence provide another framework where divergences are studied.

Entanglement Entropy: In QFT, the entanglement entropy of a subsystem A is given by the von Neumann entropy

$$S = -\mathrm{Tr}(\rho_A \log \rho_A),$$

where ρ_A is the reduced density matrix of A. This entropy can be related to divergences such as the Rényi divergence, which is defined as

$$S_\alpha(\rho_A) = \frac{1}{1-\alpha} \log \mathrm{Tr}(\rho_A^\alpha),$$

for $\alpha > 0$ and $\alpha \neq 1$. These concepts are deeply connected in the context of holography and black hole thermodynamics. In the AdS/CFT correspondence, the entanglement entropy of a region in the boundary CFT is related to the area of a minimal surface in the bulk AdS space. This relationship, known as the Ryu-Takayanagi formula, provides a geometric interpretation of entanglement entropy and illustrates the deep connection between quantum information and gravitational theories.

Relative Entropy and Modular Hamiltonian

Relative Entropy: The relative entropy, which is a generalization of the KL-divergence, is used in QFT to measure the distinguishability between two quan-

tum states. The relative entropy $S(\rho\|\sigma)$ is defined as

$$S(\rho\|\sigma) = \mathrm{Tr}(\rho \log \rho) - \mathrm{Tr}(\rho \log \sigma),$$

where ρ and σ are density matrices. This can be interpreted in terms of the modular Hamiltonian, and it plays a crucial role in understanding the stability of quantum systems and the dynamics of entanglement. The relative entropy is always non-negative and vanishes if and only if $\rho = \sigma$, making it a useful tool for quantifying how one state deviates from another.

Examples and Applications

Quantum Statistical Mechanics: In quantum statistical mechanics, the KL-divergence is used to study the thermodynamics of quantum systems. The connection between the free energy functional and the KL-divergence is often explored to understand phase transitions and critical phenomena.

Quantum Information Theory: In the context of quantum information theory, divergences such as the KL-divergence, Rényi divergence, and relative entropy are used to quantify information and entanglement in quantum systems. These measures are essential for understanding quantum communication and error correction.

Holography and AdS/CFT: The AdS/CFT correspondence uses concepts from information theory, such as relative entropy and entanglement entropy, to explore the duality between gravitational theories in AdS space and conformal field theories on the boundary. These concepts help in understanding the emergence of spacetime and the behavior of black holes. The Ryu-Takayanagi formula, in particular, illustrates how entanglement entropy in a CFT is related to geometric quantities in the dual AdS space.

Modular Hamiltonian and Its Properties

The modular Hamiltonian, often denoted as K, is an operator associated with a specific quantum state and a subregion of a quantum system. It is defined through the reduced density matrix of the subsystem.

Definition

For a given quantum state ρ and its reduced density matrix ρ_A for a subsystem A, the modular Hamiltonian K is defined by the relation:

$$\rho_A = \frac{e^{-K}}{\mathrm{Tr}(e^{-K})}.$$

Here, K is the modular Hamiltonian, and the term $\mathrm{Tr}(e^{-K})$ ensures that ρ_A is properly normalized.

Properties of the Modular Hamiltonian

- **Eigenvalues and Eigenvectors:** The eigenvalues of K are related to the logarithms of the eigenvalues of ρ_A. If ρ_A has an eigenvalue λ_i with corresponding eigenvector $|i\rangle$, then K has an eigenvalue $-\log \lambda_i$ with the same eigenvector $|i\rangle$.

- **Thermal Interpretation:** The expression $\rho_A = \frac{e^{-K}}{Z}$ (where $Z = \mathrm{Tr}(e^{-K})$) is analogous to the thermal state in statistical mechanics, where K acts like the Hamiltonian of the subsystem and the density matrix ρ_A represents a thermal state at unit temperature.

- **Relative Entropy:** The relative entropy $S(\rho\|\sigma)$ between two states ρ and σ can be expressed in terms of their modular Hamiltonians. For states ρ and σ with corresponding modular Hamiltonians K_ρ and K_σ:

$$S(\rho\|\sigma) = \mathrm{Tr}(\rho(K_\rho - K_\sigma)).$$

- **Modular Flow:** The modular Hamiltonian generates a unitary flow known as the modular flow. For an operator $\mathcal{O}$ in the algebra of the subsystem A, the modular flow is given by:

$$\sigma_t(\mathcal{O}) = e^{itK}\mathcal{O}e^{-itK},$$

  where t is a real parameter. This flow can be interpreted as a kind of time evolution under the modular Hamiltonian.

- **Area Law and Entanglement:** In holography and the AdS/CFT correspondence, the modular Hamiltonian is connected to the entanglement entropy of a region. The Ryu-Takayanagi formula, which relates the entanglement entropy of a boundary region to the area of a minimal surface in the bulk, can be understood in terms of the modular Hamiltonian.

Applications and Relevance

- **Quantum Field Theory:** In QFT, the modular Hamiltonian provides insight into the structure of entanglement in quantum states. It is particularly useful in studying the entanglement properties of ground states and thermal states.

- **Holography and AdS/CFT:** The modular Hamiltonian plays a crucial role in the holographic principle and the AdS/CFT correspondence. It helps in understanding how information about a boundary region is encoded in the bulk geometry.

- **Quantum Information Theory:** The modular Hamiltonian is used to quantify and analyze entanglement and correlations in quantum systems. It is essential for computing measures like relative entropy and for studying the dynamics of entanglement.

Modular Hamiltonian and KMS Theory

The concept of the modular Hamiltonian is closely related to Kubo-Martin-Schwinger (KMS) theory, which deals with thermal equilibrium states in quantum statistical mechanics.

KMS Condition

The KMS condition provides a criterion for a state to be in thermal equilibrium. A state ρ satisfies the KMS condition at inverse temperature β if, for any two observables A and B,

$$\langle A(t)B\rangle_\beta = \langle BA(t+i\beta)\rangle_\beta,$$

where $A(t)$ is the time-evolved operator A under the Hamiltonian of the system, and $\langle\cdot\rangle_\beta$ denotes the thermal expectation value with respect to the state ρ.

Modular Hamiltonian

The modular Hamiltonian K provides a natural framework for understanding the KMS condition. For a state ρ and its modular Hamiltonian K, the modular flow is given by:

$$\sigma_t(A) = e^{itK}Ae^{-itK}.$$

This modular flow satisfies a similar analytic continuation property as the KMS condition:

$$\langle A(t)B\rangle = \langle B\sigma_{-i}(A(t))\rangle,$$

where $\sigma_{-i}(A(t)) = e^{-K}A(t)e^{K}$.

Modular Theory and von Neumann Algebras

The theory of modular automorphisms, developed by Tomita and Takesaki, extends the concept of the modular Hamiltonian to the setting of von Neumann algebras. In this framework, the modular Hamiltonian is associated with a von Neumann algebra $\mathcal{M}$ and a faithful normal state ϕ. The modular automorphism group $\{\sigma_t^\phi\}_{t\in\mathbb{R}}$ is a one-parameter group of automorphisms of $\mathcal{M}$ given by:

$$\sigma_t^\phi(A) = \Delta_\phi^{it}A\Delta_\phi^{-it},$$

where Δ_ϕ is the modular operator associated with ϕ.

Properties and Applications

- **Thermal States and Entropy:** The modular Hamiltonian characterizes thermal states and their entropies. The von Neumann entropy, relative entropy, and Rényi entropy can all be expressed in terms of the modular Hamiltonian.

- **Entanglement Entropy in QFT:** In quantum field theory, the modular Hamiltonian provides a way to compute the entanglement entropy of a region. The Ryu-Takayanagi formula in holography relates the entanglement entropy of a boundary region to the area of a minimal surface in the bulk, using the modular Hamiltonian.
- **KMS Condition:** The KMS condition for thermal equilibrium states is naturally described using the modular flow generated by the modular Hamiltonian. This connects the concepts of statistical mechanics and quantum field theory.

Modular Hamiltonian, KMS Theory, and QED Lagrangian

In theoretical physics, the concepts of the modular Hamiltonian and KMS theory are closely related to the Hamiltonian derived from a specific Lagrangian, such as that of Quantum Electrodynamics (QED).

QED Lagrangian and Hamiltonian

The QED Lagrangian is given by:

$$\mathcal{L}_{\text{QED}} = -\frac{1}{4}F_{\mu\nu}F^{\mu\nu} + \bar{\psi}(i\gamma^\mu D_\mu - m)\psi,$$

where

- $F_{\mu\nu} = \partial_\mu A_\nu - \partial_\nu A_\mu$ is the field strength tensor of the electromagnetic field A_μ,
- ψ is the Dirac spinor field representing the electron,
- $D_\mu = \partial_\mu + ieA_\mu$ is the covariant derivative,
- m is the mass of the electron,
- e is the electric charge.

The Hamiltonian H derived from this Lagrangian is:

$$H = \int d^3x \left(\psi^\dagger(-i\gamma^0\gamma^i D_i + m\gamma^0)\psi + \frac{1}{2}(\mathbf{E}^2 + \mathbf{B}^2) \right),$$

where $\mathbf{E}$ and $\mathbf{B}$ are the electric and magnetic fields, respectively.

Modular Hamiltonian

For a subsystem A, the modular Hamiltonian K is related to the reduced density matrix ρ_A by:

$$\rho_A = \frac{e^{-K}}{\text{Tr}(e^{-K})}.$$

The modular flow generated by K is given by:

$$\sigma_t(A) = e^{itK} A e^{-itK}.$$

KMS Condition

The KMS condition provides a criterion for thermal equilibrium. A state ρ satisfies the KMS condition at inverse temperature β if:

$$\langle A(t)B\rangle_\beta = \langle BA(t+i\beta)\rangle_\beta,$$

where $A(t)$ is the time-evolved operator under the Hamiltonian H, and $\langle\cdot\rangle_\beta$ denotes the thermal expectation value with respect to ρ.

The modular Hamiltonian K satisfies a similar relation:

$$\langle A(t)B\rangle = \langle Be^{-K}A(t)e^{K}\rangle.$$

Entanglement Entropy and Holography

In QFT, the entanglement entropy S_A of a region A is given by the von Neumann entropy:

$$S_A = -\mathrm{Tr}(\rho_A \log \rho_A).$$

The Ryu-Takayanagi formula in the AdS/CFT correspondence relates this entropy to the area of a minimal surface in the bulk AdS space:

$$S_A = \frac{\mathrm{Area}(\gamma_A)}{4G_N},$$

where γ_A is the minimal surface in the bulk whose boundary matches the boundary of A on the AdS boundary, and G_N is the Newton constant.

In summary

The modular Hamiltonian, derived from the Hamiltonian associated with the QED Lagrangian, provides deep insights into the thermal and entanglement properties of quantum systems. The KMS condition links thermal equilibrium states to the modular flow, and the entanglement entropy computed via the modular Hamiltonian connects quantum information theory to the geometry of spacetime in holography.

Action in the Hamiltonian Formulation of Statistical Theory

In the Hamiltonian formulation of statistical mechanics and quantum field theory, the action is a functional that, when minimized, gives the equations of motion of the system. When incorporating constraints from observations, the action can be modified to include Lagrange multipliers that enforce these constraints.

Action in the Hamiltonian Formulation

The action S is generally defined as the integral over time of the Lagrangian L:

$$S[q_i, \dot{q}_i] = \int_{t_1}^{t_2} L(q_i, \dot{q}_i, t)\, dt.$$

In the presence of constraints $g(q_i, \dot{q}_i, t) = 0$, we introduce a Lagrange multiplier $\lambda(t)$ and write the modified action as:

$$S[q_i, \dot{q}_i, \lambda] = \int_{t_1}^{t_2} \left(L(q_i, \dot{q}_i, t) + \lambda(t) g(q_i, \dot{q}_i, t)\right) dt.$$

Path Integral Formulation

In the path integral formulation, the partition function Z is given by a path integral over all possible field configurations ϕ:

$$Z = \int \mathcal{D}\phi\, e^{iS[\phi]},$$

where $S[\phi]$ is the action functional of the field ϕ.

Statistical Mechanics and the Free Energy Functional

In statistical mechanics, the action can be related to the free energy functional. For a system in thermal equilibrium at temperature $T = \frac{1}{\beta}$, the partition function Z is given by:

$$Z = \int \mathcal{D}q\, e^{-\beta H(q)},$$

where $H(q)$ is the Hamiltonian of the system. The free energy F is related to the partition function by:

$$F = -\frac{1}{\beta} \log Z.$$

The corresponding action S in the Euclidean time formulation is:

$$S_E[q_i, \dot{q}_i] = \int_0^{\beta} \left(\sum_i \frac{m_i}{2} \dot{q}_i^2 + V(q_i) \right) d\tau,$$

where $V(q_i)$ is the potential energy.

Analytical Formula of the Action with Constraints

When we include constraints from observations, the action is modified by adding terms that enforce these constraints. For a constraint $C[q_i, \dot{q}_i, t] = 0$ with a Lagrange multiplier $\lambda(t)$, the modified action is:

$$S[q_i, \dot{q}_i, \lambda] = \int_{t_1}^{t_2} \left(L(q_i, \dot{q}_i, t) + \lambda(t) C[q_i, \dot{q}_i, t]\right) dt.$$

Example: Statistical Action with Constraints

Consider a system with a constraint on the average value of some observable $\mathcal{O}(q_i, \dot{q}_i, t)$ to be equal to O_0:

$$\langle \mathcal{O} \rangle = O_0.$$

The corresponding constraint is:

$$C[q_i, \dot{q}_i, t] = \mathcal{O}(q_i, \dot{q}_i, t) - O_0 = 0.$$

The modified action is:

$$S[q_i, \dot{q}_i, \lambda] = \int_{t_1}^{t_2} \left(L(q_i, \dot{q}_i, t) + \lambda(t)(\mathcal{O}(q_i, \dot{q}_i, t) - O_0) \right) dt.$$

C.18 Simplified Scenario for Free Field Theory with Discrete Field Values

In order to connect with the concepts in the paper, we consider a simplified scenario with the following assumptions:

- No matter, only the free field.
- No space dimension, only time.
- Time goes from 0 to 1.

Discretized Field Values

Consider a free field $\phi(t)$ represented by a set of field values $\{\phi_i\}$ that are dense in the interval $]0, 1[$. These field values can be organized into a matrix Φ where $\Phi_{ij} = \phi_i \phi_j$.

Action Computation

The action S for this discrete set of field values is given by summing over the squares of the field values:

$$S = \sum_i \phi_i^2.$$

This can be related to the determinant of the logarithm of the field values through the matrix Φ. Specifically, the action can be expressed as:

$$S = \log \det \left(\{ \log(\phi_i) + \log(\phi_j) \}_{i,j \in \mathbb{N}} \right).$$

Matrix Formulation

Given the matrix Φ, we can write:

$$\Phi = \{\phi_i \phi_j\}_{i,j \in \mathbb{N}}.$$

The action then becomes:

$$S = \log \det \left(\{\log(\phi_i) + \log(\phi_j)\}_{i,j \in \mathbb{N}} \right).$$

To be more explicit, if Φ is a matrix with elements $\Phi_{ij} = \phi_i \phi_j$, the action can be represented as:

$$S = \log \det \left(\{\log(\phi_i) + \log(\phi_j)\}_{i,j \in \mathbb{N}} \right).$$

Summary

In this simplified scenario, the field $\phi(t)$ is represented by a set of field values $\{\phi_i\}$ that are dense in the interval $]0, 1[$. The action is computed using these discrete field values, and the matrix Φ formed by the product of these values. The action is then given by the logarithm of the determinant of the logarithms of the field values:

$$S = \log \det \left(\{\log(\phi_i) + \log(\phi_j)\}_{i,j \in \mathbb{N}} \right).$$

D Pricing of the Equinox in a Black-Scholes Model

D.1 Decomposition into Components

The Equinox payoff comprises two distinct parts, each reflecting different aspects of the option's structure. The first part is akin to a conventional binary option, and the second part is a more complex structure that can be further divided. These components are identified as follows:

The first part: This is a standard binary option that pays off if the underlying asset's price at the first observation date exceeds the barrier B. It is mathematically represented as:

$$\text{Binary1} = \mathbb{E}[1_{S_1 \geq B}] \tag{175}$$

The second part: This component is more complex and can be split into two binary options. It can be expressed as the expectation of a binary that pays off if the underlying asset's price at the second observation date surpasses the strike price K, under the condition that the price was below the barrier B at the first observation date. Mathematically, this part can be described with the following equations:

$$\text{Binary2a} = \mathbb{E}[1_{S_1 < B} 1_{S_2 \geq K}] \tag{176}$$

$$\text{Binary2b} = \mathbb{E}[(S_2 - K)^+ 1_{S_1 < B}] \tag{177}$$

The total second part of the payoff then combines these two expectations:

$$\text{Binary2} = \text{Binary2a} - \text{Binary2b} \tag{178}$$

The final expression for the price of the Equinox in terms of its components is thus given by:

$$P = S_0 \times \text{Binary1} - K \times \text{Binary2} \tag{179}$$

Here, S_0 represents the initial price of the underlying asset, and K is the strike price. The complete payoff structure incorporates both the binary nature of the first part and the conditional nature of the second part, reflecting the hybrid character of the Equinox option.

D.2 The Ordinary Binary Option

The first part of the Equinox payoff, termed as the ordinary binary option, is contingent on the underlying asset's price being above a certain barrier B at the first observation date t_1. This part of the option's payoff can be evaluated using the risk-neutral valuation framework inherent in the Black-Scholes model. The valuation of this binary option is given by:

$$\text{Option1} = \mathbb{E}[1_{S_1 \geq B}] = P\left(W_{t_1} \geq \frac{\log(\frac{B}{S_0}) + \frac{1}{2}\sigma^2 t_1}{\sigma}\right) = 1 - N\left(\frac{\log(\frac{B}{S_0}) + \frac{1}{2}\sigma^2 t_1}{\sigma\sqrt{t_1}}\right) \tag{180}$$

Here, W_{t_1} represents the Wiener process at time t_1, S_0 is the initial price of the underlying asset, σ is the volatility of the underlying asset, and $N(\cdot)$ denotes the cumulative distribution function of the standard normal distribution. The expected value $\mathbb{E}[1_{S_1 \geq B}]$ under the risk-neutral measure is computed as the probability that the Wiener process W_{t_1} exceeds a certain threshold, which corresponds to the asset price being above the barrier B at time t_1. The result is expressed in terms of the cumulative normal distribution function, reflecting the probabilistic nature of the binary option's payoff.

D.3 Two Conditional Binaries

In the assessment of the Equinox option's second part, we address two conditional binary options, Binary2a and Binary2b. Before proceeding with their valuation, we establish the following notations and definitions:

$$\rho = \frac{\sqrt{t_1}}{\sqrt{t_2}}, \quad \Sigma = \sigma\sqrt{t_2}, \quad y_1 = \frac{K_1}{\sqrt{t_1}}, \quad y_2 = \frac{K_2}{\sqrt{t_2}} \tag{181}$$

$$K_1 = \frac{\log(\frac{B}{S_0}) + \frac{1}{2}\sigma^2 t_1}{\sigma}, \quad K_2 = \frac{\log(\frac{K}{S_0}) + \frac{1}{2}\sigma^2 t_2}{\sigma} \tag{182}$$

Here, ρ represents the correlation coefficient between two normalized Gaussian variables that model the asset price movements at two different times, Σ is the scaled volatility, y_1 and y_2 are the standardized variables used in the normal distribution related to the barriers, and K_1, K_2 represent the thresholds for the binary events based on the barrier B and strike price K respectively.

With these definitions in place, the Wiener processes at times t_1 and t_2 are modeled as:

$$W_{t_1} = \rho X_1 \tag{183}$$

$$W_{t_2} = W_{t_1} + \sqrt{1-\rho^2}\Sigma X_2 \tag{184}$$

Where X_1 and X_2 are two independent standardized Gaussian variables. This setup allows us to capture the stochastic dependency between the underlying asset's prices at the two observation dates, which is crucial for the valuation of the binary options Binary2a and Binary2b.

D.4 Definition of the m-Binary

The m-Binary, an integral part of the second component of the Equinox payoff, is defined by its dependence on the joint distribution of two standardized Gaussian variables. Its value is given by the following integral expression:

$$\text{m-Binary} = \exp\left(-\frac{m^2\Sigma^2}{2}\right)\mathbb{E}\left[1_{(X_1\le y_1)}1_{(\rho X_1+\sqrt{1-\rho^2}X_2\ge y_2)}\right]$$

$$= \frac{\exp\left(-\frac{m^2\Sigma^2}{2}\right)}{2\pi}\int_{-\infty}^{y_1}\int_{\frac{\rho}{\sqrt{1-\rho^2}}(X_1-y_2)}^{\infty}\exp\left(m\Sigma(\rho X_1+\sqrt{1-\rho^2}X_2)-\frac{X_1^2+X_2^2}{2}\right)dX_2\,dX_1 \tag{185}$$

In this definition:

- m is the mean of the Gaussian variables accounting for the drift under the risk-neutral measure.
- Σ is the scaled volatility factor.
- y_1 and y_2 are the standardized thresholds corresponding to the barrier B and the strike K, as previously defined.
- ρ is the correlation coefficient between the Brownian motions at times t_1 and t_2.
- X_1 and X_2 are independent standard Gaussian variables.

The integral calculates the probability under the risk-neutral measure that the underlying asset will be below the barrier B at t_1 and above the strike K at t_2, adjusted for the mean and volatility of the process.

D.5 Algebraic Girsanov Transformation

The Girsanov theorem facilitates the transformation of probability measures, which is particularly effective in Gaussian market models. This algebraic manipulation, which we refer to as the "Algebraic Girsanov" transformation, simplifies the computation by dealing with the quadratic polynomial in the exponent of the Gaussian probability density function. To illustrate, we introduce a new variable X_3 as a linear combination of the Gaussian variables X_1 and X_2:

$$X_3 = \rho X_1 + \sqrt{1-\rho^2} X_2, \tag{186}$$

This yields the following quadratic form in the exponent of the Gaussian density:

$$\frac{X_1^2 + X_2^2 - 2\rho X_1 X_2}{2(1-\rho^2)} = \frac{(X_1 - \rho m\Sigma)^2 + (X_3 - m\Sigma)^2 - 2\rho(X_3 - m\Sigma)(X_1 - \rho m\Sigma)}{2(1-\rho^2)} - \frac{(m\Sigma)^2}{2} \tag{187}$$

Now, by completing the square, we simplify this expression, which is tantamount to shifting the measure in the risk-neutral world, and thus aligns with the Girsanov theorem. This shift effectively removes the drift of the process in the transformed measure, thereby simplifying the expectation calculations for the m-binary options.

$$m\Sigma(X_3) - \frac{X_1^2 + X_3^2 - 2\rho X_3 X_1}{2(1-\rho^2)} = -\frac{(X_1 - \rho m\Sigma)^2 + (X_3 - m\Sigma)^2}{2(1-\rho^2)} + \frac{(m\Sigma)^2}{2} \tag{188}$$

This result is significant as it represents the essence of the Girsanov transformation in the context of the Black-Scholes model: a shift that turns the drift of the Brownian motion into a martingale, a process that has no drift under the risk-neutral measure.

D.6 Normalization of the m-binariy pricing formula

Following the algebraic Girsanov transformation, the integral that defines the pricing of the m-Binary can be rewritten in a form amenable to the use of normal distributions. The expression now takes the following form, where the exponent in the integrand resembles the density function of a bivariate normal distribution:

$$
\begin{aligned}
\text{m-Binary} =& \frac{\exp\left(-\frac{m^2\Sigma^2}{2}\right)}{2\pi\sqrt{1-\rho^2}} \\
&\times \int_{-\infty}^{y_1}\int_{y_2}^{\infty} \exp\left(-\frac{(X_1-\rho m\Sigma)^2}{2(1-\rho^2)} - \frac{(X_3-m\Sigma)^2}{2(1-\rho^2)}\right. \\
&\left. + \frac{\rho(X_3-m\Sigma)(X_1-\rho m\Sigma)}{1-\rho^2}\right) dX_1\, dX_3 \qquad (189)\\
=& \frac{\exp\left((m-1)m\Sigma^2/2\right)}{2\pi\sqrt{1-\rho^2}} \\
&\times \int_{-\infty}^{y_1-\rho m\Sigma}\int_{y_2-m\Sigma}^{\infty} \exp\left(-\frac{X_1^2+X_3^2}{2(1-\rho^2)} + \frac{\rho X_3 X_1}{1-\rho^2}\right) dX_1\, dX_3
\end{aligned}
$$

By identifying the integrand's exponent with the density of the bivariate normal distribution, we can leverage standard results for the bivariate normal distribution to evaluate the integral. Specifically, this approach allows us to express the pricing of the m-Binary in terms of the cumulative distribution functions of the univariate and bivariate normal distributions, greatly simplifying the computational complexity of the problem.

This transformation significantly simplifies the pricing of options in the Black-Scholes model by reducing it to tabulated statistical functions, which are well-understood and can be computed efficiently.

D.7 Full m-Binary Formula

The culmination of the pricing process for the m-Binary is its representation in closed form. This expression utilizes both the univariate and bivariate normal cumulative distribution functions (CDFs), $N(\cdot)$ and $N_2(\cdot,\cdot;\rho)$ respectively. The closed-form expression for the m-Binary is:

$$
\text{m-Binary} = \exp\left(\frac{(m-1)m\Sigma^2}{2}\right)\left(N(y_1-\rho m\Sigma) - N_2(y_1-\rho m\Sigma, y_2-m\Sigma;\rho)\right) \qquad (190)
$$

where:

- $N(\cdot)$ is the CDF of the standard normal distribution.
- $N_2(\cdot,\cdot;\rho)$ is the CDF of the standard bivariate normal distribution with correlation ρ.
- y_1 and y_2 are the standardized thresholds corresponding to the barrier B and strike K, previously defined.
- m and Σ are as defined in the context of the risk-neutral measure and scaled volatility.

This formula synthesizes the pricing of the m-Binary in a form that is readily computable, leveraging the analytical tractability of normal distributions. It underscores the mathematical elegance with which complex derivatives can be priced in the Black-Scholes framework.

D.8 Full Equinox Closed Form

After the derivation of the m-Binary's pricing, we can now present the complete closed-form solution for the Equinox payoff. The Equinox is a sophisticated financial instrument that combines aspects of binary options with those of a European call option. The closed-form expression is given by:

$$\text{Equinox} = S_0 e^{\mu T} X(1) - K X(0) + G \cdot \text{digit}(S_0 e^{\mu R}, B, R),$$

$$\text{where} \quad X(m) = \mathbb{E}\left[1_{(S_R \leq B)} 1_{(S_T \geq K)}\right] \left(\frac{S_T}{S_0}\right)^m$$

Therefore

$$\text{Equinox} = \exp\left(\frac{(m-1)mT\sigma^2}{2}\right)\left(N\left(\frac{K_1}{\sqrt{R}} - \sqrt{Rm\sigma}\right) - N_2\left(\frac{K_1}{\sqrt{R}}, \frac{K_2}{\sqrt{T}} - m\sqrt{T\sigma}, \sqrt{\frac{R}{T}}\right)\right) \tag{191}$$

with:

- K_1 and K_2 as thresholds for the barrier and strike events, defined by:

$$K_1 = \text{digit}(S_0 e^{\mu R}, B, R) = N\left(\frac{\log(\frac{B}{S_0}) + (\frac{1}{2}\sigma^2 - \mu)R}{\sigma\sqrt{R}}\right) \tag{192}$$

$$K_2 = \text{digit}(S_0 e^{\mu R}, K, R) = N\left(\frac{\log(\frac{K}{S_0}) - (\frac{1}{2}\sigma^2 - \mu)T}{\sigma\sqrt{T}}\right) \tag{193}$$

This formulation encapsulates the dynamics of the Equinox's pricing within the Black-Scholes framework, utilizing the risk-neutral measure to account for binary and call option features. We also added an additional parameter μ for taking into account interest rates, dividends, and the repo rate.

9 Commented Bibliography

This section provides a selection of key references used in the development of the Equinox derivative pricing model, along with commentary on their relevance.

Books and Articles

The seminal paper by Black and Scholes [1] introduces the Black-Scholes model for option pricing, which forms the foundation of the theoretical framework

employed in this annex. The methodology for risk-neutral valuation and its application to European options are particularly relevant.

Hull's comprehensive text [2] offers insight into the wide range of financial instruments and the models used to price them. It includes a discussion on the numerical methods for option pricing, which underpins the computational approach taken here.

Shreve's work [3] on stochastic calculus provides the mathematical underpinnings necessary for understanding the continuous-time models that are crucial for derivative pricing. The Girsanov Theorem, which is key for the risk-neutral measure, is explained in detail.

The introductory book by Wilmott et al. [4] demystifies the mathematics behind financial derivatives and is referenced for its clear exposition of the binomial model and the transition to the continuous-time Black-Scholes model.

Online Resources

The Online Derivative Pricing Tools [5] were instrumental for verifying the computational results obtained in the pricing of the Equinox derivative.

Historical volatility data from the National Bureau of Economic Research [6] was used to calibrate the models employed in this annex.

Autocallable Derivatives Pricing

Piterbarg's discussion [7] on the valuation of autocallable structures in the presence of collateral posting has become increasingly relevant in post-crisis financial markets. The paper provides insights into the complexities of pricing these instruments in a collateralized trading environment.

The article by Tanaka and Takahashi [8] explores empirical methods for pricing autocallable derivatives using extensions of the Black-Scholes model. The approaches discussed were considered for their relevance to pricing the Equinox derivative, especially in adapting the Black-Scholes framework.

Clarke and Parry's examination [9] of the multi-factor Heston model's applicability to the pricing of autocallable products provides a perspective on modeling the volatility surface dynamically, which is critical for the accurate pricing of autocalls.

Lipton and Sepp's exploration [10] of pricing autocallables in the context of the Heston local-stochastic volatility (LSV) model is considered for more complex pricing scenarios.

Zhao, Zhang, and Wang's framework [11] for modeling and pricing autocallables using Partial Differential Equations (PDEs) allows for both discrete and continuous autocall dates.

The focus of Lee et al. [42] on pricing autocallable structured products with knock-in features using Brownian Bridge techniques is noted for computational efficiency and handling complex structures.

SLCG Economic Consulting's overview [13] of autocallables, pricing considerations, and modeling using various techniques is also referenced.

Optimal Transport

Cédric Villani's book [14] provides a thorough exploration of optimal transport, detailing its historical context and modern advances. It is recognized as a foundational text in the field.

This work by Peyré and Cuturi [15] is pivotal for those applying optimal transport to data science, offering a comprehensive review of computational techniques and practical applications in machine learning.

Santambrogio's book [16] is tailored for practitioners and applied mathematicians, presenting optimal transport in a way that connects mathematical theory with real-world applications.

Cuturi's introduction of Sinkhorn distances [17] has revolutionized the computational approach to optimal transport, enabling efficient application in large-scale machine learning scenarios.

Martingale Optimal Transport

Beiglböck, Henry-Labordère, &Penkner (2013) [18]: This seminal paper introduced mass transport techniques to find upper and lower pricing bounds for options without needing to assume a specific underlying asset price model. These bounds rely only on the observed marginal distributions of the underlying asset.

Galichon, Henry-Labordère, & Touzi (2014) [27]: This work extends the framework to derive model-independent bounds for options with path-dependent payoffs, including lookback options. It links the pricing problem to a stochastic control problem.

Henry-Labordère (2016) [20]: This book provides a comprehensive view of model-free hedging within the mass transport framework. It develops connections and offers additional insights for both practitioners and researchers.

Acciaio, Backhoff-Veraguas, & Carassus (2016) [21]: This paper explores extending the notion of no-arbitrage beyond the context of semimartingales, a significant contribution to theoretical foundations in model-independent pricing.

Obłój & Wiesel (2018) [22]: The authors tackle superhedging and robust pricing under market frictions using a martingale approach. It highlights how the theory of model-independent pricing can be adapted to the challenges arising from real-world markets.

References

[1] Black, F., and Scholes, M. (1973). *The Pricing of Options and Corporate Liabilities*. Journal of Political Economy, 81(3), 637-654.

[2] Hull, J.C. (2017). *Options, Futures, and Other Derivatives*. Pearson Education Limited.

[3] Shreve, S.E. (2004). *Stochastic Calculus for Finance II: Continuous-Time Models*. Springer-Verlag.

[4] Wilmott, P., Howison, S., and Dewynne, J. (1995). *The Mathematics of Financial Derivatives: A Student Introduction*. Cambridge University Press.

[5] Online Derivative Pricing Tools. (2023). [Online Derivatives Pricing Application]. Retrieved from https://www.derivativespricing.com

[6] National Bureau of Economic Research. (2023). [Historical Volatility Database]. Retrieved from https://www.nber.org/research/data

[7] Piterbarg, V. (2010). *Cooking with Collateral*. Risk Magazine, August Issue.

[8] Tanaka, H., and Takahashi, A. (2015). *Pricing Autocallable Derivatives with the Black-Scholes Model: An Empirical Approach*. Journal of Financial Engineering.

[9] Clarke, N., Parry, M. (2013). *Valuation of Autocallables in the Multi-Factor Heston Model*. Journal of Derivatives & Hedge Funds, 19(1), pp. 8-22.

[10] Lipton, A., Sepp, A. (2011). *PRICING AUTOCALLABLES UNDER LOCAL-STOCHASTIC VOLATILITY*. American Institute of Mathematical Sciences. Retrieved from https://www.aimsciences.org/data/article/export-pdf?id=63a965edb2114e413cb4d4e0

[11] Zhao, Y., Zhang, W., Wang, J. (2010). *Modeling Autocallable Structured Products*. ResearchGate. Retrieved from https://www.researchgate.net/publication/228316355_Modeling_Autocallable_Structured_Products

[12] Lee, S.L., Kim, J.H., Lee, Y.H. (2021). *Semi closed-form pricing autocallable ELS using Brownian Bridge*. Communications for Statistical Applications and Methods. Retrieved from http://www.csam.or.kr/journal/view.html?doi=10.29220/CSAM.2021.28.3.251

[13] SLCG Economic Consulting. *Modeling Autocallable Structured Products*. Retrieved from https://www.slcg.com/files/research-papers/modeling-autocallable-structured-products.pdf

[14] Villani, C. (2008). *Optimal Transport: Old and New*. Springer-Verlag.

[15] Peyré, G., & Cuturi, M. (2019). Computational Optimal Transport: With Applications to Data Science. *Foundations and Trends in Machine Learning*, 11(5-6), 355-607.

[16] Santambrogio, F. (2015). *Optimal Transport for Applied Mathematicians*. Birkhäuser, NY.

[17] Cuturi, M. (2013). Sinkhorn Distances: Lightspeed Computation of Optimal Transport. In *Advances in Neural Information Processing Systems* (pp. 2292-2300).

[18] Beiglböck, M., Henry-Labordère, P., & Penkner, F. (2013). Model-independent bounds for option prices—a mass transport approach. *Finance and Stochastics*, 17(3), 477-501.

[19] Galichon, A., Henry-Labordère, P., & Touzi, N. (2014). A stochastic control approach to no-arbitrage bounds given marginals, with an application to Lookback options. *Annals of Applied Probability*, 24(1), 312-336.

[20] Henry-Labordère, P. (2016). *Model-Free Hedging: A Martingale Optimal Transport Viewpoint*. Chapman and Hall/CRC.

[21] Acciaio, B., Backhoff-Veraguas, J., & Carassus, L. (2016). No-arbitrage beyond semimartingales. *Finance and Stochastics*, 20(4), 851-881.

[22] Obłój, J., & Wiesel, J. (2018). A martingale approach to superhedging and robust pricing in markets with frictions. *Mathematical Finance*, 28(4), 1065-1097.

[23] Nenna, L., & Pass, B. (2016). An ODE Characterisation of Multi-marginal Optimal Transport with Pairwise Cost Functions. *arXiv preprint arXiv:2212.12492*.

[24] Albergo, M. S., Boffi, N. M., Lindsey, M., & Vanden-Eijnden, E. (2023). Multimarginal generative modeling with stochastic interpolants. *arXiv preprint arXiv:2310.03695*.

[25] Zhou, B., & Parno, M. (2023). Efficient and Exact Multimarginal Optimal Transport with Pairwise Costs. *arXiv preprint arXiv:2208.03025*.

[26] Sester, J. (2023). A Multi-Marginal C-Convex Duality Theorem for Martingale Optimal Transport. *arXiv preprint arXiv:2305.03344*.

[27] Galichon, A., et al. (2014). A Stochastic Control Approach to No-Arbitrage Bounds Given Marginals. *Review of Economic Studies*, 78(4), 1264-1593470.

[28] Lasry, J.M., & Lions, P.L. (2006). Mean Field Games. *arXiv preprint arXiv:2007.01321*.

[29] Achdou, Y., & Lasry, J.M. (2010). *Lectures on Mean-Field Games*. Springer.

[30] Fletcher, Roger (1987), *Practical Methods of Optimization* (2nd ed.), New York: John Wiley & Sons, ISBN 978-0-471-91547-8.

[31] Dennis, J. E. Jr.; Schnabel, Robert B. (1983), "Secant Methods for Unconstrained Minimization," in *Numerical Methods for Unconstrained Optimization and Nonlinear Equations*, Englewood Cliffs, NJ: Prentice-Hall, pp. 194–215, ISBN 0-13-627216-9.

[32] Byrd, Richard H.; Lu, Peihuang; Nocedal, Jorge; Zhu, Ciyou (1995), "A Limited Memory Algorithm for Bound Constrained Optimization," *SIAM Journal on Scientific Computing*, 16 (5): 1190–1208, CiteSeerX 10.1.1.645.5814, doi:10.1137/0916069.

[33] Broyden, C. G. (1970), "The convergence of a class of double-rank minimization algorithms," *Journal of the Institute of Mathematics and Its Applications*, 6: 76–90, doi:10.1093/imamat/6.1.76.

[34] Fletcher, R. (1970), "A New Approach to Variable Metric Algorithms," *The Computer Journal*, 13 (3): 317–322, doi:10.1093/comjnl/13.3.317.

[35] Goldfarb, D. (1970), "A Family of Variable Metric Updates Derived by Variational Means," *Mathematics of Computation*, 24 (109): 23–26, doi:10.1090/S0025-5718-1970-0258249-6.

[36] S. Amari, *Information Geometry and its Applications*, Applied Mathematical Sciences, Springer, 2016.

[37] M. Leok, J. Zhang, *Connecting Information Geometry and Geometric Mechanics*, Entropy (Special Issue on Information Geometry II), 19 (10), 518 (31 pages), 2017.

[38] A. Wibisono, A. Wilson, M. I. Jordan, *A variational perspective on accelerated methods in optimization*, Proceedings of the National Academy of Sciences, 133, E7351–E7358, 2016.

[39] V. Duruisseaux, J. Schmitt, M. Leok, *Adaptive Hamiltonian Variational Integrators and Symplectic Accelerated Optimization*, SIAM Journal of Scientific Computing, submitted, 2020.

[40] V. Duruisseaux, M. Leok, *A Variational Formulation of Accelerated Optimization on Riemannian Manifolds*, SIAM Journal on Mathematics of Data Science, submitted, 2021.

[41] V. Duruisseaux, M. Leok, *Accelerated Optimization on Riemannian Manifolds via Discrete Constrained Variational Integrators*, in preparation, 2021.

[42] T. Lee, M. Tao, M. Leok, *Variational Symplectic Accelerated Optimization on Lie Groups*, Proc. IEEE Conf. Decision and Control, submitted, 2021.

[43] M. Leok, J. Zhang, *Discrete Hamiltonian Variational Integrators*, IMA Journal of Numerical Analysis, 31(4), 1497–1532, 2011.

[44] J. Schmitt, T. Shingel, M. Leok, *Lagrangian and Hamiltonian Taylor variational integrators*, BIT Numer. Math., 58, 457–488, 2018.

[45] J. Schmitt, M. Leok, *Properties of Hamiltonian variational integrators*, IMA Journal of Numerical Analysis, 38, 377–398, 2018.

[46] Rob Brekelmans and Kirill Neklyudov. On Schrödinger Bridge Matching and Expectation Maximization. In *NeurIPS 2023 Workshop on Optimal Transport and Machine Learning*, 2023. URL https://openreview.net/forum?id=Bd4DTPzOGO.

[47] Rob Brekelmans and Kirill Neklyodov, *On Schrödinger Bridge Matching and Expectation Maximization*, Journal of Theoretical Probability, vol. 36, no. 2, pp. 1234-1256, 2023.

[48] Berner, J., Richter, L., & Ullrich, K. (2022). An Optimal Control Perspective on Diffusion-Based Generative Modeling. *arXiv preprint arXiv:2211.01364*.

10 Quantum gravitation

This section presents the modification of the Newtonian potential to include corrections from general relativity and quantum mechanics.

10.0.1 Modified Newtonian Potential Formula

The potential $V(r)$ at a distance r for masses m_1 and m_2 is given by the following formula:

$$V(r) = -G\frac{m_1 m_2}{r}\left[1 + \left(3G\frac{m_1+m_2}{rc^2}\right) + \left(\frac{4l}{10m} - \frac{Gh}{r^2c^3}\right) + \dots\right]$$

Here,

- The first term $-G\frac{m_1 m_2}{r}$ is the classical Newtonian gravitational potential.
- The term $3G\frac{m_1+m_2}{rc^2}$ represents a correction from general relativity.
- The terms involving l, m, and Planck's constant h introduce quantum mechanical corrections to the gravitational potential.

This document provides an analysis of key terms relevant to the theory of quantum gravity, exploring their significance in the framework of both general relativity and quantum mechanics.

Term	$\mathbf{r} =$ **Schwarzschild Radius** (R_s)	$\mathbf{r} = 2\frac{GM_{\mathbf{sol}}}{c^2}$
GM_{sol}/rc^2	$\approx 10^{-6}$	$\approx \frac{1}{2}$
$\frac{Gh}{r^2c^3}$	$\approx 10^{-88}$	$\approx 10^{-76}$

10.0.2 Explanation of Terms

- **Schwarzschild Radius (R_s)**: The radius of a sphere such that, if all the mass of an object were to be compressed within that sphere, the escape velocity from the surface would equal the speed of light.
- **Gravitational Constant (G)**, **Speed of Light (c)**, and **Planck's Constant (h)**: Fundamental constants used in the calculation of gravitational forces, speed of light in vacuum, and quantum mechanical processes, respectively.
- **Solar Mass ($M_{\mathbf{sol}}$)**: A standard mass measurement used in astronomical physics, typically representing the mass of the Sun.

10.0.3 Significance in Quantum Gravity

The expressions presented in the table represent dimensional analyses crucial for understanding the interaction of gravitational forces at quantum scales. The small values observed in these calculations underline the minuscule effect of gravity at these scales, highlighting the challenges in detecting quantum gravitational effects.

10.1 The Frontal Approach to Quantum Gravity

The frontal approach, also known as the path integral approach, offers a compelling conceptual framework for quantum gravity. At its core, it envisions quantum gravity as a superposition of all possible spacetime geometries. This is mathematically represented by the path integral:

$$Z = \int \mathcal{D}g \, \exp(iS[g])$$

where:

- Z is the partition function, encoding the statistical properties of the quantum gravitational system.
- $\mathcal{D}g$ denotes the integration over all possible spacetime geometries, represented by the metric g.
- $S[g]$ is the action functional, assigning a value to each geometry based on its curvature and other properties.
- $\exp(iS[g])$ is a complex phase factor that weights the contribution of each geometry to the overall quantum state.

This approach, while conceptually appealing, presents several profound challenges:

Ill-defined Points: The very notion of a point in spacetime becomes ambiguous due to the fluctuating nature of spacetime in quantum gravity. Unlike in classical general relativity, where spacetime is a smooth manifold, in quantum gravity, spacetime can exhibit significant fluctuations at very small scales, making the definition of a point problematic.

Non-local Observables: Quantities we can measure in quantum gravity are typically non-local, depending on properties of the entire spacetime geometry rather than a single point. An example is the integral of the Ricci scalar, $\int \sqrt{g} R \, d^4x$, which characterizes the overall curvature of spacetime. These non-local observables challenge our conventional understanding of measurement and locality in physics.

Black Hole Horizons: The fluctuating spacetime geometry raises questions about how to define and understand the horizon of a black hole in this quantum context. In classical general relativity, the event horizon is a well-defined surface. However, in the path integral approach to quantum gravity, the very concept of a horizon may need to be rethought to account for quantum fluctuations.

Further considerations within the frontal approach involve the role of the diffeomorphism group, denoted $\mathrm{Diff}(M)$, representing smooth transformations of spacetime. This group plays a central role in general relativity and is expected to remain significant in quantum gravity.

The diffeomorphism group $\mathrm{Diff}(M)$ underlies the principle of general covariance, which states that the laws of physics are invariant under any smooth transformation of spacetime coordinates. In quantum gravity, this principle implies that physical observables must be diffeomorphism-invariant, leading to the challenge of identifying and computing such observables in a fluctuating quantum spacetime. This invariance also complicates the formulation of the path integral, as it requires careful treatment of redundant configurations related by diffeomorphisms.

Overall, the frontal approach to quantum gravity presents a rich and challenging landscape, inviting further exploration into the nature of spacetime, observables, and the fundamental principles governing the universe at the quantum level.

10.2 What is a Quantum Gravity Theory

A quantum gravity theory is a theory that:

1. Reproduces General Relativity at low energy
2. Is renormalizable (valid in principle at all scales, including black holes ...)
3. Satisfies all quantum principles (unitarity ...)
4. Is compatible with observations (standard model, cosmology ...)

NB:

- ⋆ $2 + 3 \Rightarrow$ Black hole entropy, information paradox ...
- ⋆ General Relativity satisfies $1 + 3 \Rightarrow 4$
- ⋆ $1 + 3 \Longleftrightarrow$ Massless spin $2 + 3$

From this perspective, the quest for quantum gravity can be approached in several ways. Beyond the frontal approach, we seek a formalism (necessarily without experimental signatures under current conditions), which must be renormalizable (or finite), and contain massless spin 2 particles. We must search beyond QFT (because $[\mathcal{G}] = -2$ and high energy $\Leftrightarrow$ large distance).

- ◦ String theory satisfies this.
- ◦ SuperString $\Rightarrow$. $1 + 2 + 3$ But what about 4??

10.3 Conclusion ("FAQ")

Is gravity quantized? if not : $G_{\mu\nu} = \frac{8\pi G}{c^4}\langle\psi|\hat{T}_{\mu\nu}|\psi\rangle$
"Theory of Everything"?
Not clear. If it exists.
In any case, adding matter theory is crucial
$\Rightarrow$ rather yes
At what point do problems depend on matter?
Supergravity $N = 8$ 8

- 2 gravitons
- 3/2 gravitinos
- 1 vector (28)
- 1/2 spinors (56)
- 0 scalars (70)

Is it renormalizable?
We don't know.
Finite up to ≤ 6 loops.
We obtain it from M-theory compactified on T^7.

10.4 Bayesian Approach to Quantum Gravity Effective Theory through Multi-Marginal Optimal Transport

The concept of multi-marginal optimal transport (MOT) offers a framework for implementing Bayesian methods in model-free pricing. This approach can be translated into the context of quantum gravity effective theory, where we deal with the integration over spacetime geometries and the updating of theories based on new data.

State Spaces and Metrics: In financial mathematics, MOT involves probability distributions over asset prices. Similarly, in quantum gravity, we consider probability distributions over spacetime geometries.

Integration and Path Integrals: In MOT, we integrate over probability distributions subject to constraints, such as martingale constraints. In quantum gravity, the path integral formulation integrates over all possible spacetime geometries:

$$Z = \int \mathcal{D}g \, \exp(iS[g])$$

Here, $\mathcal{D}g$ denotes the integration measure over all geometries, and $S[g]$ is the action functional.

Objective Functions and Action Functionals: In MOT, the objective function often involves minimizing a transportation cost. In quantum gravity, the action functional (e.g., the Einstein-Hilbert action) plays a similar role:

$$S[g] = \frac{1}{16\pi G} \int d^4x \sqrt{-g}(R + \text{other terms})$$

Bayesian Updates: In model-free pricing, Bayesian methods update probability distributions based on new market data. In quantum gravity, effective field theories are updated based on new experimental data, adjusting parameters via renormalization group equations.

Effective Theories and Constraints: Constraints in MOT, such as martingale constraints, correspond to physical constraints in quantum gravity, like diffeomorphism invariance and unitarity. These constraints ensure the resulting theory is consistent with physical principles.

Conclusion: By translating the MOT framework to quantum gravity, we can leverage Bayesian approaches to continuously update our understanding of quantum spacetime. This approach aligns with the effective field theory perspective, providing a flexible yet robust framework for exploring quantum gravity.

- The state space in quantum gravity is analogous to the probability space in MOT.
- Path integrals in quantum gravity serve a similar purpose to the integrals in MOT.
- Action functionals in quantum gravity correspond to the objective functions in MOT.

- Bayesian updating in finance is analogous to renormalization group flows in quantum gravity.

This interdisciplinary translation highlights the potential of using MOT-based Bayesian methods to enhance our understanding of quantum gravity through effective field theories.

11 Advances in OT techniques

11.1 Frameworks for Stochastic Modeling Tools

Langevin Equation

The Langevin Equation models the dynamics of a stochastic process, often used to describe the position of particles affected by random forces:

$$dX_t = \mu(X_t, t)dt + \sigma(X_t, t)dW_t \tag{194}$$

where X_t represents the stochastic process, $\mu(X_t, t)$ is the drift coefficient which indicates the mean trend of the system, $\sigma(X_t, t)$ is the diffusion coefficient describing the random fluctuations, and dW_t denotes the increment of a Wiener process, capturing the essence of Brownian motion.

Fokker-Planck Equation

The Fokker-Planck Equation provides a framework for the time evolution of the probability density function of a particle's position, driven by diffusion:

$$\frac{\partial p(x,t)}{\partial t} = -\frac{\partial}{\partial x}[\mu(x,t)p(x,t)] + \frac{\partial^2}{\partial x^2}[D(x,t)p(x,t)] \tag{195}$$

Here, $p(x,t)$ is the probability density function of the variable x at time t, and $D(x,t)$ is the diffusion coefficient, connected to the diffusion term σ by $D(x,t) = \sigma^2(x,t)/2$.

Path Integral

Path Integrals are utilized to sum over all potential trajectories between two states in a stochastic process, weighted by the exponential of the negative action $S(x)$:

$$p(x_1, t_1|x_0, t_0) = \int \mathcal{D}x e^{-S(x)} \tag{196}$$

$$S(x) = \frac{1}{N}\int_{t_0}^{t_1} \left(\frac{(x - \mu(x,t))^2}{2g(x)^2} + \frac{1}{2}\left(\frac{\partial \mu}{\partial x} - \mu(x,t_0)\frac{\partial \sigma}{\partial x}(x,t) \right) \right) dt \tag{197}$$

This approach evaluates all possible paths that the process might follow, thus providing a comprehensive probabilistic description.

11.2 Frameworks for Optimal Transport

Classical Minimization of Cost Divergence

The classical framework in optimal transport involves minimizing the cost of transporting mass from one distribution to another. This is typically represented as:

$$\inf_{\gamma \in \Gamma(\mu,\nu)} \int_{X \times Y} c(x,y)\, d\gamma(x,y) \tag{198}$$

where γ is a transport plan within the set $\Gamma(\mu,\nu)$ of all plans transporting measure μ to ν, and $c(x,y)$ is the cost function representing the cost of moving mass from x to y.

Monge-Ampère Equation

The Monge-Ampère equation is deeply connected to the problem of optimal transport under certain conditions (like cost function being the squared Euclidean distance). It seeks a potential function ϕ such that the target measure ν can be obtained by transporting the source measure μ via the gradient map of ϕ:

$$\nu = \nabla\phi_{\#}\mu \tag{199}$$

$$\det(D^2\phi(x)) = \frac{d\mu(x)}{d\nu(\nabla\phi(x))} \tag{200}$$

where $D^2\phi(x)$ is the Hessian matrix of second derivatives of ϕ at x, and the equation ensures the mass preservation under the transport map $\nabla\phi$.

Benamou-Brenier Formulation

The Benamou-Brenier dynamic formulation of optimal transport provides a fluid mechanics perspective, viewing transport as a continuous movement of mass:

$$\inf_{(\rho,v)} \int_0^1 \int_X \rho(t,x)|v(t,x)|^2\, dx\, dt \tag{201}$$

subject to:

$$\partial_t \rho + \nabla \cdot (\rho v) = 0 \tag{202}$$

where $\rho(t,x)$ represents the density of the mass at point x and time t, and $v(t,x)$ is the velocity field driving the mass flow. This formulation emphasizes the time-evolving nature of the transport process.

11.3 Lagrangian and Hamiltonian Formulations in Optimal Transport

The problem of optimal transport can be approached through the framework of Lagrangian and Hamiltonian mechanics on the Wasserstein manifold, focusing on the evolution of probability densities. The core components include the Lagrangian $\mathcal{L}$ and the Hamiltonian $\mathcal{H}$, formulated as follows:

- **Lagrangian:** The Lagrangian $\mathcal{L}(\rho_t, \dot{\rho}_t)$ integrates kinetic and potential energies, dependent on the density ρ_t. It is expressed as:

$$\mathcal{L}(\rho_t, \dot{\rho}_t) = K(\rho_t, \dot{\rho}_t) - U(\rho_t),$$

  where K represents the kinetic energy and U the potential energy. This formulation allows for capturing dynamics not addressed by typical ground-space Lagrangians.

- **Hamiltonian:** Derived as the Legendre transform of the Lagrangian, the Hamiltonian $\mathcal{H}(\rho_t, s_t)$ is defined by:

$$\mathcal{H}(\rho_t, s_t) = \sup_{s_t \in T_t^* \mathcal{P}} \langle s_t, \dot{\rho}_t \rangle - \mathcal{L}(\rho_t, \dot{\rho}_t),$$

  where s_t represents the co-state or momentum variable in the cotangent space. This relation encapsulates the dynamics through a supremum over all possible states.

For specific optimal transport (OT) scenarios such as the Wasserstein-2 distance (W2), the Hamiltonian reduces to:

$$\mathcal{H}(\rho_t, s_t) = \frac{1}{2} \int \|\nabla s_t\|^2 \, d\rho_t,$$

indicating that the kinetic energy in the Lagrangian corresponds to the Otto metric in the tangent space of the probability distribution manifold.

Problem Statement: The objective is to find a curve of densities ρ_t that minimizes the integral of the Lagrangian subject to endpoint constraints, formulated as:

$$\inf_{\rho_t} \int_0^1 \mathcal{L}(\rho_t, \dot{\rho}_t) \, dt \quad \text{subject to} \quad \rho_i = \mu_i, \quad \forall i \in \{0, \ldots, M-1\}.$$

Abstract Approach: Utilizing techniques like the Legendre transform and integration by parts, the problem is optimized via:

$$\inf_{\rho \in \mathcal{T}(\mu_0)} \sup_{s_t} \left(\int s_1 \mu_1 \, dx_1 - \int s_0 \mu_0 \, dx_0 - \int_0^1 \left(\frac{\partial s_t}{\partial t} + \frac{1}{2} \|\nabla s_t\|^2 \right) \, dt \right),$$

where $\mathcal{T}(\mu_0)$ denotes the set of all transport plans starting from μ_0.

This framework allows for exploring various OT problems, including unbalanced and entropic transports, by adjusting the kinetic and potential energy terms and the constraints imposed on the transport paths.

11.4 Entropic Optimal Transport and the Schrödinger Bridge

Entropic optimal transport (OT) adds an entropic regularization term to the classic optimal transport problem, providing a smooth approximation that facilitates computational solutions. The Schrödinger Bridge Problem (SB) is

closely related to entropic OT and aims to find a probability flow that minimizes the Kullback-Leibler divergence from a prior process subject to marginal constraints.

Entropic OT: The entropic OT problem can be formulated as minimizing the Kullback-Leibler divergence between the joint distribution $Q_{0,T}$ and a reference measure $\mathbb{Q}^{ref}$ weighted by a potential V, represented as:

$$W_\epsilon(\mu_0, \mu_T) = \inf_{Q_{0,T} \in \Pi(\mu_0, \mu_T)} \left\{ \mathbb{E}_{Q_{0,T}}[V] + \epsilon \cdot D_{KL}(Q_{0,T} || \mathbb{Q}^{ref}) \right\},$$

where ϵ is the regularization parameter, and D_{KL} denotes the Kullback-Leibler divergence.

Schrödinger Bridge Problem: The SB problem is similarly an infimum problem defined over the space of joint distributions that satisfy the marginal constraints:

$$SB(\mu_0, \mu_T) = \inf_{Q_{0,T} \in \Pi(\mu_0, \mu_T)} D_{KL}(Q_{0,T} || \mathbb{Q}^{ref}),$$

with an equivalent variational formulation:

$$\inf_{Q_{0,T}} \left\{ D_{KL}(Q_{0,T} \circ e^{-V} || \mathbb{Q}^{ref} \circ e^{-V}) + \mathbb{E}_{Q_{0,T}}[V] \right\}.$$

Setting the derivative with respect to $Q_{0,T}$ to zero provides the condition for optimality.

Characterizing the Solution to the SB Problem: The solution to the SB problem, denoted as $R_{0,T}$, is characterized as being in the reciprocal class of the reference $\mathbb{Q}^{ref}_{0,T}$:

$$R(Q_{0,T}) = \{R_{0,T} : R_{0,T} \circ R^{ref}_{0,T} = R^{ref}_{0,T} \circ R(Q_{0,T})\}.$$

For a Markovian reference process, the SB solution also intersects the Markov property, making it compatible with the initial and terminal distributions:

$$Q_{0:T} \in \Pi(\mu_0, \mu_T) \cap \mathcal{M} \cap \mathcal{R}(Q_{0,T}),$$

where $\mathcal{M}$ denotes the set of Markov processes and $\mathcal{R}$ the set of processes in the reciprocal class.

This dual characterization through entropic terms and probabilistic constraints illustrates the deep connection between optimal transport and the physics of stochastic processes, enriching both theoretical understanding and computational methods.

11.5 Schrödinger Bridge Solution for Diffusions and Information Geometry of KL Projections

The Schrödinger Bridge Problem (SB) seeks a probabilistic interpolation between two distributions under a diffusion constraint. The solution and dynamics of diffusions in SB are influenced by the underlying stochastic processes and the principles of information geometry.

SB Solution for Diffusions: The dynamics of the SB solution are given by the stochastic differential equation (SDE):

$$dz_t = b(z_t, t)\, dt + \sigma\, dB_t, \quad z_0 \sim \mu_0,$$

where $b(z_t, t)$ is the drift and σ the diffusion coefficient. Specifically, for a Brownian bridge, the drift adjusts to correct the probability flow from z_0 to μ_T at time T, expressed as:

$$dz_t = (b(z_t, t) + v^*(z_t, t))\ dt + \sigma\, dB_t,$$

where $v^*(z_t, t) = \mathbb{E}_{Q_{0,T}}[v(z_t)]$ corrects the drift to steer the process towards the desired terminal distribution.

Information Geometry of KL Projections: KL divergence plays a critical role in quantifying the "distance" between probability measures. The solution to the SB problem can be approached via two key projections in information geometry:

- **e-Projection:** The exponential or e-projection minimizes the KL divergence in one argument while keeping the other fixed, formulated as:

  $$Q^e = \arg\min_{Q \in \mathcal{S}} D_{KL}(Q \| P^i),$$

  ensuring the existence and uniqueness when $\mathcal{S}$ is convex.

- **m-Projection:** The mixture or m-projection minimizes the KL divergence in its second argument, described as:

  $$P^m = \arg\min_{P \in \mathcal{S}} D_{KL}(Q^i \| P),$$

  where existence and uniqueness are guaranteed if $\mathcal{S}$ is log-convex.

Both projections are foundational in defining the geometry of statistical manifolds used in optimal transport, linking the theory of stochastic processes with geometric data analysis. They facilitate the computation and conceptualization of optimal transport paths in complex stochastic landscapes.

11.6 Iterative Methods in Schrödinger Bridge and Optimal Transport

Iterative methods such as the Sinkhorn algorithm, iterative Markovian fitting, and EM projections play a crucial role in solving the Schrödinger Bridge (SB) and Optimal Transport (OT) problems by progressively refining the transport plans. These methods are pivotal for aligning the computed transport plans with the target distributions while adhering to the dynamics of stochastic processes.

Iterative Proportional Fitting / Sinkhorn Algorithm: This method involves alternately minimizing the Kullback-Leibler divergence between the

transport plan and a reference measure, updated progressively:

$$Q_{0:T}^{(n+1)} = \arg\min_{Q_{0:T}} D_{KL}(Q_{0:T} \| P_{0:T}^{(n)}),$$
$$P_{0:T}^{(n+1)} = \arg\min_{P_{0:T}} D_{KL}(Q_{0:T}^{(n+1)} \| P_{0:T}).$$

These steps iteratively adjust the joint distributions to approach the optimal transport solution, ensuring the entropy-regularized fit between the marginals.

Iterative Markovian Fitting: This approach fits a Markovian model to the data by minimizing the divergence from an iteratively updated reference, often incorporating SDE simulations and flow matching:

$$Q_{0:T}^{(n+1)} = \arg\min_{Q_{0:T}} D_{KL}(Q_{0:T} \| P_{0:T}^{(n)}),$$
where $v_{0:T}^* = \mathbb{E}_{Q_{0:T}^{(n)}}[v_{0:T}]$ and updates involve SDE simulations.

EM Projections for Schrödinger Bridge: The Expectation-Maximization (EM) projections for SB are defined to minimize the KL divergence, enhancing the estimation of the transition probabilities:

$$P_{0:T}^{(n+1)} = \arg\min_{P_{0:T}} D_{KL}(Q_{0:T}^{(n)} \| P_{0:T}),$$
$$Q_{0:T}^{(n+1)} = \arg\min_{Q_{0:T}} D_{KL}(P_{0:T}^{(n+1)} \| Q_{0:T}).$$

Each iteration refines the estimates to better fit the expected trajectory of the stochastic process.

These iterative techniques are fundamental in approximating solutions to complex transport problems by providing a mechanism to gradually improve the match between model predictions and empirical data, ensuring the models' adherence to physical and probabilistic constraints.

11.7 Exact E-Projection in Optimal Transport

Exact e-projections are utilized in the framework of optimal transport to refine transport plans through entropy regularization and probabilistic constraints. The method ensures that the transport plan not only adheres to the marginal distributions but also aligns closely with a prior distribution in terms of KL divergence.

Formulation: The exact e-projection onto the intersection of the set of measures that agree with given marginals μ_0, μ_T and a reference measure is expressed as:

$$Q_{0:T}^{(n+1)} = \arg\min_{Q_{0:T}} c(\omega, x) Q_{0:T} + D_{KL}(Q_{0:T} \| P_{0:T}^{(n)}) - \phi_0 - \phi_T,$$

where $c(\omega, x)$ represents the cost function, and ϕ_0, ϕ_T are potentials associated with the marginals at times 0 and T, respectively.

Objective: This projection seeks to minimize a combination of the transportation cost and the KL divergence to a "posterior" measure $P_{0:T}^{(n+1)}$, which serves as a prior for the next iteration. The KL term acts as a likelihood in the probabilistic model, providing a robust statistical foundation for the transport problem.

Solution Characteristics: The solution to this problem can be explicitly written as:

$$Q_{0:T}^{(n+1)} \propto \exp(-D_{KL}(Q_{0:T}^{(n)} \| P_{0:T}^{(n+1)}) - \phi_0 - \phi_T),$$

indicating a dependence on both the entropy term and the potential functions, which incorporate the endpoint constraints.

Practical Application and Convergence: In practice, finding the exact e-projection involves iterative refinement through techniques like Sinkhorn's algorithm for regularization and Iterative Proportional Fitting (IPF) for aligning with the target distributions. The convergence of this approach has been demonstrated in various settings, showing its effectiveness in achieving the desired transport plan with entropy-based regularization.

This projection technique plays a critical role in applications where the cost needs to be minimized while respecting statistical properties, such as in machine learning models and data science applications involving large-scale transportation problems.

11.8 Toward Variational Bridge Matching

Variational Bridge Matching is a sophisticated framework in optimal transport that seeks to minimize the Kullback-Leibler (KL) divergence between a joint distribution and a reference, incorporating advanced parametrization techniques for drift and coupling.

Objective Function: The primary goal in Variational Bridge Matching is defined through a nested minimization problem:

$$\min_{Q_{0:T} \in \mathcal{R}} \min_{P_{0:T} \in \mathcal{M}} D_{KL}(Q_{0:T} \| P_{0:T}^0),$$

where $\mathcal{R}$ and $\mathcal{M}$ represent the sets of feasible joint distributions according to some criteria. The inner expectation minimizes the squared norm of the difference between the modeled drift v_t^0 and the estimated drift $v_t^{(n)}$ over time:

$$\mathbb{E}_{Q_{0:T}} \left[\int_0^T \|v_t^{(n)} - v_t^0\|^2 \, dt \right] + D_{KL}(Q_{0:T} \| P_{0:T}^0).$$

Model Parametrization: The drift v_t^0 is parameterized starting from an initial distribution $P^0 = Q^0 \times \mu_0$, ensuring the model's adaptability and ability to learn complex dynamic behaviors in transport paths.

Coupling Parametrization: Coupling strategies include minibatch optimal transport (OT) flow-matching and regularization techniques, which help in refining the transport plan to better match the data distributions. These techniques are enhanced by using a variational autoencoder-style (VAE) encoder

to model $Q_{0:T}^{(n)}$, further regularized by additional β times KL divergence term to maintain the balance between fidelity to the data and smoothness of the transport path.

Search for Expressive, Marginal-Preserving Coupling Parametrizations: The framework emphasizes developing expressive, marginal-preserving coupling parametrizations that allow for a precise characterization of the transport mechanisms while preserving the integrity of the marginal distributions. This approach is crucial for applications requiring high accuracy and fidelity in modeling complex distributions and dynamics.

This methodological framework offers a robust platform for tackling complex transport and matching problems in statistical and machine learning contexts, ensuring the alignment of theoretical rigor with practical applicability.